Univerzita Karlova v Praze

1. lékařská fakulta

Studijní program: Biochemie a patobiochemie

Mgr. Andrea Špolcová

Vliv různých druhů antidiabetických intervencí na vývoj neurodegenerativních změn v mozku diabetických myší a potkanů

Impact of different types of antidiabetic interventions on the development of neurodegenerative changes in brains of diabetic mice and rats

Disertační práce

Školitelka: RNDr. Lenka Maletínská, CSc.

Spoluškolitelka: Dr. Marie-Christine Galas

Konzultant: Prof. MUDr. Martin Haluzík, DrSc.

Praha, 2015

ve spolupráci s

UNIVERSITE LILLE 2 DROIT ET SANTE

FACULTE DE MEDECINE HENRI WAREMBOURG

Année : 2015

THESE POUR LE DIPLOME D'ETAT

DE DOCTEUR EN MEDECINE

Impact de différents traitements antidiabétiques sur le développement de pathologies neurodégénératives dans le cerveau de rats et de souris diabétiques

Impact of different types of antidiabetic interventions on the development of neurodegenerative changes in brains of diabetic mice and rats

Prohlášení:

Prohlašuji, že jsem závěrečnou práci zpracovala samostatně a že jsem řádně uvedla a citovala všechny použité prameny a literaturu. Současně prohlašuji, že práce nebyla využita k získání jiného nebo stejného titulu.

Souhlasím s trvalým uložením elektronické verze mé práce v databázi systému meziuniverzitního projektu Theses.cz za účelem soustavné kontroly podobnosti kvalifikačních prací.

V Praze, dne …….....

ANDREA ŠPOLCOVÁ

……..

Identifikační záznam:

ŠPOLCOVÁ, Andrea. *Vliv různých druhů antidiabetických intervencí na vývoj neurodegenerativních změn v mozku diabetických myší a potkanů [Impact of different types of antidiabetic interventions on the development of neurodegenerative changes in brains of diabetic mice and rats]*. Praha, 2015. Stran, příloh. Disertační práce. Univerzita Karlova v Praze, 1. lékařská fakulta, Ústav organické chemie a biochemie Akademie věd České republiky, v.v.i. Vedoucí disertační práce Maletínská, Lenka.

ABSTRAKT

Alzheimerova nemoc (AN) je neurologické onemocnění způsobené dvěma patologickými znaky; extracelulárními plaky amyloidního beta peptidu a intracelulárními neurofibrilárními shluky tvořených hyperfosforylovaným proteinem Tau.

Jelikož diabetes mellitus druhého typu (DM2T) je rizikovým faktorem pro rozvoj AN, byl v první části mé disertační práce zkoumán možný vztah mezi hyperfosforylací proteinu Tau a centrální inzulínovou rezistencí, a to v hipokampech fa/fa potkanů a MSG myší, zvířecích modelů pre-diabetu, který je vyvolán obezitou. U 8 měsíců starých fa/fa potkanů a 6 měsíců starých MSG myší docházelo ke snížené fosforylaci inzulínové signalizační kaskády, která vedla ke zvýšené aktivaci glykogensynthasy kinázy-3Beta (GSK-3β), což je hlavní kináza způsobující hyperfosforylaci proteinu Tau. Následně byla pozorována zvýšená fosforylace proteinu Tau na Ser396 a Thr231. Tento jev nebyl pozorován u 2 měsíců starých MSG myší.

Druhá část mé práce byla zaměřena na nové analogy potenciálně neuroprotektivního anorexigenního neuropeptidu, peptidu uvolňujícího prolaktin (PrRP), které byly navrženy na ÚOCHB AV ČR. Palmitoylace umožnila přechod PrRP přes hematoencefalickou bariéru, čímž byl umožněn jeho centrální anorexigenní účinek.

Ve třetí části byl zkoumán vliv 14denního subkutánního (SC) podávání liraglutidu, nejpoužívanější látky k léčbě DM2T s centrálním anorexigenním účinkem, a palmitovaného PrRP31 na aktivaci inzulínové signalizační kaskády a hyperfosforylaci proteinu Tau v hipokampech 6 měsíců starých MSG myší. Obě látky zvýšily aktivaci inzulínové signalizační kaskády, a dále snížily hyperfosforylaci proteinu Tau na Thr212, Thr231 a Ser396. Vliv 2měsíčního SC podávání palmitovaného PrRP31 byl také zkoumán na Thy-Tau22 myších, modelu AN-podobné Tau patologie, které exprimují lidský mutovaný protein Tau. Léčba vyústila ve sníženou fosforylaci proteinu Tau na Thr231, Ser396 a Ser404.

Naše studie odhalily škodlivý vliv pre-diabetu na vývoj hyperfosforylace proteinu Tau, jednoho ze znaků AN, a její snížení po podání anorexigenních látek. Anorexigenní látky se tudíž jeví jako potenciální látky k léčbě neurodegenerativních onemocnění.

KLÍČOVÁ SLOVA:

Alzheimerova nemoc, inzulínová rezistence, obezita, glykogensyntáza kináza-3Beta, hyperfosforylace proteinu Tau, fa/fa potkani, MSG myši, Thy-Tau22 myši, peptid uvolňující prolaktin, liraglutid

RÉSUMÉ

La maladie d'Alzheimer est une maladie neurodégénérative caractérisée par l'accumulation extracellulaire de β-amyloïde (plaques amyloïdes) et la présence, dans le milieu intracellulaire, de neurofibrilles dues à l'hyperphosphorylation de la protéine Tau.

Le diabète de type 2 étant un facteur de risque de développement de la maladie d'Alzheimer, la première partie de cette thèse porte sur la possible relation entre la résistance à l'insuline dans le système centrale et l'hyperphosphorylation de la protéine Tau. Pour cela, deux modèles d'animaux pré-diabétiques ont été considérés : des rats transgéniques fa/fa et des souris traitées avec du glutamate monosodique (MSG). Dans les cas des rats fa/fa âgés de 8 mois et des souris MSG âgées de 6 mois, une plus faible phosphorylation de la cascade de réponse à l'insuline conduit à une plus forte activation de la principale kinase de la protéine Tau (la glycogen-synthase kinase-3Beta, GSK-3β), ce qui entraine une plus importante phosphorylation de la protéine Tau (Ser386 et Thr231). Ce phénomène est moindre chez les animaux âgés de 2 mois.

La seconde partie de cette thèse porte sur l'étude d'un neuropeptide développé dans notre institut (prolactin-releasing peptide, PrRP) à activité neuroprotectrice et anorexigène. La palmitylation du peptide PrRP permet à celui-ci de franchir la barrière hémato-encéphalique et d'exercer son action anorexigène.

Dans une troisième partie, l'effet de l'administration sous-cutanée de liraglutide (le principe actif à effet anorexigène centrale le plus utilisé dans de le cas de diabète de type 2) et de peptide PrRP31 palmytoylé sur la cascade de réponse à insuline et l'hyperphosphorylation de la protéine Tau, a été étudié dans le cas de souris MSG âgées de 6 mois. Après 14 jours de traitement, une amélioration de la cascade de réponse à l'insuline et une réduction du taux de phosphorylation de la protéine Tau (Thr212, Thr231, Ser396) ont été observées. D'autre part, des souris transgéniques Thy-Tau22, un modèle de souris développant une pathologie de Tau similaire à la maladie d'Alzheimer, présentent une réduction de la phosphorylation de la protéine Tau (Thr231, Ser 396 et Ser404) après 2 mois d'injection sous-cutanée du peptide PrRP31.

Notre étude, d'une part, met en lumière l'effet délétère du pré-diabète, lié à l'obésité, dans le développement de pathologies de la protéine Tau, et, d'autre part, démontre l'effet bénéfique de composés à action anorexigène sur l'hyperphosphorylation de la protéine Tau. Ainsi, des composés tels que le peptide étudié ici pourraient trouver une application dans le traitement de maladies neurodégénératives.

MOTS-CLÉS

Maladie d'Alzheimer, résistance à l'insuline, obésité, glycogen-synthase kinase -3Beta, protéine Tau, hyperphosphorylation, rats transgéniques fa/fa, souris MSG, souris transgéniques Thy-Tau22, prolactin-releasing peptide, liraglutide

ABSTRACT

Alzheimer's disease (AD) is neurological disorder characterized by extracellular beta amyloid plaques and intracellular neurofibrillary tangles formed by hyper-phosphorylated Tau protein.

Since type 2 diabetes mellitus (T2DM) is a risk factor of AD development, in the first part of the thesis, a potential relationship between hyper-phosphorylation of Tau protein and central insulin resistance was followed in hippocampi of two models of obesity-induced pre-diabetes, fa/fa rats, and mice with monosodium glutamate (MSG) induced obesity. In both 8-month-old fa/fa rats and 6-month-old MSG mice a decreased phosphorylation of insulin signaling cascade resulted in an increased activation of main Tau kinase glycogen-synthase kinase-3Beta (GSK-3β) and an increased Tau phosphorylation at epitopes Ser396 and Thr231. This phenomenon was less developed in 2-month-old animals.

The second part of the thesis was focused on a potential neuroprotective anorexigenic neuropeptide, prolactin-releasing peptide (PrRP), designed at our Institute. Palmitoylation enabled PrRP to cross the blood-brain barrier and employ its central anorexigenic activity.

In the third part of the thesis, an effect of 14-day-long SC administration of liraglutide, the most used anti-T2DM drug with central anorexigenic effect, and palmitoylated PrRP31 on insulin signaling cascade and Tau hyper-phosphorylation was examined in the hippocampi of 6-month-old MSG mice. Both compounds streamlined insulin signaling cascade, and also attenuated Tau phosphorylation at Thr212, Thr231, and Ser396. The effect of 2-month-long SC administration of palmitoylated PrRP31 was examined also in a model of AD-like Tau pathology, Thy-Tau22 mice overexpressing mutated human Tau protein. The treatment resulted in decreased Tau protein phosphorylation at Thr231, Ser396 and Ser404.

Our study revealed a deleterious effect of obesity-related pre-diabetes on the development of Tau pathology, and the beneficial effect of anorexigenic compounds on the hyper-phosphorylation of Tau. Anorexigenic peptides thus showed potency for possible treatment of neurodegenerative disorders.

KEY WORDS:

Alzheimer's disease, insulin resistance, obesity, glycogen-synthase kinase – 3Beta, Tau protein hyper-phosphorylation, fa/fa rats, MSG mice, Thy-Tau22 mice, prolactin-releasing peptide, liraglutide

ACKNOWLEDGEMENT

First of all I would like to express my gratitude to my PhD thesis supervisors, Dr. Lenka Maletínská, and Dr. Marie-Christine Galas for giving me the opportunity to work in their groups and also for their useful guidance and sharing their expertise during the elaboration of my thesis. I would like to acknowledge Professor Martin Haluzík, MD and Dr. Jaroslav Kuneš for their advice during my thesis writing. I would also like to thank the whole team of Antiobesity peptides of Dr. Maletínská from the Institute of Organic chemistry and Biochemistry AS CR, especially to Dr. Blanka Železná for her valuable advice during my research and comments during my thesis writing, Veronika Pražienková, MSc. for binding studies measurement, and especially for maintenance of all laboratory, Barbora Mikulášková, MSc. and Barbora Judita Kasperová for their help with the experimental part of my thesis, Jana Zemenová, MSc. for drug exposure measurement, Martina Holubová, PhD for RIA and ELISA measurement, and associated professor Zdenko Pirník for c-fos immunohistochemistry. Furthermore, I would also like to acknowledge with much appreciation Miroslava Blechová, MSc. for peptide synthesis, associated professor Tomáš Elbert for peptide iodination, Ondřej Pačes, MSc. from Development workshops of IOCB for Y-maze system development, and Hedvika Vysušilová for her excellent technical assistance.

I would like to thank to whole team of Dr. Luc Buée for a warm welcome to their group Alzheimer&Tauopathies from INSERM UMR-S-1172 in Lille, France, especially to group of Dr. Marie-Christine Galas, namely to Lucie Delattre MSc. for teaching me the method of immunohistochemistry, Alban Chauderlier, MSc., Marie Violet, PhD and Meliza Sendid-Chouala for their kind help with experimental part of my thesis, and to Meryem Tardivel and IMPRT (Institut de Médecine Prédictive et de Recherche Thérapeutique, Lille) for access to the confocal microscopy platform.

Last but not least, I would like to thank my family, who have encouraged me throughout my studies, especially to my partner Tomáš for his support.

The PhD thesis was supported by the Grant Agency of the Czech Republic No. P303/12/0576 and P303/10/1368, by the Academy of Sciences of the Czech Republic RVO: 61388963, by the Technology Agency of the Czech Republic TE01020028, by Mobility grant Barrande No. 7AMB12FR011 (Ministry of Education) and by Campus France.

CONTENTS

ABBREVIATIONS 11

1 INTRODUCTION 13

1.1 Alzheimer's disease 13
1.1.1 AD discovery 13
1.1.2 AD spreading in the brain 14
1.1.3 AD diagnostics 16
1.1.4 Current AD treatment 16
1.1.5 Hallmarks of AD 17
1.1.6 Risk factors of AD development 21
1.2 Animal models of AD, obesity, and T2DM 24
1.2.1 Models of AD 24
1.2.2 Models of T2DM 26
1.3 Neuroprotective effect of insulin-sensitizing/anorexigenic compounds 29
1.3.1 Leptin 30
1.3.2 Metformin 30
1.3.3 Incretins 31
1.3.4 Gliptins 35
1.3.5 Prolactin-releasing peptide 35

2 AIMS OF THE THESIS 38

3 MATERIALS & METHODS 39

3.1 Material 39
3.1.1 Chemicals 39
3.1.2 Instruments 39
3.1.3 Kits 39
3.2 Animal models 40
3.2.1 Housing & measurement of metabolic parameters 40
3.3 Preparation of hippocampi for Western blotting 42
3.3.1 Western blotting 42
3.4 Brain preparation for paraffin-embedded immunohistochemistry 44
3.4.1 Immunohistochemistry 44
3.5 Testing of lipidized prolactin-releasing peptide analogs 45
3.5.1 Peptide synthesis and iodination 45
3.5.2 Binding to intact plated cells 45
3.5.3 Acute food intake in lean mice 45
3.5.4 Fos and GPR10 receptor immunohistochemistry 46
3.6 Intervention with anti-diabetic and/or anorexigenic compound 46
3.6.1 Peptides 46
3.6.2 MSG mice: 14-day-long treatment with palm-PrRP31 or liraglutide 46
3.6.3 Thy-Tau22 mice: 2-month-long treatment with palm^{11}-PrRP31 47

3.7 Statistical analyses 48
4 RESULTS 49
4.1 fa/fa rats 49
4.1.1 Metabolic parameters of fa/fa rats 49
4.1.2 Insulin signaling cascade in hippocampi of fa/fa rats and their controls 51
4.1.3 Phosphorylation of Tau protein in hippocampi of fa/fa rats 53
4.2 MSG mice 54
4.2.1 Metabolic parameters of MSG mice 54
4.2.2 GSK-3β activation and Tau protein phosphorylation in hippocampi of MSG mice at the age of 2 and 6 months 54
4.3 Testing of lipidized analogs of PrRP31 56
4.3.1 Affinity to GPR10 receptor 56
4.3.2 Food intake after acute peripheral administration 57
4.3.3 c-Fos activation after peripheral administration 58
4.4 Long-term treatment with palmitoylated PrRP31 and liraglutide 59
4.4.1 6-month-old MSG obese male mice 59
4.5 Nine-month-old Thy-Tau22 female mice 67
4.5.1 Spatial memory testing in Y-maze before and after 2-month-long palm^{11}-PrRP31 treatment 67
4.5.2 Metabolic parameters of Thy-Tau22 mice and their age-matched WT controls after 2-month-long treatment with palm^{11}-PrRP31 67
4.5.3 Activation of Tau kinases and hyper-phosphorylation of Tau protein at different epitopes after treatment with palm^{11}-PrRP31 70
5 DISCUSSION 72
5.1 Pathological changes in the hippocampi of obese pre-diabetic rodents 73
5.1.1 Metabolic parameters 73
5.1.2 Central insulin signaling cascade 74
5.1.3 Tau hyper-phosphorylation in hippocampi 75
5.2 Lipidization of prolactin-releasing peptide 77
5.3 Effect of long-term treatment with anorexigenic compounds on Tau protein phosphorylation and spatial memory 78
5.3.1 Fourteen-day-long treatment of 6-month-old MSG mice with liraglutide or palm-PrRP31 78
5.3.2 Two-month-long treatment with palm^{11}-PrRP31 of Thy-Tau22 mice 80
5.4 Models of T2DM and AD-like Tau pathology and possible treatment: conclusions and perspectives 81
6 CONCLUSIONS 84
7 REFERENCES 85

ABBREVIATIONS

Aβ	amyloid-beta peptide
AD	Alzheimer's disease
ANOVA	analysis of variance
APP	amyloid precursor protein
Arc	nucleus arcuatus
AUC	area under curve
BBB	blood-brain barrier
CA	cornu ammonis/Ammon's horn
cdk5	cyclin-dependent kinase 5
CNS	central nervous system
CSF	cerebrospinal fluid
db	diabetic gene
DG	dentate gyrus
DIO	diet-induced obesity
DPP-IV	dipeptidyl peptidase IV
EIA	enzyme immunoassy
ELISA	enzyme-linked immunosorbent assay
fa	fatty gene
GIP	glucose-dependent insulinotropic peptide
GLP-1	glucagon-like peptide 1
GLUT	glucose transporter
GSK-3	glycogen-synthase kinase 3
HFD	high-fat diet
ICV	intracerebroventricular
IL	interleukin
IP	intraperitoneal
IR	insulin receptor
IRS-1	insulin receptor substrate 1
JNK	c-Jun N-terminal kinase
KO	knock-out
MAP	microtubule-associated protein
MAPK/ERK1/2	mitogen-activated protein kinase/extracellular-regulated kinase 1/2
MRI	magnetic resonance imaging
MSG	monosodium glutamate
NFT	neurofibrillary tangles
NPY	neuropeptide Y
NTS	nucleus tractus solitarius
PDK-1	phosphoinositide-dependent protein kinase 1
PI3K	phosphoinositide 3 kinase

PKA	protein kinase A
PP2A	protein phosphatase 2A
PrRP	prolactin-releasing peptide
PS	presenilin
PVN	paraventricular nucleus
QUICKI	quantitative insulin sensitivity check index
RIA	radioimmunoassay
SC	subcutaneous
SEM	standard error of mean
slm	stratum lacunosum-moleculare
SWE	Swedish mutation
T2DM	type 2 diabetes mellitus
Tau	Tau protein
TNF-α	tumor necrosis factor α
WAT	white adipose tissue
ZDF	Zucker diabetic fatty rats

1 INTRODUCTION

1.1 Alzheimer's disease

Alzheimer's disease (AD) is an age-associated neurological disorder, and it is the most common type of dementia, accounting for 60 - 80% of all dementia cases. AD not only reduces the quality of life of patients but also negatively influences the social and economic situation of patients' families (Alzheimer's, 2014).

1.1.1 AD discovery

The disease was for the first time described by German psychiatrist Dr. Alois Alzheimer (Fig. 1A) at the beginning of the 20th century. He worked in Municipal Mental Asylum in Frankfurt am Main, where a 51-year-old woman, Auguste Deter (Fig. 1B), was brought with early-onset dementia accompanied with serious memory loss, no sense of place or time, hallucination, and depression (Goedert and Spillantini, 2006). After her death, Alzheimer revealed extensive lesions in her brain, along with the presence of plaques and neurofibrillary tangles (NFT), mainly in the cerebral cortex. Alzheimer considered the tangles as the usual sign of ageing. A few years after his discoveries his colleague Emil Kraepelin proposed to name the disease after Alois Alzheimer (Zilka and Novak, 2006).

A/ **B/**

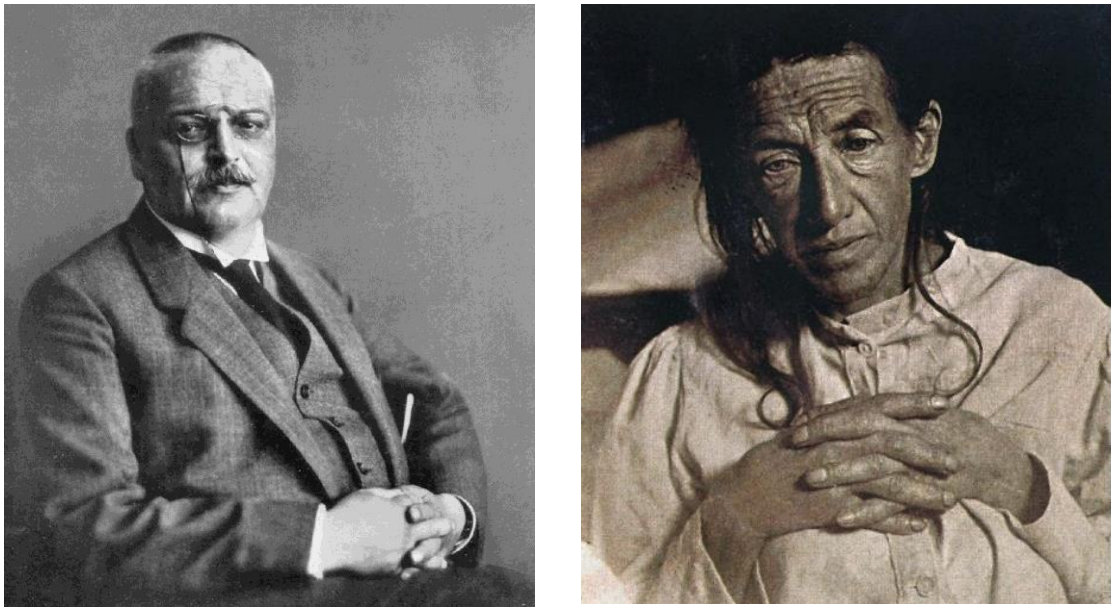

Fig. 1 A/Dr. Alois Alzheimer (www.kliniken-schmieder.de), and B/ Auguste Deter, the first patient diagnosed with Alzheimer's disease (www.best-alzheimers-products.com)

1.1.2 AD spreading in the brain

In AD brain, neuronal loss, loss of synapses, and a decreased level of neurotransmitters are observed, mainly in the brain regions important for memory formation and language, as shown in Fig. 2A. One of the first regions damaged during AD is hippocampus (Fig. 2B). Hippocampus is a part of the limbic system, located under the cerebral cortex in medial temporal lobe, which is the center important for memory and maintenance of emotions (Moser, 2011). It consists of dentate gyrus (DG) and cornu ammonis/Ammon's horn 1 - 3 (CA), and it is the crucial center for memory storage; it secures the transmission of short-term memories to the long-term memory (Squire, 1992).

A/

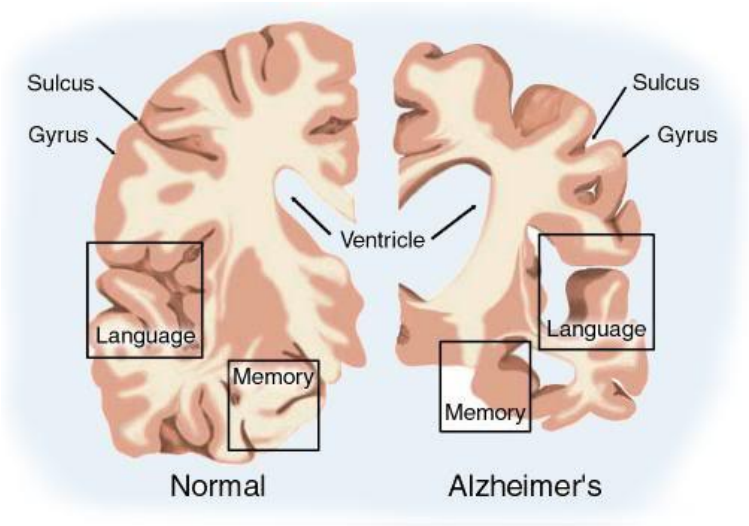

B/

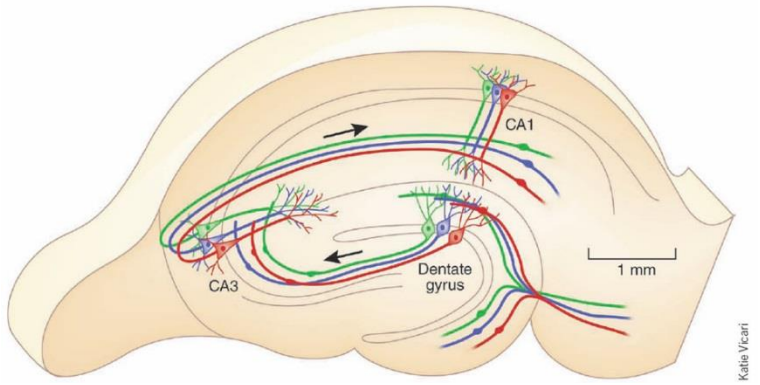

Fig. 2 A/ AD-caused brain damage (http://www.brightfocus.org)/ and B/ hippocampus (Moser, 2011), one of the first centers affected by AD

The AD pathology progression in the brain is shown in Fig. 3. It was established by Heiko Braak, who observed that in AD brain, three main stages can be recognized,

each of which can be subdivided into two phases. The first stage of AD is called the transentorhinal stage; this is a preclinical stage with no apparent symptoms in patient's behavior. There is starting pathology in entorhinal cortex and in CA1 of the hippocampus. Further, the disease spreads to other hippocampal regions, as well as to the centers such as amygdala and thalamus. This phase of the disease is called the limbic stage; there are starting clinical symptoms, when the disease starts to manifest with a small cognitive decline: forgetting recently learnt information, problems to recognize family members, problems with speaking, and with movements. Later, alterations in the person's behavior, such as apathy, aggression, and psychosis, are observed. The last stage of AD is called the isocortical stage. In this stage the pathology is also observed in the neocortex, the brain ventricles are widened and brain weight is reduced. The patients are disoriented and finally they are unable to take care of themselves. On average, nine years after the diagnosis the patients die. According to the statistics, at present, AD is the 6th common cause of the death (Alzheimer's, 2014; Braak et al., 2011; Giordano et al., 2007; Serrano-Pozo et al., 2011; Schultz et al., 2004).

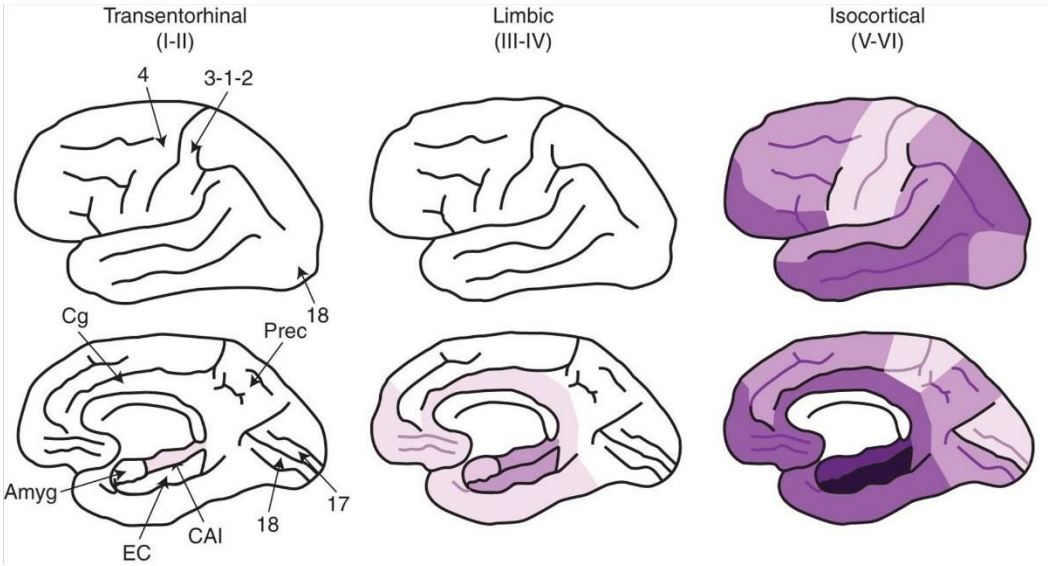

Fig. 3 Braak stages of AD progression (Serrano-Pozo et al., 2011)

Abbreviations: 3-1-2 - primary sensory cortex; 4 - primary motor cortex; 17 - primary visual cortex; 18 - associative visual cortex; Amyg - amygdala; CAI - cornu ammonis 1; Cg - cingulate cortex; EC - entorhinal cortex; Prec - precuneus

1.1.3 AD diagnostics

To date, the only certain way to truly diagnose AD has been a postmortem brain autopsy. During the life of the patient with dementia only some memory tests approximately determining the stage of dementia can be done. The tests assess the thinking ability and memory performance; according to the reached score, the stage of dementia can be determined (Alzheimer's, 2014; Sperling et al., 2011). With technology development, more methods start to be used for AD diagnosis, such as magnetic resonance imaging (MRI) or positron emission tomography, which monitor the brain changes, such as widening of the brain ventricles, and lesions in specific brain areas connected to the memory (Fan et al., 2008).

Large effort is invested into finding biomarker that would unequivocally diagnose the preclinical stage of AD, because the pathology develops for a long time, maybe decades, before the dementia emerges (Sperling et al., 2011). In cerebrospinal fluid (CSF), the concentration of amyloid-beta peptide (Aβ) 1-42 is increasing long before the memory impairment starts to manifest. Further, during AD, the CSF Aβ concentration starts to decrease, probably due to storage of amyloid peptide 1-42 in the form of non-soluble amyloid senile plaques (Hampel et al., 2014; Shaw et al., 2009). On the contrary, CSF concentration of hyper-phosphorylated Tau protein, another AD hallmark, starts to increase later during AD development; the increase is caused by release of Tau from damaged neurons (Andersson et al., 2008; Hampel et al., 2014; Shaw et al., 2009).

1.1.4 Current AD treatment

In spite of immense research of AD, the exact mechanism of the development of the disease remains unknown. Furthermore, there is no sufficient treatment of AD; only drugs slowing down the AD progression are available. The first group of drugs used at mild to moderate AD are inhibitors of acetylcholinesterase, such as galantimide, rivastigmine, or donezepil, for cognitive improvement. In later stages, antagonists of N-methyl-D-aspartate receptors are prescribed, such as memantin, which reduce the pathologically increased level of glutamate (State Institute for Drug Control, 2012).

1.1.5 Hallmarks of AD

Histopathologically, AD is characterized by two hallmarks: first, extracellular senile plaques, which are formed by Aβ, and second, intracellular NFT, formed by hyper-phosphorylated Tau protein (Tau). As shown in Fig. 4, amyloid plaques are obvious in pre-clinical stage of AD, and precede manifestation of dementia, while NFT formation increases later during the AD progression.

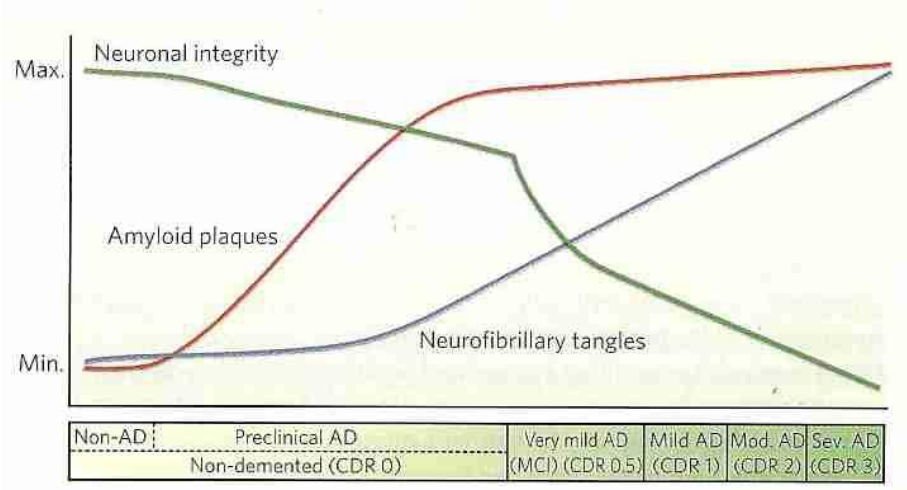

Fig. 4 Development of pathological changes during AD (www.benbest.com)

1.1.5.1 Senile plaques

Extracellular senile plaques are formed by aggregated Aβ peptides, which differ in length and contain 42– 43 amino acids. Aβ originates from amyloid precursor protein (APP). APP is a transmembrane protein; by different mRNA transcription three isoforms containing 770, 751 and 695 amino acids are formed. APP is not only present in the central nervous system (CNS), but also in the periphery. Its main function is not properly known, but in CNS it has a positive effect on synaptic formation and plasticity, neural activity, and memory (Priller et al., 2006; Turner et al., 2003). Physiologically, APP is processed in non-amyloidogenic pathway by α-secretase. Under pathophysiological condition, APP starts to be processed in amyloidogenic pathway, where it is cleaved by β- and γ-secretases, which results in formation of 42-43 long amino acid Aβ chains forming toxic oligomers. They polymerize into fibrils and are finally stored as senile plaques, as shown in Fig. 5. Moreover the plaques are responsible for mitochondrial oxidative damage, production of free radicals, and inflammatory processes (Tabaton et al., 2010).

γ-secretase is a large molecular membrane complex which consists of presenilins (PS), nicastrin, anterior pharynx defective homolog 1, and presenilin enhancer 2. Mutations in this complex are known to cause the early-onset familial form of AD. Enormous effort was made to find γ-secretase inhibitors to cure AD, but because of its important function in the Notch pathway, necessary for neuronal development, the inhibitors had a deleterious effect (Krishnaswamy et al., 2009).

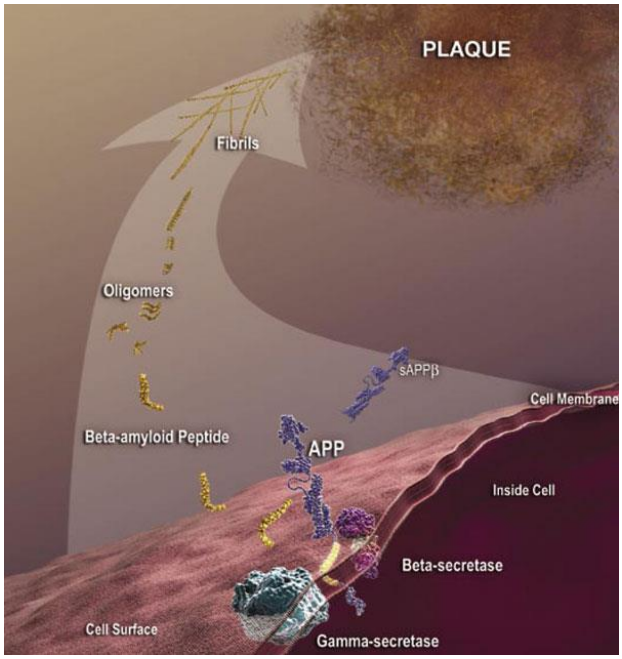

Fig. 5 Amyloid plaque formation (www.nia.nih.gov)

1.1.5.2 Neurofibrillary tangles

NFT are intracellular aggregates of Tau protein.

1.1.5.2.1 Tau functions

Together with MAP1, 2 and 4, Tau belongs to the family of microtubule-associated proteins (MAP). It promotes the tubulin assembly into microfilaments, helps to stabilize the microtubules and thus to stabilize the axons of neurons (Weingarten et al., 1975). Due to its function, Tau protein is mainly expressed in CNS, but is also found in peripheral tissues such as muscles, heart, or kidney. The human Tau protein gene is located at chromosome 17q21. The primary transcript of this gene contains 16 exons. Depending on alternative splicing of exons 2, 3 and 10 of the primary transcript, six different Tau protein isoforms are found in the brain (Goedert et al., 1989), as shown in Fig. 6. Similar 18-amino acid peptides called repeats, coded by exon 9, 10, 11, or 12,

are located at the C-terminal part of the Tau protein and serve as microtubule-binding domains. Tau isoforms without exon 10 are called Tau3R, including exon 10 Tau4R. In human brain, there is equal representation of 4R and 3R isoforms, but in adult rodent brain, mainly 4R isoforms are present (Buee et al., 2000; Lee and Leugers, 2012).

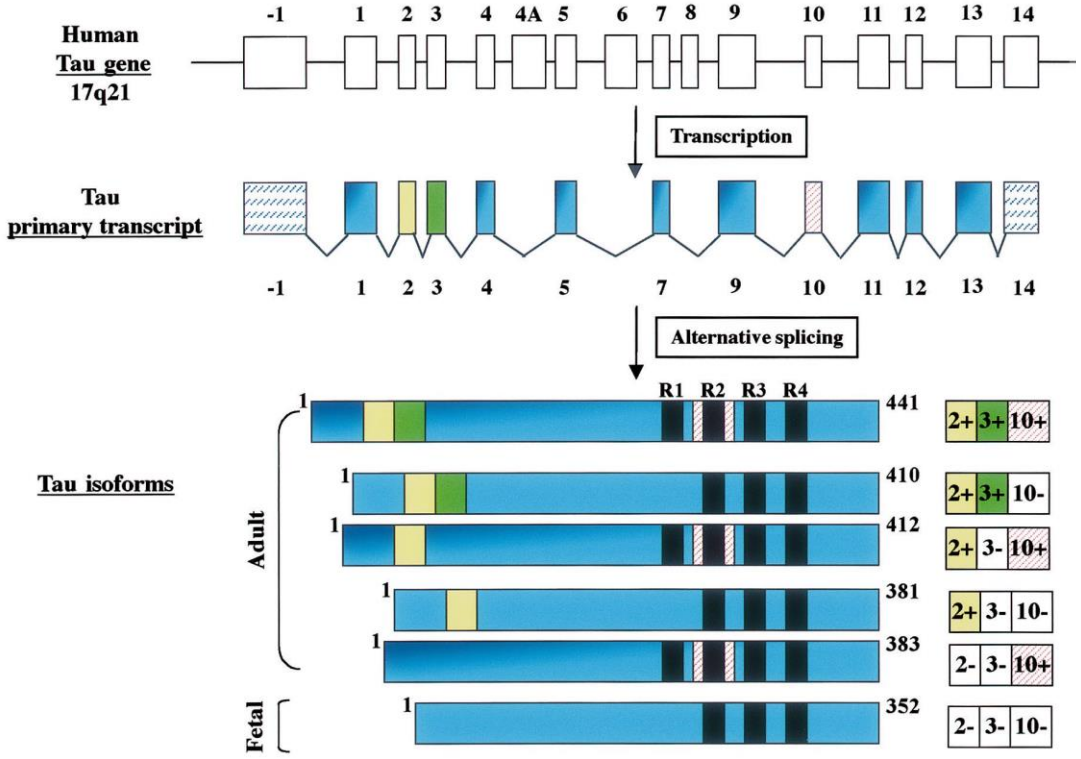

Fig. 6 Human Tau gene, primary transcript, and Tau protein isoforms in the brain (Buee et al., 2000)

1.1.5.2.2 Post-translational modifications

The Tau protein can undergo several post-translational modifications, such as phosphorylation, O-GlcNAcylation, or glycation, which are important for its biological function.

Phosphorylation

Tau contains 80 possible phosphorylation sites, which are mainly serines and threonines. Phosphorylation is under the control of many protein kinases and protein phosphatases which can phosphorylate and dephosphorylate the Tau protein, respectively, either directly or indirectly. Phosphorylation is crucial for the Tau function, as shown in Fig. 7; aberrant Tau phosphorylation negatively influences its physiological function in microtubule assembly and stabilization (Lindwall and Cole,

1984), and moreover, it is responsible for Tau aggregation into paired helical filaments, which are the hallmark of AD (Grundke-Iqbal et al., 1986a; Grundke-Iqbal et al., 1986b).

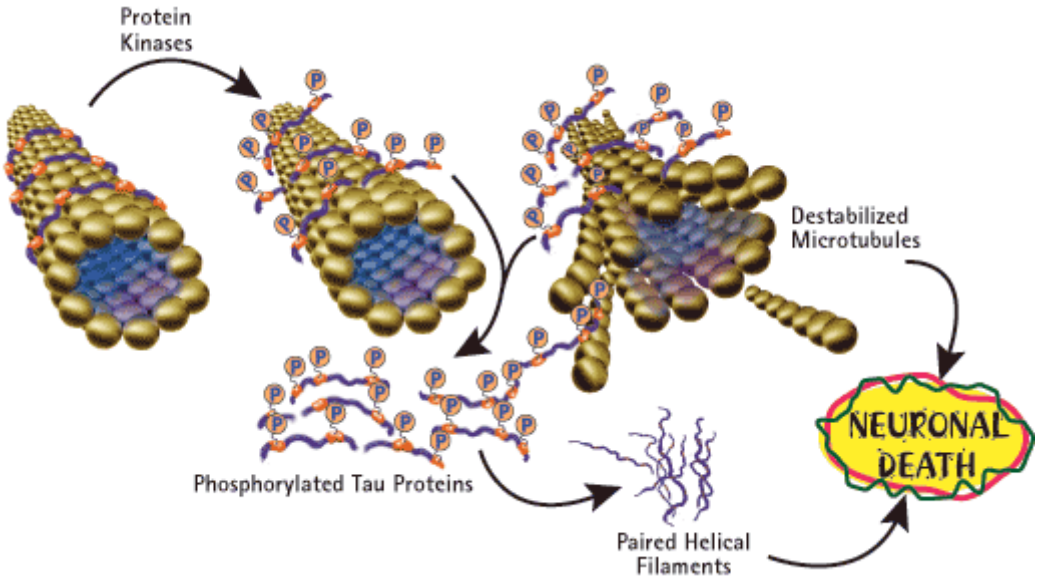

Fig. 7 Process leading to formation of neurofibrillary tangles (http://www.nottingham.ac.uk/)

Physiologically, Tau contains about 2-3 moles of phosphate/mole of protein, whereas pathophysiologicaly, 9-10 moles of phosphate/mole of protein are found in the AD brain (Kopke et al., 1993). The most important kinases implicated in Tau hyper-phosphorylation are glycogen-synthase kinase-3beta (GSK-3β) (Cho and Johnson, 2004; Takashima, 2006), c-Jun N-terminal kinase (JNK) (Atzori et al., 2001), cyclin-dependent kinase 5 (cdk5) (Alvarez et al., 2001; Jicha et al., 1999), mitogen-activated protein kinase/extracellular regulatory kinase (MAPK/ERK) (Ekinci and Shea, 1999), or protein kinase A (PKA) (Lee and Leugers, 2012). Table 1 shows the phosphorylation sites at Tau protein for the kinases.

Each of abnormal Tau phosphorylations results in different disturbances in the Tau function. For example, phosphorylation at epitope Thr231 and Ser262 reduces the ability to bind to microtubules, phosphorylation at Ser396 and Ser404 turns Tau to be more fibrillogenic, and phosphorylation of Ser422 results in increased aggregation of the Tau protein (Alonso et al., 2010; Johnson and Stoothoff, 2004).

The leading role in Tau dephosphorylation is played by protein phosphatase 2A (PP2A), which comprises more than 70 % of the brain phosphatase activity, the others

are protein phosphatase 1 and 5, phosphatase and tensin homolog etc. (Martin et al., 2013).

Table 1 Tau protein epitopes phosphorylated in AD pathology and responsible kinases (Lee and Leugers, 2012)

Phosphorylated epitopes	Tau protein kinase				
adult Tau	**cdk5**	**GSK3β**	**JNK**	**MAPK**	**PKA**
Thr181			●	●	
Ser199		●		●	
Ser202	●		●	●	
Thr205	●		●	●	●
Ser214	●	●			●
Thr217		●	●	●	
Thr231	●	●	●	●	
Ser396	●	●	●	●	
Ser404	●	●	●	●	

O-GlcNAcylation

It was discovered that brain glucose metabolism, which is essential for normal brain function, is impaired in AD and can lead to decreased O-GlcNAcylation of Tau protein. In brains of patients with type 2 diabetes mellitus (T2DM) and AD, decreased numbers of GLUT 1 and GLUT 3 were observed. Consequently, the decreased brain intracellular glucose level caused attenuation of hexosamine biosynthetic pathway, which resulted in decreased O-GlcNAcylation of the Tau protein. Decreased O-GlcNAcylation positively correlated with increased hyperphosphorylation of the Tau protein at epitopes implicated in AD development (Gong et al., 2006; Liu et al., 2009a; Liu et al., 2009b).

1.1.6 Risk factors of AD development

1.1.6.1 Ageing

The most important risk factor of AD is age; due to the increasing age of the population, about 100 million people are estimated to be suffering from AD in 2050. The incidence of AD is about 3 % in persons older than 65, 19 % in persons older than 75 and 47 % in persons older than 85, but it is not the normal part of ageing (Alzheimer's, 2014). The memory impairment due to ageing is caused by brain shrinkage and loss of synaptic plasticity, mainly in the hippocampus, and the shrinkage

is more pronounced in patients with AD. The regular shrinkage is about 0.5 % of brain weight per year, as it was discovered by the MRI method, but in AD patients the brain can be reduced by about 200 – 400 g of total brain weight, which is about 30% reduction (Fox et al., 1996; Chan et al., 2001).

1.1.6.2 Obesity

Obesity, especially abdominal obesity, is related to a variety of neurodegenerative conditions as well as altered brain morphology and cognitive ability (Lee, 2011). In fact, strong evidence suggests that mid-life obesity is a risk factor specifically for later-life development of AD-related dementia (Hassing et al., 2009; Xu et al., 2011). It was demonstrated that the prevalence of AD is greater in countries with higher intake of high fat and/or calorie diets than in those where diets low in fat are consumed (Panza et al., 2004). It was shown that high-fat diet (HFD) modulated changes in hippocampal function via glucotoxicity or disrupted insulin signaling, suggesting a potential connection between obesity and AD (Cai et al., 2012). Several lines of evidence show that a common feature in the pathophysiology of obesity is low-grade inflammation, as it was demonstrated by an increase in pro-inflammatory cytokines such as interleukin 6 (IL-6) and tumor necrosis factor α (TNF-α) (Burdge and Calder, 2005; Greenberg and Obin, 2006). Furthermore, obesity is characterized by leptin dysregulation leading to leptin resistance, which was recently linked to AD development (Bonda et al., 2014). Leptin is produced by adipose tissue, directly interacts with the hippocampus, and is important for synaptic plasticity, neurogenesis and memory consolidation. AD patients, compared to their body mass index-matched controls, were found to have a higher level of leptin in cerebrospinal fluid (Arnoldussen et al., 2014).

1.1.6.3 Type 2 diabetes mellitus

Recently, epidemiological studies have revealed that there is higher incidence of AD in patients with T2DM (Leibson et al., 1997; Schrijvers et al., 2010). T2DM is a serious metabolic and endocrine disorder characterized by resistance to the effect of insulin in the periphery, finally leading to an increased glucose level in the blood. One of the major risk factor for T2DM development is obesity which contributes to the development of insulin resistance through several mechanisms, such as increased plasma concentration of free fatty acids leading to impaired β-cell function, increased

levels of pro-inflammatory cytokines such as TNF–α, or IL-6, and disturbances in hormone levels (increased levels of glucagon and leptin, decreased level of adiponectin) (Kahn et al., 2006; Tahrani et al., 2011). Moreover, it was discovered that T2DM and AD have several common features, which are impaired glucose metabolism, insulin resistance, higher level of cholesterol, increased inflammation and oxidative stress, Aβ aggregation, increased Tau phosphorylation, activation of GSK-3β, and above all, both diseases are age-dependent (de la Monte and Wands, 2008; Doble and Woodgett, 2003; Gotz et al., 2009; Li and Holscher, 2007; Takeda et al., 2010). Therefore, Suzanne de la Monte proposed a new term for AD: type 3 diabetes mellitus (Steen et al., 2005).

1.1.6.3.1 Type 3 diabetes mellitus

After the discovery of insulin receptors (IR) in the brain, mainly in the cortex and hippocampus (Havrankova et al., 1978a), and after the finding that insulin is present in the brain at a substantially higher concentration compared to the blood plasma (Havrankova et al., 1978b), many functions for insulin in the CNS were discovered. Insulin is almost exclusively produced in the pancreas by β-cells of the islets of Langerhans, and it crosses the blood-brain barrier (BBB) through saturable transporters. In the periphery, insulin is important for glucose uptake by skeletal muscles and adipose tissue. In the CNS, insulin is required for neuronal synaptic and dendritic plasticity, for learning, and memory formation (Banks et al., 2012; Zhao et al., 1999). It was discovered that ageing causes a significant decrease in the IR number, concentration of insulin itself, and thus leads to impaired insulin signaling and memory deficits in elderly people (Banks et al., 2012; Steculorum et al., 2014).

After insulin binding to the IR, autophosphorylation of the tyrosine kinase domain of IR causes phosphorylation of insulin receptor substrate 1 (IRS-1) which further phosphorylates the regulatory subunit of phosphoinositide 3 kinase (PI3K) p85. This leads to phosphorylation of 3-phosphoinositide-dependent protein kinase 1 (PDK-1) at Ser241 and downstream activation of Akt. Akt is fully activated by phosphorylation at both Thr308 and Ser473. Activated Akt phosphorylates GSK-3β at Ser9, or GSK-3α at Ser21, which inhibits the kinase activity of GSK-3. As shown in Fig. 8, in case of central insulin resistance, activation of the insulin signaling cascade is impaired, which is manifested by decreased phosphorylation of the implicated kinases and finally by a decreased phosphorylation of GSK-3β on its inhibition site Ser9. This decreased

phosphorylation leads to GSK-3β activation, and GSK-3β is one of the most important kinases implicated in hyper-phosphorylation of Tau (Jolivalt et al., 2008; Liu et al., 2011).

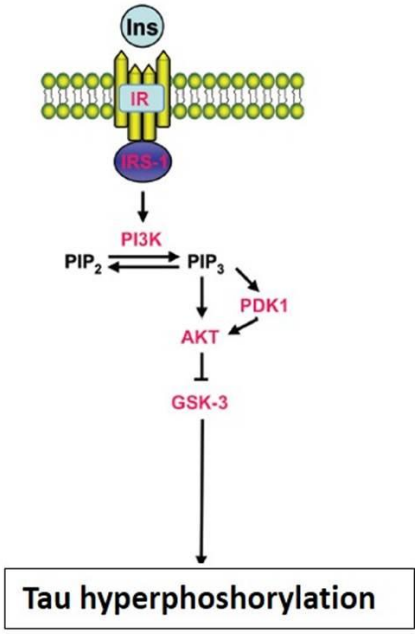

Fig. 8 Insulin signaling pathway and subsequent Tau hyper-phosphorylation (Liu et al., 2011)

1.2 Animal models of AD, obesity, and T2DM

The animal models are an important and fundamental part of medical research. Several rodent models were designed to investigate the pathological processes leading to development of AD, obesity, or T2DM. In recent years, many models combining all of the above-mentioned diseases were used to examine the effect of obesity and related T2DM on the development of neurological disorders, such as dementia or AD.

1.2.1 Models of AD

1.2.1.1 APP transgenic mouse model

Mutation in APP, leading to increased Aβ production, was observed in early onset familial cases of AD in several families in Sweden, hence this mutation is called Swedish mutation (SWE) (Lannfelt et al., 1994). To examine the impact of this mutation on AD development, transgenic mice with mutation in APP (also called Tg2576 mice) were created. They are characterized by early-onset Aβ deposits, reduced

synaptic plasticity and impaired learning abilities (Chapman et al., 1999; Irizarry et al., 1997).

1.2.1.2 APP/PS1 transgenic mouse model

This transgenic mouse model combined the Swedish mutation of APP and mutation in presenilin 1 ($PS1_{M146V}$). Mutation in PS1 was discovered to enhance production of the Aβ fragments of 42-43 amino acids that are supposed to be more fibrillogenic (Borchelt, 1998). APP/PS1 mice are characterized by a more pronounced increase in Aβ deposits in the hippocampus and cortex, compared to their littermates without mutations, impaired score in behavioral experiments and increased brain oxidative stress markers (Arendash et al., 2001; Holcomb et al., 1998; Mohmmad Abdul et al., 2004).

1.2.1.3 3xTgAD mouse model

This transgenic mouse model combines both pathological hallmarks of AD. Mice have mutations in APP_{SWE} and $PS1_{M146V}$, which causes formation of Aβ plaques, and mutation in Tau_{P301L}, which leads to formation of NFT (Ramsden et al., 2005). Amyloid pathogenesis is observed prior to Tau pathology (Oddo et al., 2003a). Mice are characterized by impaired memory, synaptic dysfunction, presence of Aβ, and hyper-phosphorylation of Tau protein (Oddo et al., 2003b).

1.2.1.4 Thy-Tau22 mouse model

To examine the role of Tau pathology in AD development, the Thy-Tau22 mouse model was created. It is a model of AD-like Tau pathology, with overexpression of human 4R-Tau protein carrying mutations G272V and P301S found in frontotemporal dementia with parkinsonism-17 tauopathies. With age, mice develop memory deficits, and Tau hyper-phosphorylation at different epitopes, such as Ser202, Thr205, Thr212, Ser214, Thr231, Ser396, mainly in the CA1 region of the hippocampus. With increasing age, hyper-phosphorylated Tau forms non-soluble aggregates which are stored as NFT in neurons (Schindowski et al., 2006; Van der Jeugd et al., 2011). Hyper-phosphorylated Tau correlated to impaired spatial memory proven in several memory tests, such as Morris water maze, or Y-maze (Van der Jeugd et al., 2013).

1.2.2 Models of T2DM

In the recent years, models of T2DM became important tools for AD research due to the discovery that insulin resistance associated with T2DM is a risk factor for the AD development.

1.2.2.1 db/db mice

The db/db mouse model is a model of obesity and T2DM. Obesity is caused by a spontaneous mutation in the diabetic gene (db) of leptin receptor, which causes impaired leptin signaling (Chen et al., 1996). These mice are characterized by early-onset hyperinsulinemia and hyperglycemia, and diabetic dyslipidemia (Kobayashi et al., 2000).

In the brain cortex of db/db mice, age-dependent hyper-phosphorylation at Ser396, Thr231 and Ser199/202 of Tau protein was observed (Kim et al., 2009). Furthermore, age-dependent reduction of brain weight was observed, with significant cortical atrophy that can be connected to impaired spatial memory observed in the db/db mice (Ramos-Rodriguez et al., 2013). The db/db mice showed reduced hippocampal synaptic plasticity and neurogenesis, and consequently impaired cognition (Stranahan et al., 2008).

1.2.2.2 Zucker fatty (fa/fa) rats

Zucker fatty rats, shown in Fig. 9, are the model of obesity, pre-diabetes, and hypertension. They obtained their name after the scientists Lois M. Zucker and Theodore F. Zucker who using fa/fa rats examined the genetics of obesity. Similarly as in the db/db mice, obesity is caused by spontaneous mutation of the leptin receptor on the "fatty" (fa) gene leading to early-onset obesity development (Kurtz et al., 1989; Zucker and Antoniades, 1972). Zucker "fatty" rats develop similarly as their lean littermates until the 4^{th} week of age; then a rapid accumulation of adipose tissue, mainly abdominal, is observed. The increase in adipose tissue is more pronounced due to hyperphagia and decreased energy expenditure (Durham and Truett, 2006). Fa/fa rats are characterized by hyperleptinemia, and hyperinsulinemia, but they are normoglycemic (Zucker and Antoniades, 1972). In this rat model, cognitive impairment was observed in the go/no-go delayed alteration task with a VIDA test (variable interval

between trials), which is used for examination of the hippocampus dysfunction (Winocur et al., 2005).

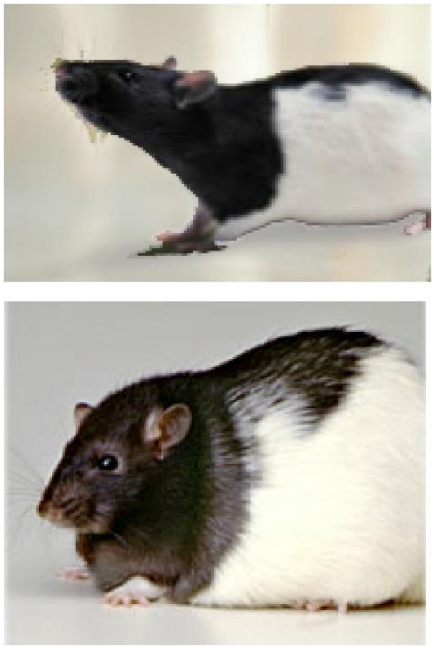

Fig. 9 Zucker fa/fa rat (lower panel) and its lean control (upper panel) (http://www.atkinsdietbulletinboard.com/)

1.2.2.3 Zucker diabetic fatty rats

Zucker diabetic fatty (ZDF) rats were selected from fa/fa rats by crossbreading hyperglycemic individuals. Similarly as fa/fa rats, ZDF rats are characterized by obesity, insulin resistance, increased levels of triglycerides and cholesterol, and moreover by severe hyperglycemia (Leonard et al., 2005; Peterson et al., 1990). In the frontal brain of 17-week-old ZDF rats, an increased amount of aggregated hyper-phosphorylated Tau protein was detected (Talaei et al., 2014).

1.2.2.4 MSG obese mice

The MSG obese mouse model (Fig. 10A) serves as a model of obesity and pre-diabetes. Obesity is caused by subcutaneous (SC) administration of monosodium glutamate (MSG) to newborn mice, when MSG is able to cross BBB and cause specific lesions in *nucleus arcuatus* (Arc) (Fig. 10B), the hypothalamic center implicated in food intake regulation. In MSG mice, compared to their controls, the total number of neurons in Arc is reduced by about 75 %; however, the number of neurons does not differ significantly in other brain regions (Elefteriou et al., 2003; Olney, 1969).

MSG mice are characterized by growth hormone insufficiency, pituitary and optic nerve atrophy, and infertility, hyperleptinemia and insulin resistance, which is more pronounced in males compared to females (Maletínská et al., 2006; Olney, 1969). The imbalance between food intake and energy expenditure in MSG obese mice leads to hypophagia and an increased storage of adipose tissue. Compared to their controls, MSG obese mice accumulate even 8 times higher weight of white adipose tissue (WAT). Excessive adipose tissue storage can also be caused by the growth hormone insufficiency, because of the lipolytic activity of the growth hormone (Fain et al., 1965; Matysková et al., 2008).

A/ **B/**

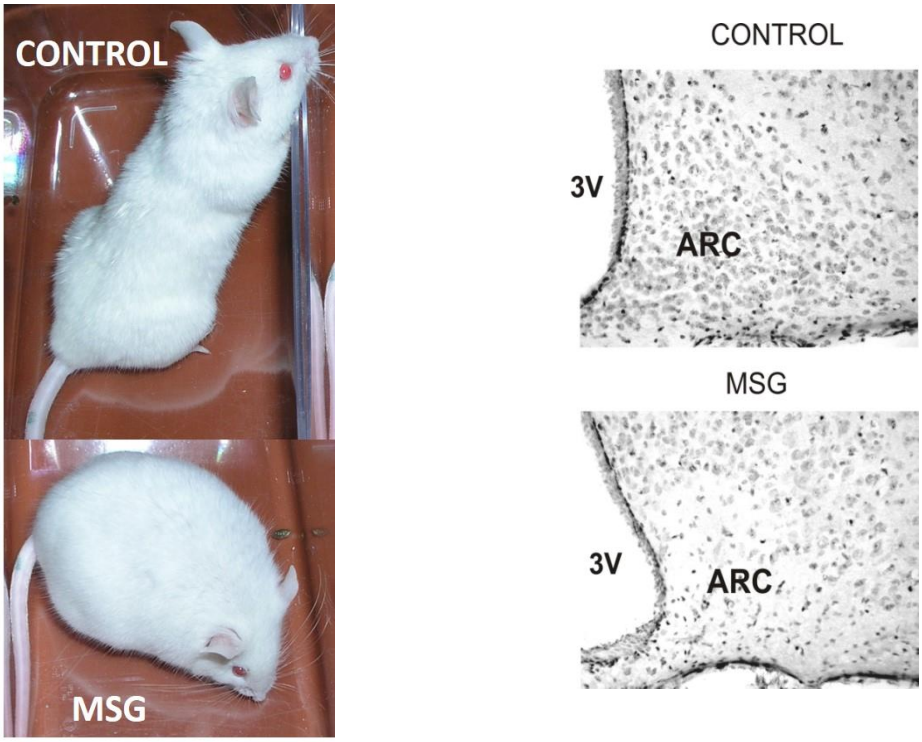

Fig. 10 A/ MSG obese mouse (lower panel) and its control (upper panel) B/ Disappearance of neurons in nucleus arcuatus in MSG mice (Zelezná et al., 2009)

1.2.2.5 Model of diet-induced obesity

Rodents with diet-induced obesity (DIO) represent a model of late onset obesity caused by consumption of food rich in the fat content; this obesity model is similar to obesity spread in developed countries connected with over-consumption of HFD and lack of physical activity. Animals are fed with HFD since young age. Many types of HFD are employed, differing in the fat origin and content. Already after two weeks of

feeding HFD, an increase in WAT is observed, which consequently leads to hyperleptinemia and leptin resistance, and finally also to insulin resistance and hyperglycemia (Buettner et al., 2007; Youngren et al., 2001).

Furthermore, in several mouse or rat models of AD and/or T2DM, such as Thy-Tau22 mice (Leboucher et al., 2013), 3xTg AD mice (Knight et al., 2014), or rats on HFD (Winocur and Greenwood, 1999), it was discovered that HFD feeding for several weeks leads to memory impairment in the spatial memory test, and to increased phosphorylation of the Tau protein, even though the exact mechanisms responsible for these phenomena are not fully understood. There is a possible implication of neuronal insulin resistance, and neuroinflammation, but to date the evidence has been quite controversial (Knight et al., 2014; Leboucher et al., 2013; Pratchayasakul et al., 2011; Takalo et al., 2014; Winocur and Greenwood, 1999).

1.3 Neuroprotective effect of insulin-sensitizing/anorexigenic compounds

At present, no effective treatment for AD and other progressive neurodegenerative disorders is available. The current drug treatments are not able to repair or prevent further degeneration. Recently, because of the newly discovered link between T2DM and AD, a possible new strategy for prevention/treatment of neurodegenerative diseases has emerged.

The IR are present in the brain regions connected with memory formation and learning, namely in the cortex and hippocampus (Wickelgren, 1998). Activation of IR was observed after spatial memory testing in the rat hippocampal CA1 region suggesting the implication of insulin in memory processing (Zhao et al., 1999). Memory impairment due to insulin resistance or disruption in the insulin signaling pathway was proved in different animal models. Moreover, it was discovered that central insulin administration, intranasal or intracerebroventricular (ICV), improved the learning ability (Banks et al., 2012). Unfortunately, because of the high incidence of insulin resistance in AD patients, it is not possible to use insulin for AD treatment. However, it is hypothesized that agents increasing insulin sensitivity could ameliorate insulin function in CNS, and thus could be used for the AD treatment.

1.3.1 Leptin

Leptin, hormone produced by adipose tissue, is responsible for energy homeostasis maintenance and food intake regulation. Its level correlates with the amount of WAT. Leptin influences the function of pancreatic β-cells producing insulin, as well as the expression of insulin itself. In obese individuals, hyperinsulinemia and diabetes, both risk factors for AD development, were connected with impaired leptin signaling (Seufert, 2004). In patients with AD, a decreased plasma level of leptin was observed; conversely, its increased concentration was found in CSF. The expression of the leptin receptor, which is also expressed in the hippocampus (Elmquist et al., 1998), was reduced in AD patients (Bonda et al., 2014).

In vitro and *in vivo* studies revealed the effect of leptin on lowering Aβ production (Greco et al., 2009b; Greco et al., 2010), and leptin treatment of CRND8 mice, AD transgenic mouse with APP_{SWE} mutation, also enhanced the memory (Greco et al., 2010). *In vitro* studies proved the leptin effect on lowering phosphorylation of Tau protein (Greco et al., 2009a; Greco et al., 2009b), and thus leptin was proposed as a potential AD therapy (Tezapsidis et al., 2009).

1.3.2 Metformin

Metformin is the most-used oral anti-T2DM drug belonging to the class of biguanides. It reduces glucose production in the liver and moreover, has an insulin-sensitizing effect in other peripheral tissues. Concerning AD, ambiguous effects were obtained when examining its function in Aβ production. First, it was discovered that metformin increases Aβ production in primary neuronal cultures or neuroblastoma cells producing APP through increased activation of β-secretase (Chen et al., 2009). However, another study proved decreased β-secretase activation and protein levels in *in vitro* and *in vivo* experiments, when the metformin treatment was performed in the presence of insulin (Hettich et al., 2014). Spatial memory of adult mice was improved after metformin treatment in mice owing to increased neurogenesis (Wang et al., 2012). Regarding the effect of metformin on Tau hyper-phosphorylation, attenuated phosphorylation of Tau was observed at different epitopes, namely Ser202, 262 and 356, associated with dephosphorylation by PP2A, whose activity is enhanced by metformin (Kickstein et al., 2010). Another possible mechanism for the beneficial effect

of metformin on Tau pathology was demonstrated by metformin-induced insulin-sensitizing effect on neuronal cells; the resulting activation of insulin signaling cascade led to attenuated phosphorylation of Tau at Ser396 (Gupta et al., 2011). A similar effect of metformin treatment was observed in hippocampi of db/db mice. Compared to control mice, db/db mice at the age of 24 weeks exhibited impaired spatial memory, decreased level of synaptophysin, protein implicated in synaptic transmission also used for quantification of synapses, increased Tau phosphorylation at Ser396 and Thr231, as well as increased activity of JNK. 18-week-long intraperitoneal (IP) metformin administration resulted in an increased synaptophysin level, decreased JNK activity, and attenuated Tau phosphorylation at Ser396 and Thr231 in hippocampi (Li et al., 2012a).

1.3.3 Incretins

Two most important human naturally occurring incretins are glucose-dependent insulinotropic polypeptide (GIP) and glucagon-like peptide 1 (GLP – 1). Both hormones are secreted by enteroendocrine cells when the glucose concentration is increased in the intestine; GIP is secreted by K cells, which are mainly present in the upper small intestine, and GLP-1 by L cells, which are mainly found in the lower small intestine. GIP and GLP-1 receptors belong to the family of G-protein coupled receptors. They are present in the pancreas in α- and β-cells; a large number was also found throughout the brain, in the region important for memory formation, such as the hippocampus. GIP and GLP-1 secretion from enteroendocrine cells trigger the insulin secretion from β-cells of the pancreas. They were discovered when it was observed that insulin secretion is higher after oral glucose gavage than intravenous administration (Perley and Kipnis, 1967) where insulin secretion depends only on blood glucose (Drucker, 2006; Holscher, 2014b; Vilsboll and Holst, 2004).

Beside stimulation of insulin secretion, both GIP and GLP-1 inhibit glucagon secretion, which also supports lowering of blood glucose levels (Vilsboll and Holst, 2004). Recently, neuroprotective properties of GIP and GLP-1 were described as reviewed in (Holscher and Li, 2010).

The problem with naturally occurring incretins is their low stability due to the cleavage of their N-terminal sequence by dipeptidyl peptidase IV (DPP IV). Therefore, their analogs with prolonged stability have been invented.

1.3.3.1 GIP analogs

There are several potent, more stable analogs of GIP, with modification at the first three amino acids at the N-terminal part which are cleaved off by DPP IV (Gault et al., 2003). GIP contains 42 amino acids but the shorter fragments, truncated at the C-terminus of the peptide, have biological activity similar to GIP (Hinke et al., 2001).

GIP analogs with L-Ala^2 changed for D-Ala decreased glucose levels and protected pancreatic β-cells from apoptosis (Widenmaier et al., 2010). After acute or chronic administration, these analogs showed a beneficial effect on hippocampal synaptic plasticity in C57Bl mice (Faivre et al., 2012), improved impaired neuronal synaptic plasticity and long term potentiation in mice on HFD (Porter et al., 2011), and also a reduced blood glucose level. Finally, in APP/PS1 mice spatial memory and synaptic plasticity were also improved after 30-day-long administration, and amyloid plaques and neuroinflammation were reduced (Faivre and Holscher, 2013b). Thus, the GIP analogs have a potential to be used for treatment of neurodegenerative diseases.

1.3.3.2 Analogs of GLP-1

Except for the beneficial effect of GLP-1 on insulin secretion, and blood glucose lowering, other positive effects were observed after treatment with more stable analogs of GLP-1 that resisted the cleavage by DPP IV, such as exenatide or liraglutide.

It was discovered that GLP-1 receptors are present in the brain centers responsible for food intake regulation, and that GLP-1-agonist treatment led to decreased food intake and body weight (Lockie, 2013; van Bloemendaal et al., 2014). GLP-1 receptors are also expressed in the brain centers important for memory formation and learning, such as the hippocampus. In experiments with GLP-1 knockout mice, reduced synaptic plasticity and memory formation was observed (Abbas et al., 2009). On the contrary, over-expression of GLP-1 receptor in hippocampus enhanced the memory and learning (During et al., 2003). Long-lasting stable GLP-1 receptor agonists used for T2DM treatment such as lixisenatid (Cai et al., 2014; McClean and Holscher, 2014b), (Val^8)GLP-1 (Gengler et al., 2012; McGovern et al., 2012) which can also be palmitoylated (Lennox et al., 2013), exenatide (Bomba et al., 2013; Bomfim et al., 2012; Chen et al., 2012), or liraglutide (Han et al., 2013; Hansen et al., 2015; Long-Smith et al., 2013; McClean et al., 2011; McClean and Holscher, 2014a; Parthsarathy and Holscher, 2013; Porter et al., 2010; Porter et al., 2013; Yang et al., 2013) were

shown to display neuroprotective properties in *in vitro* or *in vivo* experiments, such as beneficial effects on synaptic plasticity, spatial memory, and Aβ plaques reduction. The two latter analogs, exenatide and liraglutide, are now in clinical trials as potential AD treatments (Holscher, 2014a).

1.3.3.2.1 Exenatide

Exenatide is a synthetic analog of exendin 4, GLP-1 agonist, which was discovered in the saliva of lizard *Gila monster* (Drucker and Nauck, 2006). It is a frequently prescribed anti-T2DM drug that enhances pancreatic β-cell proliferation through PI3K/Akt signaling activation (Wang et al., 2015), and has potential neuroprotective properties (Bomba et al., 2013; Bomfim et al., 2012; Chen et al., 2012).

The neuroprotective action of exenatide was observed due to improvement of the impaired insulin signaling cascade. A study on APP/PS1 mice showed that exenatide is able to reduce IRS-1 phosphorylation on serine epitopes, which is the sign of insulin signaling impairment that resulted from Aβ-induced activation of JNK, specific for Ser and Thr phosphorylation (Bomfim et al., 2012). In another study, exenatide increased activation of the insulin signaling pathway that resulted in increased phosphorylation at inhibitory Ser9 of GSK-3β, the main Tau protein kinase, and thus decreased phosphorylation of the Tau protein at different epitopes. Moreover, the exenatide treatment improved the impaired spatial memory in Morris water maze test (Chen et al., 2012). No effect on spatial memory performance was observed after exenatide treatment in the 3xTgAD mouse model, which combines Aβ and Tau pathology (Bomba et al., 2013). On the other hand, streptozotocin-induced increa of Aβ and APP in the hippocampus in the 3xTgAD mouse model was prevented by 16-week-long exenatide treatment (Li et al., 2010).

1.3.3.2.2 Liraglutide

Liraglutide, shown in Fig. 11, is a stable, long-lasting GLP-1 receptor agonist and the most used anti-T2DM drug, which is now also approved by U.S. Food and Drug Administration as an anti-obesity drug. Liraglutide is only slightly modified GLP-1,with Lys^{34} changed for Arg, and palmitic acid bound through glutamic acid at Lys^{16}. Lipidization enables liraglutide non-covalent binding to serum albumin, resulting in better stability and availability in the blood plasma (Drucker and Nauck, 2006).

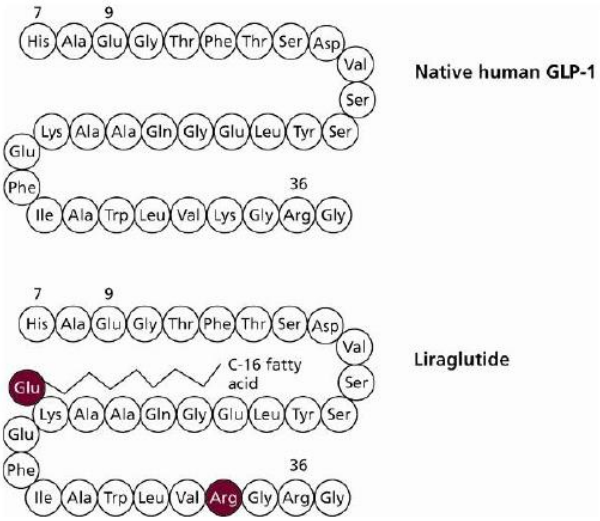

Fig. 11 Structure of naturally occurring human GLP-1 (upper panel)and structure of liraglutide, modified analog of GLP-1 (lower panel) (Sjöholm, 2010)

Neuroprotective properties of liraglutide were examined in various rodent models. Chronic liraglutide administration to APP/PS1 mice improved spatial memory, increased hippocampal long-term potentiation, levels of synaptophysin and neurogenesis marker doublecortin, and decreased the level of both soluble Aβ and β-amyloid plaques (McClean et al., 2011). Similar neuroprotective effects on reduction of Aβ and increased synaptic plasticity were observed at different ages in APP/PS1 mice, where the AD pathology is age-dependently increased (McClean and Holscher, 2014a; Parthsarathy and Holscher, 2013). Enhanced spatial memory and an augmented number of neurons in CA1 of the hippocampus after liraglutide treatment was also observed in the SAMP8 mouse model (senescence-accelerated mouse prone 8), a mouse model of accelerated ageing (Hansen et al., 2015). Liraglutide treatment prevented the memory impairment caused by $A\beta_{25-35}$ intrahippocampal injection to rats (Han et al., 2013). Improved synaptic plasticity after 21-day-long liraglutide treatment in the hippocampus was observed in ob/ob mice, model of obesity and T2DM, where liraglutide also reduced the glucose level and improved insulin sensitivity (Porter et al., 2013). Similarly, not only metabolic parameters, such as body weight, insulin resistance, or glucose level, were improved after 28-day-long liraglutide administration in the DIO mouse model, but also enhanced learning ability and increased hippocampal long-term potentiation were detected (Porter et al., 2010).

Liraglutide was also qualified to improve central insulin resistance in APP/PS1 mice, which was manifested by increased phosphorylation of IRS-1 at Ser616 (Long-Smith et al., 2013). Furthermore, in rats with T2DM and on HFD, where attenuation of the insulin signaling cascade and hyper-phosphorylation of the Tau protein at different epitopes were observed, 4-week-long liraglutide treatment led to enhanced activation of kinases implicated in the insulin signaling cascade including increased phosphorylation of inhibitory Ser9 of GSK-3β, and finally decreased phosphorylation of the Tau protein at Ser199, 202 and 396 (Yang et al., 2013).

1.3.4 Gliptins

Gliptins are inhibitors of DPP-IV, the enzyme responsible for degradation of naturally occurring incretins. Many molecules of gliptins were prepared, some of them are now used as oral anti-T2DM drugs (Drucker and Nauck, 2006). In mouse models of streptozotocin-induced AD, where streptozotocin was administered intracerebrally, treatment with saxagliptin or vildagliptin improved spatial memory and learning, increased GLP-1 brain concentration, and also reduced the level of Aβ 42 and the level of both hyper-phosphorylated and total Tau protein (Kosaraju et al., 2013a; Kosaraju et al., 2013b). In APP/PS1 mice, a similar effect was observed using sitagliptin; the treatment resulted in reduced Aβ plaques and APP in the hippocampus and increased GLP-1 brain concentration (D'Amico et al., 2010). On the contrary, in OLETF (Otsuka Long-Evans Tokushima Fatty) obese, diabetic, and hyperglycemic rats, sitagliptin treatment augmented Tau hyper-phosphorylation at different epitopes and increased the kinase activity of GSK-3β (Kim et al., 2012).

1.3.5 Prolactin-releasing peptide

Prolactin-releasing peptide (PrRP) is an anorexigenic neuropeptide belonging to the family of RF amide peptides with C-terminal arginine and phenylalanine amide sequence. Naturally, two isoforms of PrRP from one prepropeptide are found in the organism: a peptide containing 31 amino acids (PrRP31) or a peptide containing 20 amino acids (PrRP20), as shown in Fig. 12. The first described PrRP effect was prolactin release from pituitary tumor cell-line RC-4B/C (Hinuma et al., 1998), which gave the name to the peptide, but this effect was soon questioned.

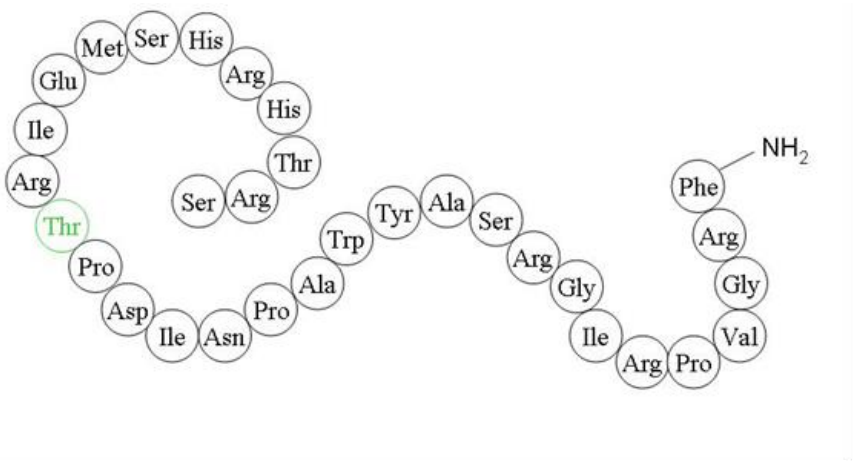

Fig. 12 Structure of human prolactin-releasing peptide

The structure of prolactin-releasing peptide containing 31 amino acids; the green Thr is the beginning of PrRP20.

PrRP is produced in neurons in many brain regions, such as *nucleus tractus solitarius* (NTS), ventrolateral reticular nucleus, and in hypothalamic paraventricular (PVN) and dorsomedial nuclei (Lee et al., 2000; Maruyama et al., 1999).The PrRP receptor, GPR10, which that belongs to the G-protein coupled receptor family, is extensively expressed in the whole brain; it can be found in anterior pituitary, amygdala, hypothalamus, brainstem, and medulla oblongata. In the periphery, GPR10 can be found in adrenal medulla, and its significantly increased expression was observed in human and rat pancreas (Fujiwara et al., 2005; Lee et al., 2000; Maruyama et al., 1999; Nieminen et al., 2000). The presence of PrRP in hypothalamic nuclei implicated in maintaining the energy balance suggested its role in food intake and weight regulation (Lawrence et al., 2000a). This function was supported by the finding that both PrRP KO mice (Mochiduki et al., 2010; Takayanagi et al., 2008), and GPR-10 KO mice (Bjursell et al., 2007; Gu et al., 2004) developed early-onset obesity. In rats, an anorexigenic effect was observed after ICV administration of PrRP31 (Lawrence et al., 2000b; Lawrence et al., 2004). Moreover, the weight loss was also accompanied by increased body temperature and oxygen consumption, which is an indirect evidence of increased energy expenditure. The increased mRNA expression of uncoupling protein 1 in brown adipose tissue also supports the increase of energy expenditure (Ellacott et al., 2003).

For its proper biological function, arginine in position 30 is required. Phenylalanine, or another aromatic amino acid with aromatic ring attached at least to

one CH2 group, in position 31, is important for GPR10 binding (Boyle et al., 2005). Modified analogs of naturally occurring neuropeptide PrRP20 maintained the same biological activity as PrRP31 in *in vitro* experiments (Langmead et al., 2000; Maixnerova et al., 2011). These analogs showed affinity to GPR10 comparable to PrRP31 or PrRP20 (Maletinska et al., 2011). After ICV administration to fasted mice , a significant decrease in food intake was observed (Maletinska et al., 2011).

It seems that PrRP could also act as an insulin sensitizing agent, but the proper mechanism must be elucidated.

2 AIMS OF THE THESIS

- **Characterization of Tau phosphorylation in the brains of obese pre-diabetic animal models**

Obesity and related T2DM, characterized by insulin resistance and high glucose levels, are considered as risk factors for AD development; in the brains of AD patients, the impaired insulin signaling cascade was observed, leading to increased phosphorylation of Tau protein, one of the hallmarks of AD. The first aim of the thesis was to examine the possible neuropathological changes in central insulin signaling cascade activation and phosphorylation of Tau protein caused by obesity and pre-diabetes, the state preceding T2DM in two rodent models of obesity – fa/fa rats and MSG mice.

- **Characterization of the new lipidized analogs of prolactin-releasing peptide in *in vitro* and *in vivo* experiments**

Anorexigenic neuropeptides are promising compounds in obesity treatment; however, their application is limited due to their low stability and inability to cross BBB and manifest their anorexigenic action when administered peripherally. In our laboratory at IOCB AS CR, new more stable lipidized analogs of anorexigenic neuropeptide PrRP were designed. The second aim of the thesis was to characterize lipidized PrRP regarding their affinity to PrRP receptor in *in vitro* binding experiments and acute anorexigenic effect when administered peripherally in *in vivo* experiments in mice.

- **Investigation of the effect of anorexigenic peptides on the development of Tau phosphorylation in hippocampi of obese MSG mice, and Thy-Tau22 mice with AD-like Tau pathology**

GLP-1 receptor agonists are frequently used anti-T2DM drugs and moreover, their neuroprotective properties were proven in several experiments. It was shown that in the CNS their effect is exclusively anorexigenic. The third aim of my thesis was to test the possible neuroprotective properties of stable anorexigenic analogs of PrRP and GLP-1 analog liraglutide after long-term intervention in MSG mice, model of obesity and pre-diabetes, and in Thy-Tau22 mice, model of AD-like Tau pathology.

3 MATERIALS & METHODS

3.1 Material

3.1.1 Chemicals

Complete Protease Inhibitor Cocktail	F. Hoffmann – La Roche Ltd, Basel, Switzerland
Luminata Clasico/Crescendo	Merck Millipore Headquarters, Billerica, MA, USA
$Na^{125}I$	Izotop, Budapest, Hungary
Precision Plus Protein Standard	Bio-Rad, Hercules, CA, USA
Triton X-100	Koch-Light Lab. Colnbrook, Berks, UK

All other commonly used chemicals were purchased from Sigma Aldrich (St. Louis, MO, USA) in p.a. quality.

3.1.2 Instruments

Bullet Blender® homogenizer	Next Advance Inc., Averill Park, NY, USA
ChemiDoc™	Bio-Rad, Hercules, CA, USA
CO_2 incubator MCO 18AIC	Sanyo, Osaka, Japan
Cryostat Microm HM520	Microm International, Walldorf, Germany
γ-counter Wizard 1470	PerkinElmer Life and Analytical Sciences, Waltham, MA, USA
ELISA reader Infinite F50	Tecan Group Ltd., Männedorf, Switzerland
Glucometer Glucocard	Arkray, Kyoto, Japan
Mini-PROTEAN 3	Bio-Rad, Hercules, CA, USA
PowerPac™ HC Power Supply	Bio-Rad, Hercules, CA, USA
XCell SureLock	Invitrogen, NY, USA

3.1.3 Kits

Insulin RIA kit	Linco Research, St. Charles, MI, USA
Leptin ELISA kit	Millipore, St. Charles, MI, USA
PrRP(1-31) EIA high-sensitivity kit	Peninsula Laboratories International, Inc. San Carlos, CA, USA

3.2 Animal models

All animal experiments performed in the Czech Republic followed the ethical guidelines for animal experiments and the Czech Republic Act No. 246/1992.

The experiments with fa/fa rats were performed in Poland (Jagellonian University in Krakow) in collaboration with the Institute of Experimental Endocrinology, Bratislava, Slovak Academy of Sciences, and followed the ethical standards of the Declaration of Helsinki. This study conformed to national and international guidelines and was approved by the authors' institutional review board.

3.2.1 Housing & measurement of metabolic parameters

3.2.1.1 fa/fa rats – genetic obesity model

The rats obtained at the age of 9 weeks from Harlan (Udine, Italy) were housed at Jagellonian University in Krakow, Poland, and had free access to standard diet and water.

For experiments, young (12 weeks old) and old (33 weeks old) obese male fa/fa rats and their age-matched lean controls, with dominant homozygotes Fa/Fa or heterozygotes Fa/fa, (n = 6 animals per group) were used. The overnight-fasted rats were sacrificed by decapitation. Blood glucose was measured at Synlab (Bratislava, Slovakia) using a multi-analyzer COBAS Integra 800 (Roche Diagnostics Ltd., Rotkreuz, Switzerland). Concentrations of serum leptin and insulin levels were determined using radioimmunoassay (RIA) kits (Millipore, USA) following the manufacturer's instructions. The quantitative insulin sensitivity check index (QUICKI) was calculated as QUICKI = $1/[(\log(I_0) + \log(G_0)]$, where I_0 is the fasting plasma insulin level (μU/ml) and G_0 is the fasting blood glucose level (mg/dl). The measurements of the serum lipids were performed in the Laboratory Diagnostics Unit of The University Hospital in Krakow using commercially available kits (Roche Molecular Diagnostics, Pleasanton, CA, USA).

3.2.1.1.1 Intraperitoneal glucose tolerance test

IPGTT was performed in all studied groups, two days prior to euthanasia. 16-hour fasted animals were IP administered 50% glucose at a dose of 2 g/kg of body weight. Blood glucose was measured from the tail vein by a glucometer (Accu-Chek active,

Roche Diagnostics, Germany) before the experiment (time 0) and 30, 60, 90 and 120 min after glucose administration.

3.2.1.2 MSG mice – chemical obesity model

NMRI mice, obtained from Charles River Laboratories (Sulzfeld, Germany), were housed at the certified animal facility of the Institute of Organic Chemistry and Biochemistry AS CR at the campus of Academy of Sciences in Krč, Prague, Czech Republic. The mice had free access to water and standard chow diet (Mlýn Kocanda, Jesenice, Czech Republic), which contained 66 % calories as carbohydrates, 25 % as protein, and 9 % as fat; its energy content was 3.4 kcal/g.

For MSG-induced obesity, newborn males were SC administered with L-glutamic acid monosodium salt hydrate (Sigma, St. Louis, USA) at a dose 4 mg/g of body weight at postnatal days 2 – 8 as previously described (Maletínská et al., 2006). These MSG obese mice were fed with the same standard diet as the untreated control group. The food and body weight was monitored once per week. For the study, MSG and control mice at the age of 2 and 6 months were used.

Overnight fasted MSG obese mice and their controls at the ages 2 and 6 months (n = 10 animals per group) were sacrificed by decapitation starting at 8:00 a.m. The trunk blood was collected, glucose was measured using glucometer Glucocard (Arkray, Tokyo, Japan), and the plasma was separated and stored at -20 °C. The WAT (subcutaneous and visceral fat) and the liver of all mice were dissected, weighed, frozen in liquid nitrogen and stored in -80°C. The rate of adiposity is expressed as the ratio of the total adipose tissue weight to the total body weight. Concentrations of serum leptin were measured using the ELISA kit (Millipore, St. Charles, MI, USA) and plasma insulin using RIA kits (Millipore, St. Charles, MI, USA and Linco Research, St. Charles, MI, USA) following the manufacturer's instructions.

3.2.1.3 Thy-Tau22 mice – Tau pathology model

Thy-Tau22 female mice and their age-matched controls were a kind gift from INSERM Laboratory UMR-S-1172, Lille, France, the research group "Alzheimer & Tauopathies". Mice arrived to Prague at the age of 7 months and were housed 3-4 per cage in the certified animal facility of the Institute of Physiology AS CR, Prague, Czech Republic, with free access to water and Altromin diet (Altromin, Eastern Westphalia,

Germany). Mice were sacrificed at the age of 9 months; decapitation and measurement of metabolic parameters was performed following the procedure described in chapter 3.2.1.2.

3.3 Preparation of hippocampi for Western blotting

After the decapitation, the brains were maintained on ice to prevent tissue degradation. In fa/fa rats, all hippocampus was used for Western blotting; in MSG and Thy-Tau22 mice only one half of the brain was used. Hippocampi were then dissected and homogenized in cold lysis buffer (62.5 mM Tris-HCl buffer with pH 6.8, 1% deoxycholate, 1% Triton X-100, 50 mM NaF, 1 mM Na_3VO_4 and complete protease inhibitor (Roche Applied Science, Mannheim, Germany)) using a Bullet Blender homogenizer (Next Advance, Inc., Averill Park, NY, USA). The lysates were sonicated for 1 min, protein concentration was measured using a Pierce BCA protein assay kit (Thermo Fisher Scientific, Inc., Waltham, MA, USA) following manufacturer's instructions and the lysates were diluted to a final concentration 1 µg/µl in Laemmli sample buffer (62.5 mM Tris-HCl with pH 6.8, 2% SDS, 10% glycerol, 0.01% bromophenol blue, 5% β-mercaptoethanol, 50 mM NaF and 1 mM Na_3VO_4). The sample aliquots were stored at -20 °C.

3.3.1 Western blotting

For the method of Western blot (WB), the samples were sonicated for 1 min and boiled at 100 °C for 2 min. Ten µl per sample was resolved using 5/10% SDS-PAGE electrophoretic Mini-PROTEAN Tetra Cell module (Bio-Rad, Hercules, CA, USA) in electrode buffer (25 mM Tris, 192 mM glycin, 1% SDS) at constant voltage 200 V for 45 min. The resolved proteins were transferred onto nitrocellulose membrane (Bio-Rad, Hercules, CA USA) using an XCell II^{TM} blot module (Invitrogen, Carlsbad, CA, USA) in transfer buffer (25 mM Tris, 192 mM glycin, 20% methanol) at constant voltage 30 V for 90 min. Membranes were blocked in 5% non-fat milk or BSA in TBS/Tween-20 buffer (20 mM Tris, 136 mM NaCl, 0.1% Tween-20, 50 mM NaF, and 5 mM Na_3VO_4), and then incubated overnight in the corresponding antibody at 4 °C; dilution is shown in Table 2. Afterwards, the membranes were incubated for 1 h in an appropriate anti-mouse or anti-rabbit IgG, HRP-linked secondary antibody (both Cell Signaling

Technology, Beverly, MA, USA) at room temperature, and developed using ECL solution Luminata Classico/Crescendo Western HRP Substrates (Merck Millipore, Darmstadt, Germany). Chemiluminescence was visualized in a ChemiDoc™ System (Bio-Rad, Hercules, CA, USA) and quantified using Image Lab Software (Bio-Rad, Hercules, CA, USA). The exact protein level on each membrane was normalized to β-actin as an internal loading control. In the figures in the chapter Results, only representative pictures of WB are presented, without each single β-actin.

Table 2 Summary of primary antibodies used for WB and their appropriate dilution

Antibody	Manufacturer	Dilution
Rabbit monoclonal antibody against Phospho-Akt (Ser473)	Cell Signaling Technology, Beverly, MA, USA	1:1 000 5% BSA TBS/tween-20
Rabbit monoclonal antibody against Phospho -Akt (Thr308)	Cell Signaling Technology, Beverly, MA, USA	1:1 000 5% BSA TBS/tween-20
Rabbit monoclonal antibody against total Akt	Cell Signaling Technology, Beverly, MA, USA	1:1 000 5% BSA TBS/tween-20
Rabbit monoclonal antibody against Phospho -GSK-3β (Ser9)	Cell Signaling Technology, Beverly, MA, USA	1:1 000 5% BSA TBS/tween-20
Rabbit monoclonal antibody against total GSK-3β	Cell Signaling Technology, Beverly, MA, USA	1:1 000 5% BSA TBS/tween-20
Rabbit monoclonal antibody against insulin receptor β	Cell Signaling Technology, Beverly, MA, USA	1:1 000 5% BSA TBS/tween-20
Rabbit monoclonal antibody against Phospho –PDK1 (ser241)	Cell Signaling Technology, Beverly, MA, USA	1:1 000 5% BSA TBS/tween-20
Rabbit monoclonal antibody against total PDK1	Cell Signaling Technology, Beverly, MA, USA	1:1 000 5% BSA TBS/tween-20
Rabbit monoclonal antibody against PI3 Kinase p85	Cell Signaling Technology, Beverly, MA, USA	1:1 000 5% BSA TBS/tween-20
Rabbit polyclonal antibody against Tau [pS396]	Invitrogen Grand Island, NY, USA	1:10 000 5% BSA TBS/tween-20
Rabbit polyclonal antibody against Tau [pT231]	Invitrogen Grand Island, NY, USA	1:10 000 5% BSA TBS/tween-20
Rabbit polyclonal antibody against Tau [pT212]	Invitrogen Grand Island, NY, USA	1:10 000 5% BSA TBS/tween-20
Anti-total Tau Cter	Gift from Dr. M.-C.Galas, Inserm, Lille, Francie	1:10 000 5% milk TBS/tween-20
Mouse monoclonal antibody Tau5 antibody	Invitrogen Grand Island, NY, USA	1:10 000 5% milk TBS/tween-20
Mouse monoclonal antibody Tau1 (Ser195,198,199,202)	Millipore, Billerica, MA, USA	1:10 000 5% milk TBS/tween-20
Mouse monoclonal antibody against β-actin	Sigma, St. Louis, MO, USA	1:10 000 5% milk TBS/tween-20

3.4 Brain preparation for paraffin-embedded immunohistochemistry

Immunohistochemistry was performed in MSG mouse brains. One hemisphere of each brain was fixed for 24 h in 4% paraformaldehyde (paraformaldehyde was dissolved in 0.2 M PBS buffer pH 7.4 from Sigma Aldrich, St. Louis, MO, USA), transferred to 70% ethanol, and paraffin-embedded at the histology laboratory of the Faculty of Medicine in Lille, France (Laboratoire d'histologie, Faculté de Médecine, Lille, France).

3.4.1 Immunohistochemistry

Paraffin-embedded sagittal brain slices, 5 μm thick, were deparaffinized by three times 5-min washing in toluene and then rehydrated in ethanol (5 min washing in 100, 95, 70 and 30 % mixture of ethanol in water). Antigen was unmasked by boiling for 10 min in citrate buffer pH 6 (3.75 mM citric acid, 2.5 mM disodium phosphate). Then the slices were blocked in 1% horse serum in 0.2 M PBS buffer (Sigma-Aldrich, St. Louis, MO, USA) and incubated overnight at 4 °C with the primary antibody diluted in 0.2 M PBS/0.2% Triton X-100 buffer; the appropriate dilution is presented in Table 3. After 1-h incubation with fluorescent secondary antibody Alexa 488 or Alexa 568 (Life Technologies, NY, USA) diluted in 0.2 M PBS/0.2% Triton X-100 buffer 1:1 000, the nuclei were stained using Vectashield/DAPI (4′,6-diamidino-2-phenylindole, Vector Laboratories, Burlingame, CA, USA) and mounted with cover glass. Images were acquired in a Zeiss confocal laser-scanning microscope LSM 710 (Zeiss, Oberkochen, Germany) using a 488-nm Argon laser, a 561-nm diode-pumped solid-state laser and a 405-nm ultraviolet laser with the same laser intensities to compare the images at Lille 2 University (Plate-forme d'Imagerie Moléculaire et Cellulaire). The quantification was performed using Image-J software (developed at NIH, Bethesda, MD, USA).

Table 3 Summary of primary antibodies used for immunohistochemical staining on paraffin-embedded brains

Antibody	Manufacturer	Dilution
AT8 antibody (Phospho-PHF-tau pSer202+Thr205 Antibody)	Thermo Scientific, Rockford, IL, USA	1:400 in 0.2 M PBS/0.2% Triton X-100 buffer
Rabbit polyclonal antibody against Tau [pT212]	Invitrogen Grand Island, NY, USA	1:1000 0.2 M PBS/0.2% Triton X-100 buffer

3.5 Testing of lipidized prolactin-releasing peptide analogs

3.5.1 Peptide synthesis and iodination

Lipidized analogs of rat PrRP31 with the following structure: SRAHQHSMETRTPDINPAWYTGRGIRPVGRF-NH2 and different length of fatty acid from octanoic (C8) to stearic acid (C18) attached to the N-terminus, palm^{11}-PrRP31 with the structure: SRTHRHSMEI K γ-E (N-palm) TPDINPAWYASRGIRPVGRF-NH_2 and human PrRP31 with the structure: SRTHRHSMEIRTPDINPAWYASRGIRPVGRF-NH2 were synthesized and purified at the Institute of Organic Chemistry and Biochemistry, Prague, Czech Republic as previously described by Blechova et al. (Blechova et al., 2013); lipidization was performed as previously described by Maletinská et al. (Maletinska et al., 2012). The identity and purity of the peptides was determined using HPLC and the Q-TOF micro MS technique (Waters, Milford, MA, USA).

Rat or human PrRP31 were iodinated at Tyr^{20} with Na^{125}I (Izotop, Budapest, Hungary) as described by Maletinska et al. (Maletinska et al., 2012).

3.5.2 Binding to intact plated cells

CHO-K1 cells overexpressing GPR10 receptor (Perkin Elmer, Waltham, MA, USA) were grown following the manufacturer's instruction. Saturation and competitive binding experiments were performed according to Motulsky and Neubig (Motulsky and Neubig, 2002). CHO-K1 cells were incubated with 0.5–5 nM ^{125}I-human PrRP31 in saturation experiments or with 0.03 nM ^{125}I-human PrRP31 and 10^{-11}–10^{-5} M non-radioactive lipidized analog of rat PrRP31 in competitive binding experiments in 24-well plates incubated for 60min at 25°C. Non-specific binding was determined using 10^{-5}M human PrRP31.

3.5.3 Acute food intake in lean mice

Male C57BL/6 mice were obtained from Charles Rivers Laboratories (Sulzfeld, Germany) and housed at the certified animal facility of the Institute of Organic Chemistry and Biochemistry AS CR at the campus of Academy of Sciences in Krč, Prague, Czech Republic at a temperature of 23°C and a daily cycle of 12h light and dark (lights on at 6:00). The mice were given *ad libitum* water and standard chow diet (St-1,

Mlýn Kocanda, Jesenice, Czech Republic). For the experiment, overnight (17 h) fasted mice were SC injected with saline or lipidized PrRP analogs at a dose of 5mg/kg (all dissolved in saline) (n = 6-8 animals per group). Fifteen minutes after injection, the mice were given weighed food pellets, which were subsequently weighed every 30 min for at least 6 h.

3.5.4 Fos and GPR10 receptor immunohistochemistry

c-Fos protein was determined using immunohistochemical processing. Overnight fasted male mice with free access to water (n = 4 animals per group) were SC injected with saline or PrRP31, oct-PrRP31, palm-PrRP31 at a dose of 5mg/kg. Ninety min after injection, the mice were deeply anesthetized with sodium pentobarbital (50mg/kg, IP) and perfused transcardially, the brains were treated, and c-Fos (Cell Signaling Technology, Beverly, MA, USA) immunoreactivity determined as described by Pirnik et al. (Pirnik et al., 2011). The same procedure was used to examine the expression of GPR10 receptor in the hippocampus.

3.6 Intervention with anti-diabetic and/or anorexigenic compound

3.6.1 Peptides

Palm-PrRP31 and palm^{11}-PrRP31 were synthesized at the Institute of Organic Chemistry and Biochemistry, Prague, Czech Republic as previously described in chapter 3.5.1. Liraglutide (Victoza, Novo Nordisk, Bagsvaerd, Denmark) was purchased from a pharmacy.

3.6.2 MSG mice: 14-day-long treatment with palm-PrRP31 or liraglutide

One week before the beginning of the experiment, 6-month-old MSG mice were randomly divided into groups of 10 mice, housed one per cage, and had *ad libitum* access to standard diet and water. The peptides were SC injected twice per day at 8:00 a.m. and 18:00 p.m. with saline, palm-PrRP31 at a dose 5 mg/kg, liraglutide at a dose 0.2 mg/kg of body weight, both peptide were dissolved in saline; a saline-treated group was used as a control. Every morning the mouse body weight and food consumption were monitored. Decapitation, hippocampus dissection, and pretreatment for WB or IHC is described in chapters 3.3 and 3.4.

3.6.2.1 Intraperitoneal glucose tolerance test

On day 9 of the 14-day-long treatment, IPGTT was performed. Overnight fasted mice were IP injected with glucose at a dose 2 g/kg of body weight. Blood glucose was measured using a glucometer Glucocard (Arkray, Kyoto, Japan); time 0 was glucose before IP injection, then the concentration was measured at 15, 30, 60, 90, 120 and 180 min after injection.

3.6.3 Thy-Tau22 mice: 2-month-long treatment with palm^{11}-PrRP31

Thy-Tau22 mice, 3 - 4 mice per cage, were infused for 2 months with palm^{11}-PrRP31 at a dose 5 mg/kg of body weight per day dissolved in phosphate-buffered saline (PBS)/5% Tween 80 pH 6, using SC Alzet® osmotic pumps (Alzet, Cupertino, CA, USA), which are certified to infuse 6 µl of solution every day. Both control Thy-Tau22 mice and WT mice were infused with PBS/5% Tween 80. Alzet® osmotic pumps were SC implanted in short-term ether anesthesia, and were changed after one month of the experiment. The body weight and food intake were measured three times per week.

Decapitation and tissue preparation for determination of metabolic parameters, WB or IHC is described in chapters 3.3 and 3.4.

3.6.3.1 Spatial memory test: Y-maze

Spatial memory was tested before the beginning of the treatment with palm^{11}-PrRP31 and after 2-month-long treatment of Thy-Tau22 mice.

As shown in Fig. 13, Y-maze consisted of three identical arms. On the walls of the maze, clues were placed to help the mouse to orient in the maze. First, the mouse was placed for 5 min into the maze where only two arms were opened. Then, the mouse was taken out from the maze for 2 min; meanwhile the floor of the maze was cleaned with 70 % ethanol to remove the odor, and the third "New arm" was opened. Finally, the mouse was placed through the "Start arm" into the maze with all arms opened for 1 min. The time spent in every arm was measured using the software created in the Development Workshops of IOCB AS CR, Prague where the Y-maze system was also constructed.

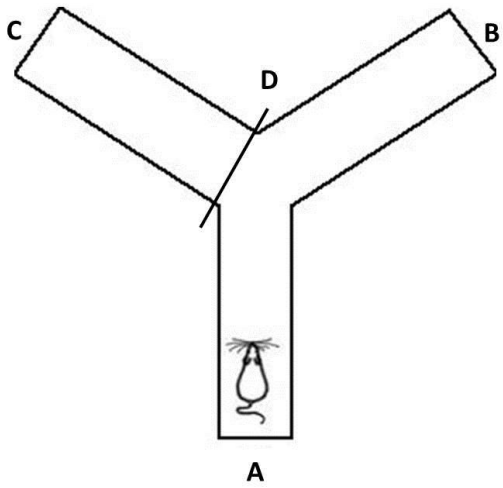

Fig. 13 Scheme of the Y-maze test

The spatial memory test Y-maze consists of three identical arms: A/ Start arm, where the mouse is placed, B/ another arm, which is opened in both sessions, C/ New arm, which is open only in the second session. D/ is the divider closing the new arm in the first session.

3.6.3.2 Drug exposure

The concentration of palm^{11}-PrRP31 was determined in blood plasma after 1- and 2-month-long Alzet® osmotic pump infusion of palm^{11}-PrRP31 using an enzyme immunoassay (EIA) high-sensitivity kit following the manufacturer's instruction.

3.7 Statistical analyses

The data are presented as the means ± SEM and were analyzed in Graph-Pad Software (San Diego, CA, USA) using a two-way analysis of variance (ANOVA), followed by a Bonferroni post-hoc test, or using an one-way ANOVA, followed by a Dunnett's post-hoc test, or a Student's t-test, as stated in the Figure and Table legends. $P < 0.05$ was considered statistically significant.

4 RESULTS

4.1 fa/fa rats

The results obtained in experiments performed in fa/fa rats presented in the following chapters were published in BMC Neuroscience (Spolcova et al., 2014).

4.1.1 Metabolic parameters of fa/fa rats

As shown in Table 4, compared to their age-matched controls the fa/fa rats developed severe obesity that was caused by non-functional leptin receptors; the body weight was significantly higher in fa/fa rats of both ages, being 50% higher than that of the age-matched control. The extreme levels of hyperleptinemia (Table 4) in fa/fa rats resulted from both the excess of adipose tissue and lack of leptin receptosr; a significantly increased level of leptin in blood was observed already in young fa/fa rats compared to their-age matched control, and was more pronounced in old fa/fa rat. Obesity was accompanied by hyperinsulinemia; significant hyperinsulinemia in fa/fa rats was represented by extreme insulin levels that reached 12-fold those of young animals and 9-fold those of old animals compared to age-matched controls. Insulin sensitivity was determined by the quantitative insulin sensitivity check index (QUICKI) where lower values indicate impaired insulin sensitivity; QUICKI was significantly decreased in both, young and old, fa/fa animals.

Table 4 Metabolic parameters of young (12-week-old) and old (33-week-old) fa/fa rats and their age-matched controls

Rats	weight [g]	leptin [ng/ml]	insulin [ng/ml]	glucose [mmol/l]	QUICKI
young control	257 ± 14	2.02 ± 1.23	0.50 ± 0.24	6.00 ± 0.42	0.537 ± 0.071
young fa/fa	386 ± 14 ***	36.72 ± 5.20**	6.26 ± 2.14**	6.27 ± 0.63	0.234 ± 0.008*
old control	457 ± 21 ***	6.33 ± 1.72	1.43 ± 0.38	6.38 ± 0.43	0.274 ± 0.010
old fa/fa	683 ± 48 ###, ooo	88.66 ± 32.71 ###, ooo	12.96 ± 4.50 ###, ooo	6.80 ± 0.51	0.216 ± 0.007 o

Data are mean ± SD, n = 6 animals per group. Significance is * P < 0,05, ** P < 0,01 and *** P < 0,001 (* vs. young control rats, # vs. young fa/fa rats, o vs. old control rats) using two-way ANOVA with Bonferroni post hoc test

There was no significant difference in the concentration of blood glucose, compared to age-matched controls, either in young or in old fa/fa rats (Table 4), but a non-significant raise in glycemia was observed in IPGTT in fa/fa rats of both ages, more increased also due to ageFig. 14 Intraperitoneal glucose tolerance test in young and old fa/fa rats and their age-matched controls is shown in Fig. 14 A and B.

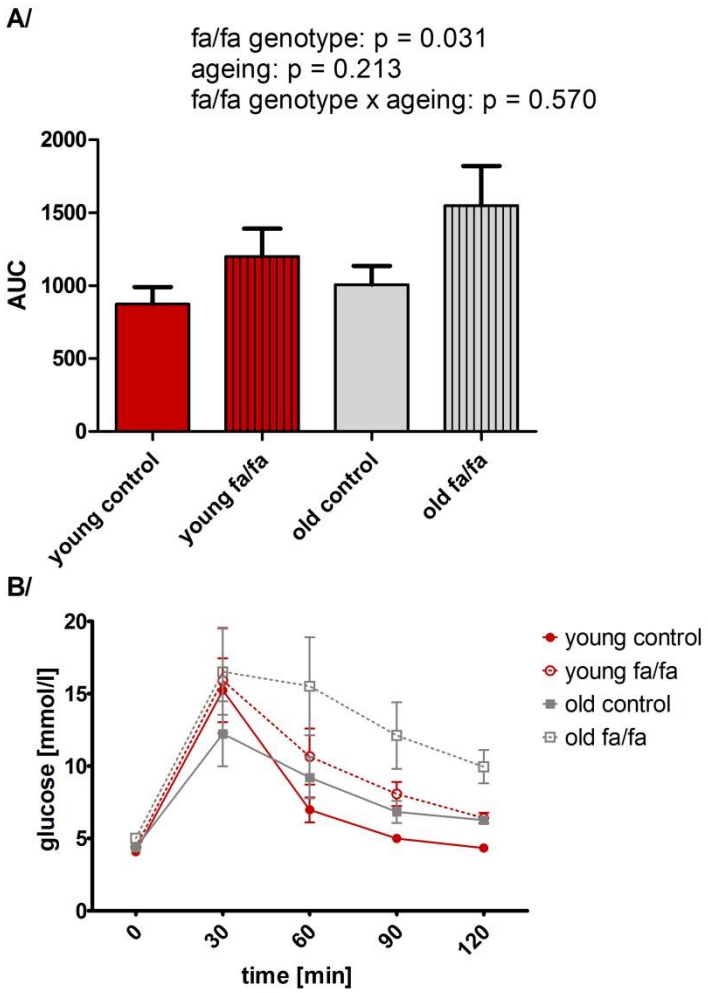

Fig. 14 Intraperitoneal glucose tolerance test in young and old fa/fa rats and their age-matched controls: A/ area under curve (AUC) B/ glucose level progress

IPGTT was performed in overnight fasted animals. Injection of 50% glucose at a dose 2g/kg was IP administered and the level of glucose was measured by a glucometer in the tail vein. Data are mean ± SEM, n = 6 animals per group. Statistical analysis was calculated by 2-way ANOVA with Bonferroni post-hoc test.

Dyslipidemia was determined by measurement of serum lipids. Both total cholesterol and cholesterol/HDL ratio were significantly increased in old fa/fa rats, compared to their lean controls, as shown in Table 5. Total cholesterol was already increased in young fa/fa rats. In the case of plasma triglyceride levels, a significant elevation was noticed only in old obese fa/fa rats compared to lean rats of the same age.

Table 5 Levels of lipids in blood serum of young and old fa/fa rats and their age-matched controls

Rats	cholesterol [mmol/l]	triglycerides [mmol/l]	HDL [mmol/l]	cholesterol/HDL
young control	2.25 ± 0.23	0.78 ± 0.12	1.40 ± 0.04	1.61 ± 0.07
young fa/fa	3.40 ± 0.41 **	2.92 ± 0.70	1.72 ± 0.08	1.99 ± 0.21
old control	2.53 ± 0.15	0.78 ± 0.10	1.65 ± 0.06	1.54 ± 0.07
old fa/fa	7.08 ± 1.17 ###, ooo	4.00 ± 0.80 oo	2.80 ± 0.48 o	2.74 ± 0.76##, ooo

Data are mean ± SEM, n = 6 animals per group. Significance is * P < 0.05, ** P < 0.01 and *** P < 0.001 (* vs. young control rats, # vs. young fa/fa rats, o vs. old control rats) using 2-way ANOVA with Bonferroni post hoc test.

4.1.2 Insulin signaling cascade in hippocampi of fa/fa rats and their controls

The effect of the fa/fa genotype and ageing on activation of the insulin signaling cascade was examined in hippocampi of fa/fa rats and their age-matched controls using the method of Western blot with specific antibodies against kinases implicated in the cascade. The data are shown in Fig. 15. First, the level of IR was determined. In the hippocampi of fa/fa rats a significant decrease in the IR protein level associated with obesity was observed already in 12-week-old animals. There was no effect of ageing on the decrease of IR, as shown in Fig. 15.

Ageing caused a significant decrease in the protein level of PI3K in both fa/fa and controls. In young 12-week-old fa/fa rats, significantly lowered PI3K was also observed compared to their age-matched controls; the level of PI3K did not differ between 33-week-old fa/fa rats and their age-matched controls. Due to the fa/fa genotype, a decrease in the phosphorylation of PDK-1 at Ser241 was observed, but it was not affected by ageing. However, ageing caused a significant reduction of phosphorylation of Akt at Thr308 in fa/fa rats and their controls. On the other hand there was no effect of the fa/fa genotype on the Akt phosphorylation at Thr308. For the full activation of Akt, the phosphorylation at Ser473 is also required. This phosphorylation was significantly

attenuated due to the fa/fa genotype, as well as by ageing. Similarly, both ageing and the fa/fa genotype caused significant reduction of phosphorylation of GSK-3β at the inhibition epitope Ser9.

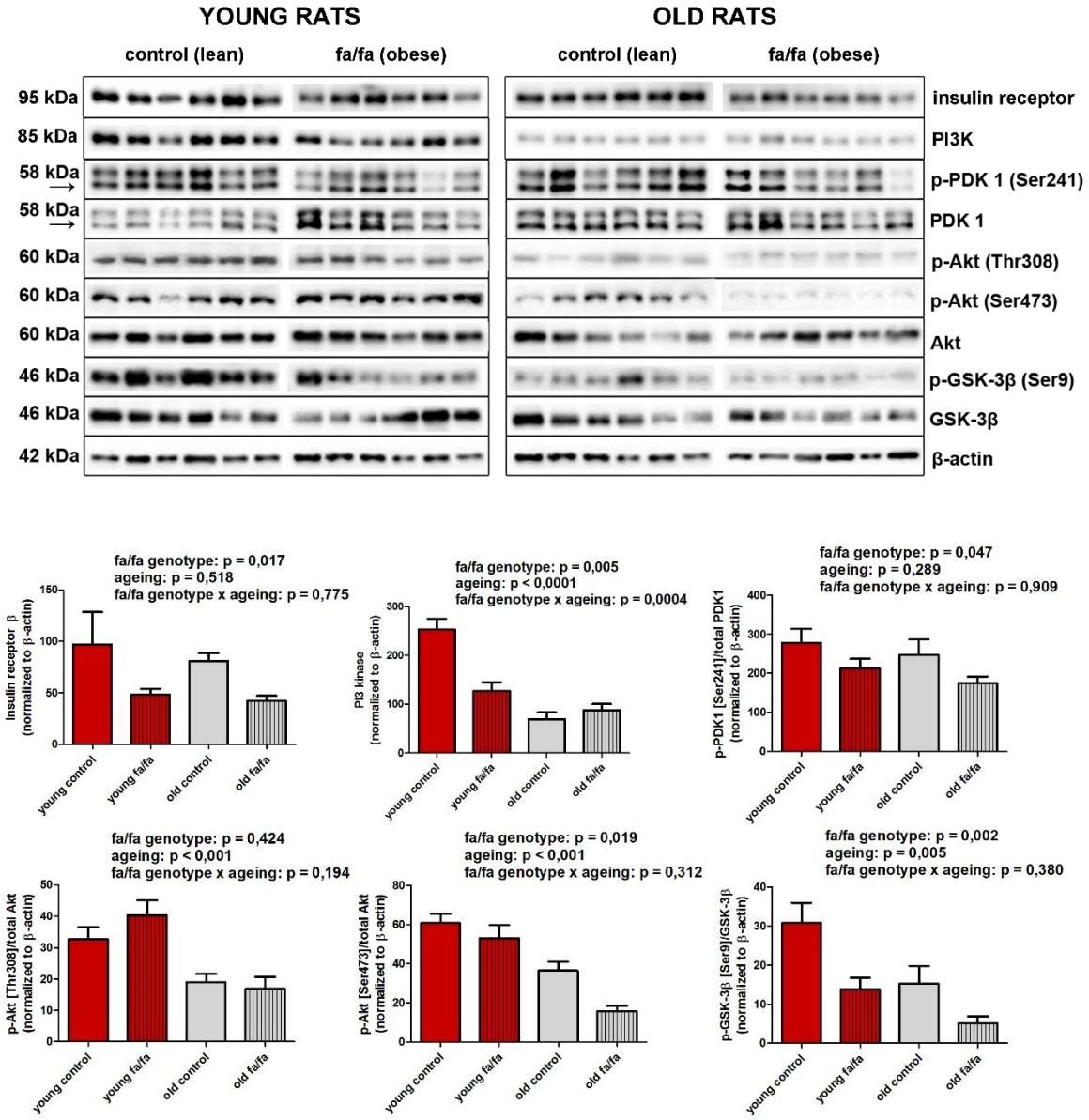

Fig. 15 Phosphorylation of kinases implicated in the insulin signaling cascade in hippocampi of 12-week- and 33-week-old fa/fa rats and their age-matched controls

Phosphorylation of kinases implicated in the insulin pathway was determined by the method of Western blot (WB) described in chapter 3.3. Data are mean ± SEM, n = 6 animals per group. Statistical analysis was calculated by 2-way ANOVA with Bonferroni post-hoc test.

4.1.3 Phosphorylation of Tau protein in hippocampi of fa/fa rats

In the hippocampi of obese fa/fa rats and their lean controls the phosphorylation of Tau protein at epitopes phosphorylated by GSK-3β was determined using the method of Western blot, and is shown in Fig. 16. The phosphorylation of Ser396 was significantly increased in fa/fa rats, compared to their controls, as well as a significant increase in phosphorylation observed due to ageing. Higher phosphorylation of Thr231 was observed in fa/fa rats already at the young age; however, there was no effect of ageing on higher phosphorylation of this epitope.

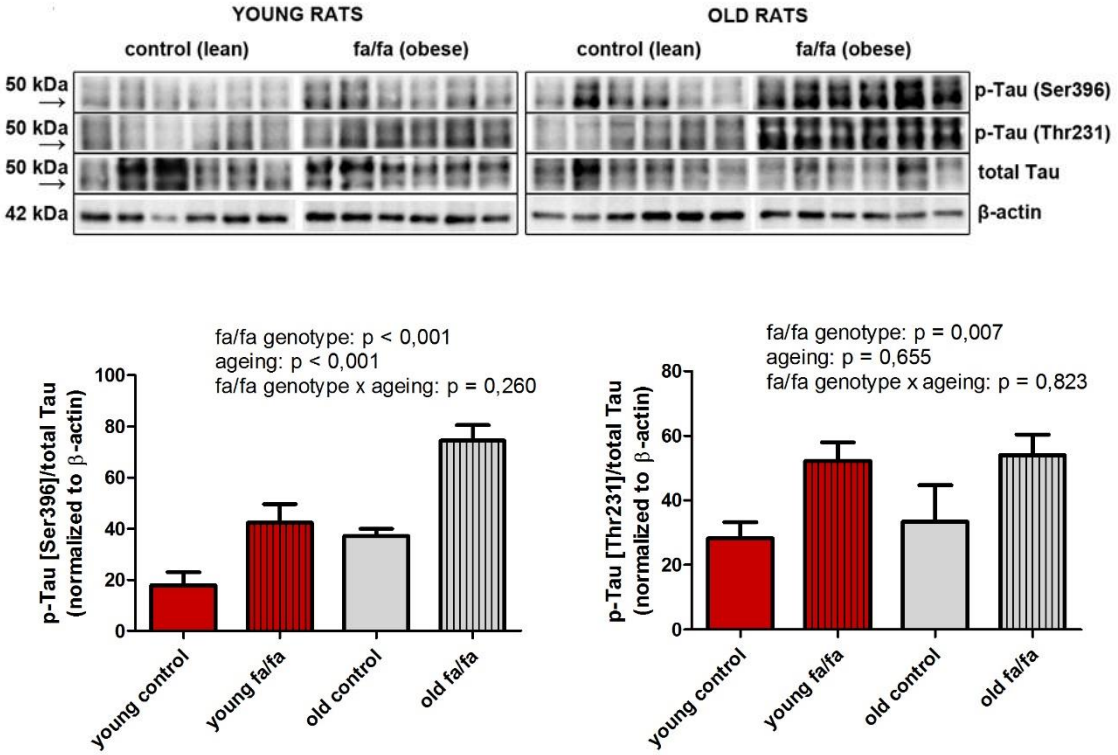

Fig. 16 Phosphorylation of Tau protein at epitopes Ser396 and Thr231 in hippocampi of 12-week- and 33-week-old fa/fa rats and their age-matched controls

Phosphorylation of Tau protein at different epitopes was determined by the method of Western blot (WB) described in chapter 3.3. Data are mean ± SEM, n = 6 animals per group. Statistical analysis was calculated by 2-way ANOVA with Bonferroni post-hoc test.

4.2 MSG mice

The results from the experiments with MSG mice were published in Journal of Alzheimer's disease (Spolcova et al., 2015).

4.2.1 Metabolic parameters of MSG mice

For the study, male MSG mice were used at the age of 2 and 6 months, as were the NMRI control mice.

The MSG treatment of newborn male NMRI mice resulted in significantly increased amounts of WAT, already in 2-month-old mice compared to age-matched controls, as shown in Table 6. However, the body weight of the MSG-obese mice did not significantly differ, either in 2- or 6-month-old animals. With an increased WAT amount, a significant increase in the leptin blood level was observed in MSG mice of both ages, compared to their age-matched controls. Fasting glucose was not significantly increased, whereas the blood insulin levels were significantly higher in MSG mice, both 2 and 6 months old. Thus, MSG mice exhibit obesity manifested by WAT accumulation and higher levels of leptin, and they are in a pre-diabetic state demonstrated by an increased insulin level but nearly normal glucose level.

Table 6 Metabolic parameters of 2- and 6-month-old male MSG mice and their age-matched controls

mice	Body weight [g]	white adipose tissue [% body weight]	leptin [ng/ml]	glucose [mmol/l]	insulin [ng/ml]
controls 2 months	40.29 ± 0.94	4.54 ± 0.47	2.07 ± 0,43	6.63 ± 0.46	0.96 ± 0.15
MSG 2 months	42.50 ± 0.59	12.04 ± 0.63 ***	27.38 ± 4.14**	8.55 ± 0.34	3.48 ± 0.57 *
controls 6 months	53.73 ± 1.84	6.88 ± 0.47	4.03 ± 1.55	6.43 ± 0.52	0.83 ± 0.27
MSG 6 months	57.18 ± 1.26	11.46 ± 0.48 ###	18.11 ± 2.91##	5.83 ± 0.45	3.64 ± 0.99#

Data are mean ± SEM (n = 10 animals per group). Significance is * P < 0.05, ** P < 0.01 and *** P < 0.001 (* vs. control 2 moths, # vs. control 6 months) using two-way ANOVA with Bonferroni post hoc test.

4.2.2 GSK-3β activation and Tau protein phosphorylation in hippocampi of MSG mice at the age of 2 and 6 months

By the method of Western blot using specific antibodies, phosphorylation at Ser9 at GSK-3β and phosphorylation of Tau protein on epitopes Ser396 and Thr231, which

are directly phosphorylated by GSK-3β were determined in the hippocampus. Results are shown in Fig. 17.

Significantly decreased phosphorylation at inhibitory Ser9 of GSK-3β leading to higher kinase activity was observed in 6-month-old control animals. Significantly increased phosphorylation of Tau protein at epitopes Ser396 and Thr231 was observed in the hippocampi of 6 months old MSG mice.

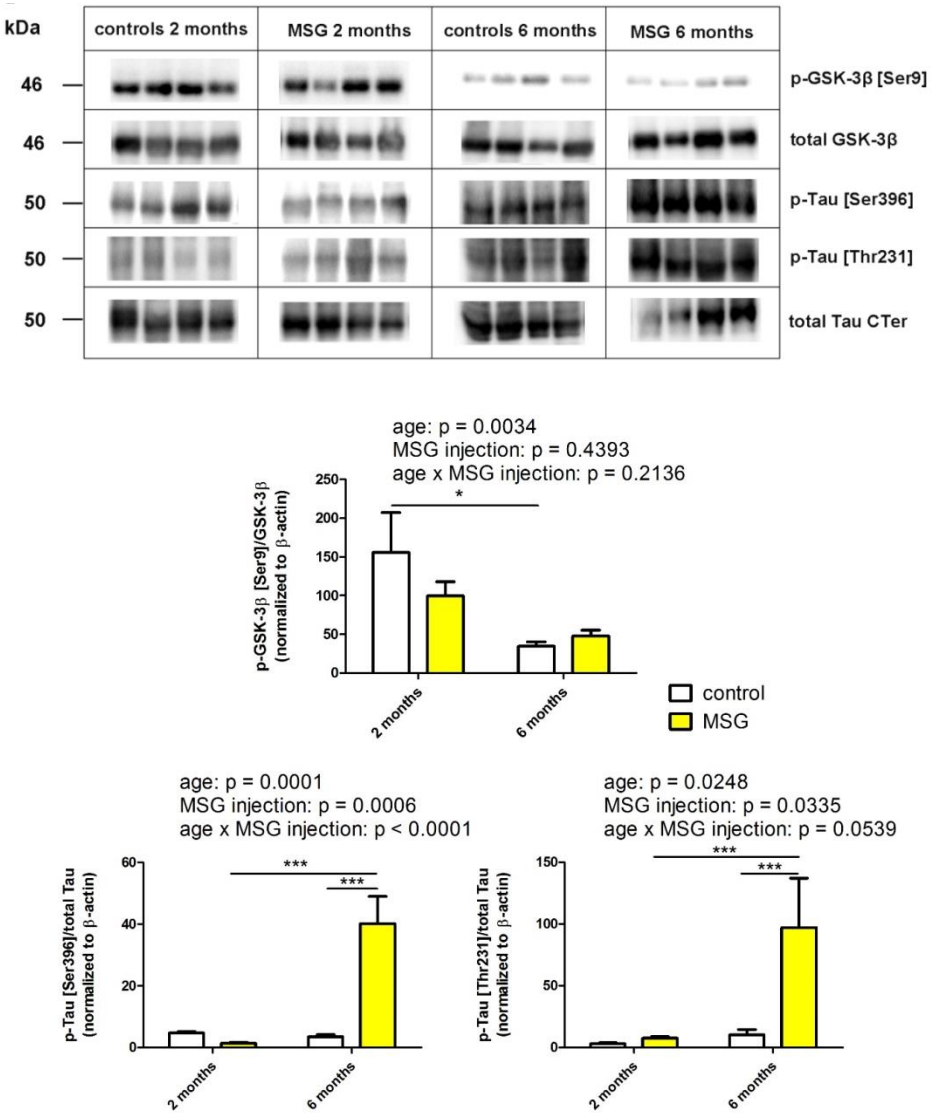

Fig. 17 Phosphorylation of GSK-3β at Ser9, and Tau protein at epitopes Ser396 and Thr231 in hippocampi of 2- and 6-month-old MSG obese mice and their controls

*Phosphorylation of GSK-3β and of Tau protein at different epitopes was determined by the method of Western blot (WB) described in chapter 3.3. Data are mean ± SEM, n = 10 animals per group. Statistical analysis was calculated by 2-way ANOVA with Bonferroni post-hoc test. Significance is * P < 0.05 and *** P < 0.001.*

4.3 Testing of lipidized analogs of PrRP31

The results were already published in the International Journal of Obesity (Maletinska et al., 2015) and patent PCT/US13/50146 Lipidated peptides as anti-obesity agents pending to IOCB AS CR was applied the 11th July 2013.

4.3.1 Affinity to GPR10 receptor

The structures of tested analogs of PrRP31 lipidized with different fatty acids are shown in Table 7. The peptide sequences were assembled on a solid support as described in the Materials and Methods. Lipidized PrRP31 analogs were modified with norleucine (Nle) in position 8 to avoid oxidation of the original Met; this change did not affect the biological activity. The purity of all peptides was higher than 95 %.

All tested analogs of PrRP31, native and lipidized, showed high binding affinity in a competitive binding experiment with human ^{125}I-PrRP31 to CHO cells overexpressing human PrRP receptor GPR10. K_i values were in a nanomolar range, as shown in Table 7. This means that lipidization of its peptide chain did not affect the affinity of PrRP to the GPR10 receptor.

Table 7 Structures and binding affinities of rat PrRP31, and its lipidized analogs to GPR10 receptor

Analog	Sequence	K_i (nM)
PrRP31	SRAHQHSMETRTPDINPAWYTGRGIRPVGRF-NH_2	3.91 ± 0.21
Nle-PrRP31	SRAHQHS Nle ETRTPDINPAWYTGRGIRPVGRF-NH_2	1.87 ± 0.42
oct-PrRP31	(N-oct)SRAHQHS Nle ETRTPDINPAWYTGRGIRPVGRF-NH_2	1.49 ± 0.07
dec-PrRP31	(N-dec)SRAHQHS Nle ETRTPDINPAWYTGRGIRPVGRF-NH_2	1.42 ± 0.55
dodec-PrRP31	(N-dodec)SRAHQHS Nle ETRTPDINPAWYTGRGIRPVGRF-NH_2	1.15 ± 0.35
myr-PrRP31	(N-myr)SRAHQHS Nle ETRTPDINPAWYTGRGIRPVGRF-NH_2	0.69 ± 0.09
palm-PrRP31	(N-palm)SRAHQHS Nle ETRTPDINPAWYTGRGIRPVGRF-NH_2	2.94 ± 0.33
palm^{11}-PrRP31	SRTHRHSMEI K γ-E (N-palm) TPDINPAWYASRGIRPVGRF-NH2	7.96 ± 1.47
stear-PrRP31	(N-stear)SRAHQHS Nle ETRTPDINPAWYTGRGIRPVGRF-NH_2	5.24 ± 0.57

Binding experiments were performed according to the protocol described in chapter 3.5.2. Data are means ± SEM of three separate experiments in duplicates. K_i was calculated using the Cheng-Prusoff equation (Cheng and Prusoff, 1973). K_d, calculated in saturation experiments, was 0.95 ± 0.20 nM. Abbreviations: Nle – norleucine, oct – octanoyl, dec – decanoyl, dodec – dodecanoyl, myr – myristoyl, palm – palmitoyl, stear – stearoyl.

4.3.2 Food intake after acute peripheral administration

Food intake was measured in lean fasted C57Bl/6 mice after acute peripheral SC injection of PrRP31 or its lipidized analogs. As shown in Fig. 18 A and B, the food intake stayed unchanged after the treatment with natural rat PrRP31 compared to the saline-injected controls. In contrast, reduction of food intake was observed after administration of some lipidized analogs of PrRP31. The most potent anorexigenic analogs were palmitoylated or stearoylated PrRP31 which significantly reduced the food intake, even after 8 hours after the administration.

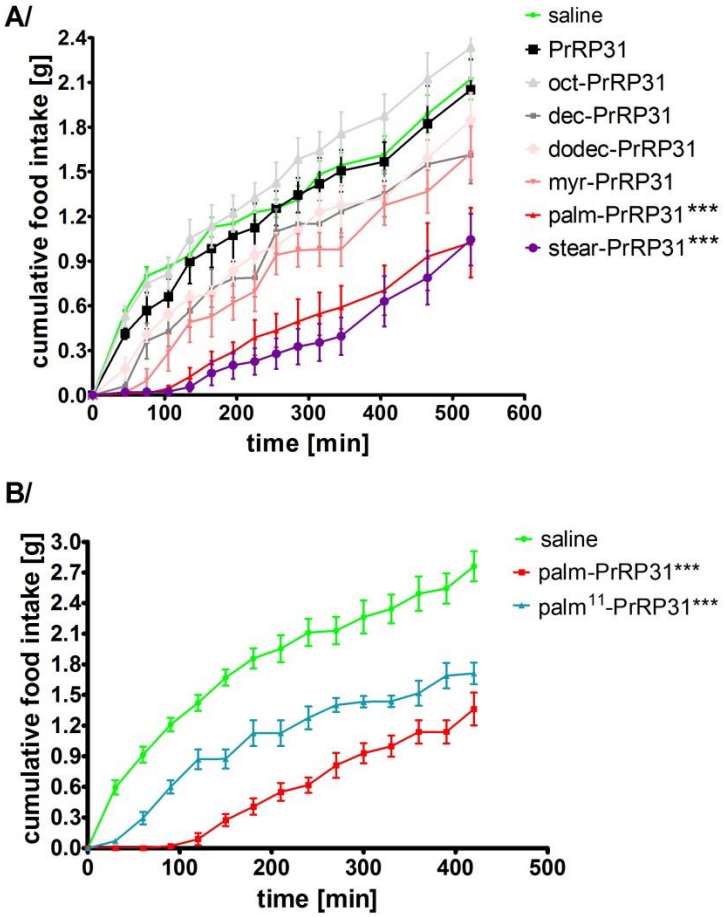

Fig. 18 Food intake after peripheral administration of lipidized analogs of PrRP31: A/ PrRP31 lipidized with fatty acids of different lengths B/ palmitoylated analogs of PrRP31

*Food intake was measured in lean fasted C57Bl/6 mice after SC injection with PrRP31 analogs lipidized with different fatty acids at a dose of 5 mg/kg, as described in chapter4.3.2.Data are mean ± SEM (n = 6 – 8 animals per group). Statistical analysis was calculated by 1-way ANOVA with Dunnett post-hoc test. Significance is *** P < 0.001.*

4.3.3 c-Fos activation after peripheral administration

By immunohistochemical staining c-Fos activation after peripheral administration of lipidized analogs was determined in the nuclei related to food intake regulation expressing GPR10 (Lee et al., 2000; Maruyama et al., 1999), which were PVN and NTS of the brain stem. The c-Fos activation corresponds with data obtained from food intake measuring. Neither in the saline-injected group nor in native PrRP31- or oct-PrRP31-treated group c-Fos was activated in any examined nuclei. Significantly increased c-Fos activation was observed after peripheral administration of palm-PrRP31 in both PVN and NTS.

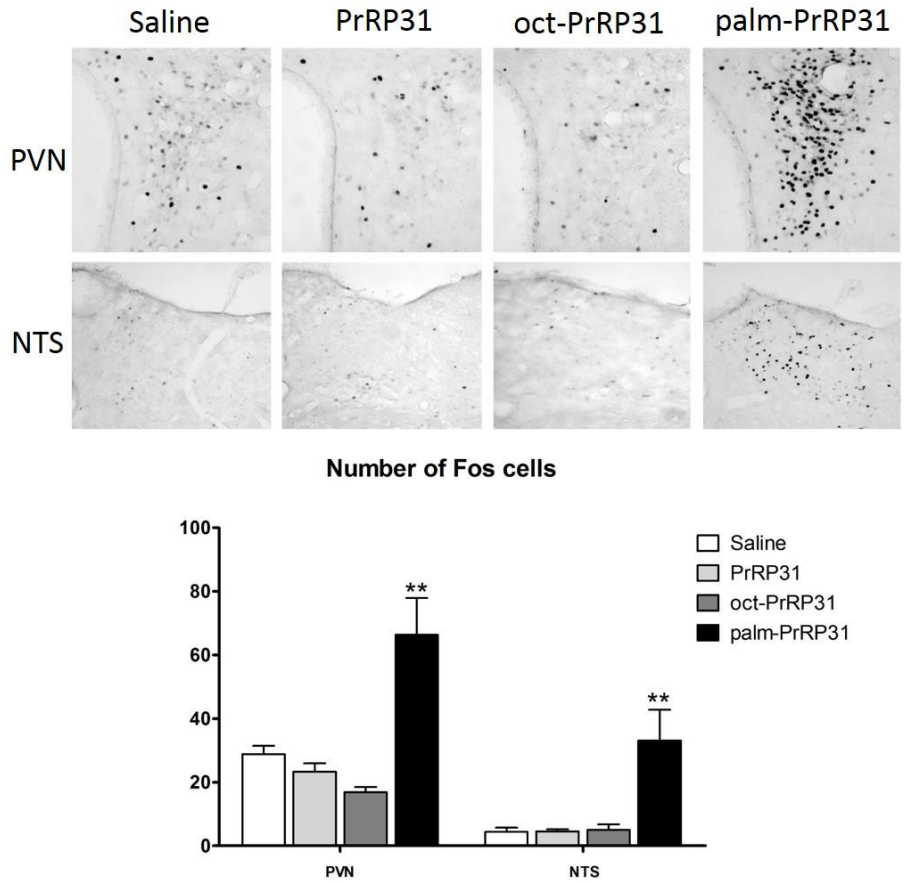

Fig. 19 Immunohistochemical staining of c-Fos protein activation after peripheral administration of PrRP31 and its lipidized analogs in paraventricular nuclei (PVN), and nucleus tractus solitaries (NTS)

*c-Fos protein activation was determined by immunohistochemical staining described in chapter 3.5.4. Data are means ± SEM (n = 4 animals per group). Statistical analysis was calculated by 1-way ANOVA with Dunnett post-hoc test. Significance is ** P < 0.01.*

4.4 Long-term treatment with palmitoylated PrRP31 and liraglutide

The results were published in Journal of Alzheimer's disease (Spolcova et al., 2015) and patent PCT/CZ2015/000047 Lipidated peptides as neuroprotective agents pending to IOCB AS CR was applied the 20th May 2015.

4.4.1 6-month-old MSG obese male mice

4.4.1.1 Metabolic parameters after 14-day-long treatment of 6-month-old MSG obese mice with palm-PrRP31 or liraglutide

Six-month-old obese male MSG mice were injected SC for 14 days either with liraglutide, or with our novel palmitoylated analog of PrRP31 at doses significantly lowering food intake. Control mice were injected with saline. Both lipidized anorexigenic peptides significantly reduced the cumulative food intake, as shown in Fig. 20A. However, compared to the saline treated group the body weight did not change after liraglutide treatment. A significant decrease of body weight was observed after palm-PrRP31 treatment on day 8 of the treatment (Fig. 20B) but on day 13 the weight loss was only non-significantly decreased compared to the saline-treated group. Weight loss also observed in saline-treated group was most likely caused by repeated injection; based on our previous experience, the NMRI mouse strain is sensitive to daily manipulation and injection.

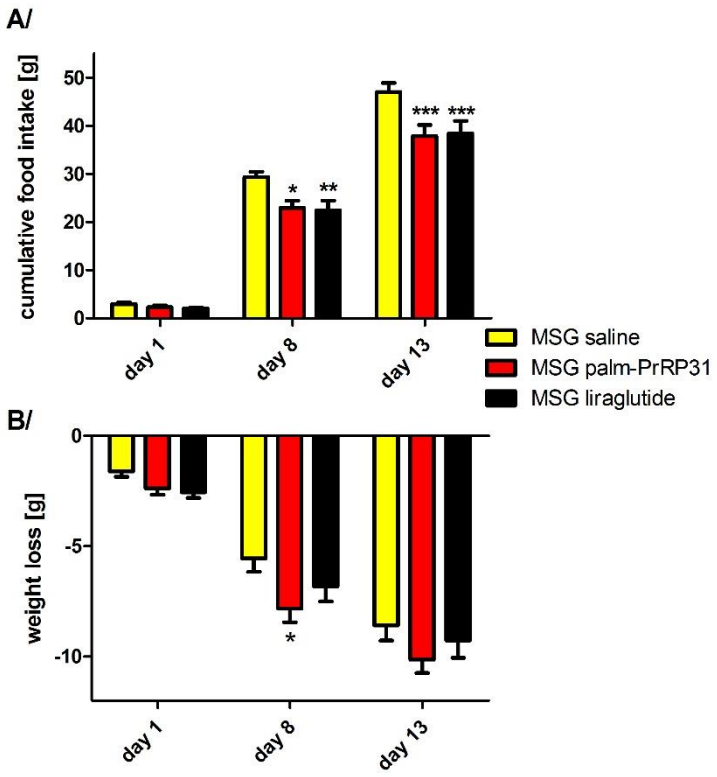

Fig. 20 A/ Cumulative food intake and B/ body weight change in 6-month-old MSG obese mice after palm-PrRP31 or liraglutide treatment

*Cumulative food intake and body weight change were measured every morning during the 14-day-long treatment with palm-PrRP31 at a dose of 5 mg/kg, or 0.2 mg/kg liraglutide as described in chapter 3.6.2. Data are mean ± SEM, n = 10 animals per group. Statistical analysis was calculated by 1-way ANOVA with Dunnett post-hoc test. Significance is * P < 0.05, **P < 0.01 and *** P < 0.001vs saline treated group.*

Table 8 shows the metabolic parameters of MSG mice after 14-day-long treatment. The amount of WAT and leptin level tended to decrease. The fasting glucose and plasma insulin levels did not significantly differ compared to the saline-treated group.

Table 8 Metabolic parameters of 6-month-old MSG mice after 14-day-long treatment with palm-PrRP31 or liraglutide

intervention	body weight [g]	white adipose tissue [% body weight]	leptin [ng/ml]	glucose [mmol/l]	insulin [ng/ml]
saline	53.08 ± 2.22	6.37 ± 0.84	23.10 ± 3.85	6.48 ± 0.42	1.53 ± 0.20
palm-PrRP31	50.07 ± 1.68	4.91 ± 0.43	21.20 ± 2.62	6.49 ± 0.32	1.57 ± 0.13
liraglutide	48.23 ± 1.70	5.38 ± 0.67	18.16 ± 2.41	5.63 ± 0.34	1.91 ± 0.27

Data are mean ± SEM (n = 10 animals per group). Data were analyzed by one-way ANOVA with Bonferroni post hoc test

On day 9 of the experiment, IPGTT was performed. The AUCs did not significantly differ either after palm-PrRP31, or liraglutide treatment compared to the saline-treated group, as shown in Fig. 21A. Only the final glucose level was significantly lower in mice treated with palm-PrRP31 compared to the control mice treated with saline (Fig. 21B).

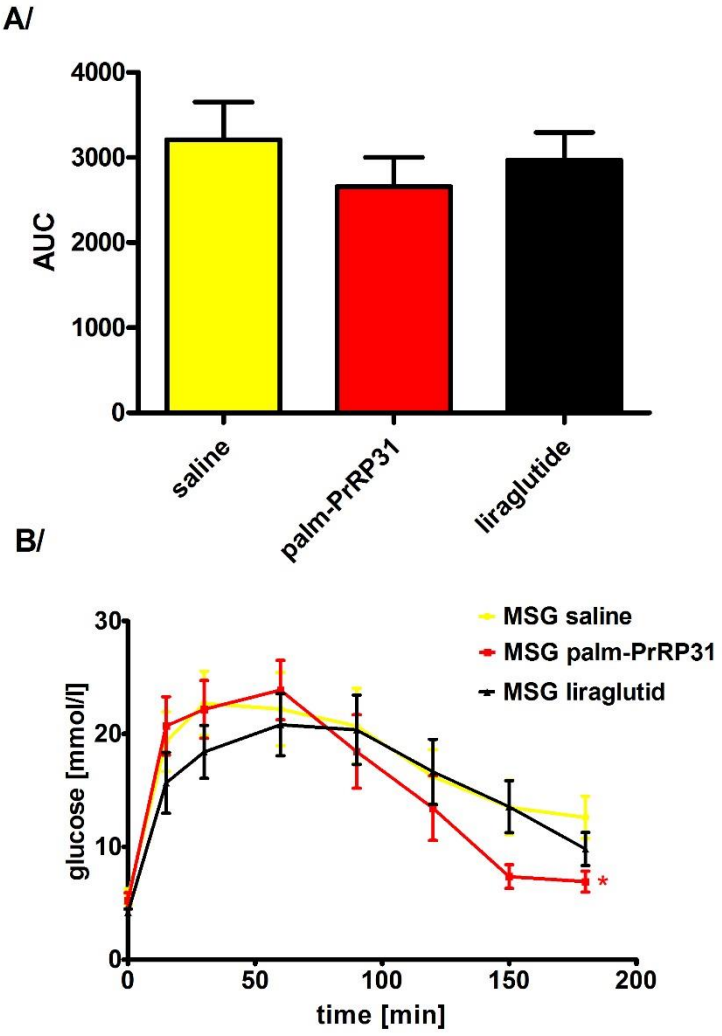

Fig. 21 Intraperitoneal glucose tolerance test in 6-month-old MSG obese mice treated with palm-PrRP31 or with liraglutide for 9 days: A/ area under curve (AUC) B/ time course of IPGTT

*IPGTT was performed in overnight fasted animals. The injection of glucose at a dose 2 g/kg was IP administered and the level of glucose was measured by a glucometer in the tail vein blood. Data are mean ± SEM, n = 10 animals per group. Statistical analysis was calculated by 2-way ANOVA with Bonferroni post-hoc test. Significance is * P < 0.05.*

4.4.1.2 GPR10 receptor in mouse hippocampi

The expression of GPR10 receptor in mice hippocampi was determined by immunohistochemical staining in hippocampi of control mice. Immunopositive cells were found in hippocampal CA1 in stratum lacunosum-moleculare (slm), as shown in Fig. 22, and the hilus of dentate gyrus.

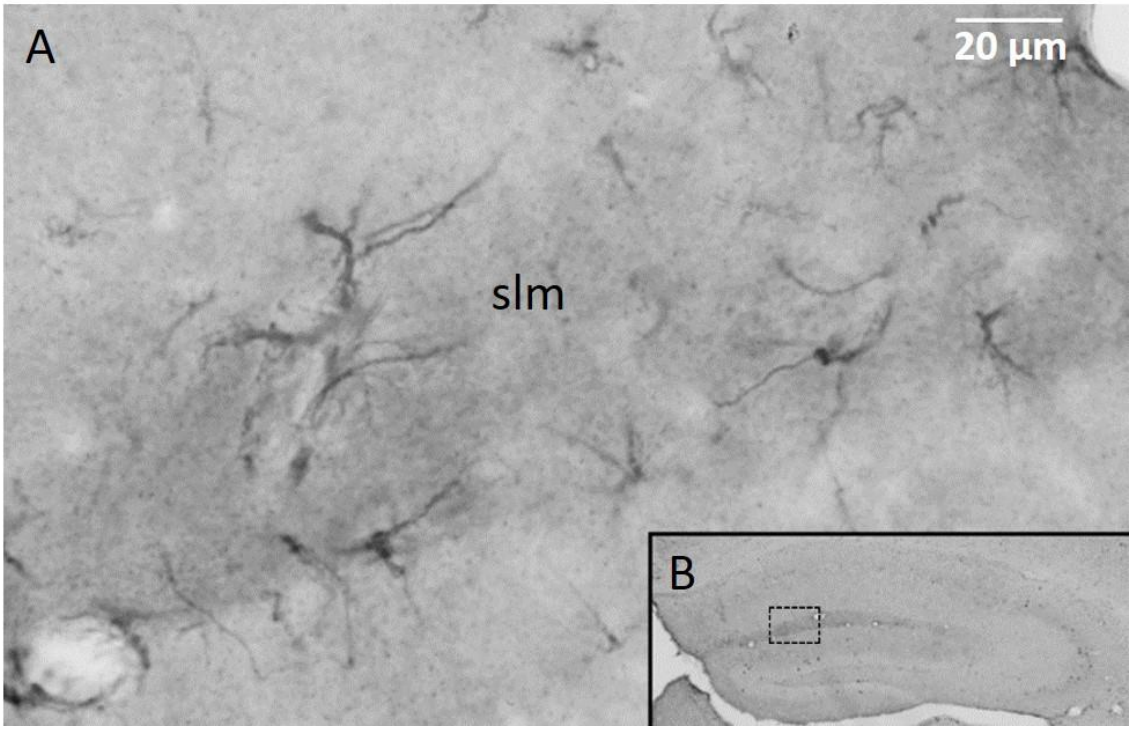

Fig. 22 GPR10 immunopositive cells in stratum lacunosum-moleculare (slm) of the CA1 subfield of the hippocampus: A/ detailed picture of slm B/ low resolution picture of hippocampus

Expression of GPR10 receptor in control mouse hippocampi was determined by immunohistochemical staining described in chapter 3.5.4.

4.4.1.3 Insulin signaling cascade in hippocampi of 6-month-old obese MSG mice after 14-day-long treatment with palm-PrRP31 or liraglutide

Fourteen-day-long treatment with palm-PrRP31 or with liraglutide resulted in increased activation of the insulin signaling cascade manifested by increased phosphorylation of the implicated kinases, as shown in Fig. 23. Enhanced phosphorylation at Ser241of PDK-1 was observed after liraglutide treatment but not after palm-PrRP31. Akt phosphorylation at the Thr308 epitope significantly increased in the palm-PrRP31-treated group but not in the liraglutide-treated group. Akt phosphorylation at Ser473 was not affected by either treatment.

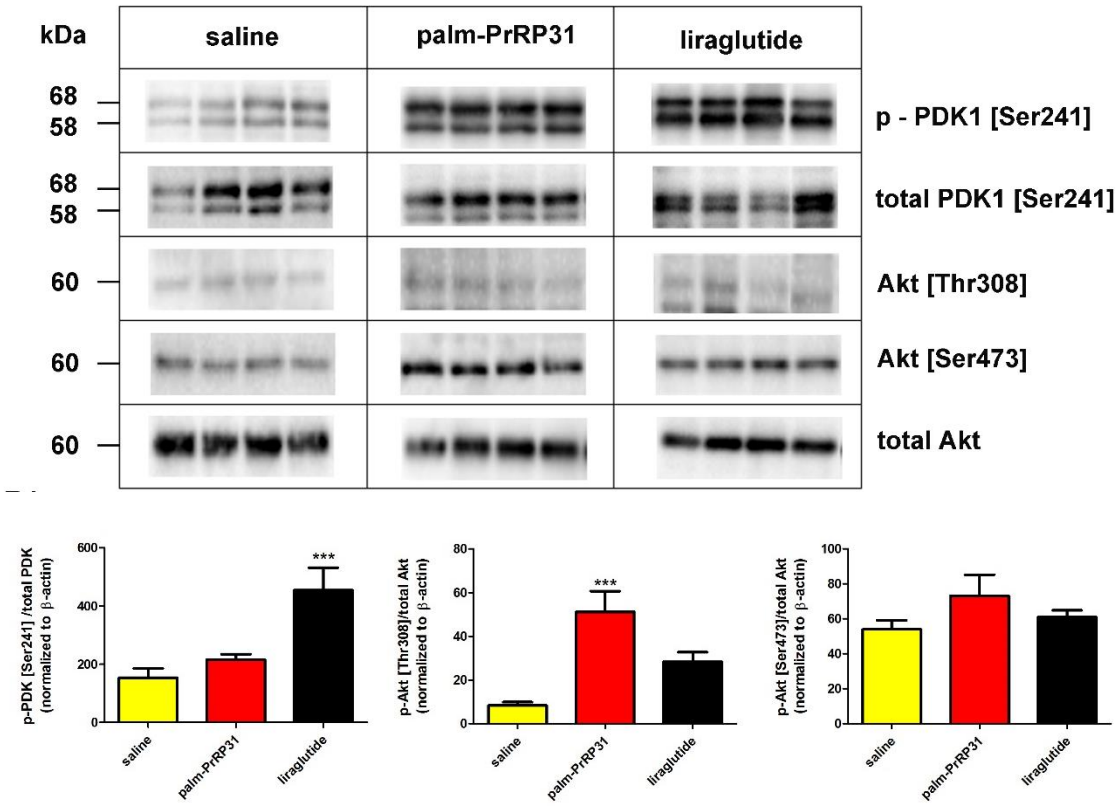

Fig. 23 Insulin signaling cascade phosphorylation in hippocampi of 6-month-old MSG obese mice after 14-day administration of palm-PrRP31 or liraglutide

*Phosphorylation of kinases implicated in the insulin pathway after treatment with anorexigenic peptides was determined by the method of Western blot (WB) described in chapter 3.3. Data are mean ± SEM, n = 10 animals per group. Statistical analysis was calculated by 1-way ANOVA with Dunnett post-hoc test. Significance is *** P < 0.001.*

4.4.1.4 Tau protein kinase phosphorylation after 14-day-long treatment with palm-PrRP31 or liraglutide in hippocampi of 6-month-old MSG mice

The phosphorylation state of kinases implicated in Tau phosphorylation was determined by immunoblotting. The results are shown in Fig. 24. Inhibitory Ser9 of GSK-3β, the primary Tau kinase, was significantly more phosphorylated after palm-PrRP31 treatment compared to the controls. The phosphorylation of MAPK/ERK1/2 and JNK, two other potent Tau kinases, was significantly lowered in the hippocampi of the MSG-obese mice after both palm-PrRP31 and liraglutide administration.

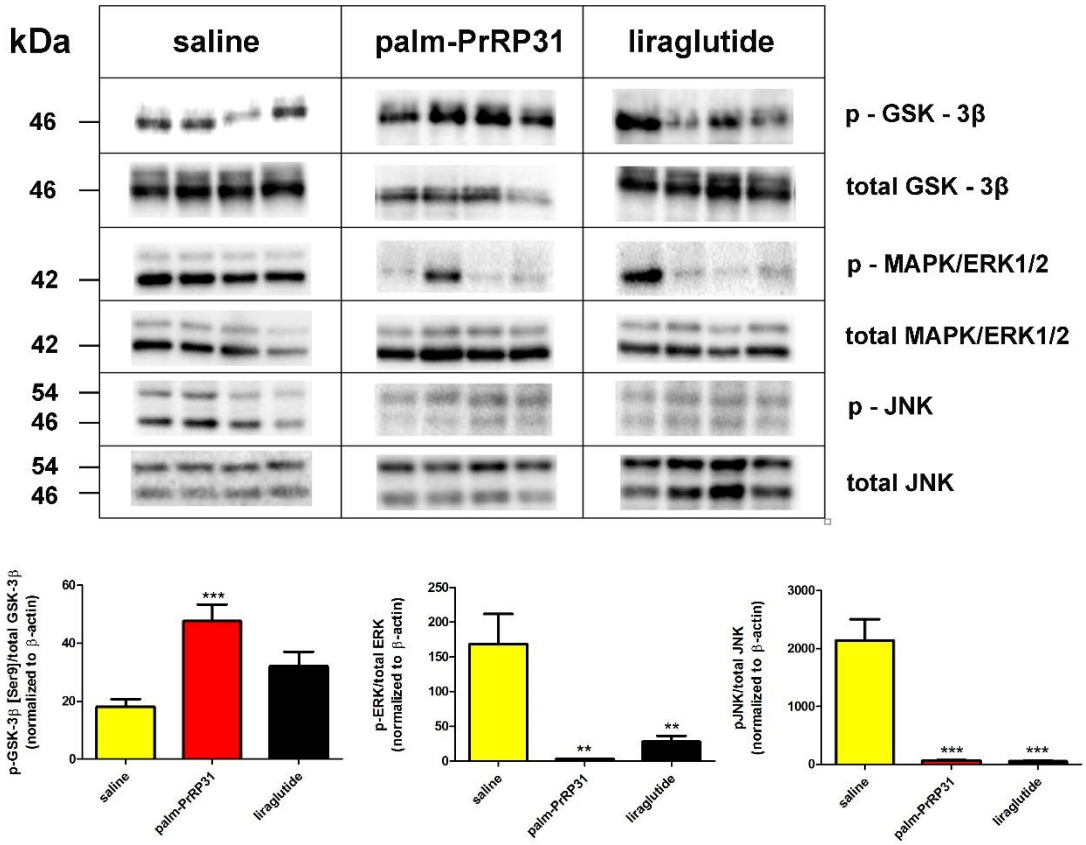

Fig. 24 Phosphorylation of kinases implicated in Tau phosphorylation in the hippocampi of 6-month-old MSG obese mice after 14-day-long intervention with palm-PrRP31 or liraglutide

*Phosphorylation of kinases implicated in Tau hyper-phosphorylation after treatment with anorexigenic peptides was determined by the method of Western blot (WB) described in chapter 3.3. Data are mean ± SEM, n = 10 animals per group. Statistical analysis was calculated by 1-way ANOVA with Dunnett post-hoc test. Significance is **P < 0,01 and *** P < 0.001.*

4.4.1.5 Phosphorylation of Tau protein at different Tau epitopes in hippocampi of 6-month-old obese MSG mice

Significantly attenuated phosphorylation at Ser396, Thr212 and Thr231 in hippocampi of 6-month-old MSG mice was observed after 14-day-long administration of both tested peptides, either palm-PrRP31 or liraglutide, using the method of Western blot (Fig. 25).

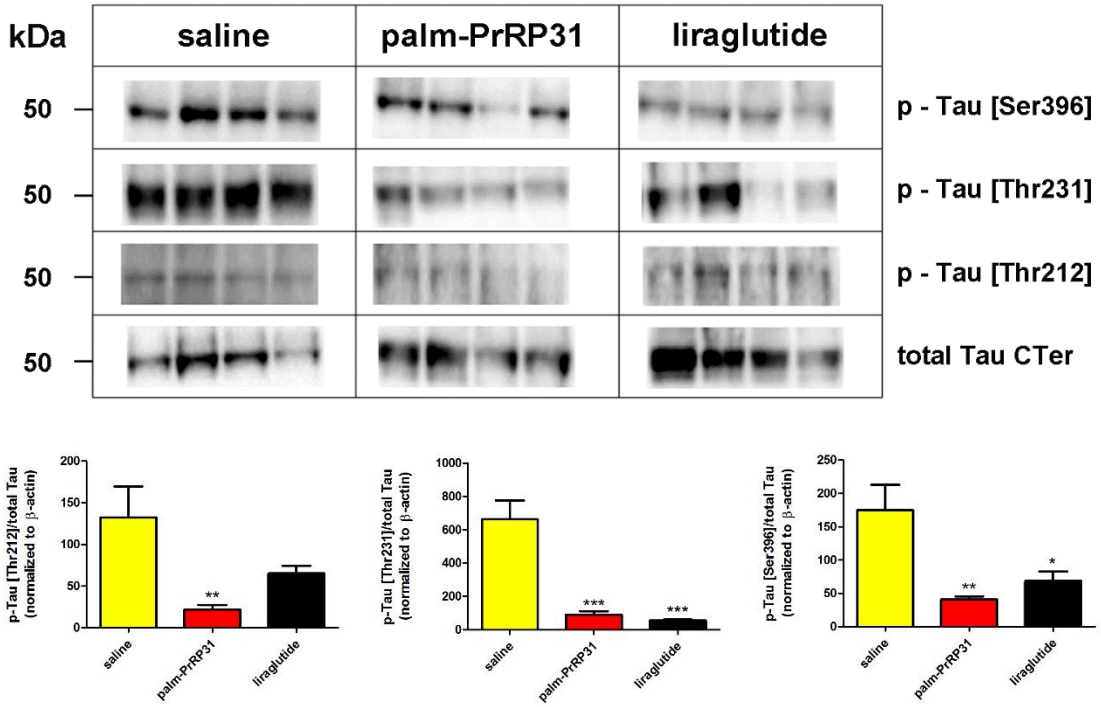

Fig. 25 Western blot analysis of Tau phosphorylation at different epitopes in hippocampi of 6-month-old MSG obese mice after 14-day-long intervention with palm-PrRP31 or liraglutide

*Phosphorylation of Tau after treatment with anorexigenic peptides was determined by the method of Western blot (WB) described in chapter 3.3. Data are mean ± SEM, n = 10 animals per group. Statistical analysis was calculated by 1-way ANOVA with Dunnett post-hoc test. Significance is * P < 0.05, **P < 0.01 and *** P < 0.001.*

To confirm the effect on hippocampal Tau phosphorylation, immunohistochemical analysis was performed. In the CA1 subfield of the hippocampus, decreased phosphorylation of the Tau protein at Thr212 and at Ser202/T205 (the antibody AT8) was detected after palm-PrRP31 or liraglutide treatment compared to that of the control group, which was manifested by weaker fluorescent signal (Fig. 26).

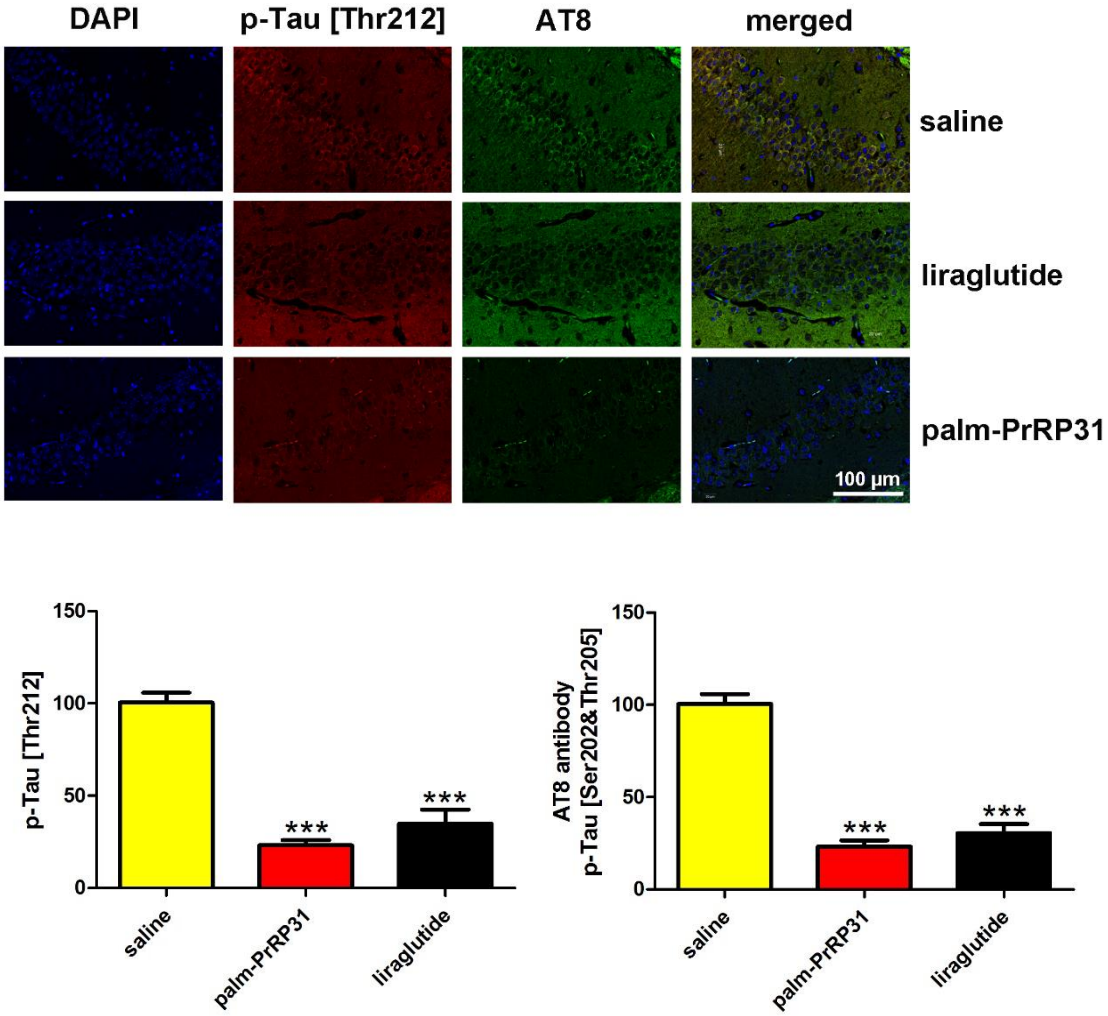

Fig. 26 Double immunohistochemical staining of Tau phosphorylation at different epitopes in hippocampi of 6-month-old MSG obese mice after 14-day-long intervention with palm-PrRP31 or liraglutide

*Phosphorylation of Tau after treatment with anorexigenic peptides was determined by immunohistochemical staining of paraffin-embedded slices as described in chapter 3.4. Data are mean ± SEM, n = 5 animals per group. Statistical analysis was calculated by 1-way ANOVA with Dunnett post-hoc test. Significance is *** P < 0.001.*

4.5 Nine-month-old Thy-Tau22 female mice

4.5.1 Spatial memory testing in Y-maze before and after 2-month-long palm^{11}-PrRP31 treatment

Spatial memory was tested in Thy-Tau22 mice using the Y-maze test before starting the treatment and after 2-month-long treatment with palm^{11}-PrRP31. Compared to WT control mice, the spatial memory was impaired in Thy-Tau22 mice before the beginning of the experiment, see Fig. 27A. The impaired memory was manifested by significantly shorter time spent in the new arm of the Y-maze and longer time spent in the start arm and other arm.

After 2-month-long treatment, the memory improved in Thy-Tau22 mice treated with palm^{11}-PrRP31 compared to vehicle-treated Thy-Tau22mice (Fig. 27B); compared to vehicle-treated Thy-Tau22 mice, mice treated with palm^{11}-PrRP31 spent significantly longer time in the new arm of the Y-maze.

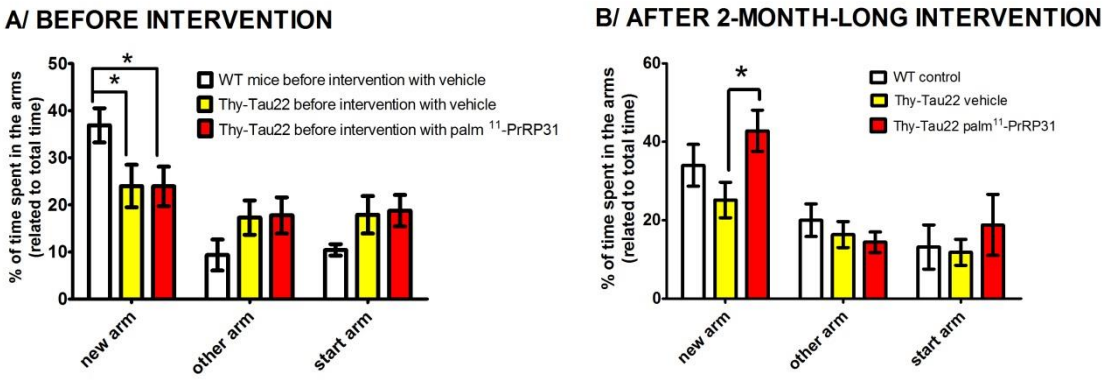

Fig. 27 Spatial memory testing of Thy-Tau22 mice and their age-matched WT controls in Y-maze: A/before the beginning of the experiment, and B/ after treatment with palm^{11}-PrRP31

*Spatial memory was tested in Y-maze following the protocol described in chapter 3.6.3.1. Data are mean ± SEM, n = 12 animals per group. Statistical analysis was calculated by Student's t-test. Significance is * P < 0.05.*

4.5.2 Metabolic parameters of Thy-Tau22 mice and their age-matched WT controls after 2-month-long treatment with palm^{11}-PrRP31

During the 2-month-long treatment, the cumulative food intake (Fig. 28A) and body weight (Fig. 28B) were measured. Palm^{11}-PrRP31-treated Thy-Tau22 mice showed no significant differences either in food intake or in body weight change

compared to vehicle-treated Thy-Tau22 mice. The body weight of WT vehicle-treated group was significantly increased compared to the Thy-Tau22-vehicle treated group; however, the cumulative food intake did not differ. The concentration of palm^{11}-PrRP31 infused by Alzet® osmotic pumps in blood plasma was determined by EIA kit after one month and two months of treatment. After one month treatment, the concentration of palm^{11}-PrRP31 was 7.39 ± 0.82 ng/ml, and after two months 20.41 ± 7.47 ng/ml.

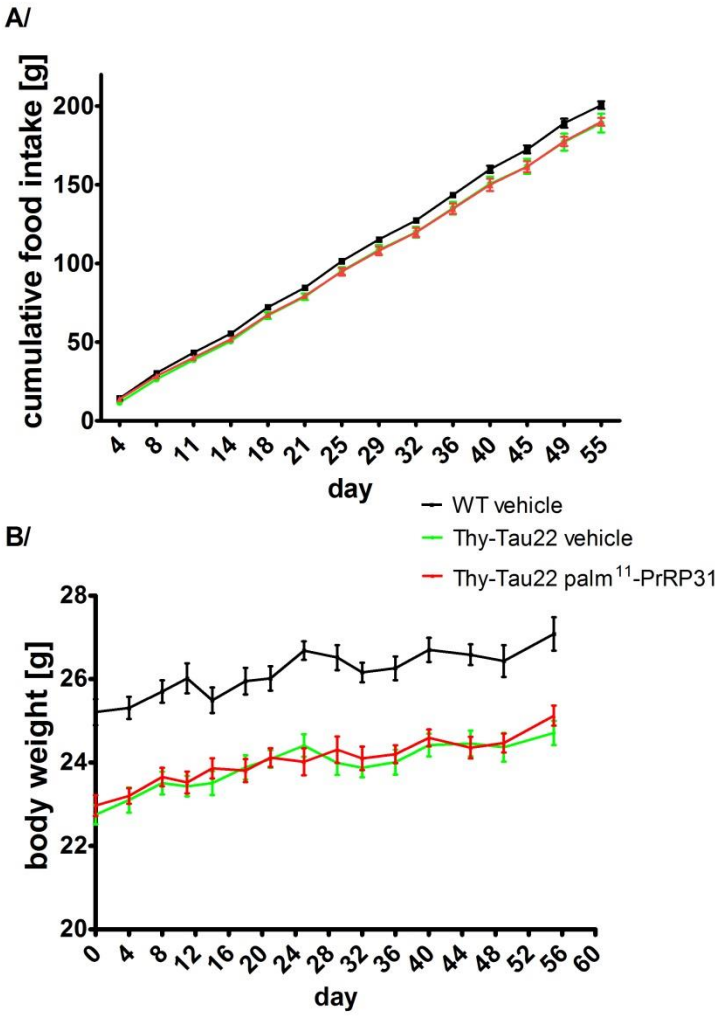

Fig. 28 A/ Cumulative food intake and B/ body weight change in Thy-Tau22 mice and their WT controls during 2-month-long palm^{11}-PrRP31 treatment

*Body weight change and cumulative food intake was measured three times per week during the 2-month-long treatment with palm^{11}-PrRP31 at a dose of 5 mg/kg/day by SC Alzet® osmotic pump as described in chapter 3.6.3. Data are mean ± SEM, n = 10 animals per group. Statistical analysis was calculated by 1-way ANOVA with Dunnett post-hoc test. Significance is ***P < 0.001 compared to Thy-Tau22 vehicle.*

After the treatment, the metabolic parameters were measured (Table 9). Compared to the Thy-Tau22-vehicle group, the WT-vehicle controls had significantly increased body weight; the body weight of palm^{11}-PrRP31-treated Thy-Tau22 mice stayed unchanged. No significant effect on WAT amount, level of leptin, insulin or glucose was observed.

Table 9 Metabolic parameters of 9-month-old overnight fasted Thy-Tau22 female mice and their age-matched WT controls after 2-month-long palm^{11}-PrRP31 treatment

mice	body weight [g]	white adipose tissue [% body weight]	leptin [ng/ml]	glucose [mmol/l]	insulin [ng/ml]
WT vehicle	23.86 ± 0.36***	2.17 ± 0.13	0.59 ± 0.13	4.55 ± 0.32	0.20 ± 0.03
Thy-Tau22 vehicle	21.47 ± 0.29	2.48 ± 0.13	0.38 ± 0.04	3.88 ± 0.38	0.19 ± 0.01
Thy-Tau22 palm^{11}-PrRP31	21.84 ± 0.24	2.76 ± 0.19	0.52 ± 0.05	4.72 ± 0.39	0.21 ± 0.02

Data are mean ± SEM (n = 12 animals per group). Data were analyzed by 1-way ANOVA with Dunnett post hoc test. Significance is ***P < 0.001 compared to Thy-Tau22 vehicle mice.

4.5.3 Activation of Tau kinases and hyper-phosphorylation of Tau protein at different epitopes after treatment with palm^{11}-PrRP31

Western blot analysis was performed in the hippocampi of vehicle-treated Thy-Tau22 mice and mice treated with palm^{11}-PrRP31. After 2-month-long treatment, significant attenuation of Tau phosphorylation at Ser396 and Ser404 (AD2 antibody) and Thr231 was observed in mice treated with palm^{11}-PrRP31 compared to the vehicle treated group (Fig. 29).

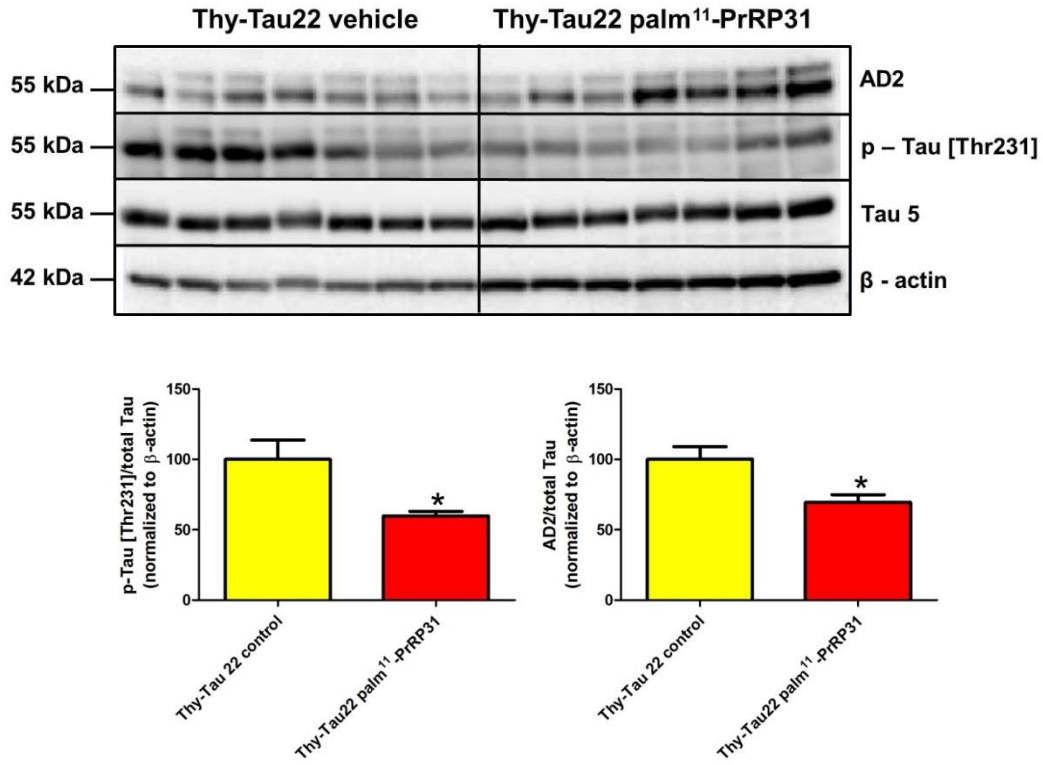

Fig. 29 Western blot analysis of Tau phosphorylation at different epitopes in hippocampi of 9-month-old Thy-Tau22 mice after 2-month-long intervention with palm^{11}-PrRP31

*Phosphorylation of Tau phosphorylation after the palm^{11}-PrRP31 treatment was determined by the method of Western blot (WB) described in chapter 3.3. Data are mean ± SEM, n = 12 animals per group. Statistical analysis was calculated by Student's t-test. Significance is * P < 0.05.*

However, no statistically significant effect on phosphorylation of GSK-3β at its inhibitory Ser9, MAPK/ERK1/2 or JNK, several kinases implicated in Tau phosphorylation, was observed (Fig. 30).

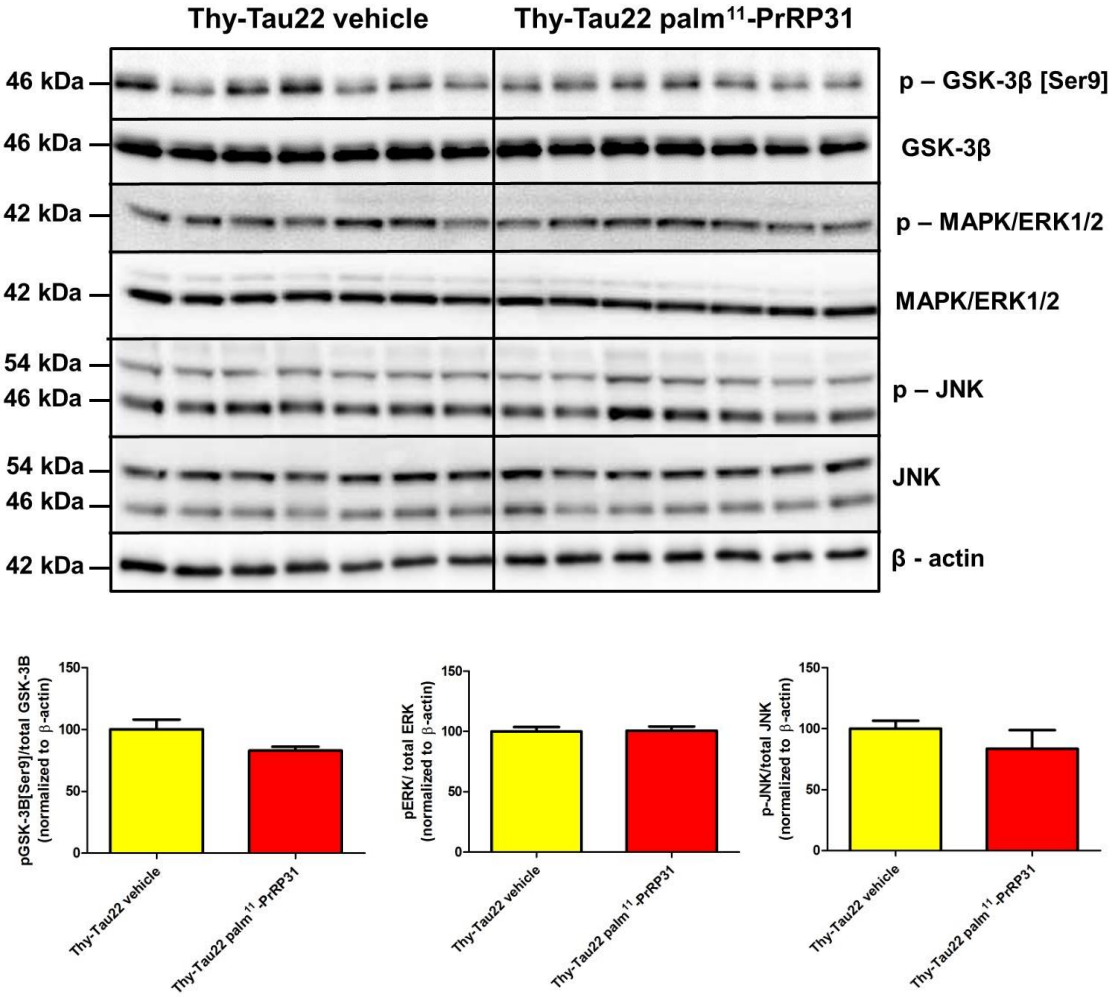

Fig. 30 Western blot analysis of kinases implicated in Tau phosphorylation in hippocampi of 9-month-old Thy-Tau22 mice after 2-month-long intervention with palm^{11}-PrRP31

Phosphorylation of Tau phosphorylation after the palm^{11}-PrRP31 treatment was determined by the method of Western blot (WB) described in chapter 3.3. Data are mean ± SEM, n = 12 animals per group. Statistical analysis was calculated by Student's t-test.

5 DISCUSSION

Obesity and related T2DM, as well as AD, are serious detrimental health complications with increasing prevalence; for example obesity is called ‘the epidemic of the 3rd millennium’. Recently, a close relationship between T2DM and AD development was discovered (Schrijvers et al., 2010), resulting in intensive research of metabolic and pathological changes, such as Tau protein hyper-phosphorylation, synaptic plasticity, or neuroinflammation, which are caused by both diseases in CNS, mainly in the hippocampus, the center of memory and learning. Considering the increasing age of the population, which is another risk factor for AD, it is estimated that there will be about 100 million people suffering from AD in 2050 (Alzheimer's, 2014). Moreover, to date, there is no sufficient AD treatment because the exact mechanisms leading to AD progression are still not fully elucidated. At present, growing evidence shows that insulin-sensitizing agents could be used for AD treatment because their neuroprotective properties, such as memory enhancement (Faivre and Holscher, 2013a), attenuated hyper-phosphorylation of Tau (Yang et al., 2013), or increased synaptic plasticity and neurogenesis (Faivre et al., 2012; Holscher, 2014b), were observed in AD and/or T2DM rodent models .

In my PhD thesis, the pathological changes of Tau protein in the hippocampi of two rodent models of obesity, fa/fa rats and MSG mice, were described. According to the previously mentioned hypothesis, the central insulin resistance, the hallmark of T2DM, attenuates the insulin signaling cascade, which leads to decreased phosphorylation of GSK-3β at Ser9 that is known to inhibit its kinase activity, and consequently hyper-phosphorylation of Tau protein at different epitopes, such as Ser396, or Thr231 (Kim et al., 2009; Liu et al., 2011; Schubert et al., 2004). Later, the beneficial effect of long-term treatment with liraglutide, an anti-T2DM drug with proven neuroprotective properties (Holscher, 2014a), and novel lipidized analogs of PrRP, anorexigenic neuropeptide with a potential neuroprotective effect, on Tau pathology was observed in the hippocampi of obese MSG mice, or Thy-Tau22 AD mice with overexpressed human Tau protein.

5.1 Pathological changes in the hippocampi of obese pre-diabetic rodents

Pre-diabetes is a state preceding T2DM, when insulin resistance is presented but the blood glucose level remains normal. To study the hippocampal phosphorylation state of the Tau protein, one of the hallmarks of AD, in relation to insulin resistance, Zucker fatty (fa/fa) rats at the age of 12 and 33 weeks and obese MSG mice at the age of 2 and 6 months were used.

5.1.1 Metabolic parameters

fa/fa rats used in this experiment, similarly as db/db mice (Kim et al., 2009), have a loss of function mutation of the leptin receptor, which is exhibited by impaired leptin signaling and increased levels of leptin and insulin. The 10-fold increased insulin levels in fa/fa rats compared to normal values indicate peripheral insulin resistance, which was proven by significantly decreased insulin sensitivity determined by the QUICKI test. Peripheral insulin resistance can also be linked to dyslipidemia observed in fa/fa rats already at a young age. In contrast to db/db mice which had a substantially increased glucose level since 8th week of age compared to control mice (Kim et al., 2009), the glucose level remained normal even in 33-week-old fa/fa rats.

MSG administration to newborn mice induced obesity development due to specific lesions in Arc despite the fact that these mice are hypophagic (Matysková et al., 2008). Arc is an important center implicated in food intake regulation; there are neurons producing orexigenic peptides, such as neuropeptide Y (NPY), anorexigenic peptides, such as cocaine- and amphetamine-regulated transcript peptide, as well as leptin receptors important for energy homeostasis control. The disturbances and decreased level of NPY was observed in MSG rats and resulted in hypophagia of MSG mice compared to their controls. In previous experiments, it was proven that MSG-treated mice (Maletínská et al., 2006), as well as hypertensive Koletsky fa/fa rats (Morton et al., 2003), did not respond to leptin administration because of the lack of functional leptin receptor in Arc. This can result in obesity development in MSG treated rodents or rodents with deficient leptin receptor. Non-functional leptin receptor could contribute to development of neurodegenerative changes since leptin is known for its neuroprotective properties (Greco et al., 2009b; Greco et al., 2010), thus, rodent models with non-

functional leptin receptor seem to be convenient for study of the possible neurodegenerative changes.

A significant increase of WAT was observed in MSG mice compared to their controls at both ages, 2 and 6 months, which corresponded with significantly increased levels of leptin. Insulin resistance manifested by an increased level of insulin was observed in MSG mice at both ages, which is in accordance with other studies of the MSG mouse model (Matysková et al., 2008; Olney, 1969). Similarly as fa/fa rats, MSG mice remained normoglycemic, even at the age of 6 months.

Disturbances in glucose, or glucosamine availability are considered as one of the possible mechanisms of Tau hyper-phosphorylation, since it was discovered that decreased GlcNAcylation of Tau protein correlates with increased phosphorylation at serines and threonines (Gong et al., 2006; Liu et al., 2009a; Liu et al., 2009b). Despite this hypothesis, in both used insulin resistant normoglycemic rodent models, fa/fa rats, even only 12-week-old, and MSG mice at the age of 6-month, increased phosphorylation of the Tau protein was observed at Ser396 and Thr231. This supports the hypothesis that insulin resistance rather than increased plasma glucose levels, sign of T2DM, leads to the Tau hyper-phosphorylation.

Both used models of obesity and pre-diabetes, fa/fa rats and MSG mice, developed hyperleptinemia caused by dysfunctional leptin receptor, and hyperinsulinemia, which were more pronounced due to ageing, but stayed normoglycemic even at older age.

5.1.2 Central insulin signaling cascade

Regarding the central insulin signaling cascade in the hippocampi of fa/fa rats the level of IR was reduced compared to controls. The reduced level of IR was also observed in the cortex and hippocampi of AD patients; the reduction could lead to impaired signaling and insulin action in the CNS (Steen et al., 2005). PI3K, and phosphorylation of PDK-1 at Ser241 was consequently significantly decreased in fa/fa rats compared to their controls; PI3K also significantly decreased with ageing. Similarly, increasing age led to reduced phosphorylation of Akt kinase at both epitopes required for full Akt activation: Thr308 and Ser473; more pronounced attenuation of phosphorylation was observed due to the fa/fa phenotype at Ser473. Consequently,

decreased phosphorylation of GSK-3β at Ser9 was observed in fa/fa rats, more pronounced in old fa/fa rats. Similarly, in obese hyperinsulinemic MSG mice, the phosphorylation of GSK-3β at Ser9 was reduced in the hippocampi of 6-month-old mice. We can therefore conclude that in both pre-diabetic models, fa/fa rats and MSG mice, peripheral insulin resistance resulted in central insulin resistance in the hippocampi, and finally to decreased phosphorylation of GSK-3β at inhibitory Ser9.

GSK-3β is the main kinase implicated in the insulin signaling cascade, as well as in Tau phosphorylation; its kinase activity is increased when there is reduced phosphorylation at Ser9 (Sutherland et al., 1993), and it is considered as one of the most potent Tau kinases that phosphorylates different Tau epitopes, predominantly at Ser199, Thr231, Ser396, and Ser413 (Michel et al., 1998). Its increased kinase activity was shown to be the cause of Tau hyper-phosphorylation in different T2DM rodent models (Schubert et al., 2004; Yang et al., 2013), as well as in human study, where impaired central insulin signaling resulted in increased activation of GSK-3β, and consequently to increased phosphorylation of Tau protein in the frontal cortex of T2DM patients; the hyper-phosphorylation was more pronounced in patients with combined T2DM and AD (Liu et al., 2011).

In our studies, the phosphorylation at inhibitory Ser9 of GSK-3β was also one of the first parameters examined in the hippocampi, and in both our models of obesity and pre-diabetes, fa/fa rats and MSG mice, the decreased kinase activity due to reduced phosphorylation of Ser9 served us as the indicator of consequent possible brain neurodegenerative changes, such as Tau protein hyper-phosphorylation.

5.1.3 Tau hyper-phosphorylation in hippocampi

Hyper-phosphorylation of two Tau epitopes, Thr231 and Ser396, important in AD pathology, has been determined; increased phosphorylation of Thr231 reduces the Tau protein ability to bind to microtubules, and Ser396 hyper-phosphorylation turns Tau protein to be more fibrillogenic (Johnson and Stoothoff, 2004). Moreover, Ser396 is directly phosphorylated by GSK-3β without priming-phosphorylation of another serine or threonine of the Tau protein (Leroy et al., 2010), and also a positive correlation between the level of Tau protein phosphorylated at Ser396 in CSF and severity of AD was found in AD patients (Hu et al., 2002). In agreement with predominant epitopes of

Tau protein phosphorylated by GSK-3β, increased Tau protein phosphorylation at Thr231 and Ser396 was observed in the hippocampi of our fa/fa rats, both 12- and 33-week-old compared to their age-matched controls; Ser396 was also more phosphorylated in fa/fa rats due to ageing. In our MSG mice the higher phosphorylation of Tau was observed only in the hippocampi of 6-month-old MSG mice. The same trend of age-dependent increase of Tau hyper-phosphorylation at Thr231 and Ser396 was observed previously in db/db mice (Kim et al., 2009); furthermore, in NIRKO mice with neuron-specific IR deficiency, the increased phosphorylation of Thr231 was observed due to reduced activation of Akt and decreased phosphorylation of GSK-3β at Ser9 (Schubert et al., 2004). Although the level of Tau phosphorylation caused by GSK-3β in MSG and fa/fa rats was different, the increased phosphorylation was observed at both pre-diabetic rodent models and was more pronounced with increasing age of the animals.

Beside the insulin signaling, the role of leptin in AD development has been studied. Deficient leptin signaling could contribute to Tau hyper-phosphorylation since a neuroprotective effect of leptin was observed via activation of AMP-dependent kinase (Greco et al., 2008), leptin dysregulation was suggested to have a detrimental impact on AD development (Bonda et al., 2014), and long-lasting hyperleptinemia was shown to accelerate Tau hyper-phosphorylation in the hippocampi (Koga et al., 2014b). Both obese fa/fa rats and MSG obese mice exhibit hyperleptinemia; fa/fa rats due to the mutated leptin receptor, and MSG mice due to the increased amount of leptin producing WAT and lesions in Arc neurons, containing leptin receptors and being the primary leptin targets (Matysková et al., 2008; Takasaki, 1978). Moreover, recently, obesity rather than insulin resistance was proposed to exacerbate the detrimental effect of DIO on the development of Tau pathology (Leboucher et al., 2013). However, the precise role of leptin signaling and obesity on the Tau pathology, and AD development should be elucidated.

Both used rodent models of obesity, hyperleptinemia, and pre-diabetes used in our studies seem to be suitable models for investigation of brain neurodegenerative changes, as well as for study of the possible intervention that could reduce or prevent the neurodegeneration.

5.2 Lipidization of prolactin-releasing peptide

Centrally acting anorexigenic neuropeptides are promising anti-obesity agents due to their specificity, low toxicity, and few side effects. However, their application as an efficient treatment is problematic since they have low stability, and most of them are unable to cross the BBB. One of these neuropeptides is PrRP. Naturally occurring PrRP is unable to cross the BBB and thus cannot reach its receptor in the hypothalamus and trigger its anorexigenic effect. In our laboratory, several new lipidized analogs of PrRP were designed; this unique modification of PrRP resulted in increased stability in the blood and moreover enabled exerting a central anorexigenic effect of PrRP even when administered peripherally.

As we have shown in our previous study (Maletinska et al., 2011), for the proper PrRP biological function the C-terminal part of the molecule is crucial. The aromatic ring at position 31 bound on CH_2 linker is required for binding to the receptor, since the change of phenylalanine to phenylglycine or to non-aromatic cyklohexylalanin resulted in loss of the binding affinity and anorexigenic effect of PrRP. Therefore, the lipidization with fatty acids of different lengths from C8 to C18 was performed at the N-terminal part of the PrRP31 molecule, namely at Ser^1 or Lys^{11}, where γ-glutamic acid was used as a linker for the fatty acid. All prepared analogs showed similar binding affinity to GPR-10 receptor; however, only the analogs lipidized with palmitoyl (C16), either at Ser^1 or at Lys^{11}, or stearyl (C18) groups significantly lowered the food intake in lean over-night fasted mice after peripheral administration. This anorexigenic effect indicates that peripherally administered lipidized PrRP analogs are probably able to cross the BBB and act centrally. This was confirmed by immunohistochemical staining of c-Fos, an early gene protein product specific of activated neurons, in food intake-regulating nuclei of the hypothalamus, or brainstem (Maletinska et al., 2015), where c-Fos immunoreactivity was enhanced after peripheral administration of peptides with C14 fatty acids or longer, whereas shorter octanoylated or natural PrRP did not induce the c-Fos reactivity. Considering the fact that the central effect of anti-T2DM drug liraglutide, a promising neuroprotective agent, whose beneficial effect on AD hallmarks was proven in several mouse models of AD and/or T2DM (Han et al., 2013; Holscher, 2014a; McClean et al., 2011; McClean and Holscher, 2014a; Porter et al., 2010) and that is now in clinical phase II as a possible AD treatment, is exclusively anorexigenic,

this brings us to the assumption that anorexigenic neuropeptide PrRP could have similar neuroprotective properties. This assumption is supported by our finding of GPR10 receptor in the stratum lacunosum-moleculare of the CA1 subfield of the hippocampus, where extensive amyloid deposits were localized (Su and Ni, 1998), and in the hilus of dentate gyrus in the mouse brain. PrRP production in the hypothalamus is controlled by neuroprotective leptin, and the anorexigenic effect of PrRP is synergistic when co-administered with leptin (Ellacott et al., 2002). In long-lasting 14-day treatment of DIO obese mice with palm-PrRP31 at a dose of 5 mg/kg SC injected twice a day, a significant reduction of food intake and body weight, was observed, thus confirming the long-lasting anorexigenic effect of this lipidized analog of PrRP31 (Maletinska et al., 2015). The same 14-day-long treatment with palm-PrRP31 was therefore chosen as an appropriately long intervention with a possible effect on neurodegenerative changes, such as Tau protein hyper-phosphorylation, in 6-month-old MSG-obese mice.

5.3 Effect of long-term treatment with anorexigenic compounds on Tau protein phosphorylation and spatial memory

My PhD thesis for the first time examined the effect of anorexigenic PrRP analogs on the development of Tau pathology in the hippocampi of 6-month-old obese pre-diabetic MSG mice and 7-month-old Thy-Tau22 mice, an AD-like Tau pathology mouse model.

5.3.1 Fourteen-day-long treatment of 6-month-old MSG mice with liraglutide or palm-PrRP31

As described previously in chapter 4.2.2, in the hippocampi of MSG mice, decreased phosphorylation of GSK-3β at Ser9 and increased phosphorylation of Tau at Thr231 and Ser396 was observed. The effect of neuroprotective liraglutide was also tested and served as a positive control because of its known beneficial effects on spatial memory, hippocampal long-term potentiation, neurogenesis, reduction of amyloid plaques, as well as attenuating phosphorylation of Tau at different epitopes (Han et al., 2013; Hunter and Holscher, 2012; McClean et al., 2011; McClean and Holscher, 2014a; Porter et al., 2010; Yang et al., 2013).

Both anorexigenic peptides were injected SC twice a day, and the weight and food intake was measured. The treatment resulted in significantly decreased food intake in comparison with the saline-treated mice that served as a control group. On the other hand, the body weight loss did not differ significantly because it seems that MSG obese mice are extremely sensitive to daily manipulation, and therefore saline-treated mice also lost weight. Regarding the metabolic parameters after the treatment, there were no significant differences, either in mice treated with liraglutide or with palm-PrRP31; only a non-significant decrease of WAT and the leptin level were observed. In IPGTT performed on day 9 of the treatment, only a significant decrease in glucose was observed in palm-PrRP31-treated mice compared to saline-treated group 180 min after the glucose load. It seems that palm-PrRP31 could have anti-diabetic properties nevertheless, its insulin-sensitizing action should be examined more precisely by a hyperinsulinemic-euglycemic clamp and also in longer-lasting treatment.

In hippocampi of 6-month-old MSG mice, the 14-day-long treatment either with liraglutide or palm-PrRP31 resulted in enhancement of the insulin signaling cascade, which was manifested by increased phosphorylation of examined kinases implicated in the insulin signaling cascade, such as p-PDK-1 at Ser241 after palm-PrRP31 and p-Akt at Thr308 after liraglutide treatment. The enhanced activation of the insulin signaling cascade by liraglutide and palm-PrRP led to increased phosphorylation of GSK-3β at inhibitory Ser9, thus decreasing its kinase activity. A similar trend was observed in rats with T2DM, where the 4-week-long liraglutide treatment also reduced GSK-3β activity by enhanced the insulin signaling cascade (Yang et al., 2013), or in AD mouse model where liraglutide treatment resulted in improvement of insulin signaling cascade effectiveness by decreased phosphorylation at Ser616 of IRS-1 (Long-Smith et al., 2013).

Beside the decreased activation of GSK-3β, one of the most potent kinases implicated in Tau hyper-phosphorylation, the treatment with palm-PrRP31 and liraglutide led to decreased phosphorylation, and thus to decreased kinase activity, of two other important Tau kinases, JNK and MAPK/ERK1/2. Similar attenuated activity of JNK was observed after treatment with other anti-diabetic drugs, such as metformin administered to db/db mice (Li et al., 2012a) or exenatide in APP/PS1 mouse model (Bomfim et al., 2012). All these kinases are known to directly phosphorylate Tau

protein at epitopes Thr212, Thr231, and Ser396, the sites which are important in Tau pathology. Analogously, in our study, after the 14-day-long SC treatment with both peptides, attenuated phosphorylation of Tau at epitopes Thr231 and Ser396 was observed in the hippocampi of MSG mice, probably due to decreased activation of the mentioned kinases. Palm-PrRP31 also attenuated phosphorylation at Thr212.

5.3.2 Two-month-long treatment with palm^{11}-PrRP31 of Thy-Tau22 mice

Because of the beneficial effect of palm-PrRP31 on the attenuation of hyper-phosphorylation of Tau protein in MSG obese mice we decided to test the effect of another, more potent analog of PrRP31 called palm^{11}-PrRP on the Tau pathology in the Thy-Tau22 mouse model, a model of AD-like Tau pathology (Schindowski et al., 2006). To avoid the stress of animals by everyday manipulation and injection, palm^{11}-PrRP at the dose 5 mg/kg/day was SC administered for two months by Alzet® osmotic pumps, which are certified to pump a defined volume of liquid per day. Pumps were implanted in short-term ether anesthesia, whose advantage is fast recovering of mice after surgery, and they were changed after one month of the treatment. The short-term anesthesia did not significantly reduce either the food intake or body weight of the animals. At the end of the experiment, the metabolic parameters of Thy-Tau22 mice and their age-matched WT controls were measured. Except for the body weight, which is known to be decreased in Thy-Tau22 mice compared to their controls (Leboucher et al., 2013), there were no significant differences in the level of WAT, glucose, leptin, or insulin in the Thy-Tau22-vehicle group compared to WT animals which is in accordance with the experiments performed by Leboucher (Leboucher et al., 2013). The 2-month-long palm^{11}-PrRP31 treatment did not result in significant changes in any measured metabolic parameter. Since Thy-Tau22 mice are not known to have any metabolic disturbances, such as hyperleptinemia or hyperinsulinemia, the data are not surprising (Leboucher et al., 2013).

Before beginning the interventions, the spatial memory was tested using Y-maze. In several previous experiments with Thy-Tau22 mice, an impaired memory in Morris water maze or Y-maze was observed (Van der Jeugd et al., 2013). In our experiment, 7-month-old Thy-Tau22 females also had significantly impaired spatial memory compared to the control WT group. The 2-month-long treatment with palm^{11}-PrRP31

resulted in spatial memory improvement when compared to the Thy-Tau22-vehicle-treated group. The memory impairment could be caused by Tau hyper-phosphorylation, mainly in the hippocampus, the center of memory and learning, which was observed in several AD models including Thy-Tau22 mice (Koga et al., 2014a; Schindowski et al., 2006). Corresponding to these finding, the treatment with palm^{11}-PrRP31 resulted in significantly attenuated Tau phosphorylation at epitopes Thr231, Ser396 and Ser404, the sites important in AD progression (Johnson and Stoothoff, 2004). However, the mechanism of action of palm^{11}-PrRP31 remains to be clarified, because no significant differences were observed in the phosphorylation state of the most important kinases implicated in Tau phosphorylation, such as GSK-3β, JNK, or MAPK/ERK1/2. Our presented results obtained in Thy-Tau22 serve as preliminary results for further studies that we plan to perform. Since liraglutide is known to improve spatial memory in other AD mouse models (the APP/PS1 mice) by increased neurogenesis and hippocampal synaptic plasticity (McClean et al., 2011), there is the possibility that palmitoylated analogs of PrRP should have similar neuroprotective properties because both lipidized peptides are anorexigenic, and regarding our study with MSG mice, it seems that both peptides have a similar mechanism of action. To verify the effect of lipidized PrRP31 on Aβ and amyloid deposits, which are known to be decreased after liraglutide treatment (Han et al., 2013; McClean and Holscher, 2014a), we plan to perform long-term treatment with lipidized PrRP in the APP/PS1 AD model.

5.4 Models of T2DM and AD-like Tau pathology and possible treatment: conclusions and perspectives

Beside the increasing age, the most important risk factor for AD development, obesity, caused mainly by unhealthy and sedentary life style, and its related complications, such as leptin and insulin resistance, T2DM, or increased level of pro-inflammatory cytokines, were characterized as important risk factors for development of neurodegenerative changes in the brain (Burdge and Calder, 2005; Greenberg and Obin, 2006). The detrimental effect of obesity caused by feeding with HFD on spatial memory, and progression of amyloid plaques and hyper-phosphorylation of Tau protein, the hallmarks of AD, were observed in different animal models of T2DM or AD (Leboucher et al., 2013; Porter et al., 2010; Ramos-Rodriguez et al., 2014). Moreover,

the increased body mass index in adults, indicator of obesity, was connected with late onset of dementia in a recent epidemiological study (Emmerzaal et al., 2015). Nevertheless, the exact pathophysiological mechanisms of neurodegeneration are still not fully understood.

Collectively, the combination of increasing prevalence of obesity, T2DM and ageing of general population calls for novel approaches able to prevent or postpone the onset of neurodegenerative diseases or slow their progression. Due to the close relationship between AD development and insulin resistance/T2DM (Schrijvers et al., 2010), the insulin-sensitizing compounds were suggested to have neuroprotective properties. GIP and GLP-1 are incretin hormones, compounds enhancing insulin secretion; both of them, as well as their more stable analogs, were shown to have beneficial effects on impaired spatial memory, amyloid plaque formation, and hyper-phosphorylation of Tau protein (Abbas et al., 2009; Bomfim et al., 2012; Faivre et al., 2012; Faivre and Holscher, 2013a; Han et al., 2013; Holscher, 2014a; Holscher, 2014b; Li et al., 2012b; Long-Smith et al., 2013; McClean and Holscher, 2014b; Porter et al., 2010; Porter et al., 2011; Yang et al., 2013). Liraglutide, stable analog of GLP-1 and most used anti-T2DM drug, is in the clinical phase as a potential AD treatment (Holscher, 2014a). Since in CNS liraglutide has an exclusively anorexigenic effect (Sisley et al., 2014), we decided to test the neuroprotective properties of other anorexigenic compounds, namely lipidized analogs of PrRP31. In our experiments we proved that palmitoylated analogs of PrRP31, similarly as liraglutide, improved the spatial memory in Y-maze, enhanced the central insulin signaling cascade resulting in decreased activation of GSK-3β, the main kinase implicated in Tau protein hyper-phosphorylation, and attenuated hyper-phosphorylation of Tau protein at different epitopes. These findings make anorexigenic compounds promising candidates for AD treatment. However, the exact mechanism of PrRP31 action is not fully understood, and we therefore plan to perform long-term treatment with our new lipidized analogs of PrRP31 in AD mouse models combined with DIO, such as APP/PS1 mice and Thy-Tau22 mice, and examine their effect on AD pathology progression.

Our studies confirmed the hypothesis that anti-diabetic and additionally anorexigenic compounds could be used as a future effective therapy for Alzheimer's disease and other neurological disorders. However, the exact mechanism leading to the

beneficial neuroprotective effects of these compounds has to be investigated and elucidated.

6 CONCLUSIONS

- In both models of obesity and pre-diabetes, fa/fa rats and MSG mice, examined in my PhD thesis, decreased phosphorylation of the insulin signaling cascade was observed, resulting in decreased phosphorylation, and thus increased kinase activity, of GSK-3β at inhibitory Ser9. Consequently, increased phosphorylation of Tau protein at different epitopes, such as Ser396, or Thr231, the epitopes phosphorylated by GSK-3β, were detected. Considering the normoglycemic state of the animals and pre-diabetes with increased insulin levels, we can conclude that insulin resistance, rather than increased glucose blood level, is associated with hyper-phosphorylation of Tau protein, the hallmark of AD.
- We designed and tested lipidized prolactin releasing peptide 31 (PrRP31) analogs. Lipidization of PrRP31 did not influence its affinity to its receptor in competitive binding experiments. Moreover, the food intake after acute peripheral SC injection of lipidized analogs of PrRP31 was significantly decreased which indicates that lipidization enabled PrRP31 to cross the blood-brain barrier, and thus to exert its central anorexigenic effect. These findings suggest the possible utilization of lipidized analogs of PrRP31 as effective anti-obesity therapeutics.
- Fourteen-day-long treatment of 6-months-old MSG obese mice with palmitoylated analog of PrRP31 and liraglutide resulted in enhanced activation of the central insulin signaling cascade, decreased activation of GSK-3β, as well as MAPK/ERK1/2 and JNK, other potent kinases implicated in Tau hyper-phosphorylation, and attenuated phosphorylation of Tau protein at different epitopes. Attenuated phosphorylation of the Tau protein was also observed in the Thy-Tau22 mice, model of AD-like Tau pathology, after 2-month-long treatment with another potent analog, palm^{11}-PrRP31. The exact mechanism of PrRP31 action has to be elucidated; nevertheless, our findings indicate that anorexigenic compounds have potential neuroprotective properties and could be used in the future as a possible treatment of neurological disorders.

7 REFERENCES

Abbas, T., Faivre, E., Holscher, C., 2009. Impairment of synaptic plasticity and memory formation in GLP-1 receptor KO mice: Interaction between type 2 diabetes and Alzheimer's disease. Behav Brain Res. 205**,** 265-71.

Alonso, A.D., Di Clerico, J., Li, B., Corbo, C.P., Alaniz, M.E., Grundke-Iqbal, I., Iqbal, K., 2010. Phosphorylation of tau at Thr212, Thr231, and Ser262 combined causes neurodegeneration. J Biol Chem. 285**,** 30851-60.

Alvarez, A., Munoz, J.P., Maccioni, R.B., 2001. A Cdk5-p35 stable complex is involved in the beta-amyloid-induced deregulation of Cdk5 activity in hippocampal neurons. Exp Cell Res. 264**,** 266-74.

Alzheimer's, A., 2014. 2014 Alzheimer's disease facts and figures. Alzheimers Dement. 10**,** e47-92.

Andersson, C., Blennow, K., Almkvist, O., Andreasen, N., Engfeldt, P., Johansson, S.E., Lindau, M., Eriksdotter-Jonhagen, M., 2008. Increasing CSF phospho-tau levels during cognitive decline and progression to dementia. Neurobiol Aging. 29**,** 1466-73.

Arendash, G.W., King, D.L., Gordon, M.N., Morgan, D., Hatcher, J.M., Hope, C.E., Diamond, D.M., 2001. Progressive, age-related behavioral impairments in transgenic mice carrying both mutant amyloid precursor protein and presenilin-1 transgenes. Brain Res. 891**,** 42-53.

Arnoldussen, I.A., Kiliaan, A.J., Gustafson, D.R., 2014. Obesity and dementia: adipokines interact with the brain. Eur Neuropsychopharmacol. 24**,** 1982-99.

Atzori, C., Ghetti, B., Piva, R., Srinivasan, A.N., Zolo, P., Delisle, M.B., Mirra, S.S., Migheli, A., 2001. Activation of the JNK/p38 pathway occurs in diseases characterized by tau protein pathology and is related to tau phosphorylation but not to apoptosis. J Neuropathol Exp Neurol. 60**,** 1190-7.

Banks, W.A., Owen, J.B., Erickson, M.A., 2012. Insulin in the brain: there and back again. Pharmacol Ther. 136**,** 82-93.

Bjursell, M., Lenneras, M., Goransson, M., Elmgren, A., Bohlooly, Y.M., 2007. GPR10 deficiency in mice results in altered energy expenditure and obesity. Biochem Biophys Res Commun. 363**,** 633-8.

Blechova, M., Nagelova, V., Zakova, L., Demianova, Z., Zelezna, B., Maletinska, L., 2013. New analogs of the CART peptide with anorexigenic potency: the importance of individual disulfide bridges. Peptides. 39**,** 138-44.

Bomba, M., Ciavardelli, D., Silvestri, E., Canzoniero, L.M., Lattanzio, R., Chiappini, P., Piantelli, M., Di Ilio, C., Consoli, A., Sensi, S.L., 2013. Exenatide promotes cognitive enhancement and positive brain metabolic changes in PS1-KI mice but has no effects in 3xTg-AD animals. Cell Death Dis. 4**,** e612.

Bomfim, T.R., Forny-Germano, L., Sathler, L.B., Brito-Moreira, J., Houzel, J.C., Decker, H., Silverman, M.A., Kazi, H., Melo, H.M., McClean, P.L., Holscher, C., Arnold, S.E., Talbot, K., Klein, W.L., Munoz, D.P., Ferreira, S.T., De Felice, F.G., 2012. An anti-diabetes agent protects the mouse brain from defective insulin signaling caused by Alzheimer's disease- associated Abeta oligomers. J Clin Invest. 122**,** 1339-53.

Bonda, D.J., Stone, J.G., Torres, S.L., Siedlak, S.L., Perry, G., Kryscio, R., Jicha, G., Casadesus, G., Smith, M.A., Zhu, X., Lee, H.G., 2014. Dysregulation of leptin signaling in Alzheimer disease: evidence for neuronal leptin resistance. J Neurochem. 128**,** 162-72.

Borchelt, D.R., 1998. Metabolism of presenilin 1: influence of presenilin 1 on amyloid precursor protein processing. Neurobiol Aging. 19**,** S15-8.

Boyle, R., Downham, R., Ganguly, T., Humphries, J., Smith, J., Travers, S., 2005. Structure-activity studies on prolactin-releasing peptide (PrRP). Analogues of PrRP-(19-31)-peptide. J Pept Sci. 11**,** 161-5.

Braak, H., Thal, D.R., Ghebremedhin, E., Del Tredici, K., 2011. Stages of the pathologic process in Alzheimer disease: age categories from 1 to 100 years. J Neuropathol Exp Neurol. 70**,** 960-9.

Buee, L., Bussiere, T., Buee-Scherrer, V., Delacourte, A., Hof, P.R., 2000. Tau protein isoforms, phosphorylation and role in neurodegenerative disorders. Brain Res Brain Res Rev. 33**,** 95-130.

Buettner, R., Scholmerich, J., Bollheimer, L.C., 2007. High-fat diets: modeling the metabolic disorders of human obesity in rodents. Obesity (Silver Spring). 15**,** 798-808.

Burdge, G.C., Calder, P.C., 2005. Plasma cytokine response during the postprandial period: a potential causal process in vascular disease? Br J Nutr. 93**,** 3-9.

Cai, H., Cong, W.N., Ji, S., Rothman, S., Maudsley, S., Martin, B., 2012. Metabolic dysfunction in Alzheimer's disease and related neurodegenerative disorders. Curr Alzheimer Res. 9**,** 5-17.

Cai, H.Y., Holscher, C., Yue, X.H., Zhang, S.X., Wang, X.H., Qiao, F., Yang, W., Qi, J.S., 2014. Lixisenatide rescues spatial memory and synaptic plasticity from amyloid beta protein-induced impairments in rats. Neuroscience. 277**,** 6-13.

D'Amico, M., Di Filippo, C., Marfella, R., Abbatecola, A.M., Ferraraccio, F., Rossi, F., Paolisso, G., 2010. Long-term inhibition of dipeptidyl peptidase-4 in Alzheimer's prone mice. Exp Gerontol. 45**,** 202-7.

de la Monte, S.M., Wands, J.R., 2008. Alzheimer's disease is type 3 diabetes-evidence reviewed. J Diabetes Sci Technol. 2**,** 1101-13.

Doble, B.W., Woodgett, J.R., 2003. GSK-3: tricks of the trade for a multi-tasking kinase. J Cell Sci. 116**,** 1175-86.

Drucker, D.J., 2006. The biology of incretin hormones. Cell Metab. 3**,** 153-65.

Drucker, D.J., Nauck, M.A., 2006. The incretin system: glucagon-like peptide-1 receptor agonists and dipeptidyl peptidase-4 inhibitors in type 2 diabetes. Lancet. 368**,** 1696-705.

Durham, H.A., Truett, G.E., 2006. Development of insulin resistance and hyperphagia in Zucker fatty rats. Am J Physiol Regul Integr Comp Physiol. 290**,** R652-8.

During, M.J., Cao, L., Zuzga, D.S., Francis, J.S., Fitzsimons, H.L., Jiao, X., Bland, R.J., Klugmann, M., Banks, W.A., Drucker, D.J., Haile, C.N., 2003. Glucagon-like peptide-1 receptor is involved in learning and neuroprotection. Nat Med. 9**,** 1173-9.

Ekinci, F.J., Shea, T.B., 1999. Hyperactivation of mitogen-activated protein kinase increases phospho-tau immunoreactivity within human neuroblastoma: additive and synergistic influence of alteration of additional kinase activities. Cell Mol Neurobiol. 19**,** 249-60.

Elefteriou, F., Takeda, S., Liu, X., Armstrong, D., Karsenty, G., 2003. Monosodium glutamate-sensitive hypothalamic neurons contribute to the control of bone mass. Endocrinology. 144**,** 3842-7.

Ellacott, K.L., Lawrence, C.B., Rothwell, N.J., Luckman, S.M., 2002. PRL-releasing peptide interacts with leptin to reduce food intake and body weight. Endocrinology. 143**,** 368-74.

Ellacott, K.L., Lawrence, C.B., Pritchard, L.E., Luckman, S.M., 2003. Repeated administration of the anorectic factor prolactin-releasing peptide leads to tolerance to its effects on energy homeostasis. Am J Physiol Regul Integr Comp Physiol. 285**,** R1005-10.

Elmquist, J.K., Bjorbaek, C., Ahima, R.S., Flier, J.S., Saper, C.B., 1998. Distributions of leptin receptor mRNA isoforms in the rat brain. J Comp Neurol. 395**,** 535-47.

Emmerzaal, T.L., Kiliaan, A.J., Gustafson, D.R., 2015. 2003-2013: a decade of body mass index, Alzheimer's disease, and dementia. J Alzheimers Dis. 43**,** 739-55.

Fain, J.N., Kovacev, V.P., Scow, R.O., 1965. Effect of growth hormone and dexamethasone on lipolysis and metabolism in isolated fat cells of the rat. J Biol Chem. 240**,** 3522-9.

Faivre, E., Hamilton, A., Holscher, C., 2012. Effects of acute and chronic administration of GIP analogues on cognition, synaptic plasticity and neurogenesis in mice. Eur J Pharmacol. 674**,** 294-306.

Faivre, E., Holscher, C., 2013a. D-Ala2GIP facilitated synaptic plasticity and reduces plaque load in aged wild type mice and in an Alzheimer's disease mouse model. J Alzheimers Dis. 35**,** 267-83.

Faivre, E., Holscher, C., 2013b. Neuroprotective effects of D-Ala(2)GIP on Alzheimer's disease biomarkers in an APP/PS1 mouse model. Alzheimers Res Ther. 5**,** 20.

Fan, Y., Resnick, S.M., Wu, X., Davatzikos, C., 2008. Structural and functional biomarkers of prodromal Alzheimer's disease: a high-dimensional pattern classification study. Neuroimage. 41**,** 277-85.

Fox, N.C., Freeborough, P.A., Rossor, M.N., 1996. Visualisation and quantification of rates of atrophy in Alzheimer's disease. Lancet. 348**,** 94-7.

Fujiwara, K., Matsumoto, H., Yada, T., Inoue, K., 2005. Identification of the prolactin-releasing peptide-producing cell in the rat adrenal gland. Regul Pept. 126**,** 97-102.

Gault, V.A., Flatt, P.R., O'Harte, F.P., 2003. Glucose-dependent insulinotropic polypeptide analogues and their therapeutic potential for the treatment of obesity-diabetes. Biochem Biophys Res Commun. 308**,** 207-13.

Gengler, S., McClean, P.L., McCurtin, R., Gault, V.A., Holscher, C., 2012. Val(8)GLP-1 rescues synaptic plasticity and reduces dense core plaques in APP/PS1 mice. Neurobiol Aging. 33**,** 265-76.

Giordano, V., Peluso, G., Iannuccelli, M., Benatti, P., Nicolai, R., Calvani, M., 2007. Systemic and brain metabolic dysfunction as a new paradigm for approaching Alzheimer's dementia. Neurochem Res. 32**,** 555-67.

Goedert, M., Spillantini, M.G., Jakes, R., Rutherford, D., Crowther, R.A., 1989. Multiple isoforms of human microtubule-associated protein tau: sequences and localization in neurofibrillary tangles of Alzheimer's disease. Neuron. 3**,** 519-26.

Goedert, M., Spillantini, M.G., 2006. A century of Alzheimer's disease. Science. 314**,** 777-81.

Gong, C.X., Liu, F., Grundke-Iqbal, I., Iqbal, K., 2006. Impaired brain glucose metabolism leads to Alzheimer neurofibrillary degeneration through a decrease in tau O-GlcNAcylation. J Alzheimers Dis. 9**,** 1-12.

Gotz, J., Ittner, L.M., Lim, Y.A., 2009. Common features between diabetes mellitus and Alzheimer's disease. Cell Mol Life Sci. 66**,** 1321-5.

Greco, S.J., Sarkar, S., Johnston, J.M., Zhu, X., Su, B., Casadesus, G., Ashford, J.W., Smith, M.A., Tezapsidis, N., 2008. Leptin reduces Alzheimer's disease-related tau phosphorylation in neuronal cells. Biochem Biophys Res Commun. 376**,** 536-41.

Greco, S.J., Sarkar, S., Casadesus, G., Zhu, X., Smith, M.A., Ashford, J.W., Johnston, J.M., Tezapsidis, N., 2009a. Leptin inhibits glycogen synthase kinase-3beta to prevent tau phosphorylation in neuronal cells. Neurosci Lett. 455**,** 191-4.

Greco, S.J., Sarkar, S., Johnston, J.M., Tezapsidis, N., 2009b. Leptin regulates tau phosphorylation and amyloid through AMPK in neuronal cells. Biochem Biophys Res Commun. 380**,** 98-104.

Greco, S.J., Bryan, K.J., Sarkar, S., Zhu, X., Smith, M.A., Ashford, J.W., Johnston, J.M., Tezapsidis, N., Casadesus, G., 2010. Leptin reduces pathology and improves memory in a transgenic mouse model of Alzheimer's disease. J Alzheimers Dis. 19**,** 1155-67.

Greenberg, A.S., Obin, M.S., 2006. Obesity and the role of adipose tissue in inflammation and metabolism. Am J Clin Nutr. 83**,** 461S-465S.

Grundke-Iqbal, I., Iqbal, K., Quinlan, M., Tung, Y.C., Zaidi, M.S., Wisniewski, H.M., 1986a. Microtubule-associated protein tau. A component of Alzheimer paired helical filaments. J Biol Chem. 261**,** 6084-9.

Grundke-Iqbal, I., Iqbal, K., Tung, Y.C., Quinlan, M., Wisniewski, H.M., Binder, L.I., 1986b. Abnormal phosphorylation of the microtubule-associated protein tau (tau) in Alzheimer cytoskeletal pathology. Proc Natl Acad Sci U S A. 83**,** 4913-7.

Gu, W., Geddes, B.J., Zhang, C., Foley, K.P., Stricker-Krongrad, A., 2004. The prolactin-releasing peptide receptor (GPR10) regulates body weight homeostasis in mice. J Mol Neurosci. 22**,** 93-103.

Gupta, A., Bisht, B., Dey, C.S., 2011. Peripheral insulin-sensitizer drug metformin ameliorates neuronal insulin resistance and Alzheimer's-like changes. Neuropharmacology. 60**,** 910-20.

Hampel, H., Lista, S., Teipel, S.J., Garaci, F., Nistico, R., Blennow, K., Zetterberg, H., Bertram, L., Duyckaerts, C., Bakardjian, H., Drzezga, A., Colliot, O., Epelbaum, S., Broich, K., Lehericy, S., Brice, A., Khachaturian, Z.S., Aisen, P.S., Dubois, B., 2014. Perspective on future role of biological markers in clinical therapy trials of Alzheimer's disease: a long-range point of view beyond 2020. Biochem Pharmacol. 88**,** 426-49.

Han, W.N., Holscher, C., Yuan, L., Yang, W., Wang, X.H., Wu, M.N., Qi, J.S., 2013. Liraglutide protects against amyloid-beta protein-induced impairment of spatial learning and memory in rats. Neurobiol Aging. 34**,** 576-88.

Hansen, H.H., Fabricius, K., Barkholt, P., Niehoff, M.L., Morley, J.E., Jelsing, J., Pyke, C., Bjerre Knudsen, L., Farr, S.A., Vrang, N., 2015. The GLP-1 Receptor Agonist Liraglutide Improves Memory Function and Increases Hippocampal CA1 Neuronal Numbers in a Senescence-Accelerated Mouse Model of Alzheimer's Disease. J Alzheimers Dis.

Hassing, L.B., Dahl, A.K., Thorvaldsson, V., Berg, S., Gatz, M., Pedersen, N.L., Johansson, B., 2009. Overweight in midlife and risk of dementia: a 40-year follow-up study. Int J Obes (Lond). 33**,** 893-8.

Havrankova, J., Roth, J., Brownstein, M., 1978a. Insulin receptors are widely distributed in the central nervous system of the rat. Nature. 272**,** 827-9.

Havrankova, J., Schmechel, D., Roth, J., Brownstein, M., 1978b. Identification of insulin in rat brain. Proc Natl Acad Sci U S A. 75**,** 5737-41.

Hettich, M.M., Matthes, F., Ryan, D.P., Griesche, N., Schroder, S., Dorn, S., Kraubeta, S., Ehninger, D., 2014. The anti-diabetic drug metformin reduces BACE1 protein level by interfering with the MID1 complex. PLoS One. 9**,** e102420.

Hinke, S.A., Manhart, S., Pamir, N., Demuth, H., R, W.G., Pederson, R.A., McIntosh, C.H., 2001. Identification of a bioactive domain in the amino-terminus of glucose-dependent insulinotropic polypeptide (GIP). Biochim Biophys Acta. 1547**,** 143-55.

Hinuma, S., Habata, Y., Fujii, R., Kawamata, Y., Hosoya, M., Fukusumi, S., Kitada, C., Masuo, Y., Asano, T., Matsumoto, H., Sekiguchi, M., Kurokawa, T., Nishimura, O., Onda, H., Fujino, M., 1998. A prolactin-releasing peptide in the brain. Nature. 393**,** 272-6.

Holcomb, L., Gordon, M.N., McGowan, E., Yu, X., Benkovic, S., Jantzen, P., Wright, K., Saad, I., Mueller, R., Morgan, D., Sanders, S., Zehr, C., O'Campo, K., Hardy, J., Prada, C.M., Eckman, C., Younkin, S., Hsiao, K., Duff, K., 1998. Accelerated Alzheimer-type phenotype in transgenic mice carrying both mutant amyloid precursor protein and presenilin 1 transgenes. Nat Med. 4**,** 97-100.

Holscher, C., Li, L., 2010. New roles for insulin-like hormones in neuronal signalling and protection: new hopes for novel treatments of Alzheimer's disease? Neurobiol Aging. 31**,** 1495-502.

Holscher, C., 2014a. Central effects of GLP-1: new opportunities for treatments of neurodegenerative diseases. J Endocrinol. 221**,** T31-41.

Holscher, C., 2014b. The incretin hormones glucagonlike peptide 1 and glucose-dependent insulinotropic polypeptide are neuroprotective in mouse models of Alzheimer's disease. Alzheimers Dement. 10**,** S47-54.

Hu, Y.Y., He, S.S., Wang, X., Duan, Q.H., Grundke-Iqbal, I., Iqbal, K., Wang, J., 2002. Levels of nonphosphorylated and phosphorylated tau in cerebrospinal fluid of Alzheimer's disease patients : an ultrasensitive bienzyme-substrate-recycle enzyme-linked immunosorbent assay. Am J Pathol. 160**,** 1269-78.

Hunter, K., Holscher, C., 2012. Drugs developed to treat diabetes, liraglutide and lixisenatide, cross the blood brain barrier and enhance neurogenesis. BMC Neurosci. 13**,** 33.

Chan, D., Fox, N.C., Jenkins, R., Scahill, R.I., Crum, W.R., Rossor, M.N., 2001. Rates of global and regional cerebral atrophy in AD and frontotemporal dementia. Neurology. 57**,** 1756-63.

Chapman, P.F., White, G.L., Jones, M.W., Cooper-Blacketer, D., Marshall, V.J., Irizarry, M., Younkin, L., Good, M.A., Bliss, T.V., Hyman, B.T., Younkin, S.G., Hsiao, K.K., 1999. Impaired synaptic plasticity and learning in aged amyloid precursor protein transgenic mice. Nat Neurosci. 2**,** 271-6.

Chen, H., Charlat, O., Tartaglia, L.A., Woolf, E.A., Weng, X., Ellis, S.J., Lakey, N.D., Culpepper, J., Moore, K.J., Breitbart, R.E., Duyk, G.M., Tepper, R.I., Morgenstern, J.P., 1996. Evidence that the diabetes gene encodes the leptin receptor: identification of a mutation in the leptin receptor gene in db/db mice. Cell. 84**,** 491-5.

Chen, S., Liu, A.R., An, F.M., Yao, W.B., Gao, X.D., 2012. Amelioration of neurodegenerative changes in cellular and rat models of diabetes-related Alzheimer's disease by exendin-4. Age (Dordr). 34**,** 1211-24.

Chen, Y., Zhou, K., Wang, R., Liu, Y., Kwak, Y.D., Ma, T., Thompson, R.C., Zhao, Y., Smith, L., Gasparini, L., Luo, Z., Xu, H., Liao, F.F., 2009. Antidiabetic drug metformin (GlucophageR) increases biogenesis of Alzheimer's amyloid peptides via up-regulating BACE1 transcription. Proc Natl Acad Sci U S A. 106**,** 3907-12.

Cheng, Y., Prusoff, W.H., 1973. Relationship between the inhibition constant (K1) and the concentration of inhibitor which causes 50 per cent inhibition (I50) of an enzymatic reaction. Biochem Pharmacol. 22**,** 3099-108.

Cho, J.H., Johnson, G.V., 2004. Primed phosphorylation of tau at Thr231 by glycogen synthase kinase 3beta (GSK3beta) plays a critical role in regulating tau's ability to bind and stabilize microtubules. J Neurochem. 88**,** 349-58.

Irizarry, M.C., McNamara, M., Fedorchak, K., Hsiao, K., Hyman, B.T., 1997. APPSw transgenic mice develop age-related A beta deposits and neuropil abnormalities, but no neuronal loss in CA1. J Neuropathol Exp Neurol. 56**,** 965-73.

Jicha, G.A., Weaver, C., Lane, E., Vianna, C., Kress, Y., Rockwood, J., Davies, P., 1999. cAMP-dependent protein kinase phosphorylations on tau in Alzheimer's disease. J Neurosci. 19**,** 7486-94.

Johnson, G.V., Stoothoff, W.H., 2004. Tau phosphorylation in neuronal cell function and dysfunction. J Cell Sci. 117**,** 5721-9.

Jolivalt, C.G., Lee, C.A., Beiswenger, K.K., Smith, J.L., Orlov, M., Torrance, M.A., Masliah, E., 2008. Defective insulin signaling pathway and increased glycogen synthase kinase-3 activity in the brain of diabetic mice: parallels with Alzheimer's disease and correction by insulin. J Neurosci Res. 86**,** 3265-74.

Kahn, S.E., Hull, R.L., Utzschneider, K.M., 2006. Mechanisms linking obesity to insulin resistance and type 2 diabetes. Nature. 444**,** 840-6.

Kickstein, E., Krauss, S., Thornhill, P., Rutschow, D., Zeller, R., Sharkey, J., Williamson, R., Fuchs, M., Kohler, A., Glossmann, H., Schneider, R., Sutherland, C., Schweiger, S., 2010. Biguanide metformin acts on tau phosphorylation via mTOR/protein phosphatase 2A (PP2A) signaling. Proc Natl Acad Sci U S A. 107**,** 21830-5.

Kim, B., Backus, C., Oh, S., Hayes, J.M., Feldman, E.L., 2009. Increased tau phosphorylation and cleavage in mouse models of type 1 and type 2 diabetes. Endocrinology. 150**,** 5294-301.

Kim, D.H., Huh, J.W., Jang, M., Suh, J.H., Kim, T.W., Park, J.S., Yoon, S.Y., 2012. Sitagliptin increases tau phosphorylation in the hippocampus of rats with type 2 diabetes and in primary neuron cultures. Neurobiol Dis. 46**,** 52-8.

Knight, E.M., Martins, I.V., Gumusgoz, S., Allan, S.M., Lawrence, C.B., 2014. High-fat diet-induced memory impairment in triple-transgenic Alzheimer's disease (3xTgAD) mice is independent of changes in amyloid and tau pathology. Neurobiol Aging. 35**,** 1821-32.

Kobayashi, K., Forte, T.M., Taniguchi, S., Ishida, B.Y., Oka, K., Chan, L., 2000. The db/db mouse, a model for diabetic dyslipidemia: molecular characterization and effects of Western diet feeding. Metabolism. 49**,** 22-31.

Koga, S., Kojima, A., Ishikawa, C., Kuwabara, S., Arai, K., Yoshiyama, Y., 2014a. Effects of diet-induced obesity and voluntary exercise in a tauopathy mouse model: implications of persistent hyperleptinemia and enhanced astrocytic leptin receptor expression. Neurobiol Dis. 71**,** 180-92.

Koga, S., Kojima, A., Kuwabara, S., Yoshiyama, Y., 2014b. Immunohistochemical analysis of tau phosphorylation and astroglial activation with enhanced leptin receptor expression in diet-induced obesity mouse hippocampus. Neurosci Lett. 571**,** 11-6.

Kopke, E., Tung, Y.C., Shaikh, S., Alonso, A.C., Iqbal, K., Grundke-Iqbal, I., 1993. Microtubule-associated protein tau. Abnormal phosphorylation of a non-paired helical filament pool in Alzheimer disease. J Biol Chem. 268**,** 24374-84.

Kosaraju, J., Gali, C.C., Khatwal, R.B., Dubala, A., Chinni, S., Holsinger, R.M., Madhunapantula, V.S., Muthureddy Nataraj, S.K., Basavan, D., 2013a. Saxagliptin: a dipeptidyl peptidase-4 inhibitor ameliorates streptozotocin induced Alzheimer's disease. Neuropharmacology. 72**,** 291-300.

Kosaraju, J., Murthy, V., Khatwal, R.B., Dubala, A., Chinni, S., Muthureddy Nataraj, S.K., Basavan, D., 2013b. Vildagliptin: an anti-diabetes agent ameliorates cognitive deficits and pathology observed in streptozotocin-induced Alzheimer's disease. J Pharm Pharmacol. 65**,** 1773-84.

Krishnaswamy, S., Verdile, G., Groth, D., Kanyenda, L., Martins, R.N., 2009. The structure and function of Alzheimer's gamma secretase enzyme complex. Crit Rev Clin Lab Sci. 46**,** 282-301.

Kurtz, T.W., Morris, R.C., Pershadsingh, H.A., 1989. The Zucker fatty rat as a genetic model of obesity and hypertension. Hypertension. 13**,** 896-901.

Langmead, C.J., Szekeres, P.G., Chambers, J.K., Ratcliffe, S.J., Jones, D.N., Hirst, W.D., Price, G.W., Herdon, H.J., 2000. Characterization of the binding of [(125)I]-human prolactin releasing peptide (PrRP) to GPR10, a novel G protein coupled receptor. Br J Pharmacol. 131**,** 683-8.

Lannfelt, L., Bogdanovic, N., Appelgren, H., Axelman, K., Lilius, L., Hansson, G., Schenk, D., Hardy, J., Winblad, B., 1994. Amyloid precursor protein mutation causes Alzheimer's disease in a Swedish family. Neurosci Lett. 168**,** 254-6.

Lawrence, C., Celsi, F., Brennand, J., Luckman, S., 2000a. Alternative role for prolactin-releasing peptide in the regulation of food intake. Nat Neurosci. 3**,** 645-6.

Lawrence, C.B., Celsi, F., Brennand, J., Luckman, S.M., 2000b. Alternative role for prolactin-releasing peptide in the regulation of food intake. Nat Neurosci. 3**,** 645-6.

Lawrence, C.B., Liu, Y.L., Stock, M.J., Luckman, S.M., 2004. Anorectic actions of prolactin-releasing peptide are mediated by corticotropin-releasing hormone receptors. Am J Physiol Regul Integr Comp Physiol. 286**,** R101-7.

Leboucher, A., Laurent, C., Fernandez-Gomez, F.J., Burnouf, S., Troquier, L., Eddarkaoui, S., Demeyer, D., Caillierez, R., Zommer, N., Vallez, E., Bantubungi, K., Breton, C., Pigny, P., Buee-Scherrer, V., Staels, B., Hamdane, M., Tailleux, A., Buee, L., Blum, D., 2013. Detrimental effects of diet-induced obesity on tau pathology are independent of insulin resistance in tau transgenic mice. Diabetes. 62**,** 1681-8.

Lee, E.B., 2011. Obesity, leptin, and Alzheimer's disease. Ann N Y Acad Sci. 1243**,** 15-29.

Lee, G., Leugers, C.J., 2012. Tau and tauopathies. Prog Mol Biol Transl Sci. 107**,** 263-93.

Lee, Y., Yang, S.P., Soares, M.J., Voogt, J.L., 2000. Distribution of prolactin-releasing peptide mRNA in the rat brain. Brain Res Bull. 51**,** 171-6.

Leibson, C.L., Rocca, W.A., Hanson, V.A., Cha, R., Kokmen, E., O'Brien, P.C., Palumbo, P.J., 1997. Risk of dementia among persons with diabetes mellitus: a population-based cohort study. Am J Epidemiol. 145**,** 301-8.

Lennox, R., Porter, D.W., Flatt, P.R., Gault, V.A., 2013. (Val(8))GLP-1-Glu-PAL: a GLP-1 agonist that improves hippocampal neurogenesis, glucose homeostasis, and beta-cell function in high-fat-fed mice. ChemMedChem. 8**,** 595-602.

Leonard, B.L., Watson, R.N., Loomes, K.M., Phillips, A.R., Cooper, G.J., 2005. Insulin resistance in the Zucker diabetic fatty rat: a metabolic characterisation of obese and lean phenotypes. Acta Diabetol. 42**,** 162-70.

Leroy, A., Landrieu, I., Huvent, I., Legrand, D., Codeville, B., Wieruszeski, J.M., Lippens, G., 2010. Spectroscopic studies of GSK3{beta} phosphorylation of the neuronal tau protein and its interaction with the N-terminal domain of apolipoprotein E. J Biol Chem. 285**,** 33435-44.

Li, J., Deng, J., Sheng, W., Zuo, Z., 2012a. Metformin attenuates Alzheimer's disease-like neuropathology in obese, leptin-resistant mice. Pharmacol Biochem Behav. 101**,** 564-74.

Li, L., Holscher, C., 2007. Common pathological processes in Alzheimer disease and type 2 diabetes: a review. Brain Res Rev. 56**,** 384-402.

Li, L., Zhang, Z.F., Holscher, C., Gao, C., Jiang, Y.H., Liu, Y.Z., 2012b. (Val(8)) glucagon-like peptide-1 prevents tau hyperphosphorylation, impairment of spatial learning and ultra-structural cellular damage induced by streptozotocin in rat brains. Eur J Pharmacol. 674**,** 280-6.

Li, Y., Duffy, K.B., Ottinger, M.A., Ray, B., Bailey, J.A., Holloway, H.W., Tweedie, D., Perry, T., Mattson, M.P., Kapogiannis, D., Sambamurti, K., Lahiri, D.K., Greig, N.H., 2010. GLP-1 receptor stimulation reduces amyloid-beta peptide accumulation and cytotoxicity in cellular and animal models of Alzheimer's disease. J Alzheimers Dis. 19**,** 1205-19.

Lindwall, G., Cole, R.D., 1984. Phosphorylation affects the ability of tau protein to promote microtubule assembly. J Biol Chem. 259**,** 5301-5.

Liu, F., Shi, J., Tanimukai, H., Gu, J., Gu, J., Grundke-Iqbal, I., Iqbal, K., Gong, C.X., 2009a. Reduced O-GlcNAcylation links lower brain glucose metabolism and tau pathology in Alzheimer's disease. Brain. 132**,** 1820-32.

Liu, Y., Liu, F., Grundke-Iqbal, I., Iqbal, K., Gong, C.X., 2009b. Brain glucose transporters, O-GlcNAcylation and phosphorylation of tau in diabetes and Alzheimer's disease. J Neurochem. 111**,** 242-9.

Liu, Y., Liu, F., Grundke-Iqbal, I., Iqbal, K., Gong, C.X., 2011. Deficient brain insulin signalling pathway in Alzheimer's disease and diabetes. J Pathol. 225**,** 54-62.

Lockie, S.H., 2013. Glucagon-like peptide-1 receptor in the brain: role in neuroendocrine control of energy metabolism and treatment target for obesity. J Neuroendocrinol. 25**,** 597-604.

Long-Smith, C.M., Manning, S., McClean, P.L., Coakley, M.F., O'Halloran, D.J., Holscher, C., O'Neill, C., 2013. The diabetes drug liraglutide ameliorates aberrant insulin receptor localisation and signalling in parallel with decreasing both amyloid-beta plaque and glial pathology in a mouse model of Alzheimer's disease. Neuromolecular Med. 15**,** 102-14.

Maixnerova, J., Spolcova, A., Pychova, M., Blechova, M., Elbert, T., Rezacova, M., Zelezna, B., Maletinska, L., 2011. Characterization of prolactin-releasing peptide: binding, signaling and hormone secretion in rodent pituitary cell lines endogenously expressing its receptor. Peptides. 32**,** 811-7.

Maletinska, L., Spolcova, A., Maixnerova, J., Blechova, M., Zelezna, B., 2011. Biological properties of prolactin-releasing peptide analogs with a modified aromatic ring of a C-terminal phenylalanine amide. Peptides. 32**,** 1887-92.

Maletinska, L., Pychova, M., Holubova, M., Blechova, M., Demianova, Z., Elbert, T., Zelezna, B., 2012. Characterization of new stable ghrelin analogs with prolonged orexigenic potency. J Pharmacol Exp Ther. 340**,** 781-6.

Maletinska, L., Nagelova, V., Ticha, A., Zemenova, J., Pirnik, Z., Holubova, M., Spolcova, A., Mikulaskova, B., Blechova, M., Sykora, D., Lacinova, Z., Haluzik, M., Zelezna, B., Kunes, J., 2015. Novel lipidized analogs of prolactin-releasing peptide have prolonged half-lives and exert anti-obesity effects after peripheral administration. Int J Obes (Lond).

Maletínská, L., Toma, R.S., Pirnik, Z., Kiss, A., Slaninová, J., Haluzík, M., Zelezná, B., 2006. Effect of cholecystokinin on feeding is attenuated in monosodium glutamate obese mice. Regul Pept. 136**,** 58-63.

Martin, L., Latypova, X., Wilson, C.M., Magnaudeix, A., Perrin, M.L., Terro, F., 2013. Tau protein phosphatases in Alzheimer's disease: the leading role of PP2A. Ageing Res Rev. 12**,** 39-49.

Maruyama, M., Matsumoto, H., Fujiwara, K., Kitada, C., Hinuma, S., Onda, H., Fujino, M., Inoue, K., 1999. Immunocytochemical localization of prolactin-releasing peptide in the rat brain. Endocrinology. 140**,** 2326-33.

Matysková, R., Maletínská, L., Maixnerová, J., Pirník, Z., Kiss, A., Zelezná, B., 2008. Comparison of the obesity phenotypes related to monosodium glutamate effect on arcuate nucleus and/or the high fat diet feeding in C57BL/6 and NMRI mice. Physiol Res. 57**,** 727-34.

McClean, P.L., Parthsarathy, V., Faivre, E., Holscher, C., 2011. The diabetes drug liraglutide prevents degenerative processes in a mouse model of Alzheimer's disease. J Neurosci. 31**,** 6587-94.

McClean, P.L., Holscher, C., 2014a. Liraglutide can reverse memory impairment, synaptic loss and reduce plaque load in aged APP/PS1 mice, a model of Alzheimer's disease. Neuropharmacology. 76 Pt A**,** 57-67.

McClean, P.L., Holscher, C., 2014b. Lixisenatide, a drug developed to treat type 2 diabetes, shows neuroprotective effects in a mouse model of Alzheimer's disease. Neuropharmacology. 86**,** 241-58.

McGovern, S.F., Hunter, K., Holscher, C., 2012. Effects of the glucagon-like polypeptide-1 analogue (Val8)GLP-1 on learning, progenitor cell proliferation and neurogenesis in the C57B/16 mouse brain. Brain Res. 1473**,** 204-13.

Michel, G., Mercken, M., Murayama, M., Noguchi, K., Ishiguro, K., Imahori, K., Takashima, A., 1998. Characterization of tau phosphorylation in glycogen synthase kinase-3beta and cyclin dependent kinase-5 activator (p23) transfected cells. Biochim Biophys Acta. 1380**,** 177-82.

Mohmmad Abdul, H., Wenk, G.L., Gramling, M., Hauss-Wegrzyniak, B., Butterfield, D.A., 2004. APP and PS-1 mutations induce brain oxidative stress independent of dietary cholesterol: implications for Alzheimer's disease. Neurosci Lett. 368**,** 148-50.

Mochiduki, A., Takeda, T., Kaga, S., Inoue, K., 2010. Stress response of prolactin-releasing peptide knockout mice as to glucocorticoid secretion. J Neuroendocrinol. 22**,** 576-84.

Morton, G.J., Niswender, K.D., Rhodes, C.J., Myers, M.G., Jr., Blevins, J.E., Baskin, D.G., Schwartz, M.W., 2003. Arcuate nucleus-specific leptin receptor gene therapy attenuates the obesity phenotype of Koletsky (fa(k)/fa(k)) rats. Endocrinology. 144**,** 2016-24.

Moser, E.I., 2011. The multi-laned hippocampus. Nat Neurosci. 14**,** 407-8.

Motulsky, H., Neubig, R., 2002. Analyzing radioligand binding data. Curr Protoc Neurosci. Chapter 7**,** Unit 7 5.

Nieminen, M.L., Brandt, A., Pietila, P., Panula, P., 2000. Expression of mammalian RF-amide peptides neuropeptide FF (NPFF), prolactin-releasing peptide (PrRP) and the PrRP receptor in the peripheral tissues of the rat. Peptides. 21**,** 1695-701.

Oddo, S., Caccamo, A., Kitazawa, M., Tseng, B.P., LaFerla, F.M., 2003a. Amyloid deposition precedes tangle formation in a triple transgenic model of Alzheimer's disease. Neurobiol Aging. 24**,** 1063-70.

Oddo, S., Caccamo, A., Shepherd, J.D., Murphy, M.P., Golde, T.E., Kayed, R., Metherate, R., Mattson, M.P., Akbari, Y., LaFerla, F.M., 2003b. Triple-transgenic model of Alzheimer's disease with plaques and tangles: intracellular Abeta and synaptic dysfunction. Neuron. 39**,** 409-21.

Olney, J.W., 1969. Brain lesions, obesity, and other disturbances in mice treated with monosodium glutamate. Science. 164**,** 719-21.

Panza, F., Solfrizzi, V., Colacicco, A.M., D'Introno, A., Capurso, C., Torres, F., Del Parigi, A., Capurso, S., Capurso, A., 2004. Mediterranean diet and cognitive decline. Public Health Nutr. 7**,** 959-63.

Parthsarathy, V., Holscher, C., 2013. Chronic treatment with the GLP1 analogue liraglutide increases cell proliferation and differentiation into neurons in an AD mouse model. PLoS One. 8**,** e58784.

Perley, M.J., Kipnis, D.M., 1967. Plasma insulin responses to oral and intravenous glucose: studies in normal and diabetic sujbjects. J Clin Invest. 46**,** 1954-62.

Peterson, R.G., Shaw, W.N., Neel, M.-A., Little, L.A., Eichberg, J., 1990. Zucker Diabetic Fatty Rat as a Model for Non-insulin-dependent Diabetes Mellitus. ILAR News. 32**,** 4.

Pirnik, Z., Bundzikova, J., Holubova, M., Pychova, M., Fehrentz, J.A., Martinez, J., Zelezna, B., Maletinska, L., Kiss, A., 2011. Ghrelin agonists impact on Fos protein expression in brain areas related to food intake regulation in male C57BL/6 mice. Neurochem Int. 59**,** 889-95.

Porter, D.W., Kerr, B.D., Flatt, P.R., Holscher, C., Gault, V.A., 2010. Four weeks administration of Liraglutide improves memory and learning as well as glycaemic control in mice with high fat dietary-induced obesity and insulin resistance. Diabetes Obes Metab. 12**,** 891-9.

Porter, D.W., Irwin, N., Flatt, P.R., Holscher, C., Gault, V.A., 2011. Prolonged GIP receptor activation improves cognitive function, hippocampal synaptic plasticity and glucose homeostasis in high-fat fed mice. Eur J Pharmacol. 650**,** 688-93.

Porter, W.D., Flatt, P.R., Holscher, C., Gault, V.A., 2013. Liraglutide improves hippocampal synaptic plasticity associated with increased expression of Mash1 in ob/ob mice. Int J Obes (Lond). 37**,** 678-84.

Pratchayasakul, W., Kerdphoo, S., Petsophonsakul, P., Pongchaidecha, A., Chattipakorn, N., Chattipakorn, S.C., 2011. Effects of high-fat diet on insulin receptor function in rat hippocampus and the level of neuronal corticosterone. Life Sci. 88**,** 619-27.

Priller, C., Bauer, T., Mitteregger, G., Krebs, B., Kretzschmar, H.A., Herms, J., 2006. Synapse formation and function is modulated by the amyloid precursor protein. J Neurosci. 26**,** 7212-21.

Ramos-Rodriguez, J.J., Ortiz, O., Jimenez-Palomares, M., Kay, K.R., Berrocoso, E., Murillo-Carretero, M.I., Perdomo, G., Spires-Jones, T., Cozar-Castellano, I., Lechuga-Sancho, A.M., Garcia-Alloza, M., 2013. Differential central pathology and cognitive impairment in pre-diabetic and diabetic mice. Psychoneuroendocrinology. 38**,** 2462-75.

Ramos-Rodriguez, J.J., Ortiz-Barajas, O., Gamero-Carrasco, C., de la Rosa, P.R., Infante-Garcia, C., Zopeque-Garcia, N., Lechuga-Sancho, A.M., Garcia-Alloza, M., 2014. Prediabetes-induced vascular alterations exacerbate central pathology in APPswe/PS1dE9 mice. Psychoneuroendocrinology. 48**,** 123-35.

Ramsden, M., Kotilinek, L., Forster, C., Paulson, J., McGowan, E., SantaCruz, K., Guimaraes, A., Yue, M., Lewis, J., Carlson, G., Hutton, M., Ashe, K.H., 2005. Age-dependent neurofibrillary tangle formation, neuron loss, and memory impairment in a mouse model of human tauopathy (P301L). J Neurosci. 25**,** 10637-47.

Serrano-Pozo, A., Frosch, M.P., Masliah, E., Hyman, B.T., 2011. Neuropathological alterations in Alzheimer disease. Cold Spring Harb Perspect Med. 1**,** a006189.

Seufert, J., 2004. Leptin effects on pancreatic beta-cell gene expression and function. Diabetes. 53 Suppl 1**,** S152-8.

Shaw, L.M., Vanderstichele, H., Knapik-Czajka, M., Clark, C.M., Aisen, P.S., Petersen, R.C., Blennow, K., Soares, H., Simon, A., Lewczuk, P., Dean, R., Siemers, E., Potter, W., Lee, V.M., Trojanowski, J.Q., Alzheimer's Disease Neuroimaging, I., 2009. Cerebrospinal fluid biomarker signature in Alzheimer's disease neuroimaging initiative subjects. Ann Neurol. 65**,** 403-13.

Schindowski, K., Bretteville, A., Leroy, K., Begard, S., Brion, J.P., Hamdane, M., Buee, L., 2006. Alzheimer's disease-like tau neuropathology leads to memory deficits and loss of functional synapses in a novel mutated tau transgenic mouse without any motor deficits. Am J Pathol. 169**,** 599-616.

Schrijvers, E.M., Witteman, J.C., Sijbrands, E.J., Hofman, A., Koudstaal, P.J., Breteler, M.M., 2010. Insulin metabolism and the risk of Alzheimer disease: the Rotterdam Study. Neurology. 75**,** 1982-7.

Schubert, M., Gautam, D., Surjo, D., Ueki, K., Baudler, S., Schubert, D., Kondo, T., Alber, J., Galldiks, N., Kustermann, E., Arndt, S., Jacobs, A.H., Krone, W., Kahn, C.R., Bruning, J.C., 2004. Role for neuronal insulin resistance in neurodegenerative diseases. Proc Natl Acad Sci U S A. 101**,** 3100-5.

Schultz, C., Del Tredici, K., Brakk, H., 2004. Neuropathology of Alzheimer's Disease. Current Clinical Neurology, Vol., Humana Press.

Sisley, S., Gutierrez-Aguilar, R., Scott, M., D'Alessio, D.A., Sandoval, D.A., Seeley, R.J., 2014. Neuronal GLP1R mediates liraglutide's anorectic but not glucose-lowering effect. J Clin Invest. 124**,** 2456-63.

Sjöholm, Å., 2010. Liraglutide Therapy for Type 2 Diabetes: Overcoming Unmet Needs. Pharmaceuticals. 3**,** 18.

Sperling, R.A., Aisen, P.S., Beckett, L.A., Bennett, D.A., Craft, S., Fagan, A.M., Iwatsubo, T., Jack, C.R., Jr., Kaye, J., Montine, T.J., Park, D.C., Reiman, E.M., Rowe, C.C., Siemers, E., Stern, Y., Yaffe, K., Carrillo, M.C., Thies, B., Morrison-Bogorad, M., Wagster, M.V., Phelps, C.H., 2011. Toward defining the preclinical stages of Alzheimer's disease: recommendations from the National Institute on Aging-Alzheimer's Association

workgroups on diagnostic guidelines for Alzheimer's disease. Alzheimers Dement. 7, 280-92.

Spolcova, A., Mikulaskova, B., Krskova, K., Gajdosechova, L., Zorad, S., Olszanecki, R., Suski, M., Bujak-Gizycka, B., Zelezna, B., Maletinska, L., 2014. Deficient hippocampal insulin signaling and augmented Tau phosphorylation is related to obesity- and age-induced peripheral insulin resistance: a study in Zucker rats. BMC Neurosci. 15, 111.

Spolcova, A., Mikulaskova, B., Holubova, M., Nagelova, V., Pirnik, Z., Zemenova, J., Haluzik, M., Zelezna, B., Galas, M.C., Maletinska, L., 2015. Anorexigenic lipopeptides ameliorate central insulin signaling and attenuate tau phosphorylation in hippocampi of mice with monosodium glutamate-induced obesity. J Alzheimers Dis. 45, 823-35.

Squire, L.R., 1992. Memory and the hippocampus: a synthesis from findings with rats, monkeys, and humans. Psychol Rev. 99, 195-231.

State Institute for Drug Control, C.R., 2012. Hodnocení vývoje distribuce vybrané skupiny léčivých přípravků. Vol. 2015, ed.^eds.

Steculorum, S.M., Solas, M., Bruning, J.C., 2014. The paradox of neuronal insulin action and resistance in the development of aging-associated diseases. Alzheimers Dement. 10, S3-11.

Steen, E., Terry, B.M., Rivera, E.J., Cannon, J.L., Neely, T.R., Tavares, R., Xu, X.J., Wands, J.R., de la Monte, S.M., 2005. Impaired insulin and insulin-like growth factor expression and signaling mechanisms in Alzheimer's disease--is this type 3 diabetes? J Alzheimers Dis. 7, 63-80.

Stranahan, A.M., Arumugam, T.V., Cutler, R.G., Lee, K., Egan, J.M., Mattson, M.P., 2008. Diabetes impairs hippocampal function through glucocorticoid-mediated effects on new and mature neurons. Nat Neurosci. 11, 309-17.

Su, Y., Ni, B., 1998. Selective deposition of amyloid-beta protein in the entorhinal-dentate projection of a transgenic mouse model of Alzheimer's disease. J Neurosci Res. 53, 177-86.

Sutherland, C., Leighton, I.A., Cohen, P., 1993. Inactivation of glycogen synthase kinase-3 beta by phosphorylation: new kinase connections in insulin and growth-factor signalling. Biochem J. 296 (Pt 1), 15-9.

Tabaton, M., Zhu, X., Perry, G., Smith, M.A., Giliberto, L., 2010. Signaling effect of amyloid-beta(42) on the processing of AbetaPP. Exp Neurol. 221, 18-25.

Tahrani, A.A., Bailey, C.J., Del Prato, S., Barnett, A.H., 2011. Management of type 2 diabetes: new and future developments in treatment. Lancet. 378, 182-97.

Takalo, M., Haapasalo, A., Martiskainen, H., Kurkinen, K.M., Koivisto, H., Miettinen, P., Khandelwal, V.K., Kemppainen, S., Kaminska, D., Makinen, P., Leinonen, V., Pihlajamaki, J., Soininen, H., Laakso, M., Tanila, H., Hiltunen, M., 2014. High-fat diet increases tau expression in the brain of T2DM and AD mice independently of peripheral metabolic status. J Nutr Biochem. 25, 634-41.

Takasaki, Y., 1978. Studies on brain lesion by administration of monosodium L-glutamate to mice. I. Brain lesions in infant mice caused by administration of monosodium L-glutamate. Toxicology. 9, 293-305.

Takashima, A., 2006. GSK-3 is essential in the pathogenesis of Alzheimer's disease. J Alzheimers Dis. 9, 309-17.

Takayanagi, Y., Matsumoto, H., Nakata, M., Mera, T., Fukusumi, S., Hinuma, S., Ueta, Y., Yada, T., Leng, G., Onaka, T., 2008. Endogenous prolactin-releasing peptide regulates food intake in rodents. J Clin Invest. 118, 4014-24.

Takeda, S., Sato, N., Uchio-Yamada, K., Sawada, K., Kunieda, T., Takeuchi, D., Kurinami, H., Shinohara, M., Rakugi, H., Morishita, R., 2010. Diabetes-accelerated memory

dysfunction via cerebrovascular inflammation and Abeta deposition in an Alzheimer mouse model with diabetes. Proc Natl Acad Sci U S A. 107, 7036-41.

Talaei, F., Van Praag, V.M., Shishavan, M.H., Landheer, S.W., Buikema, H., Henning, R.H., 2014. Increased protein aggregation in Zucker diabetic fatty rat brain: identification of key mechanistic targets and the therapeutic application of hydrogen sulfide. BMC Cell Biol. 15, 1.

Tezapsidis, N., Johnston, J.M., Smith, M.A., Ashford, J.W., Casadesus, G., Robakis, N.K., Wolozin, B., Perry, G., Zhu, X., Greco, S.J., Sarkar, S., 2009. Leptin: a novel therapeutic strategy for Alzheimer's disease. J Alzheimers Dis. 16, 731-40.

Turner, P.R., O'Connor, K., Tate, W.P., Abraham, W.C., 2003. Roles of amyloid precursor protein and its fragments in regulating neural activity, plasticity and memory. Prog Neurobiol. 70, 1-32.

van Bloemendaal, L., Ten Kulve, J.S., la Fleur, S.E., Ijzerman, R.G., Diamant, M., 2014. Effects of glucagon-like peptide 1 on appetite and body weight: focus on the CNS. J Endocrinol. 221, T1-16.

Van der Jeugd, A., Ahmed, T., Burnouf, S., Belarbi, K., Hamdame, M., Grosjean, M.E., Humez, S., Balschun, D., Blum, D., Buee, L., D'Hooge, R., 2011. Hippocampal tauopathy in tau transgenic mice coincides with impaired hippocampus-dependent learning and memory, and attenuated late-phase long-term depression of synaptic transmission. Neurobiol Learn Mem. 95, 296-304.

Van der Jeugd, A., Vermaercke, B., Derisbourg, M., Lo, A.C., Hamdane, M., Blum, D., Buee, L., D'Hooge, R., 2013. Progressive age-related cognitive decline in tau mice. J Alzheimers Dis. 37, 777-88.

Vilsboll, T., Holst, J.J., 2004. Incretins, insulin secretion and Type 2 diabetes mellitus. Diabetologia. 47, 357-66.

Wang, C., Chen, X., Ding, X., He, Y., Gu, C., Zhou, L., 2015. Exendin-4 Promotes Beta Cell Proliferation via PI3k/Akt Signalling Pathway. Cell Physiol Biochem. 35, 2223-32.

Wang, J., Gallagher, D., DeVito, L.M., Cancino, G.I., Tsui, D., He, L., Keller, G.M., Frankland, P.W., Kaplan, D.R., Miller, F.D., 2012. Metformin activates an atypical PKC-CBP pathway to promote neurogenesis and enhance spatial memory formation. Cell Stem Cell. 11, 23-35.

Weingarten, M.D., Lockwood, A.H., Hwo, S.Y., Kirschner, M.W., 1975. A protein factor essential for microtubule assembly. Proc Natl Acad Sci U S A. 72, 1858-62.

Wickelgren, I., 1998. Tracking insulin to the mind. Science. 280, 517-9.

Widenmaier, S.B., Kim, S.J., Yang, G.K., De Los Reyes, T., Nian, C., Asadi, A., Seino, Y., Kieffer, T.J., Kwok, Y.N., McIntosh, C.H., 2010. A GIP receptor agonist exhibits beta-cell anti-apoptotic actions in rat models of diabetes resulting in improved beta-cell function and glycemic control. PLoS One. 5, e9590.

Winocur, G., Greenwood, C.E., 1999. The effects of high fat diets and environmental influences on cognitive performance in rats. Behav Brain Res. 101, 153-61.

Winocur, G., Greenwood, C.E., Piroli, G.G., Grillo, C.A., Reznikov, L.R., Reagan, L.P., McEwen, B.S., 2005. Memory impairment in obese Zucker rats: an investigation of cognitive function in an animal model of insulin resistance and obesity. Behav Neurosci. 119, 1389-95.

Xu, W.L., Atti, A.R., Gatz, M., Pedersen, N.L., Johansson, B., Fratiglioni, L., 2011. Midlife overweight and obesity increase late-life dementia risk: a population-based twin study. Neurology. 76, 1568-74.

Yang, Y., Zhang, J., Ma, D., Zhang, M., Hu, S., Shao, S., Gong, C.X., 2013. Subcutaneous administration of liraglutide ameliorates Alzheimer-associated tau hyperphosphorylation in rats with type 2 diabetes. J Alzheimers Dis. 37, 637-48.

Youngren, J.F., Paik, J., Barnard, R.J., 2001. Impaired insulin-receptor autophosphorylation is an early defect in fat-fed, insulin-resistant rats. J Appl Physiol (1985). 91**,** 2240-7.

Zelezná, B., Maixnerová, J., Matysková, R., Haugvicová, R., Blokesová, D., Maletínská, L., 2009. Anorexigenic effect of cholecystokinin is lost but that of CART (Cocaine and Amphetamine Regulated Transcript) peptide is preserved in monosodium glutamate obese mice. Physiol Res. 58**,** 717-23.

Zhao, W., Chen, H., Xu, H., Moore, E., Meiri, N., Quon, M.J., Alkon, D.L., 1999. Brain insulin receptors and spatial memory. Correlated changes in gene expression, tyrosine phosphorylation, and signaling molecules in the hippocampus of water maze trained rats. J Biol Chem. 274**,** 34893-902.

Zilka, N., Novak, M., 2006. The tangled story of Alois Alzheimer. Bratisl Lek Listy. 107**,** 343-5.

Zucker, L.M., Antoniades, H.N., 1972. Insulin and obesity in the Zucker genetically obese rat "fatty". Endocrinology. 90**,** 1320-30.

WEB SITES

http://www.atkinsdietbulletinboard.com/

http://www.atkinsdietbulletinboard.com/forums/main-atkins-diet-forum/101630-weight-gain-after-calorie-restriction-diet-3.html - cited 03/06/2015

www.benbest.com

http://www.benbest.com/lifeext/Alzheimer.html - cited 03/06/2015

www.best-alzheimers-products.com:

http://www.best-alzheimers-products.com/alzheimers-disease.html - cited 03/06/2015

www.brightfocus.org

http://www.brightfocus.org/alzheimers/about/understanding/brain-with-alzheimers.html - cited 03/06/2015

http://www.nottingham.ac.uk/

http://www.nottingham.ac.uk/~mbzmail/NTM3/Tess_Alzheimers/tangles.html - cited 03/06/2015

www.kliniken-schmieder.de

http://www.kliniken-schmieder.de/behandlungs-spektrum/neurologische-erkrankungen/alzheimer.html - cited 03/06/2015

http://www.nia.nih.gov/

http://www.nia.nih.gov/alzheimers/scientific-images - cited 03/06/2015

LIST OF MY PUBLICATIONS

Publications related to PhD thesis:

1. **Spolcova, A.**, Mikulaskova, B., Krskova, K., Gajdosechova, L., Zorad, S., Olszanecki, R., Suski, M., Bujak-Gizycka, B., Zelezna, B., Maletinska, L. (2014). Deficient hippocampal insulin signaling and augmented Tau phosphorylation is related to obesity- and age-induced peripheral insulin resistance: a study in Zucker rats. *BMC Neuroscience* 15**,** 111. **IF = 2.85**
2. Maletinska, L., Nagelova, V., Ticha, A., Zemenova, J., Pirnik, Z., Holubova, M., **Spolcova, A.**, Mikulaskova, B., Blechova, M., Sykora, D., Lacinova, Z., Haluzik, M., Zelezna, B., Kunes, J. (2015). Novel lipidized analogs of prolactin-releasing peptide have prolonged half-lives and exert anti-obesity effects after peripheral administration. *International Journal of Obesity* (Lond). **IF = 5.38**
3. **Spolcova, A.**, Mikulaskova, B., Holubova, M., Nagelova, V., Pirnik, Z., Zemenova, J., Haluzik, M., Zelezna, B., Galas, M.C., Maletinska, L. (2015). Anorexigenic lipopeptides ameliorate central insulin signaling and attenuate tau phosphorylation in hippocampi of mice with monosodium glutamate-induced obesity. *Journal of Alzheimers Disease.* 45**,** 823-35. **IF = 3.61**

Publications not related to PhD thesis:

1. Maixnerova, J., **Spolcova, A.**, Pychova, M., Blechova, M., Elbert, T., Rezacova, M., Zelezna, B., Maletinska, L. (2011). Characterization of prolactin-releasing peptide: binding, signaling and hormone secretion in rodent pituitary cell lines endogenously expressing its receptor. *Peptides* 32**,** 811-7. **IF = 2.61**
2. Maletinska, L., **Spolcova, A.**, Maixnerova, J., Blechova, M., Zelezna, B. (2011). Biological properties of prolactin-releasing peptide analogs with a modified aromatic ring of a C-terminal phenylalanine amide. *Peptides* 32**,** 1887-92. **IF = 2.61**
3. Maletinska, L., Matyskova, R., Maixnerova, J., Sykora, D., Pychova, M., **Spolcova, A.**, Blechova, M., Drapalova, J., Lacinova, Z., Haluzik, M., Zelezna, B. (2011). The Peptidic GHS-R antagonist [D-Lys(3)]GHRP-6 markedly improves adiposity and related metabolic abnormalities in a mouse model of postmenopausal obesity. *Molecular and Cellular Endocrinology* 343**,** 55-62. **IF = 4.24**
4. Maletinska, L., Ticha, A., Nagelova, V., **Spolcova, A.**, Blechova, M., Elbert, T., Zelezna, B., (2013). Neuropeptide FF analog RF9 is not an antagonist of NPFF receptor and decreases food intake in mice after its central and peripheral administration. *Brain Research* 1498**,** 33-40. **IF = 2.82**
5. Holubova, M., **Spolcova, A.**, Demianova, Z., Sykora, D., Fehrentz, J.A., Martinez, J., Stofkova, A., Jurcovicova, J., Drapalova, J., Lacinova, Z., Haluzik, M., Zelezna, B., Maletinska, L. (2013). Ghrelin agonist JMV 1843 increases food intake, body weight and expression of orexigenic neuropeptides in mice. *Physiological Research* 62**,** 435-44. **IF = 1.48**
6. **Spolcova, A.**, Holubova, M., Mikulaskova, B., Nagelova, V., Stofkova, A., Lacinova, Z., Jurcovicova, J., Haluzik, M., Maletinska, L., Zelezna, B. (2014). Changes in FGF21 serum concentrations and liver mRNA expression in an experimental model of complete lipodystrophy and insulin-resistant diabetes. *Physiol Research* 63**,** 483-90. **IF = 1.48**

7. Gajdosechova, L., Krskova, K., Segarra, A.B., **Spolcova, A.**, Suski, M., Olszanecki, R., Zorad, S. (2014). Hypooxytocinaemia in obese Zucker rats relates to oxytocin degradation in liver and adipose tissue. *Journal of Endocrinology* 220**,** 333-43. **IF = 3.58**

Patents:

PCT/US13/50146. Lipidated peptides as anti-obesity agents. Patent pending to IOCB AS CR (Maletínská, L., Železná, B., Blechová, M., **Špolcová, A.**). Applied the 11th July 2013.

PCT/CZ2015/000047 Lipidated peptides as neuroprotective agents. Patent pending to IOCB AS CR (Maletínská, L., Železná, B., Blechová, M., **Špolcová, A.**, Mikulášková, B., Kuneš, J.). Applied the 20th May 2015

SUPPLEMENT

1. Spolcova, A., Mikulaskova, B., Krskova, K., Gajdosechova, L., Zorad, S., Olszanecki, R., Suski, M., Bujak-Gizycka, B., Zelezna, B., Maletinska, L. (2014). Deficient hippocampal insulin signaling and augmented Tau phosphorylation is related to obesity- and age-induced peripheral insulin resistance: a study in Zucker rats. *BMC Neuroscience* 15, 111.
2. Maletinska, L., Nagelova, V., Ticha, A., Zemenova, J., Pirnik, Z., Holubova, M., Spolcova, A., Mikulaskova, B., Blechova, M., Sykora, D., Lacinova, Z., Haluzik, M., Zelezna, B., Kunes, J. (2015). Novel lipidized analogs of prolactin-releasing peptide have prolonged half-lives and exert anti-obesity effects after peripheral administration. *International Journal of Obesity* (Lond).
3. Spolcova, A., Mikulaskova, B., Holubova, M., Nagelova, V., Pirnik, Z., Zemenova, J., Haluzik, M., Zelezna, B., Galas, M.C., Maletinska, L. (2015). Anorexigenic lipopeptides ameliorate central insulin signaling and attenuate tau phosphorylation in hippocampi of mice with monosodium glutamate-induced obesity. *Journal of Alzheimers Disease.* 45, 823-35.

BMC Neuroscience

RESEARCH ARTICLE Open Access

Deficient hippocampal insulin signaling and augmented Tau phosphorylation is related to obesity- and age-induced peripheral insulin resistance: a study in Zucker rats

Andrea Špolcová[1], Barbora Mikulášková[1], Katarína Kršková[2], Lucia Gajdošechová[2], Štefan Zórad[2], Rafał Olszanecki[3], Maciej Suski[3], Beata Bujak-Giżycka[3], Blanka Železná[1] and Lenka Maletínská[1*]

Abstract

Background: Insulin signaling and Tau protein phosphorylation in the hippocampi of young and old obese Zucker fa/fa rats and their lean controls were assessed to determine whether obesity-induced peripheral insulin resistance and aging are risk factors for central insulin resistance and whether central insulin resistance is related to the pathologic phosphorylation of the Tau protein.

Results: Aging and obesity significantly attenuated the phosphorylation of the insulin cascade kinases Akt (protein kinase B, PKB) and GSK-3β (glycogen synthase kinase 3β) in the hippocampi of the fa/fa rats. Furthermore, the hyperphosphorylation of Tau Ser396 alone and both Tau Ser396 and Thr231 was significantly augmented by aging and obesity, respectively, in the hippocampi of these rats.

Conclusions: Both age-induced and obesity-induced peripheral insulin resistance are associated with central insulin resistance that is linked to hyperTau phosphorylation. Peripheral hyperinsulinemia, rather than hyperglycemia, appears to promote central insulin resistance and the Tau pathology in fa/fa rats.

Keywords: Zucker fa/fa rats, Insulin resistance, Obesity, GSK-3β, Tau protein

Background

Insulin resistance (IR) is a state during which a higher than normal insulin level is required for glucose homeostasis. IR occurs in the periphery and in the brain, where it has recently been linked to the hyperphosphorylation of the neuronal cytoskeleton protein Tau [1], which is symptomatic for Alzheimer's neurodegeneration. After the glucose homeostasis is disturbed, an increase in the glucose level indicates the onset of type-2 diabetes (T2D).

In several clinical studies, T2D was found to increase the risk of Alzheimer's disease (AD) [2]. In the postmortem brains of both T2D and sporadic AD patients, central resistance to insulin was documented by attenuated insulin signaling, namely via a decreased phosphorylation of the insulin cascade kinases PDK1 (3-phosphoinositide-dependent protein kinase-1), Akt (protein kinase B, PKB), and GSK-3β (glycogen synthase kinase 3β), and this effect was more pronounced in patients with both T2D and AD [3]. GSK-3β acts as both the insulin cascade kinase and the primary kinase phosphorylating Tau [4,5]. The phosphorylation of Ser9 in GSK-3β by Akt inhibits the kinase activity of GSK-3β [6,7], and the attenuated phosphorylation of Ser9 logically increases the kinase activity of GSK-3β toward Tau. Central insulin resistance is linked to a hyperphosphorylation of Tau through GSK-3β [8].

Severe hyperinsulinemia and hyperglycemia, as well as the hyperphosphorylation of Ser199/202, Thr231, and Ser396 in Tau, were found to increase progressively with age in the hippocampi of db/db mice with impaired leptin receptor signaling, a rodent model of T2D [9]. An augmented phosphorylation of Ser396 in the hippocampal Tau of db/db mice was later confirmed by another

* Correspondence: maletin@uochb.cas.cz
[1]Institute of Organic Chemistry and Biochemistry, Prague 166 10, Czech Republic
Full list of author information is available at the end of the article

research team [10]. However, in whole-brain samples of db/db mice with fully developed T2D, changes in the insulin receptors and GSK-3β phosphorylation were not found [11].

Similar to db/db mice, Zucker fatty fa/fa rats have a genetically homozygous leptin receptor mutation that results in leptin dysfunction. Zucker fa/fa rats suffer from obesity induced by hyperphagia, severe hyperlipidemia, and hyperinsulinemia, resulting in IR in the liver, muscle, and adipose tissue [12-14]. The IR in fa/fa rats is established prior to adulthood, at the age of 7 weeks [15]. Unlike db/db mice, fa/fa rats are normoglycemic or have only slightly elevated glucose levels and do not develop diabetes [12,13].

In this study, insulin signaling and Tau phosphorylation were followed in the hippocampi of 12- (young) and 33-week-old (old) obese Zucker fa/fa rats and their lean controls to verify the hypothesis that peripheral insulin resistance resulting from obesity and/or old age represents a risk factor for central insulin resistance and that such possible central IR is linked to the pathologic phosphorylation of Tau protein. In short, we aimed to determine whether IR with hyperinsulinemia but normoglycemia is associated with a risk of Tau protein pathology in the hippocampus.

Results

Metabolic parameters

In old age, both the fa/fa rats and controls developed severe obesity compared with the relevant young controls ($F_{(1,20)} = 466.52$; $p < 0.001$). The fa/fa rats also showed a significantly higher body weight than did the age-matched controls ($F_{(1,20)} = 236.30$; $p < 0.001$) (Table 1). As expected, obesity in fa/fa rats resulting from impaired leptin receptor signaling was manifested by hyperleptinemia; thus, a significant age and fa/fa genotype interaction exists ($F_{(1,20)} = 12.36$; $p < 0.01$), and a subsequent Bonferroni *post-hoc* test revealed an increase in the plasma leptin levels in young fa/fa rats compared with young controls ($p < 0.01$); this increase was more pronounced in old fa/fa rats compared with old controls ($p < 0.001$) (Table 1). Obesity was accompanied by hyperinsulinemia. There were significant effects of the fa/fa genotype ($F_{(1,20)} = 71.66$; $p < 0.001$) and age ($F_{(1,20)} = 13.94$; $p = 0.001$), as well as an age x fa/fa genotype interaction ($F_{(1,20)} = 7.99$; $p = 0.01$) with plasma insulin. Significant hyperinsulinemia in fa/fa rats was represented by extreme insulin levels that reached 12-fold ($p < 0.001$) at 12 weeks of age and 9-fold at 33 weeks of age ($p < 0.001$) in lean age-matched controls. The glucose levels in all rats were similar and did not exceed normal values (Table 1). Quantitative insulin sensitivity check index (QUICKI) was significantly decreased in both 12-week-old obese ($p < 0.05$) and 33-week-old obese rats ($p < 0.05$) compared to age-matched lean controls. Both age ($p = 0.002$) and fa/fa genotype ($p = 0.012$) were accompanied with higher and longer lasting rise in glycaemia during glucose tolerance test as revealed by general linear model for repeated measures. However, there was no interaction between these factors (Figure 1). The impairment in glucose tolerance was assessed also using parameter of 2-h glycemia during IPGTT. This impairment was observed with respect to age ($F_{(1,20)} = 19.30$; $p < 0.001$) as well as to fa/fa genotype ($F_{(1,20)} = 21.44$; $p < 0.001$). There was no detected effect of an age x fa/fa genotype interaction. The area under the curve of the glucose level during IPGTT was found to increase due only to the fa/fa genotype ($F_{(1,20)} = 5.41$; $p < 0.05$).

Dyslipidemia in young and old fa/fa rats was noticed based on the serum lipid parameters. Both total cholesterol ($F_{(1,20)} = 120.38$; $p < 0.001$) and cholesterol/HDL ratio ($F_{(1,20)} = 23.55$; $p < 0.001$) were significantly increased in fa/fa rats compared with lean rats (Table 2). Statistical analysis also revealed that age significantly affected the plasma total cholesterol ($F_{(1,20)} = 58.30$; $p < 0.001$) and cholesterol/HDL ratio ($F_{(1,20)} = 4.38$; $p < 0.05$). A significant age x fa/fa genotype interaction significantly affects the plasma total cholesterol ($F_{(1,20)} = 42.83$; $p < 0.001$) and cholesterol/HDL ratio ($F_{(1,20)} = 6.26$; $p < 0.05$). As revealed in the post-hoc test, both the plasma total cholesterol were significantly increased in young and old fa/fa rats compared with their age-matched lean controls ($p < 0.001$). An age-dependent increase in this lipid parameter was observed only in fa/fa rats ($p < 0.001$). The cholesterol/HDL ratio was increased in old fa/fa rats compared with their lean age-matched rats ($p < 0.001$) and

Table 1 Metabolic parameters of fa/fa (obese) rats and their age matched controls

Rats	Weight [g]	Leptin [ng/ml]	Insulin [ng/ml]	Glucose [mmol/l]	QUICKI
Young control	257 ± 14,17	2,02 ± 1,23	0,50 ± 0,24	6,00 ± 0,42	0,537 ± 0,071
Young fa/fa	386 ± 13,68***	36,72 ± 5,20**	6,26 ± 2,14**	6,27 ± 0,63	0,234 ± 0,008*
Old control	457 ± 21,38***	6,33 ± 1,72	1,43 ± 0,38	6,38 ± 0,43	0,274 ± 0,010
Old fa/fa	683 ± 48,31$^{\#\#\#,\ ooo}$	88,66 ± 32,71$^{\#\#\#,\ ooo}$	12,96 ± 4,50$^{\#\#\#,\ ooo}$	6,80 ± 0,51	0,216 ± 0,007^{o}

Data are mean ± SD, n = 6 animals per group. Significance is *P < 0,05, **P < 0,01 and ***P < 0,001 (*vs. young control rats, $^{\#}$vs. young fa/fa rats, ^{o}vs. old control rats) using two-way ANOVA, Bonferroni post hoc test.
Significance P<0.05, P<0.01, or P<0.001 is illustrated by one, two, or three symbols, respectively. Particular symbols are for particular groups compared.

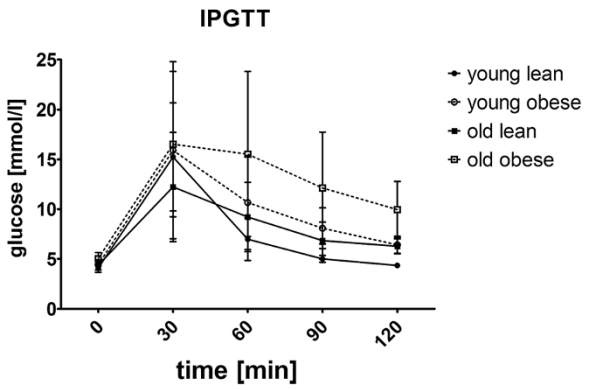

Figure 1 Graph of inraperitoneal glucose tolerance test. Before the IPGTT rats were fasted overnight. The intraperitoneal injection of 50% dextrose at dose 2 g/kg was administered and glucose was measured in the tail vein using a glucometer. Data are mean ± SD (n = 6 rats per group). Statistical analysis was calculated by two-way ANOVA, Bonferroni post hoc test.

in old fa/fa rats vs. young fa/fa rats ($p < 0.01$). In the case of plasma triglycerides levels, a significant elevation was noticed only in 33-week-old obese Zucker rats compared to lean rats of the same age.

Insulin signaling cascade in the hippocampus

Regarding the insulin cascade, a two-way ANOVA revealed a significant main effect of the fa/fa genotype ($F_{(1,20)} = 6.82$; $p < 0.05$) on insulin receptor protein expression. In Zucker fatty rats, obesity was associated with lower hippocampal insulin receptor protein levels (Figure 2). However, aging did not affect hippocampal insulin receptor protein expression ($F_{(1,20)} = 0.43$; $p < 0.52$). There was no significant interaction between age and genotype ($F_{(1,20)} = 0.78$; $p < 0.08$).

Age had a main effect on decreasing the level of PI3 kinase (PI3K) ($F_{(1,20)} = 42.03$; $p < 0.001$). The level of PI3K was also attenuated due to the fa/fa phenotype ($F_{(1,20)} = 9.84$; $p < 0.001$) (Figure 2). The two-way ANOVA revealed a significant interaction between age and genotype ($F_{(1,20)} = 17.77$; $p < 0.001$). Bonferroni's post-hoc test revealed significantly decreased levels of PI3K in young obese rats compared with young lean rats ($p < 0.001$) and in old lean rats compared with young lean rats ($p < 0.001$). No significant differences were observed between old obese and old lean rats.

As determined by the two-way ANOVA, there was significant main effect of fa/fa genotype ($F_{(1,20)} = 5.00$; $p < 0.05$) on the phosphorylation of PDK1 Ser241 in the hippocampus (Figure 2). Obesity decreased PDK1 Ser241 phosphorylation in the hippocampi of Zucker fa/fa rats. Neither a significant main effect of age nor an interaction between age and genotype was detected (Figure 2).

The two-way ANOVA revealed a significant main effect of age ($F_{(1,20)} = 27.11$; $p < 0.001$) on the phosphorylation of Akt Thr308 (Figure 2). Aging significantly attenuated the hippocampal phosphorylation of Akt Thr308 in both fa/fa and lean rats. Neither a significant effect of genotype ($F_{(1,20)} = 0.67$; $p < 0.42$) nor an interaction between age and genotype ($F_{(1,20)} = 1.80$; $p < 0.19$) was noted. Regarding the phosphorylation of Akt Ser473, significant main effects of age ($F_{(1,20)} = 31.10$; $p < 0.001$) and the fa/fa genotype ($F_{(1,20)} = 6.51$; $p < 0.05$) were observed. Both aging and obesity attenuated the phosphorylation of Akt Ser473 (Figure 2). There was no significant interaction between age and the fa/fa genotype ($F_{(1,20)} = 1.08$; $p < 0.31$).

Similarly, significant main effects of age ($F_{(1,20)} = 9.84$; $p < 0.01$) and the fa/fa genotype ($F_{(1,20)} = 12.26$; $p < 0.01$) (Figure 2) on the phosphorylation of GSK-3β Ser9 were observed. Both aging and obesity reduced the phosphorylation of GSK-3β Ser9 (Figure 2). No significant interaction between these factors was detected ($F_{(1,20)} = 0.81$; $p < 0.38$).

Table 2 Levels of lipids in blood serum of fa/fa (obese) rats and their age matched controls

Rats	Cholesterol [mmol/l]	Triglycerides [mmol/]	Cholesterol/HDL
Young control	2,25 ± 0,23	0,783 ± 0,117	1,605 ± 0,066
Young fa/fa	3,40 ± 0,41**	2,917 ± 0,703	1,988 ± 0,214
Old control	2,53 ± 0,15	0,783 ± 0,098	1,539 ± 0,067
Old fa/fa	7,08 ± 1,17$^{\#\#\#,\ ooo}$	4,000 ± 0,802^{oo}	2,736 ± 0,763$^{\#\#,\ ooo}$

Data are mean ± SD, n = 6 animals per group. Significance is *P < 0,05, **P < 0,01 and ***P < 0,001 (*vs. young control rats, $^{\#}$vs. young fa/fa rats, ^{o}vs. old control rats) using two-way ANOVA, Bonferroni post hoc test.
Significance P<0.05, P<0.01, or P<0.001 is illustrated by one, two, or three symbols, respectively. Particular symbols are for particular groups compared.

Abnormal phosphorylation of tau protein in the hippocampus

Regarding the phosphorylation of tau at Ser396 in the hippocampus, main effects of age ($F_{(1,20)} = 21.55$; $p < 0.001$) and genotype ($F_{(1,20)} = 31.16$; $p < 0.001$) were found. Both of these factors increased the phosphorylation of hippocampal tau at Ser396 (Figure 3). There was no significant interaction between age and the fa/fa genotype ($F_{(1,20)} = 1.35$; $p < 0.26$). The two-way ANOVA revealed a significant main effect of fa/fa genotype ($F_{(1,20)} = 8.86$; $p < 0.01$) on Tau Thr231 phosphorylation (Figure 3). Obesity significantly increased the phosphorylation of hippocampal Tau Thr231. Neither a significant effect of age ($F_{(1,20)} = 0.21$; $p < 0.66$) nor an interaction between age and genotype ($F_{(1,20)} = 0.05$; $p < 0.82$) was noted.

Discussion and conclusions

This study revealed attenuated insulin signaling and increased hyperphosphorylation of Tau (at Ser396 and

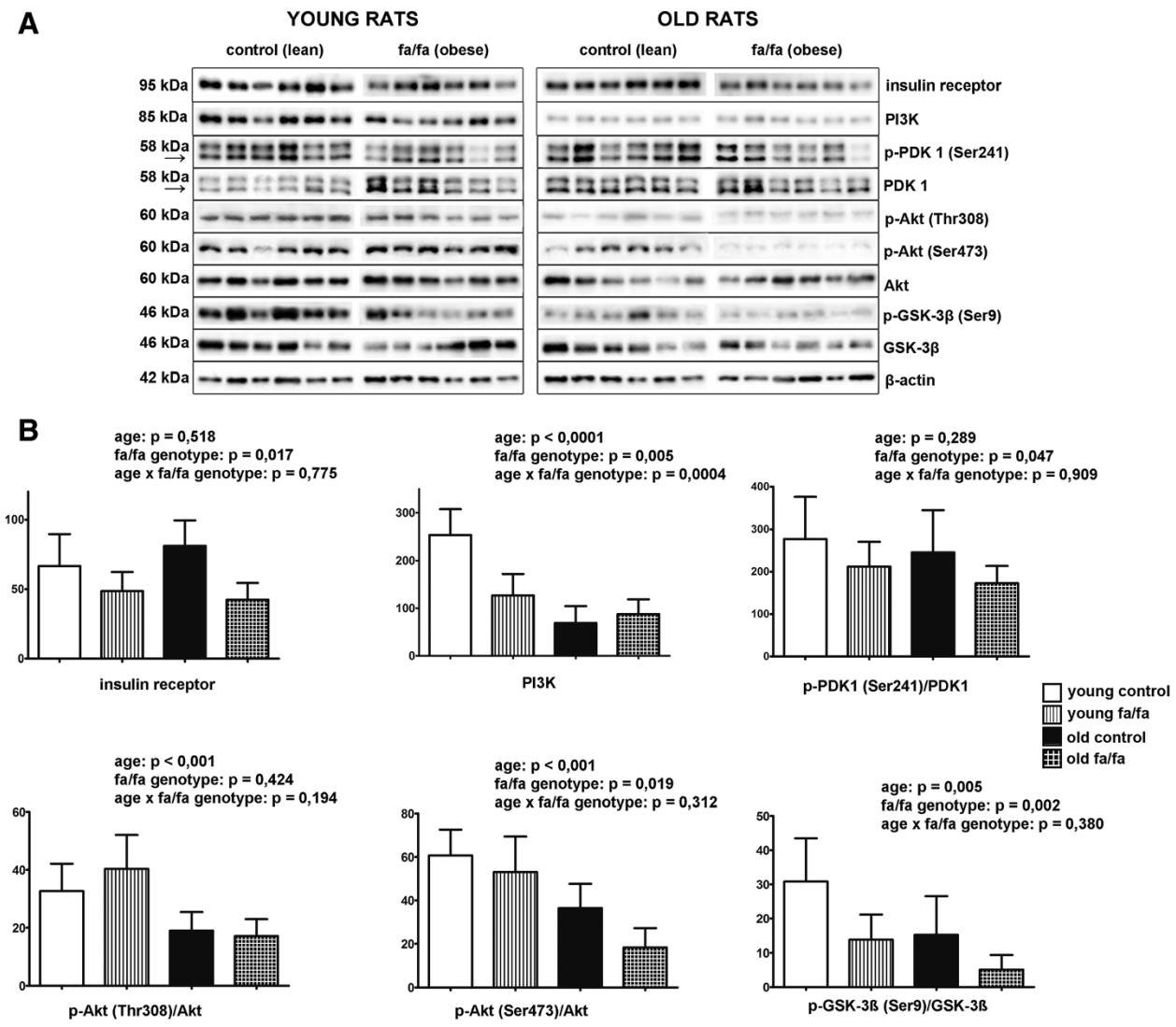

Figure 2 Insulin signaling cascade in hippocampi of fa/fa rats and their control. A Western blots of the proteins involved in insulin signaling cascade using specific antibodies (n = 6 rats per group) **B** Densitometric quantification of the western blots normalized to beta-actin: data are mean ± SD (n = 6 rats per group). Statistical analysis was calculated by two-way ANOVA, Bonferroni post hoc test.

Thr231) in the hippocampi of fa/fa rats exhibiting peripheral insulin resistance or advanced age.

Both the fa/fa rats in this study and the db/db mice in a previous work [9] exhibited impaired leptin signaling, hyperinsulinemia and blood insulin levels approximately 10-fold higher than the normal values. These data indicate that peripheral insulin resistance developed at an early age (8 and 12 weeks) in the db/db mice and the fa/fa rats, respectively. IR in the fa/fa rats was indirectly demonstrated using the QUICKI test. Dyslipidemia in the fa/fa rats could be linked to peripheral IR.

The fa/fa rats were normoglycemic even at an advanced age (33 weeks), whereas 8-week-old db/db mice had glucose levels double those of the control db + mice [9]. Glucose or glucosamine availability is considered to determine the degree of GlcNAcylation of the serines and threonines in the Tau protein that can be phosphorylated [16]. The attenuation of GlcNAcylation in favor of the augmented phosphorylation of the Tau protein has been described as a possible mechanism of Tau pathology [17-19]. On the other hand, healthy mice deprived of food for one to three days (which likely resulted in lower than normal glucose levels) exhibited reversible phosphorylation of hippocampal Tau Ser396 [20]. The fa/fa rats in the present study exhibited an obvious increase in the hyperphosphorylation of hippocampal Tau protein in the normoglycemic state. This finding supports the hypothesis that insulin ineffectiveness, rather than extreme glucose levels, is linked to Tau hyperphosphorylation.

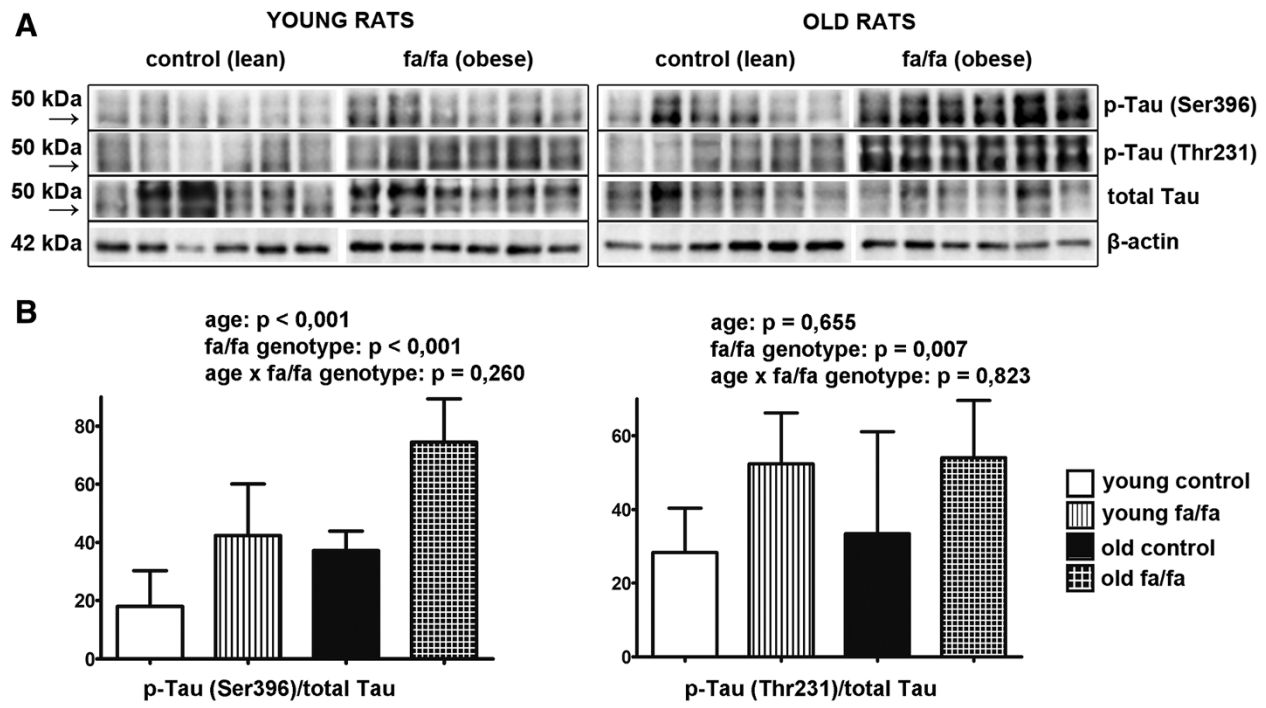

Figure 3 Hyperphosphorylation of Tau protein on different epitopes in hippocampi of fa/fa rats and their control. A Western blots of phosphorylation of Tau protein on the epitopes Ser396 and Thr231 (n = 6 rats per group) **B** Densitometric quantification of western blots normalized to β-actin: data are mean ± SD (n = 6 rats per group). Statistical analysis was calculated by two-way ANOVA, Bonferroni post hoc test.

In this study, the obese rats had significantly reduced hippocampal levels of insulin receptor and PI3 kinase protein. Statistically significantly attenuated phosphorylation of both Akt Thr308 and Ser473 was detected in old-age rats, and this effect was more pronounced in fa/fa rats. A similar trend was found for the phosphorylation of Ser9 in GSK3/β. GSK-3β, a kinase common in insulin cascading and Tau phosphorylation, is constitutively active in resting neurons, and its activity is negatively affected by Ser9 phosphorylation [6,7]. GSK-3β is the primary Tau kinase that hyperphosphorylates Tau [21-23], with Ser199, Thr231, Ser396, and Ser413 as the predominant targets [24]. Cavallini et al. [25] identified GSK-3β and also GSK-3α and MAPK13 as the most active out of 352 kinases overexpressing both Tau kinases and Tau protein [25]. Besides Akt and GSK-3β, extracellular signal-regulated kinase (ERK), is involved both in insulin signaling and Tau phosphorylation. However, there were found no differences in ERK1/2 phosphorylation between the groups in this study (not shown).

The Ser396 and Thr231 phosphorylations investigated in this study are essential in Tau protein pathology for the following reasons. Ser396 is directly phosphorylated by GSK-3β without priming (previous phosphorylation of another Ser or Thr on the Tau protein) [26]. Moreover, a positive relationship between the phosphorylation of Tau Ser396 in the cerebrospinal fluid and the severity of the disease was found in AD patients [27]. Additionally, NIRCO (neuron specific knock-out) mice without insulin receptors in brain neurons showed an increase in the phosphorylation of Tau Thr231, which resulted from the attenuated phosphorylation of Akt Ser473 and GSK-3β Ser9 [5]. Cavallini et al. [25] specified the main phosphorylation sites of Tau as Ser202, Thr231, Ser235, and Ser396/404. In addition to Ser396 and Thr231, we examined Tau phosphorylation at Ser212/214 and Ser 202 in all the groups, but the results were inconsistent.

Inefficient leptin signaling in fa/fa rats could contribute to Tau hyperphosphorylation because leptin has been reported to prevent Tau phosphorylation in neuronal cells via the activation of AMP-dependent kinase [28]. This process was later found to be stress dependent [29], making its role in Tau pathology unclear.

This study demonstrated that the phosphorylation of Ser396 and Thr231 in hippocampal Tau was related to the fa/fa obese phenotype; an interaction with the rats' age was found for Ser396 only. Analogously, in the hippocampi of db/db mice with non-functioning leptin receptors and severe IR, Tau phosphorylation at Ser 199/202, Thr231, and Ser396 was found to progress with age. Unfortunately, the previous study of

db/db mice [9] did not provide data on hippocampal insulin signaling.

In a human study [3], attenuated insulin signaling was inversely correlated with increased Tau hyperphosphorylation in the frontal cortex of T2D patients, and this correlation was more pronounced in T2D patients with AD co-morbidity. However, data on insulin, glucose, and lipid levels were not accessible because of postmortem sampling. Nevertheless, both impaired insulin signaling and Tau hyperphosphorylation in the brain were obvious in both the human study [3] and this rat study.

Peripheral IR in old-age rats appeared to result in central insulin resistance and Tau hyperprotein phosphorylation in the hippocampus. This effect was more pronounced in obese fa/fa rats, which are prone to obesity-induced IR. Based on the normoglycemic state of the IR fa/fa rats, we conclude that a pre-T2D state with IR and normoglycemia is associated with an increased risk of central pathological IR and Tau phosphorylation. The precise mechanism and the role of leptin signaling should be elucidated.

Methods

Animals

This investigation was conducted in accordance with ethical standards of the Declaration of Helsinki. This study conformed to national and international guidelines and was approved by the authors' institutional review board. All experimental procedures and animal care were carried out according to the Jagiellonian University Ethical Committee on Animal Experiments (No 75/2011).

Old (33 weeks old) and young (12 weeks old) male obese Zucker *fa/fa* rats and their age-matched lean controls (n = 6 per each group) were maintained at Jagellonian University in Krakow, Poland. Lean individuals (dominant homozygotes *Fa/Fa* or heterozygotes *Fa/fa*) served as lean controls for the obese *fa/fa* rats. The animals had free access to food and water.

The overnight-fasted rats were euthanized by decapitation. The blood glucose was measured at Synlab (Bratislava, Slovakia) using the multi-analyzer COBAS Integra 800 (Roche Diagnostics Ltd., Rotkreuz, Switzerland), and the serum leptin and insulin levels were determined using RIA kits (Millipore, USA) following the manufacturer's instructions. The measurements of the serum lipids were performed in the Laboratory Diagnostics Unit of The University Hospital in Krakow using commercially available kits (Roche Molecular Diagnostics, Pleasanton, CA, USA). The quantitative insulin sensitivity check index (QUICKI) [30] was calculated as $QUICKI = 1/[(\log(I_0) + \log(G_0)]$, where I_0 is the fasting plasma insulin level (microunits per mL), and G_0 is the fasting blood glucose level (milligrams per dL).

Intraperitoneal glucose tolerance test

All rats were subjected to an intraperitoneal glucose tolerance test (IPGTT) 2 days prior to euthanasia and after a 16-hour-long overnight fast. The rats were administered an intraperitoneal injection of 50% dextrose at a dose of 2 g/kg body weight. The blood glucose was measured using a glucometer (Accu-Chek Active, Roche Diagnostics, Germany) in the tail vein blood prior to and 30, 60, 90, and 120 min after glucose administration.

Tissue preparation for western blotting

The dissected hippocampi were homogenized in a glass microhomogenizer using lysis buffer (62.5 mM Tris–HCl buffer with pH 6.8, 1% deoxycholate, 1% Triton X-100, 50 mM NaF, 1 mM Na_3VO_4, and Complete Protease Inhibitor (Roche, Switzerland). The lysates were sonicated for 10 min and boiled for 10 minutes. The samples for electrophoresis at 1 μg/μl were diluted with a Laemmli sample buffer containing 50 mM NaF and 1 mM Na_3VO_4.

Antibodies

The following primary antibodies were used: insulin receptor rabbit mAb, PI3 kinase rabbit Ab, phospho-PDK1 (Ser241) rabbit mAb, PDK1 rabbit mAb, phospho-Akt (Thr308) rabbit mAb, phospho-Akt (Ser473) rabbit mAb, Akt rabbit mAb, phospho-GSK-3β (Ser9) rabbit mAb, and GSK-3 β rabbit mAb (all from Cell Signaling Technology, Beverly, MA, USA); phosphoTau (Ser396) rabbit mAb and phosphoTau (Thr231) rabbit mAb (clone PHF13.6 and PHF-6, respectively, both from Invitrogen, NY, USA); CTer mouse mAb for total Tau protein (gift from Dr. M.-C. Galas, Inserm U837, Lille, France); and beta-actin mouse mAb (from Sigma Aldrich). The following secondary antibodies were used: anti-mouse IgG HRP-linked antibody and anti-rabbit IgG HRP-linked antibody (both from Cell Signaling Technology, Beverly, MA, USA).

Western blotting

Samples of 2–15 μg total protein were subjected to 4/10% SDS-PAGE and transferred onto nitrocellulose (BIO-RAD) or polyvinylidene difluoride (Sigma Aldrich) membranes. The blots were blocked in 5% non-fat milk or 3% BSA in a TBS/Tween buffer (20 mM Tris, 136 mM NaCl, 0.1% Tween-20) with 50 mM NaF and 1 mM Na_3VO_4, incubated with the appropriate primary antibody, then incubated with the HRP-linked secondary antibody and developed using the SuperSignal West Femto maximum sensitivity substrate (Pierce, Rockford, IL, USA) following the manufacturer's instructions. The bands were visualized using the ChemiDoc™ System (BIO-RAD, Hercules, CA, USA) and were quantified using Image Lab Software (BIO-RAD, Hercules, CA, USA). The band intensities were normalized using actin as an internal loading compound,

and the ratios of the intensity of the band with the phosphorylated protein and the intensity of the band with the total level of protein were calculated.

Statistical analysis

The data were analyzed using IBM SPSS 19 Software and are presented as the means ± SD. The data were tested for normality by Shapiro-Wilk test. Normally distributed data were analysed by two-way analysis of variance with interaction with factors of age and fa/fa genotype. Non-normally distributed data were subjected to natural logarithm transformation followed by two-way ANOVA (insulin). Data without normal distribution despite the use of above mentioned transformation were analysed by non-parametric Kruskal-Wallis test (QUICKI, triglycerides). General Linear Model for Repeated Measures was used to evaluate differences in glycaemia during IPGTT. Total area under the curve (AUC) was calculated to describe increment of plasma glucose levels after exogenous glucose load. The overall level of statistical significance was $p < 0.05$.

Competing interests

The authors declare that there is no competing interest that could be perceived as prejudicing the impartiality of the research reported.

Authors' contributions

AS performed partly sampling and western blots and partly drafted the manuscript, BB performed western blots, KK performed sampling and partly analyses of the blood samples, LG performed sampling, analyses of the blood samples and partly drafted the manuscript, SZ was partly responsible for conception and design of the study, RO was partly responsible for the conception and design of the study. BB-G and MS were partly responsible for analyses of the blood samples, BZ and LM partly drafted the manuscript, LM was corresponding author. All authors read and approved the final manuscript.

Acknowledgements

This project was supported by GACR P303/12/0576 and RVO:61388963 (Czech Rep.), VEGA 2/0089/11 and APVV 0028–10 (Slovakia) and 2011/01 M/NZ04/03752 (Poland). The authors are indebted to Dr. M.-C. Galas, Inserm U837, Lille, France for providing the total Tau protein antibody.

Author details

[1]Institute of Organic Chemistry and Biochemistry, Prague 166 10, Czech Republic. [2]Institute of Experimental Endocrinology, Bratislava 833 06, Slovakia. [3]Jagiellonian University Medical College, Chair of Pharmacology, Krakow 310 08, Poland.

Received: 17 September 2013 Accepted: 18 September 2014
Published: 25 September 2014

References

1. Deng Y, Li B, Liu Y, Iqbal K, Grundke-Iqbal I, Gong CX: **Dysregulation of insulin signaling, glucose transporters, O-GlcNAcylation, and phosphorylation of tau and neurofilaments in the brain: Implication for Alzheimer's disease.** *Am J Pathol* 2009, **175**(5):2089–2098.
2. Kopf D, Frölich L: **Risk of incident Alzheimer's disease in diabetic patients: a systematic review of prospective trials.** *J Alzheimers Dis* 2009, **16**(4):677–685.
3. Liu Y, Liu F, Grundke-Iqbal I, Iqbal K, Gong CX: **Deficient brain insulin signalling pathway in Alzheimer's disease and diabetes.** *J Pathol* 2011, **225**(1):54–62.
4. Hong M, Lee VM: **Insulin and insulin-like growth factor-1 regulate tau phosphorylation in cultured human neurons.** *J Biol Chem* 1997, **272**(31):19547–19553.
5. Schubert M, Gautam D, Surjo D, Ueki K, Baudler S, Schubert D, Kondo T, Alber J, Galldiks N, Küstermann E, Arndt S, Jacobs AH, Krone W, Kahn CR, Brüning JC: **Role for neuronal insulin resistance in neurodegenerative diseases.** *Proc Natl Acad Sci U S A* 2004, **101**(9):3100–3105. Epub 2004 Feb 23.
6. Sutherland C, Leighton IA, Cohen P: **Inactivation of glycogen synthase kinase-3 beta by phosphorylation: new kinase connections in insulin and growth-factor signalling.** *Biochem J* 1993, **296**(Pt 1):15–19.
7. Cross DA, Alessi DR, Cohen P, Andjelkovich M, Hemmings BA: **Inhibition of glycogen synthase kinase-3 by insulin mediated by protein kinase B.** *Nature* 1995, **378**(6559):785–789.
8. Takashima A: **GSK-3 is essential in the pathogenesis of Alzheimer's disease.** *J Alzheimers Dis* 2006, **9**(3 Suppl):309–317.
9. Kim B, Backus C, Oh S, Hayes JM, Feldman EL: **Increased tau phosphorylation and cleavage in mouse models of type 1 and type 2 diabetes.** *Endocrinology* 2009, **150**(12):5294–5301.
10. Li J, Deng J, Sheng W, Zuo Z: **Metformin attenuates Alzheimer's disease-like neuropathology in obese, leptin-resistant mice.** *Pharmacol Biochem Behav* 2012, **101**(4):564–574.
11. Jolivalt CG, Lee CA, Beiswenger KK, Smith JL, Orlov M, Torrance MA, Masliah E: **Defective insulin signaling pathway and increased glycogen synthase kinase-3 activity in the brain of diabetic mice: parallels with Alzheimer's disease and correction by insulin.** *J Neurosci Res* 2008, **86**(15):3265–3274.
12. www.criver.com.
13. www.harlan.com.
14. Shiota M, Printz RL: **Diabetes in Zucker diabetic fatty rat.** *Methods Mol Biol* 2012, **933**:103–123.
15. Di Nardo F, Burattini R, Cogo CE, Faelli E, Ruggeri P: **Age-related analysis of insulin resistance, body weight and arterial pressure in the Zucker fatty rat.** *Exp Physiol* 2009, **94**(1):162–168.
16. Walgren JL, Vincent TS, Schey KL, Buse MG: **High glucose and insulin promote O-GlcNAc modification of proteins, including alpha-tubulin.** *Am J Physiol Endocrinol Metab* 2003, **284**(2):E424–E434.
17. Dias WB, Hart GW: **O-GlcNAc modification in diabetes and Alzheimer's disease.** *Mol Biosyst* 2007, **3**(11):766–772.
18. Deng Y, Li B, Liu F, Iqbal K, Grundke-Iqbal I, Brandt R, Gong CX: **Regulation between O-GlcNAcylation and phosphorylation of neurofilament-M and their dysregulation in Alzheimer disease.** *FASEB J* 2008, **22**(1):138–145.
19. Lefebvre T, Dehennaut V, Guinez C, Olivier S, Drougat L, Mir AM, Mortuaire M, Vercoutter-Edouart AS, Michalski JC: **Dysregulation of the nutrient/stress sensor O-GlcNAcylation is involved in the etiology of cardiovascular disorders, type-2 diabetes and Alzheimer's disease.** *Biochim Biophys Acta* 2010, **1800**(2):67–79.
20. Yanagisawa M, Planel E, Ishiguro K, Fujita SC: **Starvation induces tau hyperphosphorylation in mouse brain: implications for Alzheimer's disease.** *FEBS Lett* 1999, **461**(3):329–333.
21. Ishiguro K, Omori A, Takamatsu M, Sato K, Arioka M, Uchida T, Imahori K: **Phosphorylation sites on tau by tau protein kinase I, a bovine derived kinase generating an epitope of paired helical filaments.** *Neurosci Lett* 1992, **148**(1–2):202–206.
22. Yamaguchi H, Ishiguro K, Uchida T, Takashima A, Lemere CA, Imahori K: **Preferential labeling of Alzheimer neurofibrillary tangles with antisera for tau protein kinase (TPK) I/glycogen synthase kinase-3 beta and cyclin-dependent kinase 5, a component of TPK II.** *Acta Neuropathologica* 1996, **92**(3):232–241.
23. Hooper C, Killick R, Lovestone S: **The GSK3 hypothesis of Alzheimer's disease.** *J Neurochem* 2008, **104**(6):1433–1439.
24. Michel G, Mercken M, Murayama M, Noguchi K, Ishiguro K, Imahori K, Takashima A: **Characterization of tau phosphorylation in glycogen synthase kinase-3beta and cyclin dependent kinase-5 activator (p23) transfected cells.** *Biochim Biophys Acta* 1998, **1380**(2):177–182.
25. Cavallini A, Brewerton S, Bell A, Sargent S, Glover S, Hardy C, Moore R, Calley J, Ramachandran D, Poidinger M, Karran E, Davies P, Hutton M, Szekeres P, Bose S: **An unbiased approach to identifying tau kinases that phosphorylate tau at sites associated with Alzheimer disease.** *J Biol Chem* 2013, **288**(32):23331–23347.
26. Leroy A, Landrieu I, Huvent I, Legrand D, Codeville B, Wieruszeski JM, Lippens G: **Spectroscopic studies of GSK3{beta} phosphorylation of the**

neuronal tau protein and its interaction with the N-terminal domain of apolipoprotein E. *J Biol Chem* 2010, **285**(43):33435–33444.
27. Hu YY, He SS, Wang X, Duan QH, Grundke-Iqbal I, Iqbal K, Wang J: **Levels of nonphosphorylated and phosphorylated tau in cerebrospinal fluid of Alzheimer's disease patients: an ultrasensitive bienzyme-substrate-recycle enzyme-linked immunosorbent assay.** *Am J Pathol* 2002, **160**(4):1269–1278.
28. Greco SJ, Sarkar S, Johnston JM, Zhu X, Su B, Casadesus G, Ashford JW, Smith MA, Tezapsidis N: **Leptin reduces Alzheimer's disease-related tau phosphorylation in neuronal cells.** *Biochem Biophys Res Commun* 2008, **376**(3):536–541.
29. Salminen A, Kaarniranta K, Haapasalo A, Soininen H, Hiltunen M: **AMP-activated protein kinase: a potential player in Alzheimer's disease.** *J Neurochem* 2011, **118**(4):460–474.
30. Katz A, Nambi SS, Mather K, Baron AD, Follmann DA, Sullivan G, Quon MJ: **Quantitative insulin sensitivity check index: a simple, accurate method for assessing insulin sensitivity in humans.** *J Clin Endocrinol Metab* 2000, **85**(7):2402–2410.

doi:10.1186/1471-2202-15-111
Cite this article as: Špolcová *et al.*: Deficient hippocampal insulin signaling and augmented Tau phosphorylation is related to obesity- and age-induced peripheral insulin resistance: a study in Zucker rats. *BMC Neuroscience* 2014 **15**:111.

International Journal of Obesity (2015), 1–8

www.nature.com/ijo

ORIGINAL ARTICLE

Novel lipidized analogs of prolactin-releasing peptide have prolonged half-lives and exert anti-obesity effects after peripheral administration

L Maletínská[1], V Nagelová[1], A Tichá[1], J Zemenová[1,2], Z Pirník[1,3,4], M Holubová[1], A Špolcová[1], B Mikulášková[1,5], M Blechová[1], D Sýkora[2], Z Lacinová[6], M Haluzík[6], B Železná[1] and J Kuneš[1,5]

OBJECTIVES: Obesity is a frequent metabolic disorder but an effective therapy is still scarce. Anorexigenic neuropeptides produced and acting in the brain have the potential to decrease food intake and ameliorate obesity but are ineffective after peripheral application. We have designed lipidized analogs of prolactin-releasing peptide (PrRP), which is involved in energy balance regulation as demonstrated by obesity phenotypes of both PrRP- and PrRP-receptor-knockout mice.

RESULTS: Lipidized PrRP analogs showed binding affinity and signaling in PrRP receptor-expressing cells similar to natural PrRP. Moreover, these analogs showed high binding affinity also to anorexigenic neuropeptide FF-2 receptor. Peripheral administration of myristoylated and palmitoylated PrRP analogs to fasted mice induced strong and long-lasting anorexigenic effects and neuronal activation in the brain areas involved in food intake regulation. Two-week-long subcutaneous administration of palmitoylated PrRP31 and myristoylated PrRP20 lowered food intake, body weight and improved metabolic parameters, and attenuated lipogenesis in mice with diet-induced obesity.

CONCLUSIONS: Our data suggest that the lipidization of PrRP enhances stability and mediates its effect in central nervous system. Strong anorexigenic and body-weight-reducing effects make lipidized PrRP an attractive candidate for anti-obesity treatment.

International Journal of Obesity advance online publication, 14 April 2015; doi:10.1038/ijo.2015.28

INTRODUCTION

Prolactin-releasing peptide (PrRP) was originally discovered as an endogenous ligand of an orphan G-protein-coupled receptor.[1] PrRP and its receptor named GPR10 were detected in several hypothalamic nuclei,[2] suggesting an involvement of PrRP in the control of food intake and body weight.[3] PrRP was also found to have high affinity to the neuropeptide FF-2 (NPFF2) receptor, resulting in anorexigenic effect.[4] The endogenous ligand of NPFF2 receptor, NPFF, also has hyperalgesic and anti-morphine analgesic properties (for reviews, see[5,6]).

The suggestion that PrRP may act as a homeostatic regulator of food intake was supported by the finding that PrRP messenger RNA (mRNA) expression was reduced in situations of negative energy balance similarly to other anorexigenic peptides such as α-melanocyte stimulating hormone or cocaine- and amphetamine-regulated transcript peptide.[3] The intracerebroventricular administration of PrRP inhibited food intake and body weight gain in rats but did not cause conditioned taste aversion.[7] Furthermore, Fos immunoreactivity was enhanced after PrRP administration in the brain areas associated with food intake regulation.[7]

Finally, PrRP-receptor-knockout mice had significantly higher body weight at 15 weeks of age compared with wild-type mice, and this late-onset obesity was much more pronounced in female mice, which also exhibited a significant decrease in energy expenditure.[8] Similarly, PrRP-deficient mice displayed late-onset obesity, increased food intake and attenuated responses to the anorexigenic signals cholecystokinin and leptin.[9]

Taken together, these findings suggest that PrRP and other anorexigenic neuropeptides involved in food intake regulation[10,11] may have a potential in the development of future anti-obesity agents. Nevertheless, because these peptides normally regulate food intake directly in the hypothalamus, their anorexigenic potential after peripheral administration is hampered by their inability to cross the blood-brain barrier (BBB) and to reach the target brain receptors.

For the design of peptide drugs, the lipidization of peptides, that is, the attachment of fatty-acid chain to peptides through ester or amide bond is advantageous. Such modification results in an increased stability and half-life of the peptide, and it is possible that these modifications allow peptide to cross the BBB after a peripheral administration (reviewed by[12–14]). Myristoylation or palmitoylation through an amide bond on a Lys has been employed in the insulin analog detemir[15] or glucagon-like peptide 1 analog liraglutide.[16] Both of these peripherally acting lipopeptide drugs show strongly prolonged half-lives and slower biodegradation. Central effects of detemir and liraglutide have been described suggesting that the attachment of fatty acid may also enable these peptides to cross the BBB.[17]

PrRP seems to be a suitable candidate for lipidization because of its linear, one-chain peptide structure. Two biologically active

[1]Antiobesity Peptides, Institute of Organic Chemistry and Biochemistry, AS CR, Prague, Czech Republic; [2]Department of Analytical Chemistry, University of Chemistry and Technology, Prague, Czech Republic; [3]Laboratory of Functional Neuromorphology, Institute of Experimental Endocrinology, SAS, Bratislava, Slovak Republic; [4]Department of Human and Clinical Pharmacology, University of Veterinary Medicine, Košice, Slovak Republic; [5]Institute of Physiology, AS CR, Prague, Czech Republic and [6]Third Department of Medicine, Charles University in Prague, Prague, Czech Republic. Correspondence: Dr L Maletínská, Antiobesity Peptides, Institute of Organic Chemistry and Biochemistry, AS CR, Flemingovo nam. 2, Prague 6 166 10, Czech Republic.
E-mail: maletin@uochb.cas.cz
Received 29 August 2014; revised 10 February 2015; accepted 19 February 2015; accepted article preview online 16 March 2015

isoforms of PrRP, with either 31 (PrRP31) or 20 (PrRP20) amino acids contain a C-terminal Arg-Phe-amide sequence that is critical for the preservation of biological activity of PrRP.[18–20]

The aim of this study was to achieve the direct central anorexigenic activity of PrRP via its peripheral route of administration employing the lipidization of its N terminus. We tested a series of PrRP analogs modified with fatty acids of various lengths both *in vitro* and *in vivo*. The data showed that myristoylated PrRP20 and palmitoylated PrRP31 retained the biological activity of PrRP while significantly decreasing food intake and body weight and improving metabolic parameters upon peripheral administration in mice with diet-induced obesity. Thus, the lipidization of neuropeptides involved in food intake regulation might serve as a tool to retain their ability to act centrally after peripheral administration.

MATERIALS AND METHODS

Peptide synthesis and iodination

Rat PrRP analogs (for structure see Table 1), human PrRP31 (SRTHRHSMEIRTPDINPAWYASRGIRPVGRF-NH_2), scrambled peptides (SHQ RPADTHWYPRGNIeFPTIGRITARNGEVSR-NH_2 and (N-myr)SHQRPADTHWYP RGNIeFPTIGRITARNGEVSR-NH_2) and a stable analog of NPFF, 1DMe (D-YL(N-Me)FQPQRF-NH_2) were synthesized and purified as described previously.[21] Lipidization of PrRP analogs was performed as shown in[22] on fully protected peptide on resine as a last step. The purity and identity of all peptides were determined by analytical high-performance liquid chromatography and by using a Q-TOF micro MS technique (Waters, Milford, MA, USA).

Rat or human PrRP31 and 1DMe were iodinated at Tyr^{20} and D-Tyr^1, respectively, with $Na^{125}I$ (Izotop, Budapest, Hungary) as described previously.[22]

Binding to intact plated cells and cell membranes

Rat pituitary RC-4B/C cells obtained from ATCC (Manassas, VA, USA) were grown as described previously[24] and Chinese hamster ovarian (CHO)-K1 cells with GPR10 receptor (Perkin Elmer, Waltham, MA, USA) according to manufacturer's instructions. Saturation and competitive binding experiments were performed according to Motulsky and Neubig.[25] RC-4B/C or CHO-K1 cells were incubated with 0.5–5 nM ^{125}I-rPrRP31 or ^{125}I-hPrRP31, respectively, in saturation experiments or with 0.1 nM ^{125}I-rPrRP31 or with 0.03 nM ^{125}I-hPrRP31, respectively, and 10^{-11}–10^{-5}M non-radioactive ligands in competitive binding experiments. Experiments were performed on plates incubated for 60 min at 25 °C. Non-specific binding was determined using 10^{-5}M PrRP31. Binding assays on human NPFF2 receptor membranes obtained from Perkin Elmer were performed as described in.[24]

Detection of MAPK/ERK1/2 phosphorylation by western blotting

CHO-K1 cells were incubated with PrRP31, PrRP20, palm-PrRP31 or myr-PrRP20 with final concentrations from 10^{-7}–10^{-12}M for 5 min at 37 °C. The cells were lysed and western blots carried out as described in.[26]

Stability of PrRP analogs *in vitro*

Rat plasma fortified with a solution of the studied compound at a concentration of 3×10^{-6}M was incubated at 37 °C. The times of sampling were 0–24 h for PrRP31 and PrRP20 and 0–96 h for palm-PrRP31 and myr-PrRP20. Samples were collected in triplicates and stored at − 20 °C. The PrRP(1–31) EIA high-sensitivity kit (Peninsula Laboratories, San Carlos, CA, USA) was used according to the manufacturer's instructions.

Pharmacokinetics *in vivo* in mice

All animal experiments followed the ethical guidelines for animal experiments and the Act of the Czech Republic Nr. 246/1992 and were approved by the Committee for Experiments with Laboratory Animals of the ASCR.

The measurement of *in vivo* pharmacokinetics was performed as previously described.[23] C57BL/6 male mice were injected subcutaneously (SC) with PrRP31, PrRP20, palm-PrRP31 or myr-PrRP20 (dissolved in saline; Sal) at a dose of 5 mg kg^{-1} ($n = 3$), blood plasma collected and peptides determined by PrRP(1–31) EIA high-sensitivity kit.

Acute food intake in lean mice

Male C57BL/6 mice from Charles Rivers Laboratories (Sulzfeld, Germany) were housed at a temperature of 23 °C and a daily cycle of 12 h light and dark (lights on at 6:00). The mice were given *ad libitum* water and standard chow diet (St-1, Mlýn Kocanda, Jesenice, Czech Republic). Following schedules were used for food intake monitoring after single administration of peptides: (a) on the day of the food intake experiment, overnight (17 h) fasted mice were injected SC with Sal or PrRP analogs at doses of 0.1–5 mg kg^{-1} (all dissolved in Sal) ($n = 6$–8). Fifteen minutes after injection, the mice were given weighed food pellets. The pellets were weighed every 30 min for at least 6 h. (b) Freely fed mice were injected SC with Sal or PrRP analogs at a dose of 5 mg kg^{-1} (all dissolved in Sal) ($n = 6$) 30 min before lights out. Food intake was monitored every 10 min for at least 14 h using automatic food intake monitoring system (Development Workshops of IOCB, Prague, Czech Republic).

Fos immunohistochemistry

For c-Fos immunohistochemical processing, overnight-fasted male mice with the free access to water ($n = 4$) were SC injected with Sal or PrRP31, oct-PrRP31, myr-PrRP20 or palm-PrRP31 at a dose of 5 mg kg^{-1}. Ninety minutes after injection, the mice were deeply anesthetized with sodium pentobarbital (50 mg kg^{-1}, intraperitoneally) and perfused transcardially, the brains were treated and c-Fos immunoreactivity determined as described in.[27,28]

Table 1. Structures and binding affinities of PrRP analogs

Analog	*Sequence*	*Human GPR10. ^{125}I-human PrRP31 binding K_i (nM)*	*Human NPFF2.^{125}I-1DMe binding K_i (nM)*	*RC-4B/C cells. ^{125}I-rat PrRP31 binding K_i (nM)*
PrRP31	SRAHQHSMETRTPDINPAWYTGRGIRPVGRF-NH_2	3.91 ± 0.21	42.21 ± 6.76	2.38 ± 0.11
oct-PrRP31	(N-oct)SRAHQHS Nle ETRTPDINPAWYTGRGIRPVGRF-NH_2	1.49 ± 0.07	24.82 ± 13.2	0.98 ± 0.22
dec-PrRP31	(N-dec)SRAHQHS Nle ETRTPDINPAWYTGRGIRPVGRF-NH_2	1.42 ± 0.55	14.73 ± 3.10	0.68 ± 0.12
dodec-PrRP31	(N-dodec)SRAHQHS Nle ETRTPDINPAWYTGRGIRPVGRF-NH_2	1.15 ± 0.35	14.28 ± 6.40	0.38 ± 0.14
myr-PrRP31	(N-myr)SRAHQHS Nle ETRTPDINPAWYTGRGIRPVGRF-NH_2	0.69 ± 0.09	1.59 ± 0.32	0.69 ± 0.09
palm-PrRP31	(N-palm)SRAHQHS Nle ETRTPDINPAWYTGRGIRPVGRF-NH_2	2.94 ± 0.33	0.69 ± 0.36	0.51 ± 0.15
stear-PrRP31	(N-stear)SRAHQHS Nle ETRTPDINPAWYTGRGIRPVGRF-NH_2	5.24 ± 0.57	15.92 ± 14.43	0.93 ± 0.08
PrRP20	TPDINPAWYTGRGIRPVGRF-NH_2	4.4 ± 0.77	21.80 ± 9.91	2.23 ± 0.19
oct-PrRP20	(N-oct)TPDINPAWYTGRGIRPVGRF-NH_2	1.88 ± 0.31	48.13 ± 13.19	0.91 ± 0.23
dec-PrRP20	(N-dec)TPDINPAWYTGRGIRPVGRF-NH_2	2.94 ± 0.47	3.60 ± 2.57	0.41 ± 0.01
dodec-PrRP20	(N-dodec)TPDINPAWYTGRGIRPVGRF-NH_2	2.34 ± 0.25	9.97 ± 3.48	0.58 ± 0.22
myr-PrRP20	(N-myr)TPDINPAWYTGRGIRPVGRF-NH_2	4.21 ± 0.24	8.23 ± 1.97	1.02 ± 0.20

Abbreviations: dec, decanoyl; dodec, dodecanoyl; myr, myristoyl; Nle, norleucine; oct, octanoyl; palm, palmitoyl; stear, stearoyl. The means ± s.e.m. of at least three separate experiments are shown. In competitive binding, K_i was calculated using the Cheng–Prusoff equation. The concentration of the radioligand was 0.1 nM or 0.03 nM, and the K_d that was calculated from saturation experiments was 4.21 ± 0.66 nM for RC-4B/C[23] or 0.95 ± 0.20 nM for GPR10 receptor in CHO cells, respectively. K_d for NPFF2 receptor in CHO cells was 0.72 ± 0.12 nM.

Behavioral tests in mice

Locomotor activity and analgesia were measured in free-fed mice using the VideoMot system (TSE Systems, Bad Homburg, Germany) after the SC injection of Sal, PrRP31, oct-PrRP31, palm-PrRP31 and myr-PrRP20 at a dose of 5 mg kg^{-1} ($n = 5$) as described previously.[28,29]

The elevated plus maze (TSE Systems) test was used to measure anxiety/fear behavior. The total time spent in open and closed arms was measured.

Determination of prolactin release in rats and mice

Male Wistar rats (250–300 g, Harlan Laboratories, Correzzana, Italy, $n = 3$) were injected intravenously into the jugular vein with Sal, thyrotropin-releasing hormone (10 μg kg^{-1}) or palm-PrRP31 (0.5 mg kg^{-1}), or SC with Sal or palm-PrRP31 (5 mg kg^{-1}). Blood was collected from carotid artery before injections and 5 and 10 min after injections. Male C57BL/6 mice were injected SC with Sal, myr-PrRP20 or palm-PrRP31 (5 mg kg^{-1}). Blood was collected by decapitation 10 min after injection. Prolactin (PRL) in rat or mouse serum was determined with a radioimmunoassay assay kit (Izotop).

Effect of 14-day administration of palm-PrRP31 and myr-PrRP20 on food intake and metabolic parameters in mice with high-fat diet-induced obesity

From 8 weeks of age, C57BL/6 mice were supplied with a high-fat (HF) diet for 12 weeks to induce obesity. The energy content of the HF diet was 5.3 kcal g^{-1}, with 13%, 60% and 27% of the calories derived from protein, fat and carbohydrate, respectively.[30] Food intake and body weight were monitored weekly from 9 to 18 weeks of age. Mice resistant to the HF diet were withdrawn from the experiment (~10% of mice).

At the age of 19 weeks, the mice were divided into groups of 10 animals and placed into the separate cages with free access to HF diet and water. Three groups were injected SC either with Sal or with palm-PrRP31 or myr-PrRP20 at a dose of 5 mg kg^{-1} twice a day. The fourth group served as pair-fed controls to the animals treated with palm-PrRP31, and was given food amount consumed by palm-PrRP31 treated mice the previous day. The amount of the HF diet consumed and the weight of the mice were monitored daily.

At the end of the experiment, overnight-fasted mice were killed by decapitation starting at 8:00 a.m. The trunk blood was collected, and the plasma was separated and stored at −20 °C. The intraperitoneal adipose tissue (IPAT), subcutaneous adipose tissue (SCAT), the perirenal adipose tissue, the brown adipose tissue and the liver of all mice were dissected, weighed and stored at − 70 °C.

Determination of hormonal and biochemical parameters

The plasma insulin concentrations were measured with radioimmunoassay assays (Linco Research, St Charles, MI, USA), leptin concentrations were determined with enzyme-linked immuno assay (Millipore, St Charles, MI, USA), corticosterone levels were determined with radioimmunoassay assay kit (Izotop) and adrenocorticotropic hormone with enzyme-linked immuno assay (Peninsula Laboratories). The plasma glucose levels were measured using a Glucocard glucometer (Arkray, Kyoto, Japan). The plasma triglyceride levels were measured by quantitative enzymatic reactions (Sigma, St Louis, MO, USA).

Determination of mRNA expression

Samples of adipose tissue (IPAT, SCAT) and liver were processed as described in.[31] Determination of the mRNA expression of genes of interest (ACACA and FASN in liver, IPAT and SCAT; lipoprotein lipase, adiponectin and leptin in IPAT and SCAT, FABP-4 in liver, UCP-1 in brown adipose tissue) was performed using an ABI PRISM 7500 instrument (Applied Biosystems, Foster City, CA, USA). The expression of beta-2-microglobulin was used to compensate for variations in input RNA amounts and the efficiency of reverse transcription. (ACACA—acetyl-CoA carboxylase 1, FASN—fatty-acid synthase, LPL—lipoprotein lipase, SREBP—sterol regulatory element-binding protein, FABP-4—fatty-acid binding protein 4, UCP-1—uncoupling protein-1).

Analysis of binding data and statistics

The saturation binding curves were plotted using GraphPad software (San Diego, CA, USA) comparing the best fit for single binding site models (K_d, B_{max} and IC_{50} values were obtained from nonlinear regression analysis). Inhibition constants (K_i) were calculated from the IC_{50} values using the Cheng–Prusoff equation.[32]

The data are presented as the means ± s.e.m. for the number of animals indicated in the figures and tables. The data were analyzed using one-way analysis of variance followed by the Dunnett's *post hoc* test or a *t*-test, as stated in the figure and table legends, using the GraphPad Software.

RESULTS

Lipidized analogs of PrRP20 and PrRP31 are agonists of the PrRP receptor GPR10 and have high affinity to both GPR10 and NPFF2 receptors

The peptide sequences were assembled on a solid support as described in the Materials and Methods. The purity of all peptides was higher than 95%. The structures of the PrRP analogs used in this study are shown in Table 1. PrRP20 and PrRP31 were lipidized at the N terminus with fatty acids of different lengths. Lipidized PrRP31 analogs were modified with norleucine in position 8 to avoid oxidation of the original methionine. Analogously to a similar modification of the cocaine- and amphetamine-regulated transcript peptide,[33] the change of methionine for norleucine did not affect the biological activity of PrRP31.

All native and lipidized analogs of PrRP31 and PrRP20 competed with human ^{125}I-PrRP31 for binding to CHO cells overexpressing the human PrRP receptor GPR10 with K_i values in a nanomolar range, as shown in Table 1. Scrambled peptide based on PrRP20 and its myristoylated analog (structures in the Methods) were bound to GPR10 receptor with a negligible affinity, with K_i values higher than 10^{-5}M.

Natural PrRP31 and PrRP20, as well as their lipidized analogs palmitoylated PrRP31 (palm-PrRP31) and myristoylated PrRP20 (myr-PrRP20), respectively, increased the phosphorylation of MAPK/ERK1/2 in CHO cells overexpressing GPR10 receptor with an EC_{50} values in the nanomolar range (EC_{50} was 1.01 nM for PrRP31, 5.62 nM for PrRP20, 0.93 nM for palm-PrRP31 and 1.48 nM for myr-PrRP20), which confirmed the powerful agonist effects of palm-PrRP31 and myr-PrRP20 on the GPR10 receptor. The dose–response curves are shown in Supplementary Figure S1.

Lipidized PrRP analogs were bound to CHO cells overexpressing NPFF2 receptor with K_i values of 10^{-8}M range or lower, similar to native PrRP20 and PrRP31 in competition binding with a stable NPFF analog ^{125}I-1DMe (Table 1). Myristoylated and palmitoylated PrRP analogs displaced ^{125}I-1DMe with affinity equal to or higher than 1DMe ($K_i = 2.21 \pm 0.70$).

In the rat tumor pituitary cell line RC-4B/C expressing endogenously both GPR10 and NPFF2, lipidized PrRP analogs were bound with a very high affinity to these cells that increased with the length of the carbon chain of a fatty acid (Table 1).

Palm- and stear-PrRP31 and myr-PrRP20 attenuate food intake after acute peripheral administration in fasted lean mice and activate neurons in the food intake-regulating areas in the brain

Food intake was unaffected in Sal-treated controls and native PrRP31 and native PrRP20 administered SC in mice, both fasted and freely fed (Figure 1). In contrast, anorexigenic effects of several peripherally administered lipidized analogs of PrRP31 and PrRP20 were proven in fasted mice (Figure 1a and b) and freely fed mice (Figure 1c). After the acute SC administration of myr-PrRP20 and palm- and stear-PrRP31 (dose of 5 mg kg^{-1}), food intake was very significantly lowered for several hours. The effects of myr-PrRP20 and palm-PrRP31 were dose-dependent, with a dose as low as 1 mg kg^{-1} of each peptide significantly lowering food intake (Supplementary Figure S2). Scrambled myristoylated PrRP20 had no effect on food intake in mice after peripheral administration (Figure 1a). Interestingly, PrRP31 lipopeptides with myristoyl and fatty acids of shorter carbon chains and PrRP20 lipopeptides with dodecanoyl fatty acid and fatty

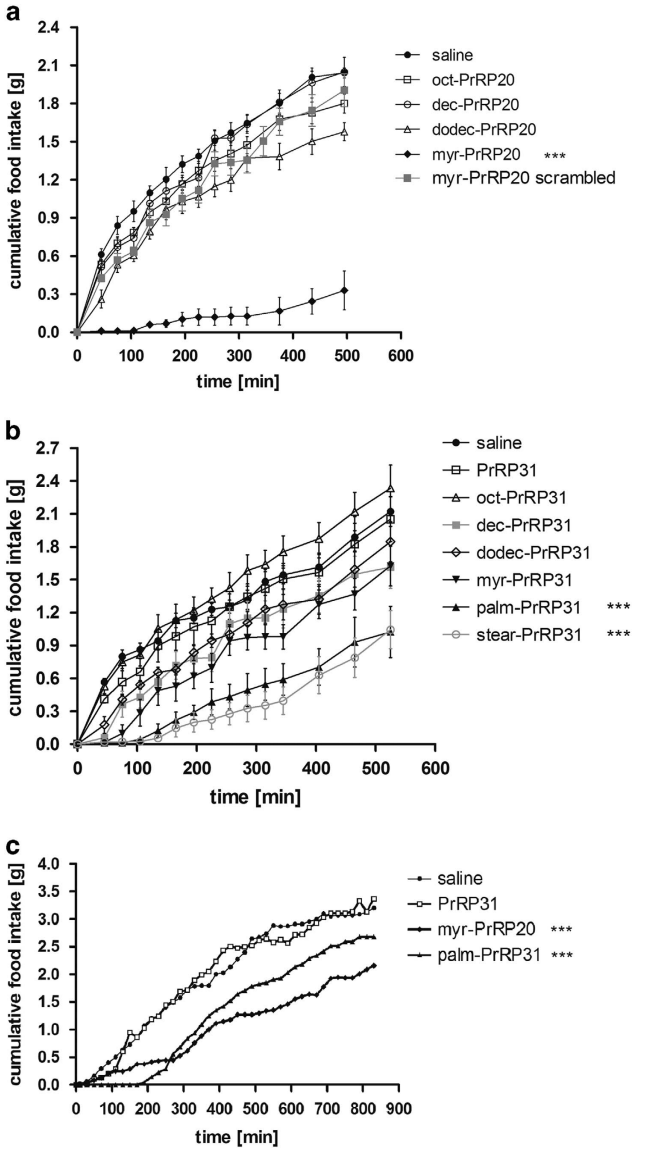

Figure 1. Palmitoylated and stearoylated PrRP31 and myristoylated PrRP20 attenuate food intake after acute peripheral administration in fasted mice. Cumulative food intake of 17 h fasted mice after acute SC administration of (**a**) lipidized PrRP20 analogs, (**b**) natural and lipidized PrRP31 analogs at a dose of 5 mg kg^{-1}, (**c**) cumulative food intake of freely fed mice after acute SC administration of saline, PrRP31, myr-PrRP20 and palm-PrRP31 (dose 5 mg kg^{-1}). Food intake is expressed in grams of food consumed ($n = 6$–8 mice per group). ***$P < 0.001$ vs saline-treated group. The significance concerns the whole time course.

acids of shorter carbon chains did not significantly affect food intake (Figure 1a and b). Although myr-PrRP20 showed a stronger anorexigenic potency at a dose of 5 mg kg^{-1} SC in fasted mice compared with palm-PrRP31 (Figures 1a and b), anorexigenic effect of both analogs was comparable in freely fed mice (Figure 1c) and moreover, palm-PrRP31 lowered food intake more significantly than myr-PrRP30 at a dose of 1 mg kg^{-1} (Supplementary Figure 2). It might be explained by higher lipophilicity and lower solubility of myr-PrRP20 compared with palm-PrRP31.

The central effect of peripherally administered palm-PrRP31 as well as myr-PrRP20 was confirmed by a significant increase in c-Fos immunoreactivity in the hypothalamic and brainstem nuclei involved in food intake regulation (Figure 2). Natural and octanoylated PrRP31 administered peripherally did not influence food intake and did not increase c-Fos immunoreactivity.

Lipidized analogs of PrRP are selective and stable anorexigenic compounds

Several behavioral tests in mice were carried out to evaluate possible side effects of selected PrRP analogs after their peripheral administration. Two analogs that did not affect food intake after SC administration, PrRP31 and oct-PrRP31, and two analogs that did significantly decrease food intake, myr-PrRP20 and palm-PrRP31, were SC administered into mice at a dose of 5 mg kg^{-1} to test their sedative effect (in the open field test), analgesic activity (in the hot plate test) and anxiety (in the elevated plus maze). Neither non-lipidized nor lipidized PrRP analogs influenced open field locomotory activity, nor did they exhibit any analgesic or hyperalgesic activity, nor were any anxiogenic effects in the elevated plus maze observed (Supplementary Figure S3).

After intravenously or SC administration, Palm-PrRP31 did not increase PRL release in rats compared with intravenously administered thyrotropin (Supplementary Figure S4a). Similarly, myr-PrRP20 and palm-PrRP31 did not significantly affect PRL release in mice after SC administration (Supplementary Figure S4b).

The degradation of selected PrRP analogs was tested in rat plasma *in vitro*. The stabilities of palm-PrRP31 and myr-PrRP20 were prolonged (> 24 h) compared with native PrRP20 or PrRP31 (half-lives ~ 10–20 min) (Figure 3a), possibly by promoting the association of these peptides with circulating plasma proteins through the attached fatty-acid moieties.

To further validate the pharmacokinetic profiles of selected analogs *in vivo*, plasma concentrations of PrRP31, PrRP20, palm-PrRP31 and myr-PrRP20 were determined after a single SC injection into mice (Figure 3b). Lipidized PrRP analogs showed longer stability and increased AUC compared with natural PrRP31 and PrRP20.

Chronic 14-days administration of palm-PrRP31 and myr-PrRP20 decreased food intake and body weight in DIO mice, improved metabolic parameters and positively affected lipid metabolism

Rodents with diet-induced obesity are considered models of the most common human obesity, which is associated with the consumption of HF food. The therapeutic potential of two selected lipidized PrRP analogs that were the most potent in the acute food intake test was assessed in diet-induced obese mice that were peripherally administered these peptides for 14-days twice per day. Figure 4 shows that the food intake and body weight in diet-induced obesity (DIO) mice were significantly lowered, mainly by the effect of palm-PrRP31. After the treatment, palm-PrRP31-treated mice weighed ~ 15% less and myr-PrRP20-treated mice ~ 10% less than Sal-treated controls. No signs of inflammation were observed during the treatment.

As shown in Table 2, palm-PrRP31 treatment significantly lowered insulin and leptin levels in blood, and decreased SCAT and perirenal fat masses. The group of mice pair-fed to palm-PrRP31 showed similar metabolic changes, suggesting that the primary effect of palm-PrRP31 is most likely due to food intake regulation. Despite the fact that the treatment of DIO mice with myr-PrRP20 decreased circulating level of leptin significantly, the masses of the dissected fat tissues were not significantly lowered (Table 2).

Plasma corticosterone level significantly increased after myr-PrRP20 and palm-PrRP31 treatment compared with Sal-treated group, but increase in adrenocorticotropic hormone level did not reach significance (Supplementary Figure S5).

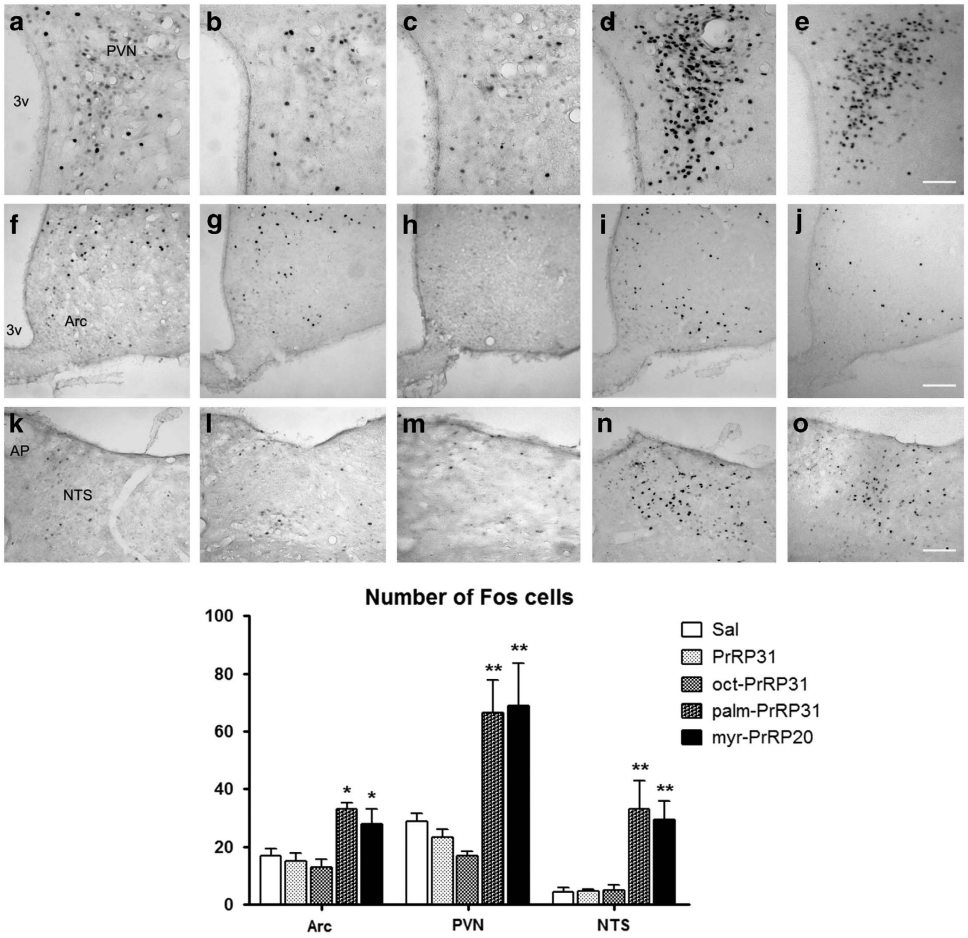

Figure 2. Effect of PrRP lipidization on cells activity in food intake-regulating areas in mouse brain. Fos immunoreactivity: the qualitative as well as quantitative assessment of Fos-immunostained cells in coronal section of PVN (**a**–**e**), Arc (**f**–**j**) and NTS (**k**–**o**) 90 min after SC application of saline (**a**, **f**, **k**) and PrRP31 (**b**, **g**, **l**), oct-PrRP31 (**c**, **h**, **m**), palm-PrRP31 (**d**, **i**, **n**) and myr-PrRP20 (**e**, **j**, **o**) at a dose of 5 mg kg^{-1} in fasted mice ($n = 4$). *$P < 0.05$, **$P < 0.01$ vs saline (Sal), PrRP31 and oct-PrRP31. PVN—paraventricular hypothalamic nucleus, Arc—arcuate hypothalamic nucleus, NTS—solitary tract nucleus, 3v—third brain ventricle. Scale bar is 50 μm for **a**–**e**, 100 μm for **f**–**o**.

Expression of UCP-1 was not changed in brown adipose tissue of palm-PrRP31 compared with Sal-treated group (Supplementary Figure S6).

As palm-PrRP31 treatment had the most attenuating effect on fat stores, we investigated the mRNA expressions of adipokines and fat metabolism-regulating enzymes only in palm-PrRP31-treated DIO mice and their pair-fed group. Decrease in the masses of all particular fats dissected resulted in a very significantly attenuated mRNA expressions of leptin (Supplementary Figure S7) but not adiponectin (not shown). In both SCAT and IPAT, the second most significant site of lipogenesis, fatty-acid synthase mRNA was significantly attenuated. Treatment with palm-PrRP31 did not decrease lipoprotein lipase mRNA expression in SCAT or in IPAT in contrast to the results observed in pair-fed animals (Supplementary Figure S7). Palm-PrRP31 treatment attenuated fat metabolism more significantly in the liver, where the mRNAs of enzymes catalyzing the *de novo* synthesis of fatty acids, ACACA and FASN, were reduced significantly and in addition to a reduction in sterol regulatory element-binding protein mRNA (Supplementary Figure S7).

DISCUSSION

In spite of their low toxicity and few side effects, the clinical potential of natural centrally acting anorexigenic neuropeptides is limited due to their low stability and poor bioavailability under physiological conditions. Our work has shown for the first time that a unique modification of PrRP by lipidization led not only to an increased stability in blood but also enabled to exert PrRP central effect after peripheral administration.

In our previous study,[20] we confirmed the importance of the C terminus, identical for both PrRP20 and PrRP31, for their biological activity. Therefore, the N terminus of both natural peptides, PrRP31 and PrRP20, was lipidized with fatty acids of different lengths to preserve their full biological activity. PrRP31 and PrRP20 lipidized by 8–18 carbon chain fatty acids retained their binding affinities to GPR10 and NPFF2 receptors over-expressed in CHO cells and to tumor cells RC-4B/C endogenously expressing both GPR10 and NPFF2 receptors with affinities similar to natural PrRP31.[20,34] Agonistic properties of the lipidized analogs of PrRP31 and PrRP20 were confirmed by an increased MAPK/EKR1/2 phosphorylation in CHO cells overexpressing GPR10 receptor.

Despite similar binding affinities and agonist character of PrRP lipidized by 8–18 carbons chain fatty acids, only palm- and stear-PrRP31 and myr-PrRP20 highly significantly and dose-dependently lowered food intake in lean overnight-fasted and freely fed mice after SC administration, whereas analogs containing fatty acids with shorter carbon chains and the natural PrRP31 or PrRP20 had no effect on food intake. These findings suggest that only palm- or stear-PrRP31 and myr-PrRP20 were probably able to cross the BBB and exert their central effect on food intake. This conclusion was

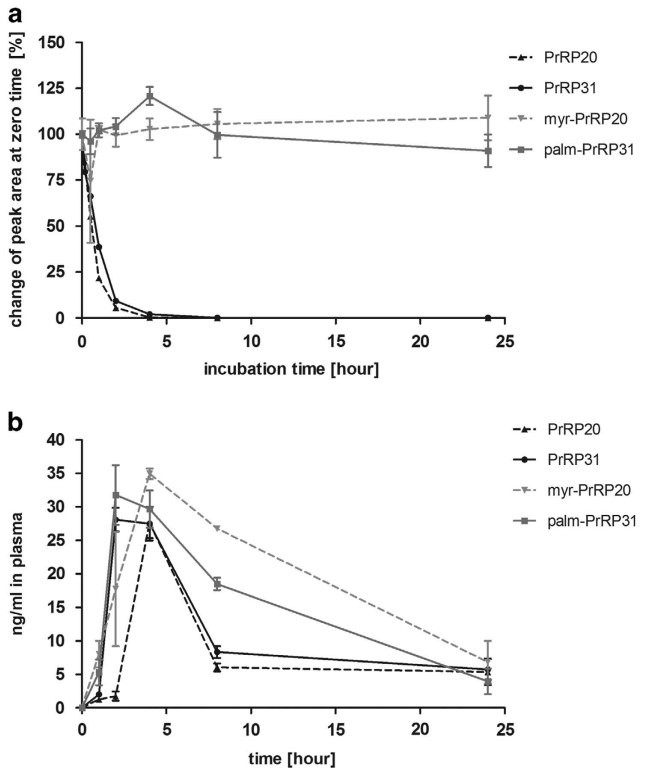

Figure 3. Pharmacokinetics of the PrRP analogs *in vitro* and *in vivo*. (**a**) Degradation profiles in rat plasma. The analog triplicates were incubated for different times in rat plasma and then submitted for immunoanalysis using EIA kit. The results are expressed as the percentage differences from the blood levels of PrRP31 at time 0 with a 10^{-6}M initial concentration. (**b**) Plasma concentrations after single SC injection (5 mg kg^{-1}) in mice ($n=3$) as measured by EIA kit.

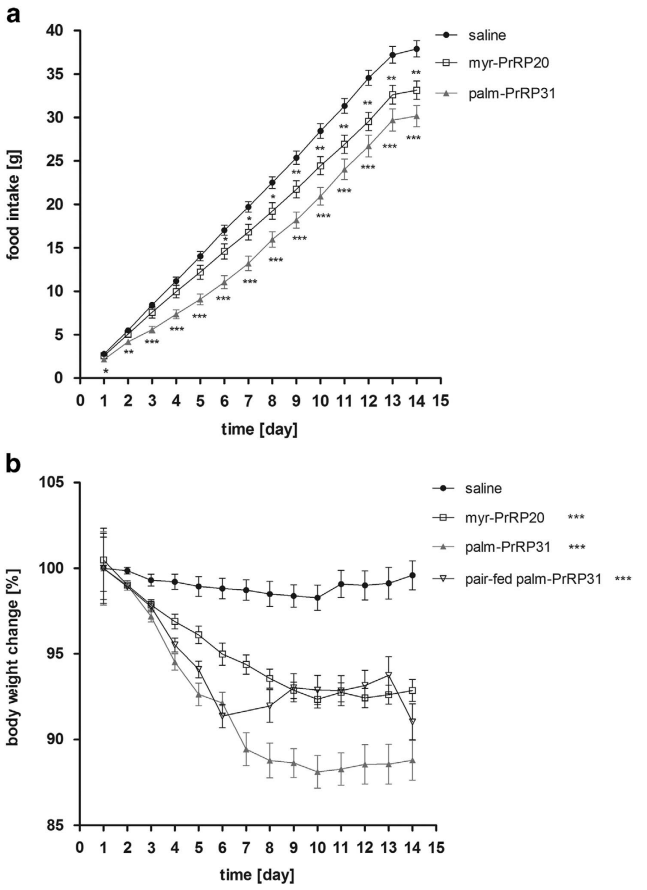

Figure 4. Palmitoylated PrRP31 and myristoylated PrRP20 reduce food intake and body weight of diet-induced obese mice**.** Effect of 14- day administration of palm-PrRP31 and myr-PrRP20 on (**a**) food intake and (**b**) body weight of DIO mice. Mice were SC administered by saline or peptides at a dose of 5 mg kg^{-1} twice daily ($n=10$). Pair-fed group received amount of food consumed by palm-PrRP31-treated group the previous day. The data were analyzed by one-way ANOVA. *$P<0.05$, **$P<0.01$, ***$P<0.001$ vs saline-treated group.

further supported by the fact that both SC administered myr-PrRP20 and palm-PrRP31 significantly enhanced c-Fos immunoreactivity in food intake-regulating hypothalamic and brainstem nuclei containing both GPR10 and NPFF2 receptors,[18,35] whereas natural and octanoylated PrRP31 did not induce these changes.

In the hypothalamus, leptin receptor and PrRP are colocalizated and have additive anorexigenic effect.[36] Anorexigenic effect of PrRP independent of leptin but dependent on CCK was suggested in the brainstem.[37]

The acute SC administration of natural PrRP31, palm-PrRP31 and myr-PrRP20 did not result in any sedative, analgetic or anxiety-inducing effects in mice. Thus, despite their high-affinity binding to NPFF2 receptor, lipidized PrRP analogs do not share the hyperalgesic activities of NPFF.[24] In spite of its name, PrRP-induced PRL release is currently considered controversial.[38] In our experiments, after intravenously or SC administration, palm-PrRP31 or myr-PrRP20 did not increase the release of PRL in rats and mice.

The long-lasting anorexigenic effect of palm- and stear-PrRP31 and myr-PrRP20 analogs could be explained by their prolonged stability owing to binding to serum albumin similar to liraglutide or palmitoylated gastric inhibitory polypeptide.[16] Our stability test confirmed that both palm-PrRP31 and myr-PrRP20 were stable for >24 h in rat plasma. *In vivo* pharmacokinetics in mice also showed longer stability and a higher area under the curve for palm-PrRP31 and myr-PrRP20 compared with natural, non-lipidized analogs.

Finally, the 2-week-long twice daily administration of palm-PrRP31 and myr-PrRP20 to mice with HF diet-induced obesity significantly decreased cumulative food intake and body weight. The time course and the extent of the effect were similar to those of liraglutide,[39,40] confirming the potential of these compounds for obesity treatment.

The decrease in body weight after 2-week palm-PrRP31 treatment in DIO mice was mediated mainly by the reduction of body fat that was accompanied by a decrease in leptin level. Decreased mRNA expressions of fatty-acid synthase in both the adipose tissue and the liver along with a decreased expression of acetyl-CoA carboxylase and sterol regulatory element-binding protein in the liver suggests that this reduction most likely resulted from a decreased *de novo* lipogenesis owing primarily to negative energy balance due to reduced food intake. In our study, changes of UCP-1 mRNA in brown adipose tissue after palm-PrRP31 treatment pointing to possible increase of energy expenditure were not found. On the other hand, significantly increased corticosterone and nonsignificantly increased adreno-corticotropic hormone plasma levels after 14-days treatment with myr-PrRP20 and palm-PrRP31 support the fact that PrRP was proposed to be implicated also in endocrine regulation of hypothalamic–pituitary–andrenal axis.[41]

In conclusion, we have demonstrated that the lipidization of PrRP enabled its central anorexigenic effect after peripheral administration in both acute and chronic settings by enhancing its stability in the blood and improving its ability to cross the BBB. Our data also confirmed that GPR10 and/or NPFF2 receptors are suitable targets for the treatment of obesity. Collectively, our data

Table 2. Metabolic parameters after 14-day SC administration of PrRP analogs in fasted DIO mice

		Group/treatment			
		Saline	*Myr-PrRP20*	*Palm-PrRP31*	*Pair-fed to palm-PrRP31*
Fat/body weight	(%)	16.15 ± 0.4	15.3 ± 0.42	12.7 ± 0.71***	14.5 ± 0.67
SCAT/body weight	(%)	8.07 ± 0.33	7.05 ± 0.19	5.38 ± 0.49***	6.95 ± 0.50
IPAT/body weight	(%)	4.66 ± 0.33	5.09 ± 0.43	4.75 ± 0.19	4.67 ± 0.46
Perirenal fat/body weight	(%)	2.94 ± 0.14	2.77 ± 0.13	2.07 ± 0.20***	2.60 ± 0.08
Liver/body weight	(%)	4.07 ± 0.20	3.60 ± 0.18	3.56 ± 0.07	3.14 ± 0.13***
Leptin	(ng ml^{-1})	53.3 ± 3.49	39.6 ± 3.47*	24.7 ± 3.39***	27.4 ± 1.91***
Glucose	(mmol l^{-1})	6.94 ± 0.28	7.52 ± 0.16	7.26 ± 0.29	5.6 ± 0.37**
Insulin	(ng ml^{-1})	4.09 ± 0.55	3.54 ± 0.47	2.37 ± 0.47*	0.79 ± 0.14***
Triglycerides	(mg dl^{-1})	72.2 ± 3.2	68.7 ± 4.16	66.8 ± 8.74	57.5 ± 5.38

Abbreviations: IPAT, intraperitoneal adipose tissue; SCAT, subcutaneous adipose tissue. All values are expressed as mean ± s.e.m. ($n = 10$ per group). Significance (one-way ANOVA) is *$P < 0.05$, **$P < 0.01$ and ***$P < 0.001$ vs saline-treated group.

suggest that lipidized PrRP analogs have potential as a possible future anti-obesity drugs.

CONFLICT OF INTEREST

The authors declare no conflict of interest.

ACKNOWLEDGEMENTS

This study was supported by the GACR No. P303/10/1368 and P303/12/0576, TACR TE01020028, grant of MSMT (No. 20/2014) and by the ASCR RVO: 61388963 and RVO:67985823. We gratefully acknowledge T Elbert for the radioiodination of peptides and H Vysušilová, Z Kopecká and I Nahodilová for excellent technical assistance.

REFERENCES

1 Hinuma S, Habata Y, Fujii R, Kawamata Y, Hosoya M, Fukusumi S *et al.* A prolactin-releasing peptide in the brain. *Nature* 1998; **393**: 272–276.
2 Ibata Y, Iijima N, Kataoka Y, Kakihara K, Tanaka M, Hosoya *et al.* Morphological survey of prolactin-releasing peptide and its receptor with special reference to their functional roles in the brain. *Neurosci Res* 2000; **38**: 223–230.
3 Lawrence C, Celsi F, Brennand J, Luckman S. Alternative role for prolactin-releasing peptide in the regulation of food intake. *Nat Neurosci* 2000; **3**: 645–646.
4 Engström M, Brandt A, Wurster S, Savola JM, Panula P. Prolactin releasing peptide has high affinity and efficacy at neuropeptide FF2 receptors. *J Pharmacol Exp Ther* 2003; **305**: 825–832.
5 Dockray GJ. The expanding family of -RFamide peptides and their effects on feeding behaviour. *Exp Physiol* 2004; **89**: 229–235.
6 Chartrel N, Bruzzone F, Leprince J, Tollemer H, Anouar Y, Do-Régo JC *et al.* Structure and functions of the novel hypothalamic RFamide neuropeptides R-RFa and 26RFa in vertebrates. *Peptides* 2006; **27**: 1110–1120.
7 Lawrence C, Ellacott K, Luckman S. PRL-releasing peptide reduces food intake and may mediate satiety signaling. *Endocrinology* 2002; **143**: 360–367.
8 Bjursell M, Lennerås M, Göransson M, Elmgren A, Bohlooly-Y M. GPR10 deficiency in mice results in altered energy expenditure and obesity. *Biochem Biophys Res Commun* 2007; **363**: 633–638.
9 Takayanagi Y, Matsumoto H, Nakata M, Mera T, Fukusumi S, Hinuma S *et al.* Endogenous prolactin-releasing peptide regulates food intake in rodents. *J Clin Invest* 2008; **118**: 4014–4024.
10 Maniscalco JW, Rinaman L. Overnight food deprivation markedly attenuates hindbrain noradrenergic, glucagon-like peptide-1, and hypothalamic neural responses to exogenous cholecystokinin in male rats. *Physiol Behav* 2013; **121**: 35–42.
11 Dodd GT, Luckman SM. Physiological Roles of GPR10 and PrRP Signaling. *Front Endocrinol (Lausanne)* 2013; **4**: 20.
12 Bellmann-Sickert K, Beck-Sickinger AG. Peptide drugs to target G protein-coupled receptors. *Trends Pharmacol Sci* 2010; **31**: 434–441.
13 Brasnjevic I, Steinbusch HW, Schmitz C, Martinez-Martinez P. Initiative ENR. Delivery of peptide and protein drugs over the blood-brain barrier. *Prog Neurobiol* 2009; **87**: 212–251.
14 Malavolta L, Cabral FR. Peptides: important tools for the treatment of central nervous system disorders. *Neuropeptides* 2011; **45**: 309–316.
15 Havelund S, Plum A, Ribel U, Jonassen I, Vølund A, Markussen J *et al.* The mechanism of protraction of insulin detemir, a long-acting, acylated analog of human insulin. *Pharm Res* 2004; **21**: 1498–1504.
16 Gault VA, Kerr BD, Harriott P, Flatt PR. Administration of an acylated GLP-1 and GIP preparation provides added beneficial glucose-lowering and insulinotropic actions over single incretins in mice with Type 2 diabetes and obesity. *Clin Sci (Lond)* 2011; **121**: 107–117.
17 Manning S, Pucci A, Finer N. Pharmacotherapy for obesity: novel agents and paradigms. *Ther Adv Chronic Dis* 2014; **5**: 135–148.
18 Roland B, Sutton S, Wilson S, Luo L, Pyati J, Huvar R *et al.* Anatomical distribution of prolactin-releasing peptide and its receptor suggests additional functions in the central nervous system and periphery. *Endocrinology* 1999; **140**: 5736–5745.
19 Boyle R, Downham R, Ganguly T, Humphries J, Smith J, Travers S. Structure-activity studies on prolactin-releasing peptide (PrRP). Analogues of PrRP-(19-31)-peptide. *J Pept Sci* 2005; **11**: 161–165.
20 Maletínská L, Spolcová A, Maixnerová J, Blechová M, Zelezná B. Biological properties of prolactin-releasing peptide analogs with a modified aromatic ring of a C-terminal phenylalanine amide. *Peptides* 2011; **32**: 1887–1892.
21 Blechová M, Nagelová V, Záková L, Demianová Z, Zelezná B, Maletínská L. New analogs of the CART peptide with anorexigenic potency: the importance of individual disulfide bridges. *Peptides* 2013; **39**: 138–144.
22 Maletínská L, Pýchová M, Holubová M, Blechová M, Demianová Z, Elbert T *et al.* Characterization of new stable ghrelin analogs with prolonged orexigenic potency. *J Pharmacol Exp Ther* 2012; **340**: 781–786.
23 Holubová M, Spolcová A, Demianová Z, Sýkora D, Fehrentz JA, Martinez J *et al.* Ghrelin agonist JMV 1843 increases food intake, body weight and expression of orexigenic neuropeptides in mice. *Physiol Res* 2013; **62**: 435–444.
24 Maletinska L, Ticha A, Nagelova V, Spolcova A, Blechova M, Elbert T *et al.* Neuropeptide FF analog RF9 is not an antagonist of NPFF receptor and decreases food intake in mice after its central and peripheral administration. *Brain Res* 2013; **1498**: 33–40.
25 Motulsky H, Neubig R. Analyzing radioligand binding data. *Curr Protoc Neurosci* 2002; **Chapter 7**: Unit 7.5.
26 Nagelová V, Pirník Z, Železná B, Maletínská L. CART (cocaine- and amphetamine-regulated transcript) peptide specific binding sites in PC12 cells have characteristics of CART peptide receptors. *Brain Res* 2014; **1547**: 16–24.
27 Pirnik Z, Bundziková J, Holubová M, Pýchová M, Fehrentz JA, Martinez J *et al.* Ghrelin agonists impact on Fos protein expression in brain areas related to food intake regulation in male C57BL/6 mice. *Neurochem Int* 2011; **59**: 889–895.
28 Maletínská L, Maixnerová J, Matysková R, Haugvicová R, Pirník Z, Kiss A *et al.* Synergistic effect of CART (cocaine- and amphetamine-regulated transcript) peptide and cholecystokinin on food intake regulation in lean mice. *BMC Neurosci* 2008; **9**: 101.
29 Maletínská L, Lignon M, Galas M, Bernad N, Pírková J, Hlavácek J *et al.* Pharmacological characterization of new cholecystokinin analogues. *Eur J Pharmacol* 1992; **222**: 233–240.
30 Kopecký J, Hodný Z, Rossmeisl M, Syrový I, Kozak LP. Reduction of dietary obesity in aP2-Ucp transgenic mice: physiology and adipose tissue distribution. *Am J Physiol* 1996; **270**: E768–E775.
31 Maletinska L, Matyskova R, Maixnerova J, Sykora D, Pychova M, Spolcova A *et al.* The Peptidic GHS-R antagonist [D-Lys(3)]GHRP-6 markedly improves adiposity and related metabolic abnormalities in a mouse model of postmenopausal obesity. *Mol Cell Endocrinol* 2011; **343**: 55–62.

32 Chang C, Cheng Y. Ribonucleotide reductase isolated from human cells. Heterogeneity among the sources. *Biochem Pharmacol* 1978; **27**: 2297–2300.
33 Maixnerová J, Hlavácek J, Blokesová D, Kowalczyk W, Elbert T, Sanda *et al*. Structure-activity relationship of CART (cocaine- and amphetamine-regulated transcript) peptide fragments. *Peptides* 2007; **28**: 1945–1953.
34 Maixnerová J, Špolcová A, Pýchová M, Blechová M, Elbert T, Rezáčová *et al*. Characterization of prolactin-releasing peptide: binding, signaling and hormone secretion in rodent pituitary cell lines endogenously expressing its receptor. *Peptides* 2011; **32**: 811–817.
35 Gouardères C, Faura CC, Zajac JM. Rodent strain differences in the NPFF1 and NPFF2 receptor distribution and density in the central nervous system. *Brain Res* 2004; **1014**: 61–70.
36 Ellacott KL, Halatchev IG, Cone RD. Characterization of leptin-responsive neurons in the caudal brainstem. *Endocrinology* 2006; **147**: 3190–3195.
37 Bechtold DA, Luckman SM. Prolactin-releasing Peptide mediates cholecystokinin-induced satiety in mice. *Endocrinology* 2006; **147**: 4723–4729.
38 Jarry H, Heuer H, Schomburg L, Bauer K. Prolactin-releasing peptides do not stimulate prolactin release *in vivo*. *Neuroendocrinology* 2000; **71**: 262–267.
39 Porter DW, Kerr BD, Flatt PR, Holscher C, Gault VA. Four weeks administration of Liraglutide improves memory and learning as well as glycaemic control in mice with high fat dietary-induced obesity and insulin resistance. *Diabetes Obes Metab* 2010; **12**: 891–899.
40 Kerr BD, Flatt PR, Gault VA. Effects of gamma-glutamyl linker on DPP-IV resistance, duration of action and biological efficacy of acylated glucagon-like peptide-1. *Biochem Pharmacol* 2010; **80**: 396–401.
41 Maruyama M, Matsumoto H, Fujiwara K, Noguchi J, Kitada C, Fujino *et al*. Prolactin-releasing peptide as a novel stress mediator in the central nervous system. *Endocrinology* 2001; **142**: 2032–2038.

Supplementary Information accompanies this paper on International Journal of Obesity website (http://www.nature.com/ijo)

Journal of Alzheimer's Disease 45 (2015) 823–835
DOI 10.3233/JAD-143150
IOS Press

Anorexigenic Lipopeptides Ameliorate Central Insulin Signaling and Attenuate Tau Phosphorylation in Hippocampi of Mice with Monosodium Glutamate-Induced Obesity

Andrea Špolcová[a,b], Barbora Mikulášková[a], Martina Holubová[a], Veronika Nagelová[a], Zdenko Pirnik[a,e,f], Jana Zemenová[a,d], Martin Haluzík[c], Blanka Železná[a], Marie-Christine Galas[b] and Lenka Maletínská[a,*]

[a]*Institute of Organic Chemistry and Biochemistry, AS CR, Prague, Czech Republic*
[b]*INSERM UMR837, Lille, France, Jean Pierre Aubert Research Centre, Faculté de Médecine-Pòle Recherche, Institut de Médecine Prédictive et de Recherche Thérapeutique, Université Droit et Santé de Lille, CHU-Lille, Lille, France*
[c]*Third Department of Medicine, First Faculty of Medicine, Charles University in Prague, Prague, Czech Republic*
[d]*Institute of Chemical Technology, Department of Analytical Chemistry, Prague, Czech Republic*
[e]*Laboratory of Functional Neuromorphology, Institute of Experimental Endocrinology, SAS, Bratislava, Slovak Republic*
[f]*Department of Human and Clinical Pharmacology, University of Veterinary Medicine, Košice, Slovak Republic*

Accepted 29 December 2014

Abstract. Numerous epidemiological and experimental studies have demonstrated that patients who suffer from metabolic disorders, such as type 2 diabetes mellitus (T2DM) or obesity, have higher risks of cognitive dysfunction and of Alzheimer's disease (AD). Impaired insulin signaling in the brain could contribute to the formation of neurofibrillary tangles, which contain an abnormally hyperphosphorylated tau protein. This study aimed to determine whether potential tau hyperphosphorylation could be detected in an obesity-induced pre-diabetes state and whether anorexigenic agents could affect this state. We demonstrated that 6-month-old mice with monosodium glutamate (MSG) obesity, which represent a model of obesity-induced pre-diabetes, had increased tau phosphorylation at Ser396 and Thr231 in the hippocampus compared with the controls, as determined by western blots. Two weeks of subcutaneous treatment with a lipidized analog of prolactin-releasing peptide (palm-PrRP31) or with the T2DM drug liraglutide, which both had a central anorexigenic effect, resulted in increased phosphorylation of the insulin cascade kinases PDK1 (Ser241), Akt (Thr308), and GSK-3β (Ser9). Furthermore, these drugs attenuated phosphorylation at Ser396, Thr231, and Thr212 of tau and of the primary tau kinases in the hippocampi of 6-month-old MSG-obese mice. We identified tau hyperphosphorylation in the obesity-induced pre-diabetes state in MSG-obese mice and demonstrated the beneficial effects of palm-PrRP31 and liraglutide, both of known central anorexigenic effects, on hippocampal insulin signaling and on tau phosphorylation.

Keywords: Alzheimer's disease, insulin signaling, liraglutide, monosodium glutamate-obese mice, obesity, pre-diabetes, prolactin-releasing peptide, tau phosphorylation

INTRODUCTION

Besides extracellular amyloid-β peptide (Aβ) plaques, Alzheimer's disease (AD) is characterized by intracellular hyperphosphorylated tau protein

*Correspondence to: Dr. Lenka Maletínská, Institute of Organic Chemistry and Biochemistry AS CR, Flemingovo nam. 2, 166 10 Prague 6, Czech Republic. Tel.: +420 220183567; Fax: +420 220183571; E-mail: maletin@uochb.cas.cz.

ISSN 1387-2877/15/$35.00

neurofibrillary tangles. Tau protein is expressed mainly in neurons where it promotes tubulin assembling to microtubules and establishes links between microtubules and other cytoskeleton components. Binding of tau to tubulin is regulated by phosphorylation of tau. Hyperphosphorylation lowers binding of tau to tubulin and promotes tau self-polymerization and aggregation to neurofibrillary tangles [1–3]. Tau is primarily phosphorylated by the following proline-directed kinases: GSK-3β (glycogen synthase kinase-3β), cdk5 (cyclin-dependent kinase 5), p44/42 MAPK/ERK1/2 (mitogen-activated protein kinases/extracellular signal-regulated kinases), and JNK (c-Jun N-terminal kinase) [4]. When tau and its various kinases were co-overexpressed in neuroblastoma cells, GSK-3α, GSK-3β, and MAPK 13 were the most effective tau kinases that phosphorylated Ser202, Thr231, Ser235, and Ser396/404, which represent the AD-relevant phosphorylation sites. Generally, GSK-3β has a kinase activity to the most phosphorylation sites of tau. Most of the kinases phosphorylate several tau epitopes, and most phosphorylation sites are targets of more than one kinase. Additionally, some epitopes can be phosphorylated only after other sites have been phosphorylated [5, 6].

GSK-3β is a participant in the insulin signaling cascade and is abundantly expressed in the central nervous system. The phosphorylation of serines 9 and 389 inhibits the kinase activity of GSK-3β [7]. Decreased insulin effectiveness with attenuated GSK-3β Ser9 phosphorylation was shown to result in enhanced GSK-3β kinase activity toward tau in both type 2 diabetes mellitus (T2DM) and AD patients [8]. Similarly, in db/db mice, which represent a rodent model of T2DM, hippocampal tau protein phosphorylation at the epitopes Ser199/202, Thr231, and Ser396, as well as spatial memory impairment, increased progressively with age-related hyperinsulinemia and hyperglycemia [9, 10]. The pathological changes in GSK-3β and tau phosphorylation identified in db/db mice were reversed with insulin administration [11].

Insulin secretagogues, such as the glucagon-like peptide-1 (GLP-1) analogs exendin-4 and liraglutide, which are used for T2DM treatment, as well as the glucose-dependent insulinotropic polypeptide (GIP) analog, have demonstrated protective effects in the brain by reducing Aβ plaques and by preventing the loss of synapses and memory impairments in AD mouse models [12–16]. In rats with intracerebroventricular (ICV) streptozotocin (STZ) treatment-induced sporadic AD [17], a decline in learning and memory and an increase in total and phosphorylated tau in the hippocampus were reversed by an ICV co-application of a GLP-1 analog [18]. Because the central effects of liraglutide have been shown to be exclusively anorexigenic and weight-attenuating [19], one question that arises is whether an anorexigenic neuropeptide produced and acting in the brain, such as prolactin-releasing peptide (PrRP) (reviewed by [20]), could affect tau phosphorylation in the hippocampus. PrRP production is under the control of leptin; PrRP-expressing neurons contain leptin receptors, and when PrRP and leptin were ICV co-administered to rats, these drugs had additive anorexigenic and energy expenditure-increasing effects [21]. The neuroprotective properties of leptin include lowering tau phosphorylation in tau-overexpressing SH-SY5Y cells [22]. Leptin attenuated Aβ formation and improved cognitive performance in CRND8 mice overexpressing amyloid-β precursor protein (AβPP) [23, 24]. A non-functioning leptin receptor was the cause of worsened spatial memory in Zucker diabetic fatty rats [25] and in db/db mice [26].

In this study, we aimed to determine whether tau hyperphosphorylation could be detected during the pre-diabetes state, which is a frequent condition in elderly individuals. A useful rodent model of pre-diabetes includes mice or rats with obesity induced by monosodium glutamate (MSG) subcutaneous injections administered to newborns, which result in specific lesions in the arcuate nucleus (ARC) of the hypothalamus. MSG-obese rodents develop obesity with increased adiposity at a sustained body weight [27] because of a lower metabolic rate rather than elevated food intake [28]. Hyperinsulinemia at nearly normoglycemia [29] supports the use of MSG- obese mice as a model of pre-diabetes.

In this study, we also aimed to determine how repeated administration of the GLP-1 agonist liraglutide, which is an anti-T2DM drug promoting insulin secretion that has also a central body weight-reducing effect, and our unique centrally acting anorexigenic lipidized PrRP analog, affected metabolic parameters connected with pre-diabetes in the periphery and insulin signaling and tau phosphorylation in the hippocampus.

MATERIALS AND METHODS

Peptides

The palmitoylated PrRP analog palm-PrRP31 (N-palm-SRTHRHSMEIRTPDINPAWYASRGIRPVG RF-NH_2) was synthesized and purified at the Institute

of Organic Chemistry and Biochemistry, Prague, Czech Republic as previously described [30]. PrRP lipidization was performed as previously described in [31] on a fully protected peptide on resin as the final step. The purity and identity of the peptide was determined using analytical HPLC and a Q-TOF micro MS technique (Waters, Milford, MA, USA).

Liraglutide (Victoza, Novo Nordisk, Maloev, Denmark, 6 mg/ml in an injection pen) was obtained from a pharmacy.

Experimental animals

All animal experiments followed the ethical guidelines for animal experiments and the Czech Republic Act No. 246/1992. The experiments were approved by the Committee for Experiments with Laboratory Animals of the Academy of Sciences of the Czech Republic.

NMRI mice (Charles River, Sulzfeld, Germany) were housed at 23°C with a daily 12-h light and dark cycle (lights on at 6 a.m.). The mice had free access to water and a standard chow diet (Mlýn Kocanda, Jesenice, Czech Republic), which contained 25%, 9%, and 66% calories as protein, fat, and carbohydrates, respectively, and 3.4 kcal/g energy content.

For MSG-induced obesity, newborn male NMRI mice were subcutaneously (SC) administered L-glutamic acid sodium salt hydrate (Sigma-Aldrich, St. Louis, MO, USA) (4 mg/g body weight) at postnatal days 2–8 as previously described [28].

Body weight was monitored once per week up to the age of 6 months. Overnight fasted MSG-obese mice and their controls at ages 2 and 6 months ($n = 10$) were sacrificed by decapitation starting at 8:00 a.m. The trunk blood was collected, and the plasma was separated and stored at −20°C. The white adipose tissue (i.e., subcutaneous, abdominal, and perirenal fat), the liver and the hippocampus of all mice were dissected and weighed. The rate of adiposity was expressed as the fat-to-body weight ratio (the ratio of the total adipose tissue weight to the total body weight).

Effects of 14-day administration of palm-PrRP31 and liraglutide on body weight, food intake, metabolic parameters, insulin signaling, and tau phosphorylation in MSG-obese mice

At 6 months old, one week before the beginning of the experiment, the MSG-obese mice were randomly divided into groups of 10 mice and placed in individual cages with free access to food and water. The following week, the mice were subjected to a 14-day administration of peptides. Three groups were SC injected with saline, palm-PrRP31 (5 mg/kg), or liraglutide (0.2 mg/kg, both peptides dissolved in saline) twice per day (at 8:00 a.m. and 6:00 p.m.). The amount of food consumed and the weights of the mice were monitored daily.

At the end of the experiment, overnight fasted mice were sacrificed by decapitation starting at 8:00 a.m. Blood was collected, and tissues were dissected as previously described in section Experimental animals.

Glucose tolerance test

An intraperitoneal glucose tolerance test (IPGTT) was performed on day 9 of the 14-day treatment. Overnight fasted MSG-obese mice were IP injected with glucose (2 g/kg) at 8:00 a.m. (time 0). Then, blood glucose was measured at 0, 15, 30, 60, 90, 120, and 180 min following injection using a Glucocard glucometer (Arkray, Kyoto, Japan).

Determination of hormonal and biochemical parameters

The plasma insulin concentrations were measured using RIA (Millipore, St. Charles, MI, USA and Linco Research, St. Charles, MI, USA), and the leptin concentrations were determined using ELISA (Millipore, St. Charles, MI, USA). The serum glucose levels were measured using a Glucocard glucometer. All measurements were performed according to the protocols recommended by the manufacturers.

Antibodies used for immunoblotting and immunohistochemistry

The following antibodies were used: phospho-PDK1 (3-phosphoinositide-dependent kinase 1) rabbit mAb, PDK1 rabbit mAb, phospho-Akt (Thr308) rabbit mAb, phospho-Akt (Ser473) rabbit mAb, Akt rabbit mAb, phospho-GSK-3β (Ser9) rabbit mAb, GSK-3 β rabbit mAb, phospho-MAPK/ERK1/2 mouse mAb, total MAPK/ERK1/2 mouse mAb, phospho-JNK rabbit mAb, total JNK rabbit mAb, anti-mouse IgG HRP-linked antibody, anti-rabbit IgG horseradish peroxidase (HRP)-linked antibody (purchased from Cell Signaling Technology, Beverly, MA, USA). Anti-Tau[pSer^{396}] rabbit mAb, anti-Tau[pThr^{231}] rabbit mAb were purchased from Invitrogen, NY, USA and AT8 antibody was purchased from Thermo Scientific, Waltham, MA, USA. Tau CTer mouse mAb was

identified previously [32] and anti-β-actin antibody produced in mouse were obtained from Sigma-Aldrich, St. Louis, MO, USA.

Tissue preparation for immunoblotting

The hippocampi were separated from the dissected brains and homogenized in cold lysis buffer (62.5 mM Tris-HCl buffer with pH 6.8, 1% deoxycholate, 1% Triton X-100, 50 mM NaF, 1 mM Na_3VO_4 and complete protease inhibitor (Roche Applied Science, Mannheim, Germany)) using a Bullet Blender homogenizer (Next Advance, Inc., Averill Park, NY, USA). During tissue handling, all samples were kept on ice. The lysates were sonicated for 1 min. The protein concentration was determined using a Pierce BCA protein assay kit (Thermo Fisher Scientific, Inc., Waltham, MA, USA). The lysates were diluted to a final concentration of 1 μg/μl in Laemmli sample buffer (62.5 mM Tris-HCl with pH 6.8, 2% SDS, 10% glycerol, 0.01% bromophenol blue, 5% β-mercaptoethanol, 50 mM NaF, and 1 mM Na_3VO_4) and stored at −20°C.

Immunoblotting

The samples for immunoblotting were sonicated for 1 min and boiled at 100°C for 2 min. Then, 10 μg/10μl of each sample was resolved using 5/10% SDS-PAGE electrophoresis. The proteins were transferred onto a nitrocellulose membrane, blocked in 5% non-fat milk or BSA in TBS/Tween-20 buffer (20 mM Tris, 136 mM NaCl, 0.1% Tween-20, 50 mM NaF, and 5 mM Na_3VO_4) and incubated overnight in the corresponding antibody diluted in 5% non-fat milk or 5% BSA in TBS/Tween-20 buffer at 4°C. After incubation for 1 h with a HRP-linked secondary antibody at room temperature, the membranes were developed using Luminata Classico/Crescendo/Forte Western HRP Substrates (Merck Millipore, Darmstadt, Germany), visualized in a ChemiDoc™ System (Bio-Rad, Hercules, CA, USA) and quantified using Image Lab Software (Bio-Rad, Hercules, CA, USA). To compare obtained data the electrophoresis and transfer were performed at the same time in one electrophoretic or transfer system and membranes were visualized in the ChemiDoc™ System altogether. The protein level was normalized to β-actin as a housekeeping protein.

Tissue preparation for immunohistochemistry

One hemisphere of each brain was fixed for 24 h in 4% paraformaldehyde, transferred to 70% ethanol and embedded in paraffin at the histology laboratory of the Faculty of Medicine, Lille, France (Laboratoire d'histologie, Faculté de Médecine, Lille, France).

Phosphorylated tau immunohistochemistry

Five-micrometer thick paraffin-embedded sagittal brain slices were deparaffinized by washing three times in toluene, rehydrated in ethanol (100, 95, 70, and 30%) and unmasked by boiling for 10 min in citrate buffer pH 6 (3.75 mM acid citrate, 2.5 mM disodium phosphate). After 1 h of blocking in 1% horse serum in PBS buffer (Sigma-Aldrich, St. Louis, MO, USA), the slices were incubated overnight at 4°C with the appropriate antibody diluted in PBS/0.2% Triton X-100 buffer. Then, the slices were incubated for 1 h with secondary antibody Alexa 488 or Alexa 568 (Life Technologies, NY, USA). The nuclei were stained with Vectashield/DAPI (4′,6-diamidino-2-phenylindole, Vector Laboratories, Burlingame, CA, USA). Images were acquired on a Zeiss confocal laser-scanning microscope LSM 710 using a 488-nm Argon laser, a 561-nm diode-pumped solid-state laser and a 405-nm ultraviolet laser with the same laser intensities to compare the images at Lille 2 University (Plate-forme d'Imagerie Moléculaire et Cellulaire).

Prolactin releasing hormone receptor (PrRP-R) immunohistochemistry

Overnight fasted untreated control male NMRI mice ($n = 4$, body weight 45.6 ± 1.3 g) with the free access to water were used for PrRP-R immunohistochemical processing. The mice were deeply anesthetized with sodium pentobarbital (50 mg/kg, IP) and transcardially perfused with 0.1 M phosphate buffer (PB, pH 7.4) containing 4% paraformaldehyde. The brains were subsequently removed, postfixed in the same fixative overnight at 4°C, and infiltrated with 20% sucrose in 0.1 M PB for 48 h at 4°C. The brains were cut into 30-μm thick coronal sections at −22°C in a Leica CM1950 cryostat (Leica Microsystems GmbH, Germany), and the free-floating sections were collected in cold (4°C) PB.

The free-floating sections were repeatedly washed in cold PB, followed by preincubation in 3% H_2O_2 for 40 min at room temperature. Then, the sections were incubated with rabbit PrRP-R polyclonal antiserum (1:200, LifeSpan BioSciences, Inc., LS-C177303) and diluted in 0.1 M PB containing 4% normal goat serum (Gibco, Grand Island, NY, USA), 0.5% Triton X-100 (Sigma-Aldrich, St. Louis, MO, USA), and 0.1%

sodium azide for 48 h at 4°C. After several rinses in PB, the sections were incubated with biotinylated goat anti-rabbit IgG (1:500, VectorStain Elite ABC, Vector Laboratories, Burlingame, CA, USA) diluted in 0.1 M PB containing 4% NGS and 1% Triton X-100 for 90 min at room temperature. The PB rinses were followed by incubation with the avidin-biotin peroxidase complex (1:250, VectorStain Elite ABC, Vector Laboratories, Burlingame, CA), which was diluted in 0.1 M PB containing 1% Triton X-100 for 90 min at room temperature. PB washing was followed by a wash in 0.05 M Tris-HCl (pH 6.0). The PRLHR antigenic sites were visualized with 0.01% 3,3′-diaminobenzidine tetrahydrochloride (DAB, Sigma-Aldrich, St. Louis, MO, USA) dissolved in 0.05 M Tris-HCl containing 0.0012% H_2O_2 for 3–5 min. Finally, the sections were mounted on glass, air-dried, and coverslipped with DPX mounting medium (Thermo Fisher Scientific, Inc., Waltham, MA, USA). Immunostaining of the negative control, which did not display antiserum immunolabeling, included the substitution of the primary antiserum with normal rabbit serum and the sequential elimination of the primary or secondary antibody from the staining series. The PrRP-R immunoreactive cells were evaluated separately in each side of the coronal sections ($n = 2$-3 sections per mouse) within the dentate gyrus and the CA1-CA3 fields of the hippocampus of the hippocampal formation (from bregma −1.46 to −1.94 mm) according to the mouse brain atlas [33]. Images of representative sections were acquired using a digital camera (Olympus DP70) and an Olympus AX70 light microscope.

Statistical analyses

The data are presented as the means ± SEM for the number of animals indicated in the Figures and Tables. The data were analyzed using a two-way analysis of variance (ANOVA), followed by a Bonferroni *post-hoc* test, or using a one-way ANOVA, followed by a Dunnett's *post-hoc* test or a *t*-test, as stated in the Figure and Table legends, using Graph-Pad Software (San Diego, CA, USA). $p < 0.05$ was considered statistically significant.

RESULTS

Six-month-old MSG-obese mice developed increased tau phosphorylation

The male MSG-obese mice and their age-matched controls were characterized by fat and body weight and by the metabolic parameters connected with obesity and diabetes at 2 and 6 months old (Table 1). The body weights of the MSG-obese mice did not significantly differ from their age-matched controls at 2 or 6 months old. However, the total amount of white adipose tissue and the resultant leptin levels were significantly higher in the MSG-obese mice compared with those amounts and levels of their age-matched controls. Fasting glucose levels were not significantly increased in the MSG-obese mice, whereas the insulin levels were significantly higher in the MSG-obese mice at both 2 and 6 months old compared with those levels of their age-matched controls (Table 1). Thus, the MSG-obese mice exhibited obesity with significant fat accumulation in a pre-diabetes state (increase in insulin but not glucose levels).

The phosphorylation of inhibitory Ser9 in GSK-3β, which is the primary tau kinase, significantly decreased only in the 6-month-old controls compared with that in the 2-month-old controls (Fig. 1). Compared with the controls, the 6-month-old MSG-obese mice displayed increased phosphorylation at the Ser396 and Thr231 epitopes of hippocampal tau, whereas the 2-month-old MSG-obese mice did not display different phosphorylation levels of the Ser396 and Thr231 epitopes of hippocampal tau compared with respective age-matched controls (Fig. 1). It was the reason why 6-month-old MSG-obese mice were used in the following experiment.

Table 1
Metabolic parameters of 2 and 6 months old MSG mice and their age-matched controls

Mice	Body weight [g]	White adipose tissue [% body weight]	Glucose [mmol/l]	Insulin [ng/ml]	Leptin [ng/ml]
Controls 2 months	40.29 ± 0.94	4.54 ± 0.47	6.63 ± 0.46	0.96 ± 0,15	2.07 ± 0.43
MSG 2 months	42.50 ± 0.59	12.04 ± 0.63***	8.55 ± 0.34	3.48 ± 0.57*	27.38 ± 4.14**
Controls 6 months	53.73 ± 1.84	6.88 ± 0.47	6.43 ± 0.52	0.83 ± 0.27	4.03 ± 1.55
MSG 6 months	57.18 ± 1.26	11.46 ± 0.48 ###	5.83 ± 0.45	3.64 ± 0.99#	18.11 ± 2.91##

Data are mean ± SEM ($n = 10$ animals per group). Significance is *$p < 0.05$, **$p < 0.01$, and ***$p < 0.001$ (*versus control 2 months, #versus control 6 months) using one-way ANOVA, Bonferroni *post hoc* test.

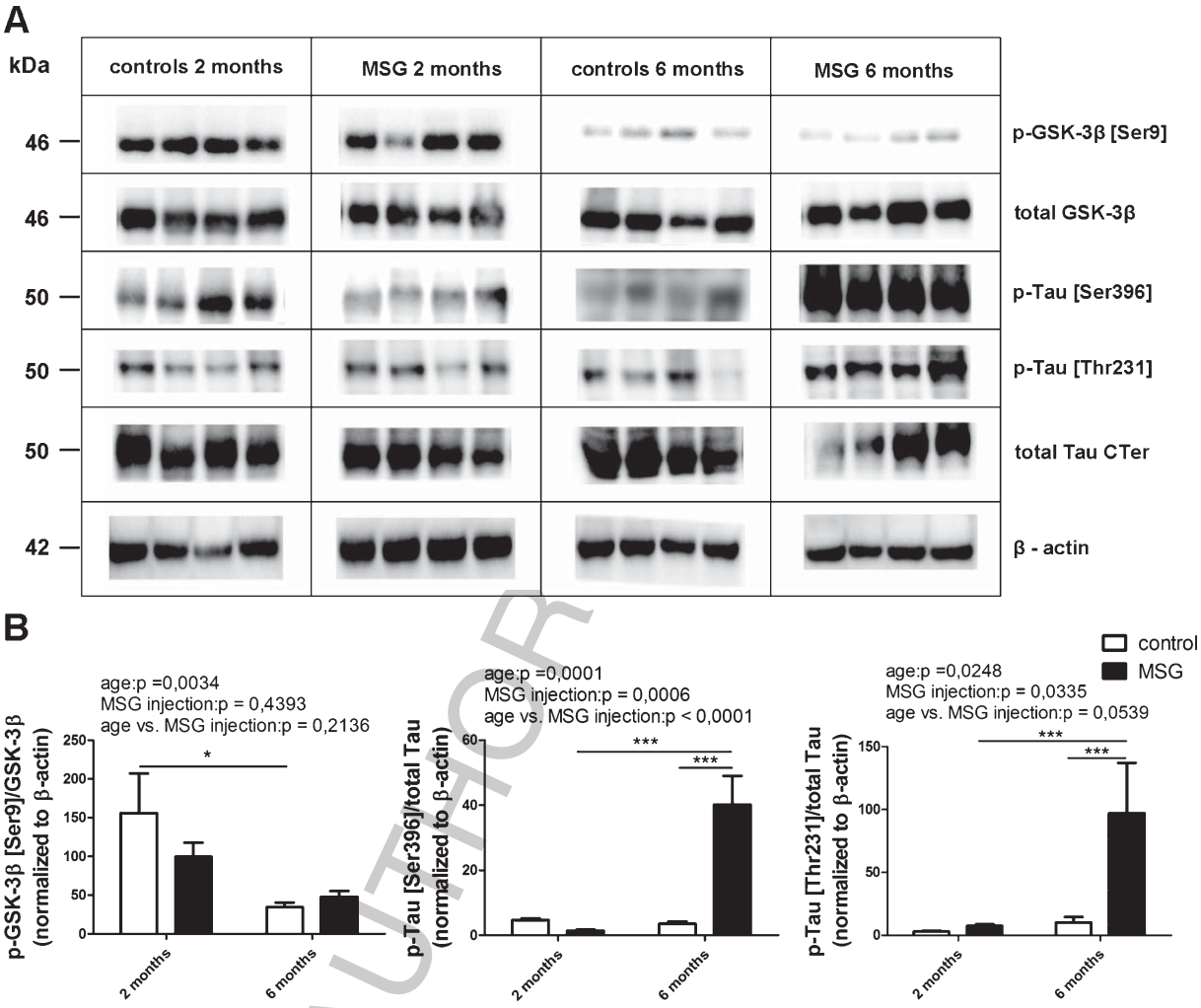

Fig. 1. MSG mice show age-related pathological tau hyperphosphorylation in the hippocampus. A) Western blot analysis of glycogen synthase kinase-3β (GSK-3β) activation and tau phosphorylation (Ser396 and Thr231 epitopes) in hippocampi lysates of 2- and 6-month-old MSG mice and their controls ($n = 10$ mice per group). B) Densitometric quantification of the Western blots normalized to β-actin. Data were analyzed by two-way ANOVA, Bonferroni *post hoc* test. Data are mean ± SEM, $n = 10$ mice per group.

Anorexigenic lipopeptides, palm-PrRP31 and liraglutide, attenuated food intake but did not affect body weight or related metabolic parameters in MSG-obese mice

To examine the effects of two anorexigenic peptides on hippocampal tau phosphorylation in 6-month-old MSG-obese mice, liraglutide and the novel analog palm-PrRP31 were SC administered twice per day for 14 days at doses that significantly lowered food intake and activated neurons in the brain areas regulating food intake after acute administration [34].

The cumulative food intake significantly decreased after treatment with both lipopeptides (Fig. 2). Weight loss did not reach significance after treatment with either palm-PrRP31 or liraglutide compared with that of the saline-treated group (Fig. 2). However, significant weight loss occurred in the saline-treated group most likely because of the repeated injections. Furthermore, based on our previous experience, the NMRI mouse strain is extremely sensitive to manipulation and to repeated injections. The white adipose tissue weight and leptin levels only tended to decrease after treatment with both peptides. The fasting glucose and insulin levels did not significantly differ from those levels of the saline-treated controls (Table 2).

IPGTT was performed in fasted mice on day 9 of the experiment (Fig. 3). The AUCs of palm-PrRP31 or liraglutide treated MSG-obese mice did not significantly differ from those AUCs for the saline-treated

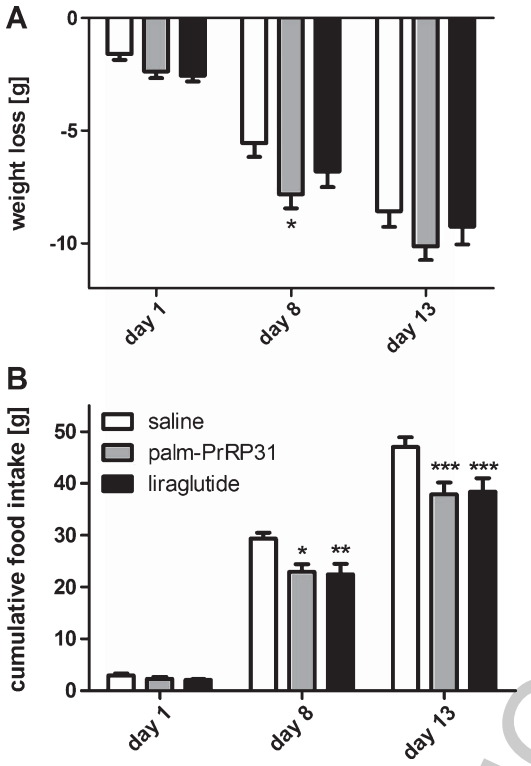

Fig. 2. Body weight change and food intake in MSG mice after palm-PrRP31 or liraglutide treatment. Effect of 14-day administration of liraglutide and palm-PrRP31 on (A) body weight change and (B) food intake of MSG mice. Mice were SC administered by saline or peptides, palm-PrRP31 at a dose of 5 mg/kg and liraglutide at a dose of 0.2 mg/kg twice daily ($n = 10$). The data were analyzed by one-way ANOVA, Bonferroni *post-hoc* test. $^{*}p < 0.05$, $^{**}p < 0.001$ and $^{***}P < 0.001$ vs saline-treated group.

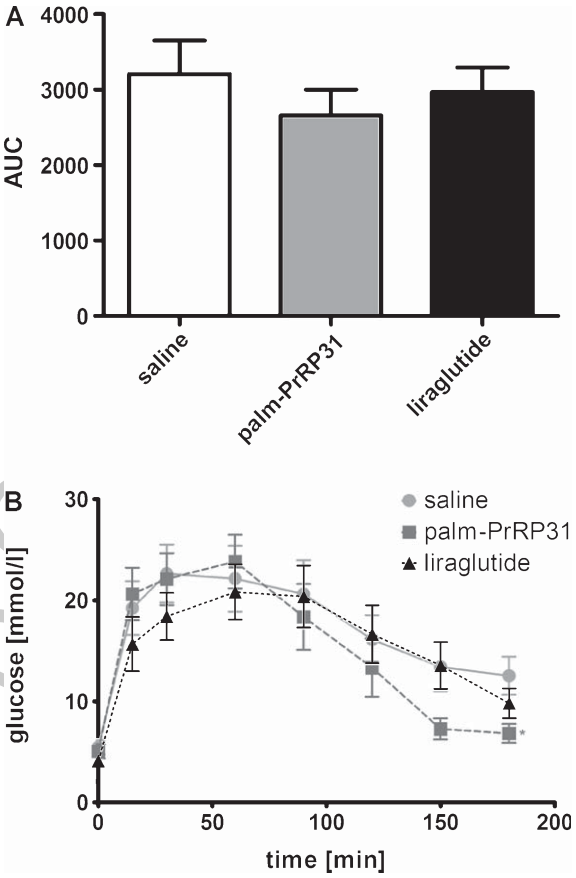

Fig. 3. Glucose tolerance test in MSG mice and their controls. Intraperitoneal glucose tolerance test (IPGTT) was performed in overnight fasted MSG mice injected IP with glucose (2 g/kg) after 9 days of saline, liraglutide, or palm-PrRP31 treatment ($n = 10$). A) Area under curve (AUC). B) Time course of IPGTT. Significance is $^{*}p < 0.05$ using one-way ANOVA, Bonferroni *post-hoc* test.

MSG-obese mice or for the control mice (Fig. 3a); only the final glucose level was significantly lower in the MSG-obese mice treated with palm-PrRP31 compared with the MSG-obese control mice treated with saline (Fig. 3b).

Palm-PrRP31 and liraglutide ameliorated insulin signaling and attenuated activity of tau kinases in the hippocampi of MSG-obese mice

The repeated administration of both palm-PrRP31 and liraglutide positively affected the hippocampal insulin signaling cascade. Figure 4 shows significant enhancement of PDK phosphorylation in the liraglutide-treated mice but not after palm-PrRP31 intervention. Akt phosphorylation at the Thr308 epitope significantly increased in the palm-PrRP31-treated group but not in the liraglutide-treated group. Akt phosphorylation at Ser473 was not affected by either treatment.

Phosphorylation at the Ser9 epitope of GSK-3β, which is the primary tau kinase, significantly increased

Table 2
Metabolic parameters of 6 months old MSG mice after 14-day treatment with palm-PrRP31 and liraglutide

Intervention	Body weight [g]	White adipose tissue [% body weight]	Glucose [mmol/l]	Insulin [ng/ml]	Leptin [ng/ml]
Saline	53.08 ± 2.22	6.37 ± 0.84	6.48 ± 0.42	1.53 ± 0.20	23.10 ± 3.85
Palm-PrRPP31	50.07 ± 1.68	4.91 ± 0.43	6.49 ± 0.32	1.57 ± 0.13	21.20 ± 2.62
liraglutide	48.23 ± 1.70	5.38 ± 0.67	5.63 ± 0.34	1.91 ± 0.27	18.16 ± 2.41

Data are mean ± SEM ($n = 10$ animals per group). Data were analyzed by one-way ANOVA, Bonferroni *post hoc* test.

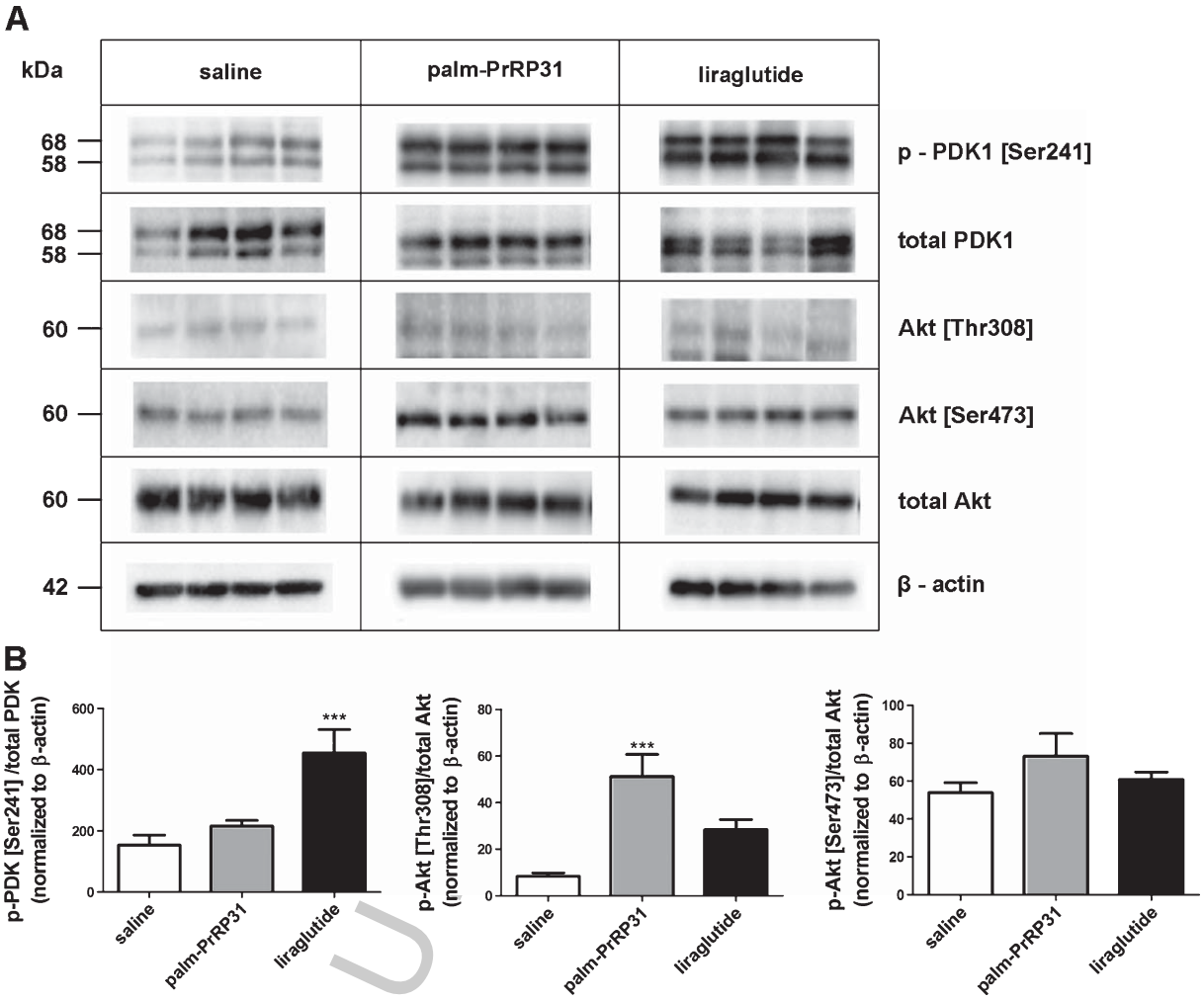

Fig. 4. Liraglutide and palm-PrRP31 enhance insulin signaling in the hippocampus. Insulin signaling cascade in hippocampi of MSG mice after palm-PrRP31 or liraglutide treatment. A) Western blots of the proteins involved in insulin signaling cascade using specific antibodies ($n = 10$ mice per group). B) Densitometric quantification of the western blots normalized to β-actin. Data are mean ± SEM. The data were analyzed by one-way ANOVA, Dunnett *post hoc* test. $^{*}p < 0.05$, $^{**}p < 0.001$, and $^{***}p < 0.001$ versus saline-treated group.

after palm-PrRP31 administration but not after liraglutide administration in the MSG-obese mice (Fig. 5).

The phosphorylation of two other potent tau kinases, ERK1/2 and JNK, was significantly lowered after both palm-PrRP31 and liraglutide administration in the hippocampi of the MSG-obese mice, as shown in Fig. 5.

Palm-PrRP31 and liraglutide reduced tau hyperphosphorylation in the hippocampi of MSG-obese mice

The phosphorylation of the hippocampal tau protein at the Thr212, Thr231, and Ser396 epitopes of the MSG-obese mice was affected by treatment with both palm-PrRP31 and liraglutide (Fig. 6). Both liraglutide and palm-PrRP31 treatment significantly decreased the hyperphosphorylation of the tau protein in these epitopes. The immunohistochemical analysis of the hippocampi confirmed these results. In the CA1 subfield of the hippocampus, the phosphorylation of the tau protein at Thr212 and at Ser202/T205 (the antibody AT8) decreased after palm-PrRP31 and liraglutide treatment compared with that of the control group (Fig. 7).

PrRP-R immunopositive cells are present in the hippocampus

PrRP-R immunopositive cells, which displayed small cell bodies and dendritic branches, were

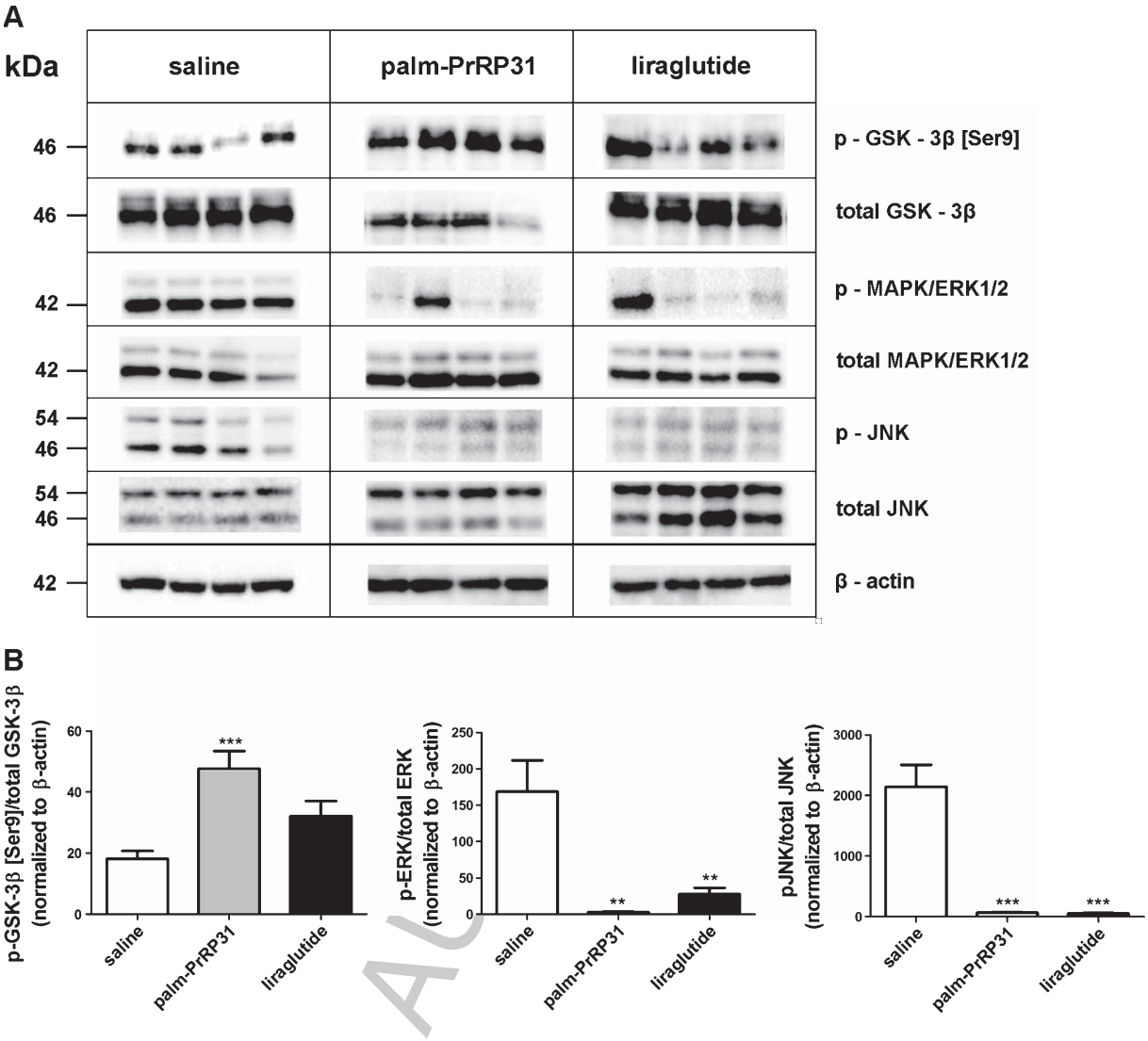

Fig. 5. Impact of liraglutide and palm-PrRP31 treatment on phosphorylation of hippocampal tau kinases GSK-3β, ERK1/2, and JNK. A) Western blots of the tau kinases phosphorylation using specific antibodies ($n = 10$ mice per group). B) Densitometric quantification of the western blots normalized to β-actin. Data are mean ± SEM. The data were analyzed by one-way ANOVA, Dunnett *post hoc* test. $^{*}p < 0.05$, $^{**}p < 0.001$, and $^{***}p < 0.001$ versus saline-treated group.

primarily detected in the stratum lacunosum-moleculare of the hippocampus (Fig. 8) and in the hilus proper of the dentate gyrus from control mice. In addition, several scattered PrRP-R cells were also detected in the stratum radiatum of the CA3 field of the hippocampus.

DISCUSSION

The primary results of this study revealed that treatment with palm-PrRP31, an analog of the anorexigenic neuropeptide PrRP that is active centrally after peripheral administration [34] and the T2DM drug liraglutide both had a central anorexigenic effect and decreased the phosphorylation of several tau kinases and of the tau protein in the hippocampus of 6-month-old pre-diabetic MSG-obese mice. Moreover, palm-PrRP31 and liraglutide abolished insulin signaling in the hippocampus in the MSG-obese mice.

MSG administration to mice or rats during the neonatal period led to "selective" lesions in the ARC [35, 36]; to pre-diabetic syndrome with mild hyperglycemia, hyperinsulinemia, and hyperleptinemia [36, 37]; and to decreased insulin sensitivity [38]. This pre-diabetic condition was also apparent in our MSG-obese mice at 2 and 6 months old.

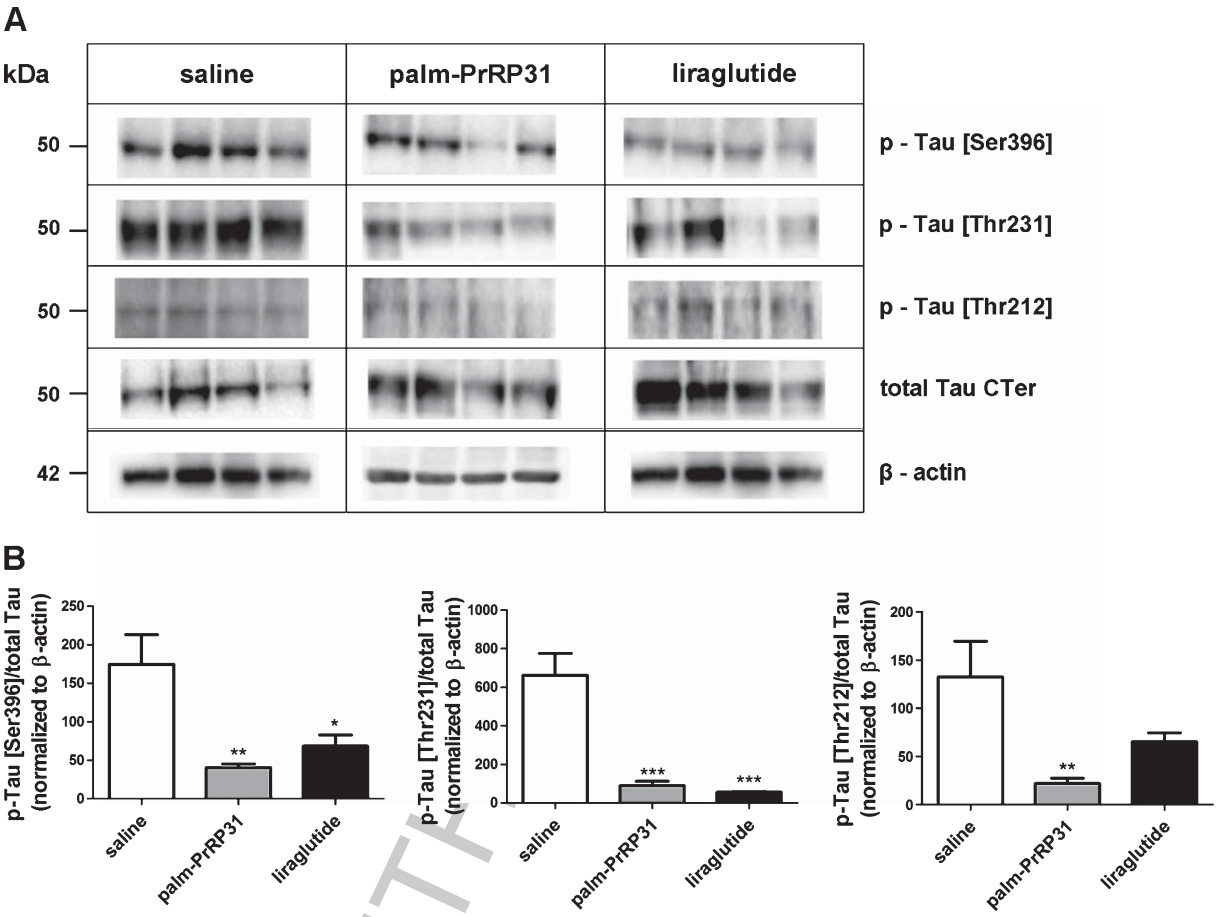

Fig. 6. Pathological hyperphosphorylation of tau protein is attenuated in hippocampi of MSG mice after liraglutide and palm-PrRP31 treatment. A) Western blots of tau phosphorylation on the epitopes Ser396, Thr231, and Thr212 ($n = 10$ mice per group). B) Densitometric quantification of western blots normalized to β-actin. Data are mean ± SEM. The data were analyzed by one-way ANOVA, Dunnett *post hoc* test. $^{*}p < 0.05$, $^{**}p < 0.001$, and $^{***}p < 0.001$ versus saline-treated group.

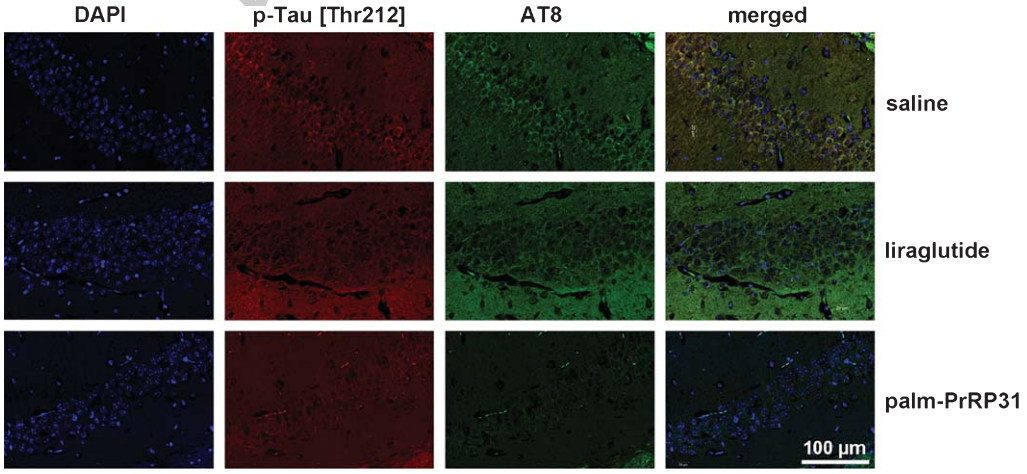

Fig. 7. Immunohistochemical staining of phosphorylated tau in hippocampi of MSG mice after liraglutide and palm-PrRP31 treatment. In hippocampal CA1 region from MSG mice, tau phosphorylation at Thr212 and at Ser202/Thr205 was detected after liraglutide or palm-PrRP31 treatment compared to saline-treated group. The nuclei were counterstained with DAPI (4′,6-diamidino-2-phenylindole).

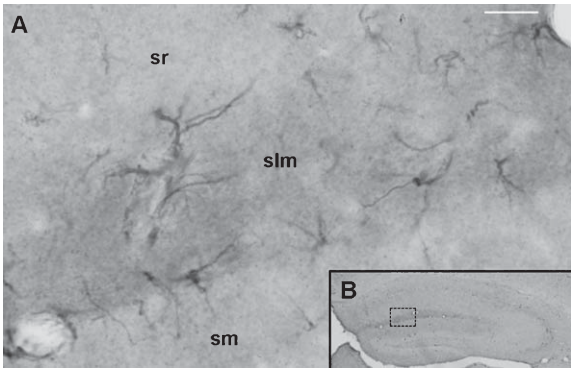

Fig. 8. The PrRP receptor immunopositive cells in the stratum lacunosum-moleculare (slm) of the control mice hippocampus. A) The detailed picture of PrRP receptor immunopositive cells in the stratum lacunosum-moleculare (slm) of the untreated control NMRI mice hippocampus. The white scale bar = 20 μm. B) The lower resolution picture of mice hippocampus with the denoted square area from which detailed pictures (A) was taken. slm, stratum lacunosum-moleculare; sm, stratum moleculare; sr stratum radiatum.

Although an age-related significant decrease in the phosphorylation of inhibitory Ser9 in GSK-3β, which augmented GSK-3β kinase activity, was obvious in controls but not in our MSG-obese mice, significantly enhanced phosphorylation of Thr231 and Ser396 of tau in the hippocampi was identified in the 6-month-old, but not in the 2-month-old, MSG-treated mice compared with controls. Tau hyperphosphorylation in pre-diabetic MSG-obese mice appears to be a progressive process similar to db/db mice with severe T2DM [9] and Zucker fa/fa rats [39]. Similarly, an increased phosphorylation at Ser396 in the neurofibrillary tangles and in dystrophic neurites has been found in the later stage of AD [40].

MSG-obese mice exhibit hyperleptinemia resulting from increased adiposity and from the loss of ARC neurons, which are the primary leptin targets [35, 36]. Recently, leptin resistance in the hippocampus was found to play a possible role in the characteristic changes associated with AD [41]. In contrast, leptin administration protected cortical and hippocampal cells from Aβ-induced expression of synaptic protein and tau hyperphosphorylation *in vitro* and *in vivo* [42].

Leptin controls PrRP production in the hypothalamus, and the anorexigenic effect of PrRP is synergistic with leptin [43]. Additionally, the present study demonstrated the presence of the PrRP receptor in the stratum lacunosum-moleculare of the CA1 subfield of the hippocampus and in the hilus of the dentate gyrus from control mice. These findings allowed rational assumption for the study of the palm-PrRP31 treatment also in obese MSG mice. Liraglutide was shown to cross the blood-brain barrier and to increase cAMP and neurogenesis in the mouse brain [44]. Learning and memory were restored after GLP-1 receptor (GLP-1R) gene transfer to the hippocampus in GLP-1R-deficient mice [45]. Although the central effect of liraglutide has recently been demonstrated to be only anorexigenic [19], liraglutide ameliorated hippocampal tau hyperphosphorylation in rats with STZ-induced severe T2DM in established DIO [46] and improved spatial memory and hippocampal neurogenesis in DIO mice [47, 48].

Moreover, different effects of diabetes on tau hyperphosphorylation have been identified in AD mouse models, in STZ-treated pR5 mice expressing P301L mutant tau [49], and in THY/Tau22 transgenic mice overexpressing human mutated tau with DIO [50]. STZ-induced diabetes exacerbated tau pathology in pR5 mice, whereas a detrimental effect of DIO on tau pathology in THY/Tau22 mice was related to obesity rather than to insulin resistance, whether peripheral or central. This study demonstrated that tau hyperphosphorylation could occur in the hippocampi of mice with obesity connected with pre-diabetes and that anorexigenic peptides with potent anti-obesity effects could attenuate this hypothetical tau hyperphosphorylation. Because the central effects of liraglutide have been proven exclusively anorexigenic and because palm-PrRP31 is an analog of a potent anorexigenic neuropeptide whose anti-diabetic effect has not yet been demonstrated, we conclude that the anorexigenic rather than anti-diabetic effects of both liraglutide and palm-PrRP31 mediated the decrease in tau phosphorylation in the hippocampi of the MSG-treated obese mice. In this study, we found that liraglutide and palm-PrRP31 attenuated the effects on tau hyperphosphorylation, although a 9-day treatment with both liraglutide and palm-PrRP31 did not affect the global utilization of glucose in the MSG-obese mice. In contrast, food intake significantly decreased after treatment with both substances.

In conclusion, 14-day peripheral administration of the anorexigenic lipopeptides, palm-PrRP31 and liraglutide, ameliorated hippocampal insulin signaling, decreased the activity of major tau kinases, and attenuated the pathological hyperphosphorylation of tau in MSG-obese mice, which are a model of obesity and pre-diabetes. These findings support the potential use of these analogs for the prevention and treatment of the tau hyperphosphorylation that is connected with obesity-related T2DM and describe, for the first time, the neuroprotective effect of PrRP.

ACKNOWLEDGMENTS

This study was supported by the Grant Agency of the Czech Republic No. P303/12/0576, and by the Academy of Sciences of the Czech Republic RVO: 61388963.

We gratefully acknowledge M. Blechová for synthesis of palm-PrRP31 analog, H. Vysušilová for excellent technical assistance, the laboratory of histology at Faculty of Medicine, Lille 2 university for preparing paraffin embedded slices, and Meryem Tardivel and IMPRT (Institut de Médecine Prédictive et de Recherche Thérapeutique, Lille) for access to the confocal microscopy platform.

Authors' disclosures available online (http://j-alz.com/manuscript-disclosures/14-3150).

SUPPLEMENTARY MATERIAL

The supplementary material is available in the electronic version of this article: http://dx.doi.org/10.3233/JAD-143150.

REFERENCES

[1] Martin L, Latypova X, Wilson CM, Magnaudeix A, Perrin ML, Yardin C, Terro F (2013) Tau protein kinases: Involvement in Alzheimer's disease. *Ageing Res Rev* **12**, 289-309.

[2] Buee L, Bussiere T, Buee-Scherrer V, Delacourte A, Hof PR (2000) Tau protein isoforms, phosphorylation and role in neurodegenerative disorders. *Brain Res Brain Res Rev* **33**, 95-130.

[3] Kolarova M, Garcia-Sierra F, Bartos A, Ricny J, Ripova D (2012) Structure and pathology of tau protein in Alzheimer disease. *Int J Alzheimers Dis* **2012**, 731526.

[4] Lee G, Leugers CJ (2012) Tau and tauopathies. *Prog Mol Biol Transl Sci* **107**, 263-293.

[5] Cavallini A, Brewerton S, Bell A, Sargent S, Glover S, Hardy C, Moore R, Calley J, Ramachandran D, Poidinger M, Karran E, Davies P, Hutton M, Szekeres P, Bose S (2013) An unbiased approach to identifying tau kinases that phosphorylate tau at sites associated with Alzheimer disease. *J Biol Chem* **288**, 23331-23347.

[6] Tenreiro S, Eckermann K, Outeiro TF (2014) Protein phosphorylation in neurodegeneration: Friend or foe? *Front Mol Neurosci* **7**, 42.

[7] Wang QM, Fiol CJ, DePaoli-Roach AA, Roach PJ (1994) Glycogen synthase kinase-3 beta is a dual specificity kinase differentially regulated by tyrosine and serine/threonine phosphorylation. *J Biol Chem* **269**, 14566-14574.

[8] Liu Y, Liu F, Grundke-Iqbal I, Iqbal K, Gong CX (2011) Deficient brain insulin signalling pathway in Alzheimer's disease and diabetes. *J Pathol* **225**, 54-62.

[9] Kim B, Backus C, Oh S, Hayes JM, Feldman EL (2009) Increased tau phosphorylation and cleavage in mouse models of type 1 and type 2 diabetes. *Endocrinology* **150**, 5294-5301.

[10] Ramos-Rodriguez JJ, Ortiz O, Jimenez-Palomares M, Kay KR, Berrocoso E, Murillo-Carretero MI, Perdomo G, Spires-Jones T, Cozar-Castellano I, Lechuga-Sancho AM, Garcia-Alloza M (2013) Differential central pathology and cognitive impairment in pre-diabetic and diabetic mice. *Psychoneuroendocrinology* **38**, 2462-2475.

[11] Jolivalt CG, Lee CA, Beiswenger KK, Smith JL, Orlov M, Torrance MA, Masliah E (2008) Defective insulin signaling pathway and increased glycogen synthase kinase-3 activity in the brain of diabetic mice: Parallels with Alzheimer's disease and correction by insulin. *J Neurosci Res* **86**, 3265-3274.

[12] Long-Smith CM, Manning S, McClean PL, Coakley MF, O'Halloran DJ, Holscher C, O'Neill C (2013) The diabetes drug liraglutide ameliorates aberrant insulin receptor localisation and signalling in parallel with decreasing both amyloid-beta plaque and glial pathology in a mouse model of Alzheimer's disease. *Neuromolecular Med* **15**, 102-114.

[13] McClean PL, Parthsarathy V, Faivre E, Hölscher C (2011) The diabetes drug liraglutide prevents degenerative processes in a mouse model of Alzheimer's disease. *J Neurosci* **31**, 6587-6594.

[14] Faivre E, Holscher C (2013) Neuroprotective effects of D-Ala(2)GIP on Alzheimer's disease biomarkers in an APP/PS1 mouse model. *Alzheimers Res Ther* **5**, 20.

[15] Li Y, Duffy KB, Ottinger MA, Ray B, Bailey JA, Holloway HW, Tweedie D, Perry T, Mattson MP, Kapogiannis D, Sambamurti K, Lahiri DK, Greig NH (2010) GLP-1 receptor stimulation reduces amyloid-beta peptide accumulation and cytotoxicity in cellular and animal models of Alzheimer's disease. *J Alzheimers Dis* **19**, 1205-1219.

[16] Yarchoan M, Arnold SE (2014) Repurposing diabetes drugs for brain insulin resistance in Alzheimer disease. *Diabetes* **63**, 2253-2261.

[17] Lannert H, Hoyer S (1998) Intracerebroventricular administration of streptozotocin causes long-term diminutions in learning and memory abilities and in cerebral energy metabolism in adult rats. *Behav Neurosci* **112**, 1199-1208.

[18] Li L, Zhang ZF, Holscher C, Gao C, Jiang YH, Liu YZ (2012) (Val(8)) glucagon-like peptide-1 prevents tau hyperphosphorylation, impairment of spatial learning and ultra-structural cellular damage induced by streptozotocin in rat brains. *Eur J Pharmacol* **674**, 280-286.

[19] Sisley S, Gutierrez-Aguilar R, Scott M, D'Alessio DA, Sandoval DA, Seeley RJ (2014) Neuronal GLP1R mediates liraglutide's anorectic but not glucose-lowering effect. *J Clin Invest* **124**, 2456-2463.

[20] Dodd GT, Luckman SM (2013) Physiological Roles of GPR10 and PrRP Signaling. *Front Endocrinol (Lausanne* **4**, 20.

[21] Ellacott K, Lawrence C, Rothwell N, Luckman S (2002) PRL-releasing peptide interacts with leptin to reduce food intake and body weight. *Endocrinology* **143**, 368-374.

[22] Greco SJ, Sarkar S, Johnston JM, Tezapsidis N (2009) Leptin regulates tau phosphorylation and amyloid through AMPK in neuronal cells. *Biochem Biophys Res Commun* **380**, 98-104.

[23] Greco SJ, Bryan KJ, Sarkar S, Zhu X, Smith MA, Ashford JW, Johnston JM, Tezapsidis N, Casadesus G (2010) Leptin reduces pathology and improves memory in a transgenic mouse model of Alzheimer's disease. *J Alzheimers Dis* **19**, 1155-1167.

[24] Fewlass DC, Noboa K, Pi-Sunyer FX, Johnston JM, Yan SD, Tezapsidis N (2004) Obesity-related leptin regulates Alzheimer's Abeta. *FASEB J* **18**, 1870-1878.

[25] Kamal A, Ramakers GM, Gispen WH, Biessels GJ (2013) Hyperinsulinemia in rats causes impairment of spatial memory and learning with defects in hippocampal synaptic

plasticity by involvement of postsynaptic mechanisms. *Exp Brain Res* **226**, 45-51.

[26] Li XL, Aou S, Oomura Y, Hori N, Fukunaga K, Hori T (2002) Impairment of long-term potentiation and spatial memory in leptin receptor-deficient rodents. *Neuroscience* **113**, 607-615.

[27] Djazayery A, Miller DS, Stock MJ (1979) Energy balances in obese mice. *Nutr Metab* **23**, 357-367.

[28] Maletínská L, Toma RS, Pirnik Z, Kiss A, Slaninová J, Haluzík M, Zelezná B (2006) Effect of cholecystokinin on feeding is attenuated in monosodium glutamate obese mice. *Regul Pept* **136**, 58-63.

[29] Remke H, Wilsdorf A, Müller F (1988) Development of hypothalamic obesity in growing rats. *Exp Pathol* **33**, 223-232.

[30] Blechová M, Nagelová V, Záková L, Demianová Z, Zelezná B, Maletínská L (2013) New analogs of the CART peptide with anorexigenic potency: The importance of individual disulfide bridges. *Peptides* **39**, 138-144.

[31] Maletínská L, Pýchová M, Holubová M, Blechová M, Demianová Z, Elbert T, Železná B (2012) Characterization of new stable ghrelin analogs with prolonged orexigenic potency. *J Pharmacol Exp Ther* **340**, 781-786.

[32] Sultan A, Nesslany F, Violet M, Begard S, Loyens A, Talahari S, Mansuroglu Z, Marzin D, Sergeant N, Humez S, Colin M, Bonnefoy E, Buee L, Galas MC (2011) Nuclear tau, a key player in neuronal DNA protection. *J Biol Chem* **286**, 4566-4575.

[33] Franklin K, Paxinos G (1997) *The mouse brain in stereotaxic coordinates*, New York: Academic Press.

[34] Maletinska L, Nagelova V, Ticha A, Spolcova A, Blechova M, Pirnik Z, Kunes J, Zelezna B (2013) Lipidized analogs of prolactin-releasing peptide reduce food intake in rodents after peripheral administration. *Biopolymers* **100**, 255-255.

[35] Takasaki Y (1978) Studies on brain lesion by administration of monosodium L-glutamate to mice. I. Brain lesions in infant mice caused by administration of monosodium L-glutamate. *Toxicology* **9**, 293-305.

[36] Matysková R, Maletínská L, Maixnerová J, Pirník Z, Kiss A, Železná B (2008) Comparison of the obesity phenotypes related to monosodium glutamate effect on arcuate nucleus and/or the high fat diet feeding in C57BL/6 and NMRI mice. *Physiol Res* **57**, 727-734.

[37] Cameron DP, Poon TK, Smith GC (1976) Effects of monosodium glutamate administration in the neonatal period on the diabetic syndrome in KK mice. *Diabetologia* **12**, 621-626.

[38] Lorden JF, Sims JS (1987) Monosodium L-glutamate lesions reduce susceptibility to hypoglycemic feeding and convulsions. *Behav Brain Res* **24**, 139-146.

[39] Spolcova A, Mikulaskova B, Krskova K, Gajdosechova L, Zorad S, Olszanecki R, Suski M, Bujak-Gizycka B, Zelezna B, Maletinska L (2014) Deficient hippocampal insulin signaling and augmented tau phosphorylation is related to obesity- and age-induced peripheral insulin resistance: A study in Zucker rats. *BMC Neurosci* **15**, 111.

[40] Su JH, Cummings BJ, Cotman CW (1994) Early phosphorylation of tau in Alzheimer's disease occurs at Ser-202 and is preferentially located within neurites. *Neuroreport* **5**, 2358-2362.

[41] Bonda DJ, Stone JG, Torres SL, Siedlak SL, Perry G, Kryscio R, Jicha G, Casadesus G, Smith MA, Zhu X, Lee HG (2014) Dysregulation of leptin signaling in Alzheimer disease: Evidence for neuronal leptin resistance. *J Neurochem* **128**, 162-172.

[42] Doherty GH, Beccano-Kelly D, Yan SD, Gunn-Moore FJ, Harvey J (2013) Leptin prevents hippocampal synaptic disruption and neuronal cell death induced by amyloid beta. *Neurobiol Aging* **34**, 226-237.

[43] Ellacott KL, Lawrence CB, Rothwell NJ, Luckman SM (2002) PRL-releasing peptide interacts with leptin to reduce food intake and body weight. *Endocrinology* **143**, 368-374.

[44] Hunter K, Holscher C (2012) Drugs developed to treat diabetes, liraglutide and lixisenatide, cross the blood brain barrier and enhance neurogenesis. *BMC Neurosci* **13**, 33.

[45] During MJ, Cao L, Zuzga DS, Francis JS, Fitzsimons HL, Jiao X, Bland RJ, Klugmann M, Banks WA, Drucker DJ, Haile CN (2003) Glucagon-like peptide-1 receptor is involved in learning and neuroprotection. *Nat Med* **9**, 1173-1179.

[46] Yang Y, Zhang J, Ma D, Zhang M, Hu S, Shao S, Gong CX (2013) Subcutaneous administration of liraglutide ameliorates Alzheimer-associated tau hyperphosphorylation in rats with type 2 diabetes. *J Alzheimers Dis* **37**, 637-648.

[47] Porter DW, Kerr BD, Flatt PR, Holscher C, Gault VA (2010) Four weeks administration of Liraglutide improves memory and learning as well as glycaemic control in mice with high fat dietary-induced obesity and insulin resistance. *Diabetes Obes Metab* **12**, 891-899.

[48] Lennox R, Porter DW, Flatt PR, Gault VA (2013) (Val(8))GLP-1-Glu-PAL: A GLP-1 agonist that improves hippocampal neurogenesis, glucose homeostasis, and beta-cell function in high-fat-fed mice. *ChemMedChem* **8**, 595-602.

[49] Ke YD, Delerue F, Gladbach A, Götz J, Ittner LM (2009) Experimental diabetes mellitus exacerbates tau pathology in a transgenic mouse model of Alzheimer's disease. *PLoS One* **4**, e7917.

[50] Leboucher A, Laurent C, Fernandez-Gomez FJ, Burnouf S, Troquier L, Eddarkaoui S, Demeyer D, Caillierez R, Zommer N, Vallez E, Bantubungi K, Breton C, Pigny P, Buée-Scherrer V, Staels B, Hamdane M, Tailleux A, Buée L, Blum D (2013) Detrimental effects of diet-induced obesity on τ pathology are independent of insulin resistance in τ transgenic mice. *Diabetes* **62**, 1681-1688.

Univerzita Karlova v Praze, 1. lékařská fakulta
Kateřinská 32, Praha 2

Prohlášení zájemce o nahlédnutí
do závěrečné práce absolventa studijního programu
uskutečňovaného na 1. lékařské fakultě Univerzity Karlovy v Praze

Jsem si vědom/a, že závěrečná práce je autorským dílem a že informace získané nahlédnutím do zpřístupněné závěrečné práce nemohou být použity k výdělečným účelům, ani nemohou být vydávány za studijní, vědeckou nebo jinou tvůrčí činnost jiné osoby než autora.

Byl/a jsem seznámen/a se skutečností, že si mohu pořizovat výpisy, opisy nebo kopie závěrečné práce, jsem však povinen/a s nimi nakládat jako s autorským dílem a zachovávat pravidla uvedená v předchozím odstavci.

Příjmení, jméno (hůlkovým písmem)	Číslo dokladu totožnosti vypůjčitele (např. OP, cestovní pas)	Signatura závěrečné práce	Datum	Podpis